NASA/TM-2020-220434

NASA ETR Quiet Zone Probe Study

Larry A. Ticatch
TEAMS 3, Hampton, Virginia

George N. Szatkowski,
Langley Research Center, Hampton, Virginia

Angelo A. Cavone and Justin K. Strickland
Analytical Mechanics Associates, Hampton, Virginia

January 2020

NASA STI Program . . . in Profile

Since its founding, NASA has been dedicated to the advancement of aeronautics and space science. The NASA scientific and technical information (STI) program plays a key part in helping NASA maintain this important role.

The NASA STI program operates under the auspices of the Agency Chief Information Officer. It collects, organizes, provides for archiving, and disseminates NASA's STI. The NASA STI program provides access to the NTRS Registered and its public interface, the NASA Technical Reports Server, thus providing one of the largest collections of aeronautical and space science STI in the world. Results are published in both non-NASA channels and by NASA in the NASA STI Report Series, which includes the following report types:

- TECHNICAL PUBLICATION. Reports of completed research or a major significant phase of research that present the results of NASA Programs and include extensive data or theoretical analysis. Includes compilations of significant scientific and technical data and information deemed to be of continuing reference value. NASA counter-part of peer-reviewed formal professional papers but has less stringent limitations on manuscript length and extent of graphic presentations.

- TECHNICAL MEMORANDUM. Scientific and technical findings that are preliminary or of specialized interest, e.g., quick release reports, working papers, and bibliographies that contain minimal annotation. Does not contain extensive analysis.

- CONTRACTOR REPORT. Scientific and technical findings by NASA-sponsored contractors and grantees.

- CONFERENCE PUBLICATION. Collected papers from scientific and technical conferences, symposia, seminars, or other meetings sponsored or co-sponsored by NASA.

- SPECIAL PUBLICATION. Scientific, technical, or historical information from NASA programs, projects, and missions, often concerned with subjects having substantial public interest.

- TECHNICAL TRANSLATION. English-language translations of foreign scientific and technical material pertinent to NASA's mission.

Specialized services also include organizing and publishing research results, distributing specialized research announcements and feeds, providing information desk and personal search support, and enabling data exchange services.

For more information about the NASA STI program, see the following:

- Access the NASA STI program home page at http://www.sti.nasa.gov

- E-mail your question to help@sti.nasa.gov

- Phone the NASA STI Information Desk at 757-864-9658

- Write to:
  NASA STI Information Desk
  Mail Stop 148
  NASA Langley Research Center
  Hampton, VA 23681-2199

NASA/TM-2020-220434

NASA ETR Quiet Zone Probe Study

Larry A. Ticatch
TEAMS 3, Hampton, Virginia

George N. Szatkowski,
Langley Research Center, Hampton, Virginia

Angelo A. Cavone and Justin K. Strickland
Analytical Mechanics Associates, Hampton, Virginia

January 2020

The use of trademarks or names of manufacturers in this report is for accurate reporting and does not constitute an official endorsement, either expressed or implied, of such products or manufacturers by the National Aeronautics and Space Administration.

Available from:

NASA STI Program / Mail Stop 148
NASA Langley Research Center
Hampton, VA 23681-2199
Fax: 757-864-6500

Abstract

The NASA Langley Research Center's Experimental Test Range is an indoor anechoic compact range far field test facility used to conduct antenna and electromagnetic radiation measurements. The Experimental Test Range was designed to simulate far field illumination in the facility test volume over a broad band of frequencies by collimating the RF energy from the 26 ft by 26 ft parabolic reflector. The quality of the antenna and radiation measurements are dependent on the uniformity of the far field plane wave generated by the compact range reflector. While this facility is going through several upgrades, this report describes an assessment of the far field plane wave conducted after resurfacing the primary reflector to improve performance and extend the range of frequencies for which this facility can operate. This assessment addresses far field uniformity probe data measured in the test volume across the facility operational frequency bands.

Introduction

The NASA Langley Research Center Experimental Test Range (ETR) is an electromagnetic (EM) anechoic research facility that is designed to operate from 300 MHz to 40 GHz to measure antenna and radiation phenomena. The facility is 40 ft wide by 40 ft high by 100 ft long and uses a 26 ft by 26 ft parabolic reflector to collimate the transmit RF signal. The plane wave test volume, or Quiet Zone, is located at the centerline of the chamber just downrange of the offset reflector focal point and antenna feed position. The reflector generates a plane wave to provide far field test conditions. The quality of the plane wave (uniformity in amplitude and phase) is established primarily by the precision of the reflector surface geometry and the alignment and radiation pattern of the transmit antennas. The shape of the center portion of the reflector (nominally 13 ft by 13 ft) is parabolic and gradually changes to an ellipse using a cosine blending function that forms a rolled edge (see Figure 1). The reflector surface tolerance geometry becomes more stringent with increasing signal frequency. As wavelengths become shorter, reflector geometry irregularities and surface roughness can result in ripples (non-uniformity) in the far field Quiet Zone pattern.

The facility is asymmetric with the feed antenna located on the left wall at the reflector parabola's focal point. The reflector is oriented such that the collimated far field plane wave is focused and generally aligned on the centerline of the facility, both left to right and floor to ceiling. The center of the Quiet Zone is approximately in the center of the chamber length. Figure 2 shows this arrangement.

This report presents the Quiet Zone magnitude and phase data recently acquired after the reflector was resurfaced (Reference 1) to remove some imperfections that were affecting the field quality at higher frequencies above 24 GHz. Data is presented from 0.3 to 34 GHz using a variety of transmit and receive antennas, and provides a general sense of the Quiet Zone size and uniformity. It should also be noted that, for this probe study, the backwall chamber doors were open to the model handling area because that wall was not populated with absorber.

Acronyms

dB	Decibels
E Field	Electric Field
EM	Electromagnetic
ETR	Experimental Test Range
H Field	Magnetic Field
H-pol (HH)	Horizontally Polarized
IF	Intermediate Filter
NASA	National Aeronautics and Space Administration
ns	Nanoseconds
RF	Radio Frequency
S1	Source/Receive Port 1
S2	Source/Receive Port 2
S21	Transmit Port 1- Receive Port 2
V-pol (VV)	Vertically Polarized

ETR Facility Arrangement

The ETR facility, as shown in Figure 2, is asymmetric with the feed antenna located on the left wall looking uprange at the reflector from the focal point.

The backwall door, where test articles are inserted into the chamber, is approximately 30 ft high and 15 ft wide. For this probe study, this door was left open to minimize backscatter in the ETR chamber because the door was

not populated with absorber. A picture of the open door is shown in Figure 3.

The feed antenna assembly consists of a feed stand with precision positioning adjustments to vary the pointing direction of the transmit antenna and to enable placing the antenna phase center at the reflector parabola focal point. For most antenna setups, the antenna can be adjusted forward and backwards, left and right, and in azimuth and elevation. Figure 4 shows a picture of a typical feed stand setup.

Reflector

The reflector is a 26 ft by 26 ft parabolic shape in the center and transitions to a rolled edge ellipse using a cosine blending function (see Figure 1). Images of the reflector are presented in Figure 5. The reflector is constructed of many panels that are connected to form a uniform 3-dimensional surface. The reflector surface is finished with conductive silver paint to form a continuous conductive reflecting surface. With the feed antenna radiating at the focal point of the parabolic reflector, the reflected energy is transformed from the near field illumination into a far field plane wave that illuminates the Quiet Zone, as show in Figure 6.

Reflector Resurfacing

An assessment of the ETR Quiet Zone was conducted to determine whether the Quiet Zone field uniformity was adequate to support the testing of 3-meter diameter high gain antennas. The assessment was initiated in response to a new NASA mandate requiring that future deep space satellites utilize Ka band (31-33 GHz) frequencies for data communications to improve data transmission bandwidths. ETR is the only NASA compact range large enough to accommodate antennas of this size.

The results of an RF and geometric study showed that the ETR reflector had some slight (± 0.050 inch) waviness in the parabolic region that reduced the field uniformity at Ka band frequencies. An 18-month activity was subsequently conducted to rework the surface of the reflector and bring the surface to within ±0.010 inch of the reflector's "ideal" geometry. Reference 1 provides a description of the resurfacing activity. The result of the resurfacing has improved the field uniformity at Ka band to within acceptable limits for high gain antenna qualification. Data presented in this report was acquired after completion of the reflector resurfacing with the goal of characterizing the post resurfacing facility Quiet Zone.

Quiet Zone

The Quiet Zone is located generally in the middle of the chamber approximately 38 ft down range from the reflector center and at 20 ft high off the chamber floor. The exact size of the Quiet Zone is a function of the radiation pattern of the transmission antennas and the performance of the reflector. In this report, the Quiet Zone extent limits are defined as the linear cross range dimension at which the amplitude taper of the measurement does not exceed a ± 1 dB threshold and the phase variation is within ± 12 degrees. Based on these definitions, a 2 dB taper in the plane wave will result in the following measurement errors: the peak antenna gain will be reduced by 0.1 dB, the 3 dB beamwidth will be increased by 0.04 deg, and the peak side lobe level will be reduced by 0.1 dB (see Reference 2).

Probe Arm

To conduct the Quiet Zone field probing measurements, a receive antenna was translated linearly along a 14 ft mechanical actuator probe arm that was supported by a circular metal column on a floor rotator. Pictures of the probe arm assembly are shown in Figure 7. The 14 ft long prober arm has a translating antenna mounting plate to attach the receive antenna. The probe arm antenna mount carriage is belt driven by a motor employing a digital encoder capable of step sizes as small as 0.05 inches. During data collection, samples are obtained uniformly across the length of the prober arm. Data presented in this report were collected in increments of 0.2 in to 1.0 inches.

The prober arm is mounted to a gear box rotator to enable rotation of the prober arm in roll from 0 deg to ± 90 deg at a height of 20 ft above the floor. Figure 8 defines the roll angle convention and locations. The entire probe arm assembly is mounted to a floor rotator to provide yaw adjustments when aligning with the transmit field. This floor rotator can provide adjustments to 0.001 deg. and is mounted to a support carriage that travels on linear rails, which enables

movement of the carriage in and out of the chamber (up and down range from transceiver) as needed. The carriage and rails can be seen in Figure 7a. The ETR facility is equipped with other carriages that supports a swept pylon and a precision antenna 3 axis test support rig. A sketch of the rail system components is shown in Figure 9.

The entire probe assembly can be controlled and managed via custom LabVIEW software applications that issue instructions to the motor controllers through an RS232 serial interface. This same software manages the data acquisition hardware and can automate the data collection process.

Probe Measurements

Probe measurements were acquired at frequencies ranging from 0.3 to 34 GHz in both horizontal and vertical polarizations and at prober arm roll orientations from 0 to ± 90 deg every 15 deg in some cases. 0 deg roll is defined as the prober arm horizontal in the chamber and parallel to the floor.

Probe data is acquired identically for each probe arm pass. That is, the probing starts with the receive antenna, which is placed in the "home position," at the right edge of the probe arm, looking uprange toward the reflector. At each scan location, the data acquisition software acquires data, then commands the probe arm receive antenna to move to the next location where a new sample is acquired. When the receive antenna has reached the final sampling location, at the left side of the probe arm, data acquisition is terminated and the data is store and processed resulting in plots for review and analysis. At this point, the receive antenna is returned to the "home position" and the polarization is changed or the probe arm is rolled to the next roll angle to collect the next data set.

Antennas

Proper feed antenna selection is critical to optimizing the size and quality of the Quiet Zone. The radiation illumination pattern from the feed antenna will determine the amplitude taper of the collimated plane wave in the Quiet Zone. If the radiation pattern is too small, the reflector will be under illuminated resulting in a smaller Quiet Zone. If the reflector is substantially over illuminated by the feed antenna, the signal strength of the plane wave will be effectively reduced, thereby resulting in a lower signal to noise measurements.

For each feed antenna used, phase center alignment to the reflector's focal point position was performed.
The feed antenna can be adjusted in translation left, right, up, and down relative to the boresight axis of the feed antenna. It can also be adjusted in azimuth, elevation and forward and aft along the boresight axis. For example, when the phase data has a curved parabolic shape, translating the feed antenna along its boresight axis will correct the alignment and result in a linear phase curve.

The antenna selections for this study was based on radiation patterns, bandwidth, and availability from the existing antenna inventory. Table 1 provides a summary of the feed antennas and corresponding prober arm receive antennas used for each measurement band. Both the transmit and receive antennas were shrouded with RF absorber to minimize scattering from stray signals and room reflections.

Three different feed antennas were used during the field probe data collection. The first feed antenna used in the probe study was ETR's original Ohio State University (OSU) custom built bowtie antenna (Reference 3). The OSU antenna was specifically designed to properly illuminate the ETR compact range reflector across the frequency band from 300 MHz to 18 GHz. The half power beamwidth was designed to be approximately 60 degrees in both the E and H planes. Two different receive horn antennas were needed to cover the entire transmission bandwidth of the bowtie feed antenna, requiring the probe measurements to be conducted in two bands: 0.3 to 6 GHz and 2 to 18 GHz. An AEL H-1734 ridge feed antenna was used as the receive antenna for the 0.3 to 6 GHz band and an AEL H-1498 was used for the 2 to 18 GHz band.

The second feed antenna used to illuminate the compact range reflector was a Seavey OSA-77C. This dual polarized circular antenna has a gain of -12 dB and 3 dB beamwidth of 60 deg. The same AEL H-1498 was used as the prober arm receive antenna for this band. While the antenna performance began to fall off beyond 8.4 GHz, the probe measurements were carried out up to 9 GHz to maintain a 2 GHz operational bandwidth to

provide sufficient range resolution to effectively incorporate software time domain gates.

The third feed antenna used in the probe measurements was the Millitech SFH-28-R31560N A17503 and covered the frequency band from 22 to 34 GHz. This antenna is dual polarized and was selected because of its performance ability to provide a sufficient Quiet Zone size and quality to accommodate measurements of a 3-meter, high gain antennas. The DRG SAS-574 was used as the receive antenna on the prober arm for measurement across the 22 to 34 GHz band.

Measurement Setup

The hardware instrumentation schematic used for the probe measurements is shown in Figure 10. During the data collection, an Agilent Technologies Programmable Network Analyzer (PNA) Model E8364C was operated in the S21 mode using a standard antenna measurement configuration. Some measurements required the use of transmit and/or receive amplification to improve the measurement response. The IF bandwidth was set to 700 Hz and averaging was set to 8 samples to improve the signal to noise ratio for each measurement. Software time domain gating was utilized to improve the measured response by eliminating spurious room reflections. The specific configurations utilized to gather data samples in each of the characterized frequency bands is presented with its corresponding data plots. A summary of the band setups are presented in Table 1.

Data Acquisition Measurements

A custom built Windows LabVIEW application was developed to interface with the RF hardware and prober arm positioning motor to control the data collection and processing. The application provides a Graphical User Interface (GUI) that allows the operator to configure and control the operation of an Agilent PNA and the linear traverse (probe arm). Dialogs within the application allow the various operational parameters to be defined and set for the PNA, probe arm, and data storage management at the start of each run. During the data collection activity, acquisition progress can be monitored on GUI. Additionally within the application, the data collection sequences can be automated; that is, given a sequence of traverse positions, the application positions the receive antenna along the traverse, initiates a data acquisition request, collects the acquired response data, and stores it to the local disk.

The significant PNA control parameters entered by the acquisition software include the following:

- Frequency Band
- Frequency Step Size
- Polarization
- Number of data averages
- Software Gate Locations
- IF Bandwidth
- Probe Arm Scan Step Size

Quiet Zone Probe Data

Probe Band 2 GHz to 18 GHz

For this test setup, Quiet Zone probe data was acquired from 2.0 to 18.0 GHz, using the ETR facility Bowtie antenna to transmit (S1) and an AEL-1498 broadband horn antenna to receive (S2). Images of these antennas and the significant input settings used to collect this data are presented in Figure 11. For this setup, the probe arm step size was set to 1.0 inch. Typical frequency performance data for this setup is presented in Figure 12 for both H-pol and V-pol. The frequency response data shown in Figure 12 is for the probe at the arm center location.

Data for this setup is presented in Magnitude, dB, and Phase, deg, of the received signal at the S2 receive antenna location as a function of probe position for both horizontal and vertical polarized antenna positions, and is shown in Figures 13a to 13p. The probe position is defined in Figure 8, where home position is with the probe located 0 inches from the right side of the prober arm (looking uprange), and probe position 168 inches is on the far left side of the arm. Probe data is presented for probe arm roll angles of 0, 45, -45, and 90 deg. The roll angles are referenced in each figure title.

Generally, the magnitude data shows a flat response across the entire prober length and across the frequency band indicating that the Bowtie Antenna fills the parabolic portion of the reflector effectively. The phase data is also generally flat, indicating that the feed antenna is properly positioned at the reflector focal point. In general, the Quiet Zone size for this setup can

be said to be 14 ft by 14 ft. Table 2 provides a summary of the mean and standard deviation for the H-pol and V- pol data at 0 and 90 deg prober roll angles for 2, 6, 10, 14 and 18 GHz.

Probe Band 0.3 GHz to 6.0 GHz

Quiet Zone probe data was acquired from 0.3 to 6.0 GHz using the ETR facility Bowtie antenna to transmit (S1) and an AEL-1734 broadband horn antenna to receive (S2). Images of these antennas and the significant input setting for these data are presented in Figure 14. For this probe setup, the probe arm step size was set to 1.0 inch. Typical frequency performance data for this setup is presented in Figure 15 for both H-pol and V-pol. The frequency response data shown in Figure 15 is for the probe at the arm center location.

Data for this setup is presented in Magnitude, dB, and Phase, deg, of the received signal at the S2 antenna location as a function of probe position for both horizontal and vertical polarized antenna positions in Figures 16a to 16v. Probe data is presented for probe arm roll angles of 0, 30, 60, 90, -30, and -60 deg. The roll angles are referenced in each figure title.

Generally, the magnitude data shows a good Quiet Zone response across the entire prober length. The phase data shows generally flat measurements across the entire prober length, also indicating good feed alignment and reflector performance. The -30 deg roll data in both polarizations shows a small linear step in both the amplitude and phase curves due to intermittent movement of the receive antenna cable when the prober arm located the antenna near the 30 inch position in V-pol and the 80 inch in H-pol. In general, the Quiet Zone size for this setup is 14 by 14 ft above 1.0 GHz and less than 13 ft by 13 ft below 1.0 GHz. Table 3 provides a summary of the mean and standard deviation for the H-pol and V-pol data at 0 and 90 deg prober roll angles for 0.3, 0.65, 1, 3 and 6 GHz.

Probe Band 7.0 GHz to 9.0 GHz

Quiet Zone probe data was acquired from 7.0 to 9.0 GHz using a circular antenna Seavey OSA-77C to transmit (S1) and an AEL-1734 antenna to receive (S2). Images of these antennas and the significant input setting for these data are presented in Figure 17. Precision probing was conducted for this band and data was acquired at 0.2 inch intervals. An Agilent Amplifier 83071A was connected to increase the transmit power. Typical frequency performance data for this setup is presented in Figure 18 for both H-pol and V-pol. The frequency response data shown in Figure 18 is for the probe at the arm center location.

Data for this setup is presented in Magnitude, dB, and Phase, deg, of the received signal at the S2 antenna location as a function of probe position for both horizontal and vertical polarized antenna positions in Figures 19a to 19bbb. In this band, the probe data was acquired every 15 deg of probe arm roll from ±90 deg. The roll angles are referenced in each figure title.

In general, probe data presented in Figure 19 has more fall off at the probe arm edges compared to the previously presented data. However, in general, the majority of the probe data is within the 2 dB limit across the extent of the probe area. Data approaching 9 GHz in V-pol was an exception to this, with significant fall off. This effect is due to the transmit feed antenna's performance falling off beyond 8.4 GHz, as specified earlier.

The high spatial density of this data collection in this band (data points every 0.2 inch. and probe arm roll angle every 15 deg) allows the magnitude data to be summarized by a representative 2-dimensional plot showing the magnitude value as a shaded color. These plots provide a quick look at the uniformity of the Quiet Zone plane wave. Data was interpolated between the roll angle cuts. Figures 20a to 20j present summary plots for both H-pol and V-pol at frequencies of 7.0, 7.5, 8.0, 8.5, and 9.0 GHz.

Figures 20a to 20j provide several useful details. First, by shifting into standard polar coordinates, the center of the plot is now the zero radial location corresponding to the center of the probe arm. The view of these plots is looking uprange toward the reflector with the probe arm "home position" on the right edge as always. However, that location now has a value of 83.5 inches. The other coordinate change in these plots is the conversion of the ±180 deg roll angle convention into a standard 0 to 360 deg polar angle. 0 deg roll is still on the right looking uprange and +90 deg roll is 90 deg on the plot. But the original -90 deg roll and the corresponding negative roll

angles are now identified as roll 270 deg to 360 deg.

Other useful details in these plots include the peak value of the summarized data, which is marked with an "x." The peak value is shown at the top right corner of the plot. This peak value is used to set the upper scale of the color bar to the nearest ½ dB greater than the maximum value. The color scale is set in ½ dB increments. The color change at 2 dB down from the upper end of the scale (Quiet Zone limit criteria) is set to be distinct, with dark green and bright blue on either side, so that the edge of the Quiet Zone can be easily seen. Additionally, an isoline is drawn at a value that is exactly 2 dB less than the maximum measurement. This provides a more precise depiction of the Quiet Zone edge for instances when the maximum value occurs near the lower boundary of the highest color interval.

As shown in Figures 20a and 20b, virtually the entire probe area is within the Quiet Zone limit criteria of ±1 dB taper and ±12 deg phase, with the exception of the vertical probe cut at 270 deg, where a portion exceeds the amplitude taper metric (see transition from green to blue in figure). By contrast, Figure 20j shows that, where the antenna does not perform well at 9 GHz, a large portion of the Quiet Zone limit criteria is not met.

In general, for this 7 to 9 GHz (S1 antenna is Seavey OSA-77C) setup, the Quiet Zone can be defined as 13 ft by 13 ft with the exception of 9 GHz. At 9 GHz in V-pol the antenna used is not acceptable for standard target testing. Table 4 provides a summary of the mean and standard deviation for the H-pol and V-pol data at 0, 90, and -90 deg prober roll angles for 7, 7.5, 8, 8.5, and 9 GHz.

Probe Band 31.0 GHz to 33.0 GHz

Quiet Zone probe data was acquired from 31.0 to 33.0 GHz using circular antenna Millitech SFH-28-R31560N A17503 to transmit (S1) and a DRG SAS-574 to receive (S2). Images of these antennas and the significant input setting for these data are presented in Figure 21. Precision probing was conducted for this bandwidth at intervals of 0.2 inches. A Lambda RLNA16G32G amplifier was connected upstream of the transmit antenna to boost the signal. Typical frequency performance data for this setup is presented in Figure 22 for both H-pol and V-pol. The frequency response data shown in Figure 22 is for the probe at the arm center location.

Data for this setup is presented in Magnitude, dB, and Phase, deg, for the received signal at the S2 antenna location as a function of probe position for both horizontal and vertical polarized antenna positions in Figures 23a to 23zz. To respond to the customer requested precision, probe data is acquired every 15 deg of probe arm roll from ± 90 deg. The roll angles are referenced in each figure title.

At Ka band with very short wavelengths, any small imperfections in the reflector surface geometry will result in a non-uniform plane wave. The magnitude scale for these data plots have been reduced to a total span of 10 dB, which allows the amplitude irregularities to be more pronounced. Based on probe measurements collected prior to the reflector resurfacing, the plane wave performance has improved. (see Reference 1).

The phase data also demonstrates the performance sensitivity at Ka band. Phase deviation is extremely sensitive to shifts in the location of the receive antenna and reflector surface irregularities. This is seen in the shift in the slope of the phase data at probe arm roll angles that are larger than ± 30 deg. It is believed that the source of the linear phase bias deviation is the result of the rotation plane of the probe arm roll axis being slightly misaligned with the transmit field. Specifically, the linear phase bias indicates the receive antenna is slightly up range or down range from the 0-degree roll angle due to a slight tilt of the prober arm roll axis.

Figures 24a-24j show 2-dimensional summary plots of the Ka band data. In general, these plots indicate that the transmit antenna could have been better aligned, yet the Quiet Zone covers the majority of the probed region. This slight misalignment is also seen in the plots in Figure 23a to 23zz, in the slope of the phase data at some probe arm positions. Near 33 GHz the Quiet Zone is reduced due to the transmit antenna, which is optimized for 31.5 GHz—but not for 33 GHz.

In general, for this 31 to 33 GHz setup, the Quiet Zone can be defined as 11.5 ft by 11.5 ft. At these frequencies, antenna alignment is sensitive and crucial to achieving the largest possible Quiet Zone. Table 5 provides a summary of the mean and standard deviation

for the H-pol and V-pol data at 0, 90, and -90 deg prober roll angles for 31, 31.5, 32, 32.5, and 33 GHz.

Probe Band 22.0 GHz to 34.0 GHz

A relatively coarse Quiet Zone probe was conducted between 22 and 34 GHz to assess this broader higher frequency performance. For this setup, a customer provided circular antenna, Millitech SFH-28-R31560N A17503, was used to transmit (S1) and a DRG SAS-574 antenna was used to receive (S2) along with a Lambda RLNA16G32G amplifier connected on the transmit antenna feed. Images of these antenna and the significant input setting for these data are presented in Figure 25. Typical frequency performance data for this setup is presented in Figure 26 for both H-pol and V-pol. The frequency response data shown in Figure 26 is for the probe at the arm center location.

Data for this setup is presented in Magnitude, dB, and Phase, deg, of the received signal at the S2 antenna location as a function of probe position for both horizontal and vertical polarized antenna positions in Figures 27a to 27l. For this setup, probe data was only acquired at roll angles of 0, 45, 90 deg. The roll angles are referenced in each figure title.

Generally, the probe data shows good Quiet Zone performance across the entire probe region. There is evidence that the transmit horn alignment could be improved. At 0 degree roll in H-pol, the amplitude plot shows slightly higher levels from 80 to 168 inches. The phase plot for this same test shows a significant taper from 0 to 30 inches. This suggests that the feed antenna was not pointed at the exact center of the reflector and was biased slightly toward the right side of the reflector. Better alignment would improve both the amplitude bias and phase taper.

Utilizing the precision probe data in the previously discussed Ka band section (31 to 33 GHz), combined with this broader high frequency scan, the Quiet Zone size for this setup of 22 to 34 GHz is 11.5 ft by 11.5 ft. Table 5 provides a summary of the mean and standard deviation for the H-pol and V-pol data at 0 and 90 deg prober roll angles for 22, 26, 30, and 34 GHz.

Summary

NASA Langley Research Center Experimental Test Range is a compact range, indoor facility designed for broad frequency use in measuring antenna performance and electromagnetic scattering. The accuracy of these measurements is directly dependent on the quality of the illuminating field. Field uniformity probing of the ETR Quiet Zone was conducted across the entire operating frequencies of the facility to establish the performance and resulting Quiet Zone area at various frequencies.

Data is presented from 0.3 to 34 GHz using a variety of transmit and receive antennas. It should also be noted that, for this probe study, the backwall door was kept open because it was not populated with absorber and range filtering was used to suppress returns from outside the test volume.

The Quiet Zone is located roughly in the middle of the 40 ft by 40 ft by 100 ft facility. Generally, the Quiet Zone dimensions for the various transmit and receive setups discussed in this report, are as follows:

0.3 GHz to 1.0 GHz	13 ft by 13 ft
1.0 GHz to 18 GHz	14 ft by 14 ft
22 GHz to 34 GHz	11.5 ft by 11.5 ft.

References

1. Schulze, Ron; Bray, Matthew; Ticatch, Larry A; Szatkowski, George; Cavone, Angelo; Flores, Nate; VanDelinder, Chris; Ayers, Matthew; Draszt, Michael; Boucher, Rick; Rooks, John: *Resurfacing the NASA Langley Experimental Test Range Reflector*. IEEE ISSN**:** 2474-2740, November, 2018

2. Wayne, David; Fordham Jeffery A.; McKenna John: Effects of a Non-Ideal Wave on Compact range Measurements. MI Technologies, AMTA, 2014

3. Lai, Albert K. Y.; Sinopoli, Albert L.; Burnside, Walter D.: A Novel Antenna for Ultra-Wide-Band Applications. IEEE 0018-926X/92, 1992

Table 1. Transmit and receive antenna used at each frequency band.

Probe Frequency Band, GHz	S1 Transmit Antenna	S1 Antenna Main Lobe Angle at Half Power, deg	S2 Receive Antenna
2 to 18	Bowtie	60	AEL H-1498
0.3 to 6	Bowtie	60	AEL H-1498
7 to 9	Seavey OSA-77C	42	AEL H-1498
31 to 33	Milltech SFH-28-R31560N A17503	60	DRG SAS-574
22 to 34	Milltech SFH-28-R31560N A17503	60	DRG SAS-574

Table 2. Mean and Standard Deviation of probe data at frequency = 2.0 GHz to 18.0 GHz using the S1 antenna = Bowtie, S2 Antenna = AEL H1498.

Probe Frequency Band, GHz	S1 Antenna	S2 Antenna
2 to 18	Bowtie	AEL H-1498

Prober Roll Angle 0 deg		Polarization	HH								
Magnitude	2.0 GHz	6.0 GHz	10.0 GHz	14.0 GHz	18.0 GHz	Phase	2.0 GHz	6.0 GHz	10.0 GHz	14.0 GHz	18.0 GHz
Mean, dB	-42.66	-54.05	-64.04	-74.46	-83.02	Mean, dB	-24.52	57.60	-103.46	71.33	-132.87
Standard Deviation, dB	0.20	0.26	0.33	0.36	0.66	Standard Deviation, dB	2.91	2.87	4.77	7.06	9.25
Prober Roll Angle 0 deg		Polarization	VV								
Magnitude	2.0 GHz	6.0 GHz	10.0 GHz	14.0 GHz	18.0 GHz	Phase	2.0 GHz	6.0 GHz	10.0 GHz	14.0 GHz	18.0 GHz
Mean, dB	-40.94	-54.01	-63.61	-74.47	-82.68	Mean, dB	140.44	-123.27	79.02	-105.89	48.55
Standard Deviation, dB	0.71	0.44	0.43	0.23	1.07	Standard Deviation, dB	2.57	4.58	8.84	11.46	10.78

Prober Roll Angle 90 deg		Polarization	HH								
Magnitude	2.0 GHz	6.0 GHz	10.0 GHz	14.0 GHz	18.0 GHz	Phase	2.0 GHz	6.0 GHz	10.0 GHz	14.0 GHz	18.0 GHz
Mean, dB	-41.40	-54.59	-63.93	-74.74	-80.97	Mean, dB	-34.65	56.56	-104.19	66.29	-149.22
Standard Deviation, dB	0.80	0.33	0.20	0.55	0.72	Standard Deviation, dB	1.66	1.68	2.14	2.44	4.55
Prober Roll Angle 90 deg		Polarization	VV								
Magnitude	2.0 GHz	6.0 GHz	10.0 GHz	14.0 GHz	18.0 GHz	Phase	2.0 GHz	6.0 GHz	10.0 GHz	14.0 GHz	18.0 GHz
Mean, dB	-41.67	-53.66	-63.31	-74.45	-80.38	Mean, dB	-36.35	55.28	-105.79	65.29	-151.05
Standard Deviation, dB	0.46	0.45	0.56	0.37	0.52	Standard Deviation, dB	3.24	2.72	5.83	9.25	11.07

Table 3. Mean and Standard Deviation of probe data at frequency = 0.3 GHz to 6.0 GHz using the S1 antenna = Bowtie, S2 Antenna = AEL H1734.

Probe Frequency Band, GHz	S1 Antenna	S2 Antenna
0.3 to 6	Bowtie	AEL H-1734

Prober Roll Angle 0 deg		Polarization	HH								
Magnitude	0.3 GHz	0.65 GHz	1.0 GHz	3.0 GHz	6.0 GHz	Phase	0.3 GHz	0.65 GHz	1.0 GHz	3.0 GHz	6.0 GHz
Mean, dB	-48.06	-52.16	-54.08	-60.65	-68.33	Mean, dB	-6.58	-15.70	-120.31	-73.94	-82.32
Standard Deviation, dB	0.42	0.38	0.34	0.29	0.20	Standard Deviation, dB	2.45	2.22	2.04	2.03	3.52
Prober Roll Angle 0 deg		Polarization	VV								
Magnitude	0.3 GHz	0.65 GHz	1.0 GHz	3.0 GHz	6.0 GHz	Phase	0.3 GHz	0.65 GHz	1.0 GHz	3.0 GHz	6.0 GHz
Mean, dB	-48.07	-51.99	-53.64	-60.70	-68.55	Mean, dB	-4.53	-13.42	-118.31	126.25	-80.11
Standard Deviation, dB	0.56	0.49	0.42	0.26	0.62	Standard Deviation, dB	2.90	2.90	2.79	1.77	2.71

Prober Roll Angle 90 deg		Polarization	HH								
Magnitude	0.3 GHz	0.65 GHz	1.0 GHz	3.0 GHz	6.0 GHz	Phase	0.3 GHz	0.65 GHz	1.0 GHz	3.0 GHz	6.0 GHz
Mean, dB	-48.03	-51.93	-53.60	-60.58	-68.59	Mean, dB	-2.04	-11.10	-116.28	126.70	-87.36
Standard Deviation, dB	0.52	0.44	0.37	0.29	0.54	Standard Deviation, dB	2.87	2.86	2.87	5.04	8.72
Prober Roll Angle 90 deg		Polarization	VV								
Magnitude	0.3 GHz	0.65 GHz	1.0 GHz	3.0 GHz	6.0 GHz	Phase	0.3 GHz	0.65 GHz	1.0 GHz	3.0 GHz	6.0 GHz
Mean, dB	-51.45	-53.03	-55.28	-59.79	-68.57	Mean, dB	-8.78	-114.55	-110.65	-82.50	-81.95
Standard Deviation, dB	0.40	0.36	0.34	0.30	0.71	Standard Deviation, dB	2.47	2.44	3.07	4.75	10.80

Table 4. Mean and Standard Deviation of probe data at frequency = 7.0 GHz to 9.0 GHz using the S1 antenna = Seavey OSA-77C , S2 Antenna = AEL H1498.

Probe Frequency Band, GHz	S1 Antenna	S2 Antenna
7 to 9	Seavey OSA-77C	AEL H-1498

Prober Roll Angle 0 deg		Polarization	HH								
Magnitude	7.0 GHz	7.5 GHz	8.0 GHz	8.5 GHz	9.0 GHz	Phase	7.0 GHz	7.5 GHz	8.0 GHz	8.5 GHz	9.0 GHz
Mean, dB	-33.54	-36.72	-37.35	-36.86	-37.17	Mean, deg	-97.77	-134.55	-140.56	-141.27	-149.51
Standard Deviation, dB	0.42	0.36	0.42	0.49	0.59	Standard Deviation, deg	1.94	1.40	1.73	2.04	2.28
Prober Roll Angle 0 deg		Polarization	VV								
Magnitude	7.0 GHz	7.5 GHz	8.0 GHz	8.5 GHz	9.0 GHz	Phase	7.0 GHz	7.5 GHz	8.0 GHz	8.5 GHz	9.0 GHz
Mean, dB	-34.20	-37.39	-37.83	-37.71	-39.67	Mean, deg	68.60	-134.69	59.53	-96.83	107.36
Standard Deviation, dB	0.38	0.35	0.39	0.46	0.45	Standard Deviation, deg	3.44	3.80	4.22	4.43	4.95

Prober Roll Angle 90 deg		Polarization	HH								
Magnitude	7.0 GHz	7.5 GHz	8.0 GHz	8.5 GHz	9.0 GHz	Phase	7.0 GHz	7.5 GHz	8.0 GHz	8.5 GHz	9.0 GHz
Mean, dB	-33.24	-36.81	-37.34	-36.81	-36.56	Mean, deg	-98.03	-128.89	-133.40	-132.10	-136.19
Standard Deviation, dB	0.46	0.47	0.48	0.52	0.56	Standard Deviation, deg	5.70	6.07	6.68	7.15	7.33
Prober Roll Angle 90 deg		Polarization	VV								
Magnitude	7.0 GHz	7.5 GHz	8.0 GHz	8.5 GHz	9.0 GHz	Phase	7.0 GHz	7.5 GHz	8.0 GHz	8.5 GHz	9.0 GHz
Mean, dB	-33.98	-37.15	-37.71	-37.49	-39.67	Mean, deg	-116.30	39.00	-127.13	75.82	-79.70
Standard Deviation, dB	0.41	0.43	0.44	0.52	1.27	Standard Deviation, deg	6.36	6.88	7.50	8.83	7.56

Prober Roll Angle -90 deg		Polarization	HH								
Magnitude	7.0 GHz	7.5 GHz	8.0 GHz	8.5 GHz	9.0 GHz	Phase	7.0 GHz	7.5 GHz	8.0 GHz	8.5 GHz	9.0 GHz
Mean, dB	-33.29	-36.82	-37.27	-36.79	-36.53	Mean, deg	-97.99	-128.27	-133.03	-131.99	-135.90
Standard Deviation, dB	0.45	0.44	0.46	0.50	0.57	Standard Deviation, deg	11.81	12.44	13.25	13.98	14.74
Prober Roll Angle -90 deg		Polarization	VV								
Magnitude	31.0 GHz	31.5 GHz	32.0 GHz	32.5 GHz	33.0 GHz	Phase	7.0 GHz	7.5 GHz	8.0 GHz	8.5 GHz	9.0 GHz
Mean, dB	-34.22	-37.36	-37.71	-37.60	-39.77	Mean, deg	75.67	-126.91	67.68	-89.24	116.48
Standard Deviation, dB	0.41	0.41	0.41	0.50	1.29	Standard Deviation, deg	10.60	11.52	12.56	12.90	15.85

Table 5. Mean and Standard Deviation of probe data at frequency = 31.0 GHz to 33.0 GHz using the S1 antenna = Milltech SFH-28-R31560N A17503 , S2 Antenna = DRG SAS-574.

Probe Frequency Band, GHz	S1 Antenna	S2 Antenna
31 to 33	Milltech SFH-28-R31560N A17503	DRG SAS-574

Prober Roll Angle 0 deg		Polarization	HH								
Magnitude	31 GHz	31.5 GHz	32.0 GHz	32.5 GHz	33.0 GHz	Phase	31 GHz	31.5 GHz	32.0 GHz	32.5 GHz	33.0 GHz
Mean, dB	-75.79	-77.74	-78.60	-79.14	-78.91	Mean, deg	57.75	158.08	-81.78	26.99	142.15
Standard Deviation, dB	0.46	0.48	0.48	0.47	0.47	Standard Deviation, deg	6.54	41.33	6.87	7.03	7.11
Prober Roll Angle 0 deg		Polarization	VV								
Magnitude	31 GHz	31.5 GHz	32.0 GHz	32.5 GHz	33.0 GHz	Phase	31 GHz	31.5 GHz	32.0 GHz	32.5 GHz	33.0 GHz
Mean, dB	-75.61	-77.57	-78.33	-78.71	-78.32	Mean, deg	-52.13	45.92	160.01	-86.57	25.32
Standard Deviation, dB	0.42	0.41	0.40	0.40	0.40	Standard Deviation, deg	9.03	8.68	8.62	9.16	9.29

Prober Roll Angle 90 deg		Polarization	HH								
Magnitude	31.0 GHz	31.5 GHz	32.0 GHz	32.5 GHz	33.0 GHz	Phase	31.0 GHz	31.5 GHz	32.0 GHz	32.5 GHz	33.0 GHz
Mean, dB	-75.83	-77.79	-78.66	-79.14	-78.76	Mean, deg	40.75	145.69	-99.57	9.09	123.80
Standard Deviation, dB	0.53	0.52	0.52	0.52	0.51	Standard Deviation, deg	22.73	23.10	23.41	23.71	24.10
Prober Roll Angle 90 deg		Polarization	VV								
Magnitude	31.0 GHz	31.5 GHz	32.0 GHz	32.5 GHz	33.0 GHz	Phase	31.0 GHz	31.5 GHz	32.0 GHz	32.5 GHz	33.0 GHz
Mean, dB	-76.00	-77.95	-78.69	-79.04	-78.56	Mean, deg	-62.98	41.35	144.38	-96.52	18.08
Standard Deviation, dB	0.61	0.60	0.60	0.59	0.59	Standard Deviation, deg	21.23	21.65	61.89	22.27	22.62

Prober Roll Angle -90 deg		Polarization	HH								
Magnitude	31.0 GHz	31.5 GHz	32.0 GHz	32.5 GHz	33.0 GHz	Phase	31.0 GHz	31.5 GHz	32.0 GHz	32.5 GHz	33.0 GHz
Mean, dB	-75.92	-77.86	-78.69	-79.15	-78.79	Mean, deg	101.71	-62.00	-28.12	89.65	-42.10
Standard Deviation, dB	0.52	0.52	0.52	0.51	0.49	Standard Deviation, deg	79.89	114.47	50.92	51.38	125.69
Prober Roll Angle -90 deg		Polarization	VV								
Magnitude	31.0 GHz	31.5 GHz	32.0 GHz	32.5 GHz	33.0 GHz	Phase	31.0 GHz	31.5 GHz	32.0 GHz	32.5 GHz	33.0 GHz
Mean, dB	-76.04	-77.97	-78.70	-79.05	-78.63	Mean, deg	84.40	-51.75	47.15	5.71	-60.09
Standard Deviation, dB	0.59	0.59	0.58	0.57	0.57	Standard Deviation, deg	47.95	47.49	47.83	144.69	73.85

Table 6. Mean and Standard Deviation of probe data at frequency = 22.0 GHz to 34.0 GHz using the S1 antenna = Milltech SFH-28-R31560N A17503 , S2 Antenna = DRG SAS-574.

Probe Band, GHz	S1 Antenna	S2 Antenna
22 to 34	Milltech SFH-28-R31560N A17503	DRG SAS-574

Prober Roll Angle 0 deg		Polarization	HH	
Magnitude	22.0 GHz	26.0 GHz	30.0 GHz	34.0 GHz
Mean, dB	-49.85	-50.48	-54.85	-62.87
Standard Deviation, dB	0.41	0.42	0.47	0.45

Phase	22.0 GHz	26.0 GHz	30.0 GHz	34.0 GHz
Mean, dB	31.33	104.09	107.86	-88.54
Standard Deviation, dB	13.94	14.87	16.84	18.59

Prober Roll Angle 0 deg		Polarization	VV	
Magnitude	22.0 GHz	26.0 GHz	30.0 GHz	34.0 GHz
Mean, dB	-50.61	-50.39	-54.61	-62.12
Standard Deviation, dB	0.51	0.49	0.44	0.45

Phase	22.0 GHz	26.0 GHz	30.0 GHz	34.0 GHz
Mean, dB	-22.34	20.13	-18.35	137.92
Standard Deviation, dB	9.74	10.66	12.68	14.38

Prober Roll Angle 90 deg		Polarization	HH	
Magnitude	22.0 GHz	26.0 GHz	30.0 GHz	34.0 GHz
Mean, dB	-49.99	-50.61	-55.06	-62.97
Standard Deviation, dB	0.41	0.46	0.54	0.51

Phase	22.0 GHz	26.0 GHz	30.0 GHz	34.0 GHz
Mean, dB	20.57	92.57	95.68	-102.00
Standard Deviation, dB	13.87	14.96	17.01	19.25

Prober Roll Angle 90 deg		Polarization	VV	
Magnitude	22.0 GHz	26.0 GHz	30.0 GHz	34.0 GHz
Mean, dB	-50.80	-50.64	-55.08	-62.50
Standard Deviation, dB	0.41	0.45	0.61	0.59

Phase	22.0 GHz	26.0 GHz	30.0 GHz	34.0 GHz
Mean, dB	12.14	56.63	24.70	-93.73
Standard Deviation, dB	11.14	12.34	14.49	135.50

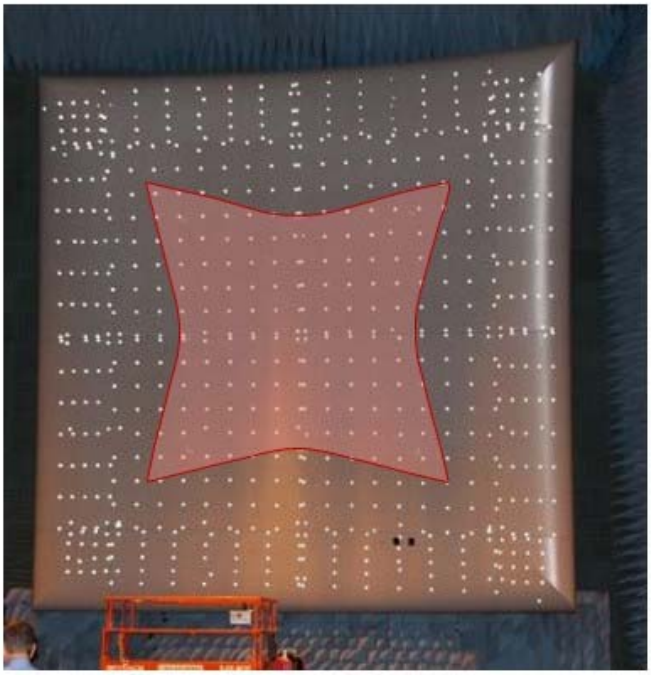

(a) View of reflector with parabolic area shaded.
Figure 1. Reflector description.

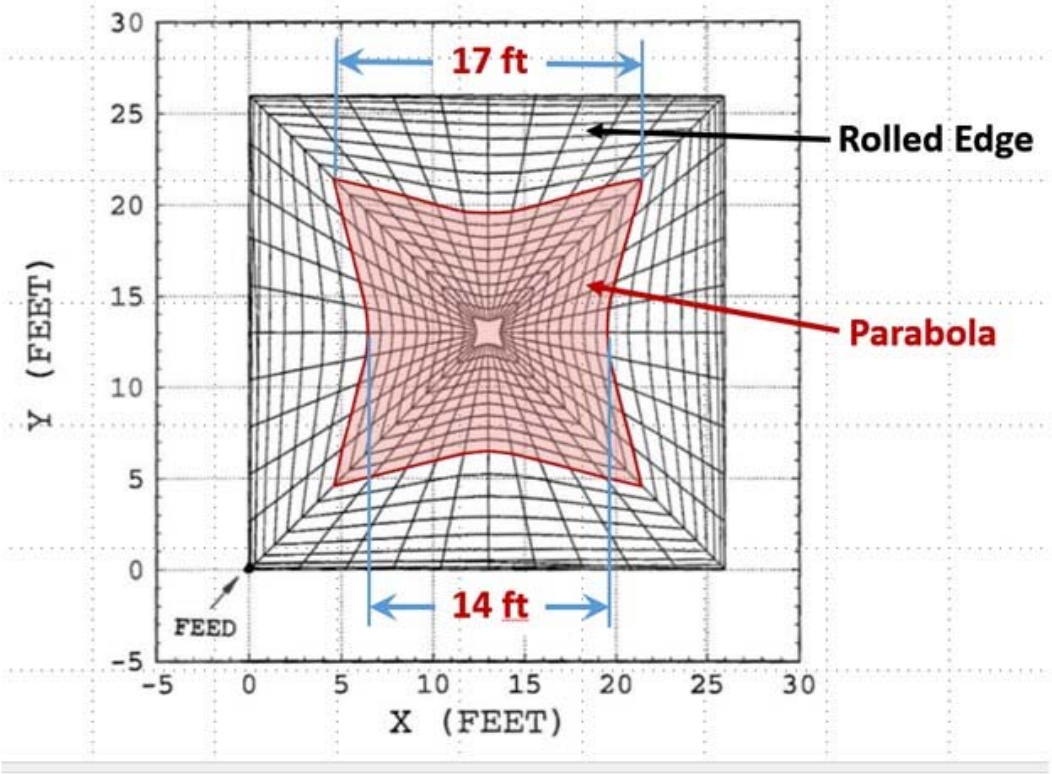

(b) Sketch of reflector with locations of parabolic region and rolled edges.
Figure 1. Concluded

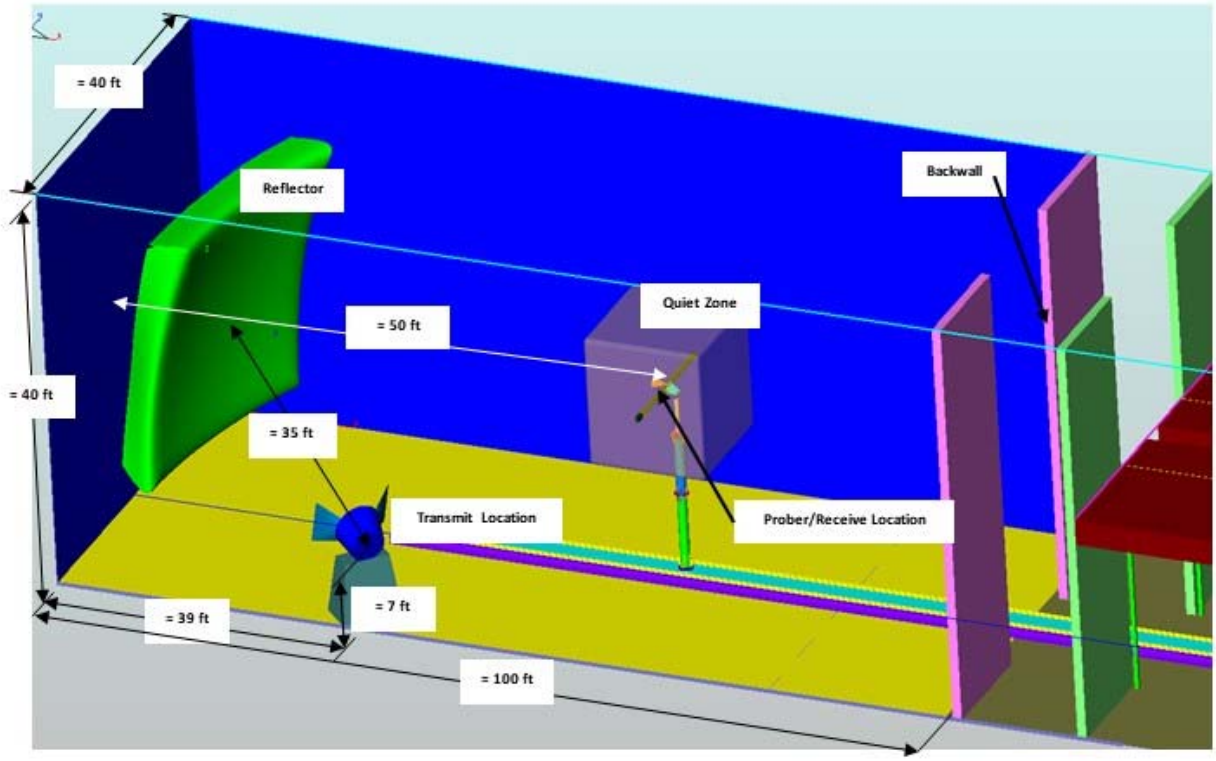

Figure 2. ETR arrangement description.

Figure 3. View of ETR backwall with backdoor open.

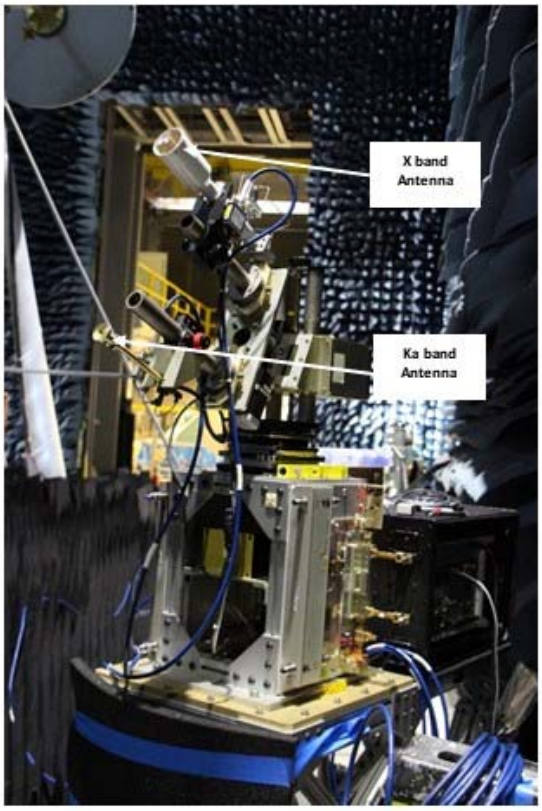

Figure 4. View of ETR typical transmit antenna feed setup.

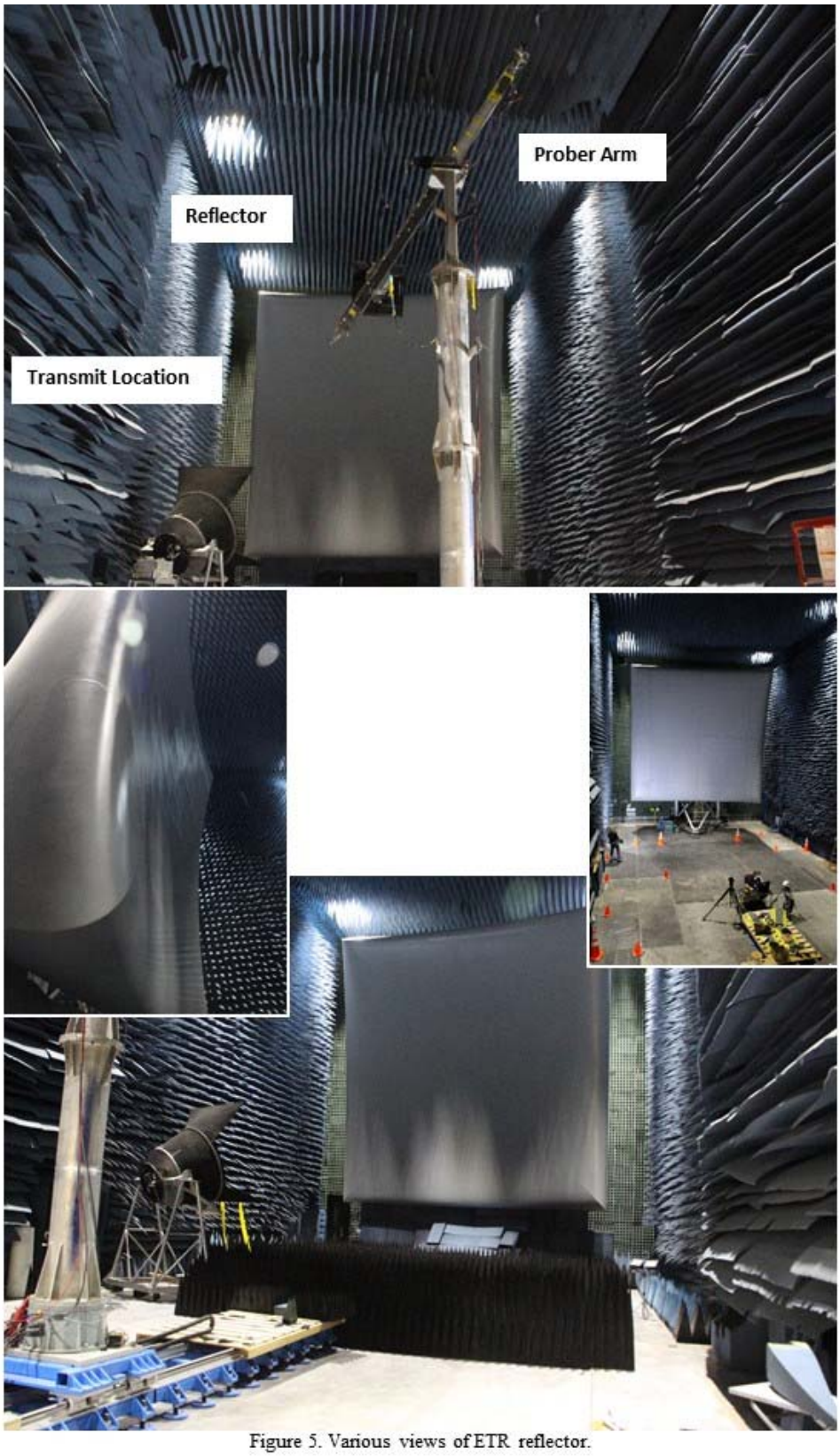

Figure 5. Various views of ETR reflector.

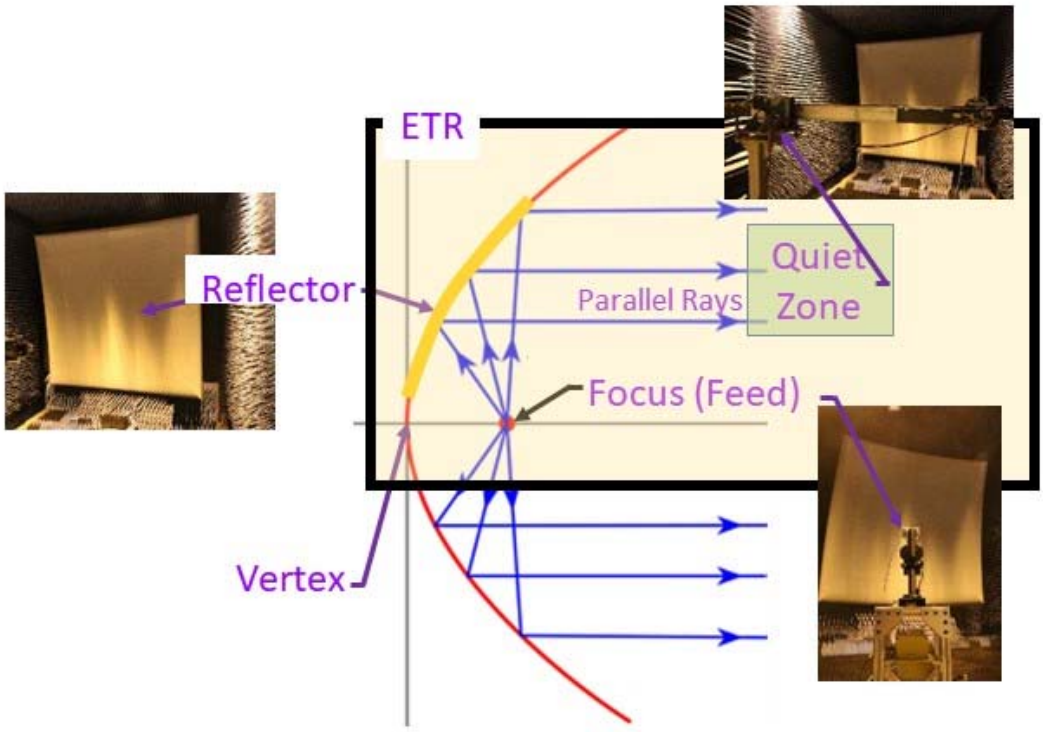

(a) Arrangement of transmit focal point, reflector, quiet zone and ray trace of wave pattern.

Figure 6. ETR transmit wave front characteristics before and after reflector bounce.

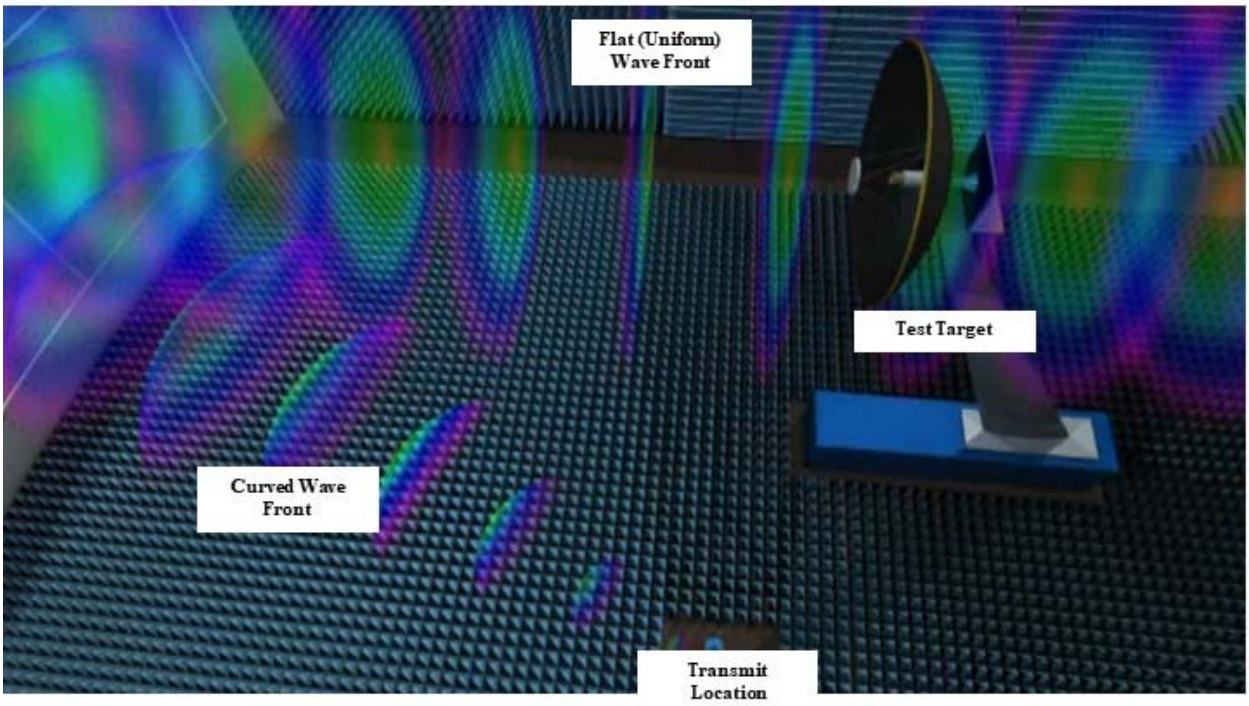

(b) Illustration of wave front characteristics before and after reflector bounce.

Figure 6. Concluded

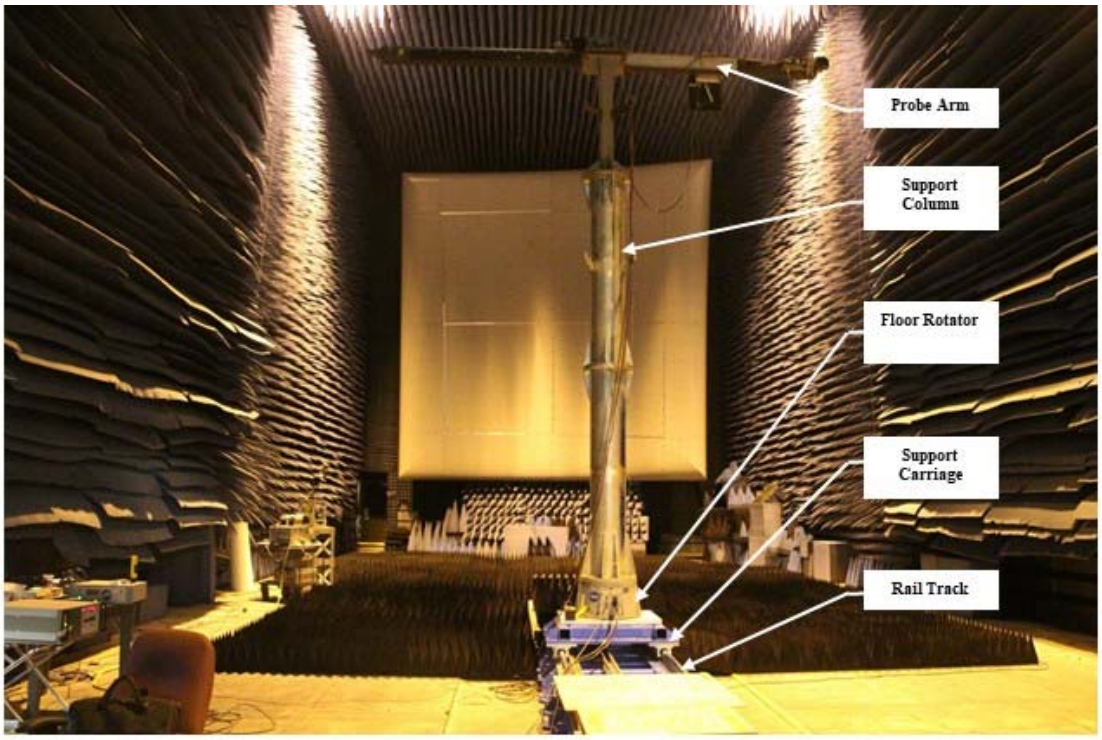

(a) Probe arm assembly components.
Figure 7. Pictures of probe arm assembly.

(b) Probe arm assembly components view looking downrange.
Figure 7. Continued.

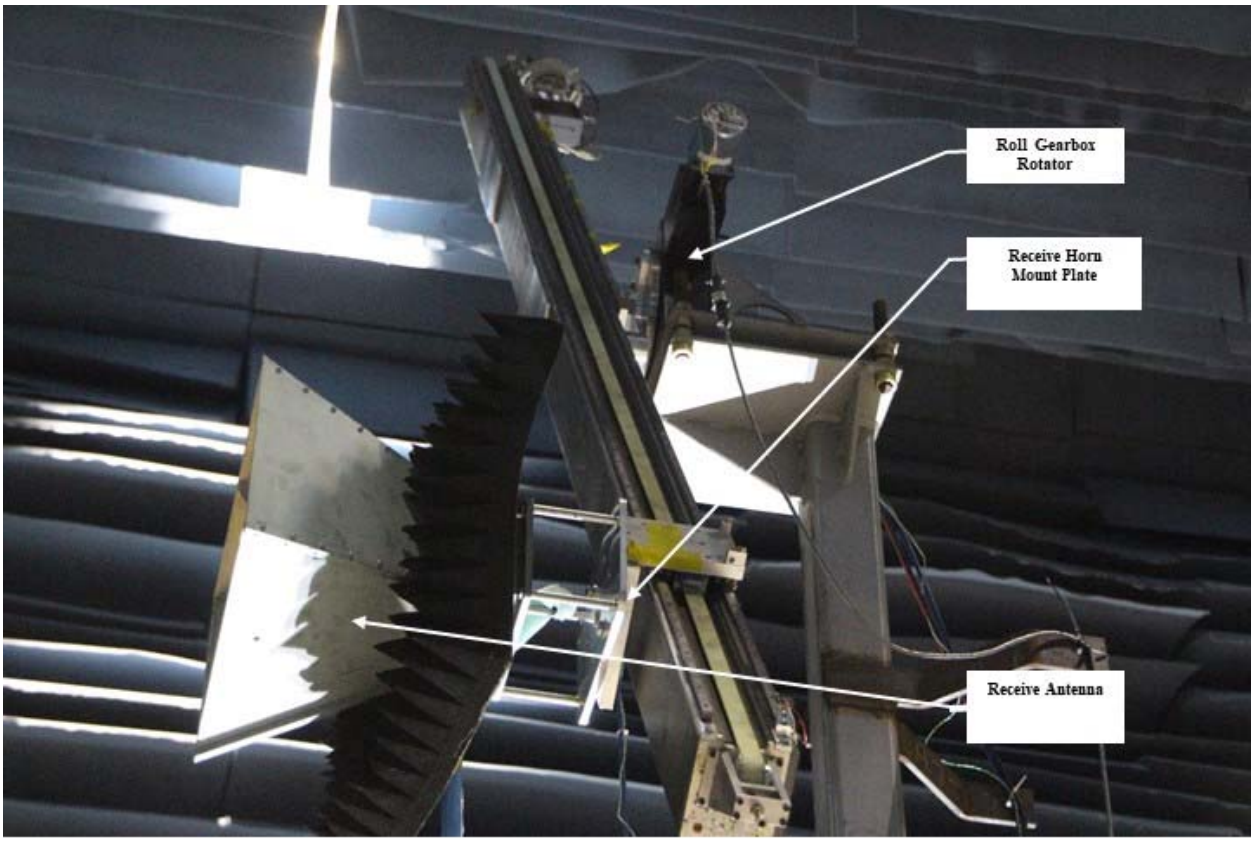

(c) Probe arm details.
Figure 7. Concluded.

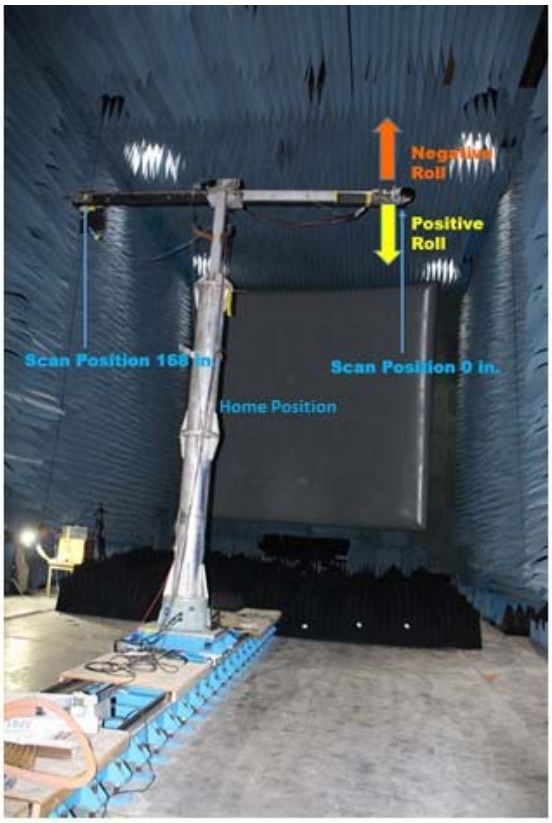

(a) Definition of probe position and positive and negative roll angle.
Figure 8. Probe arm roll angle definition.

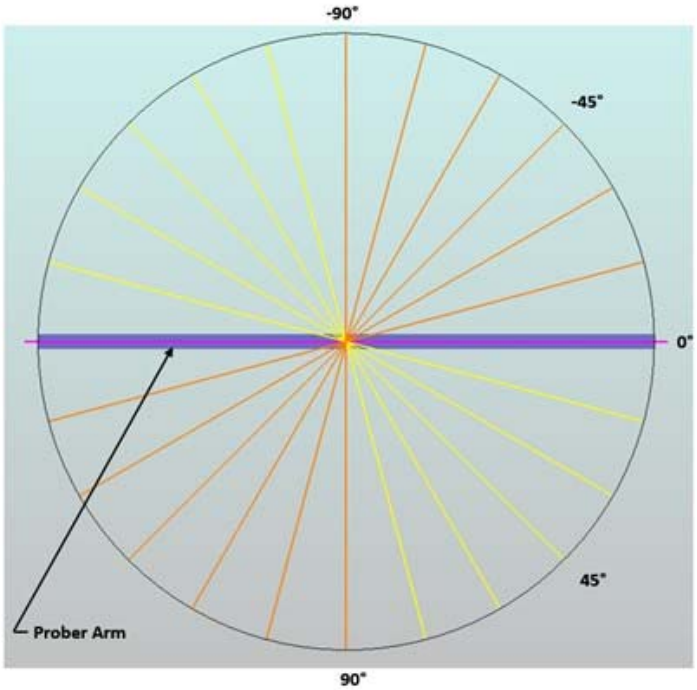

(b) Probe roll positions definition. View looking uprange. Data acquired every 15 deg from +/- 90 deg in some cases.
Figure 8. Concluded

(a) Uprange view of rail system.
Figure 9. ETR target support rail system.

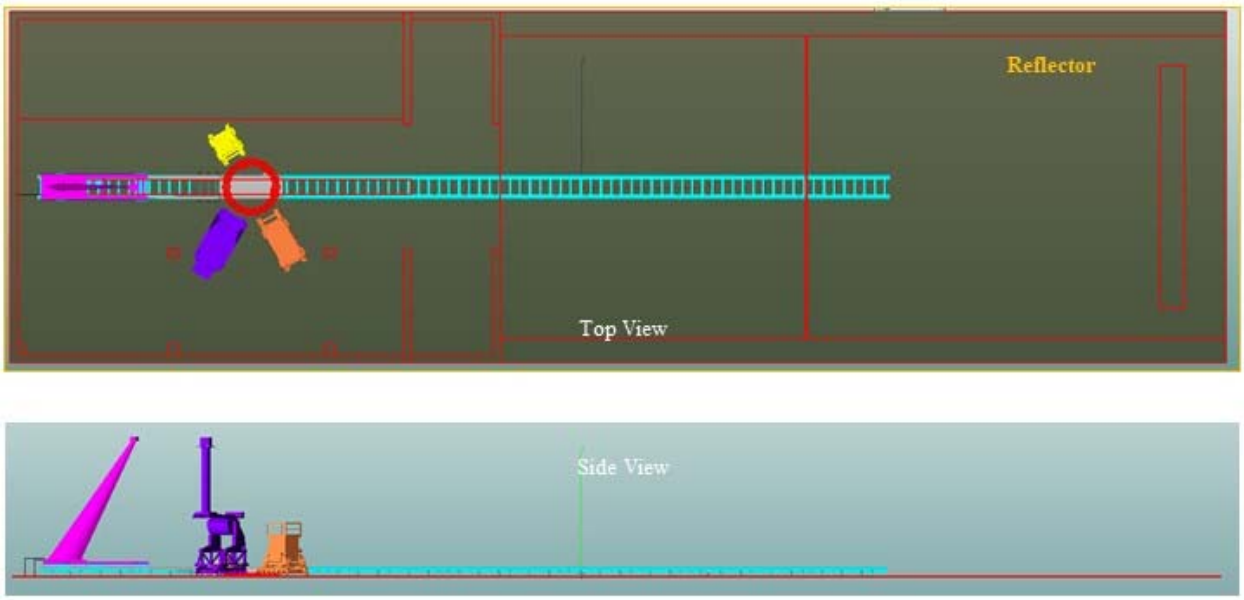

(b) Sketch of rail system components.
Figure 9. Concluded.

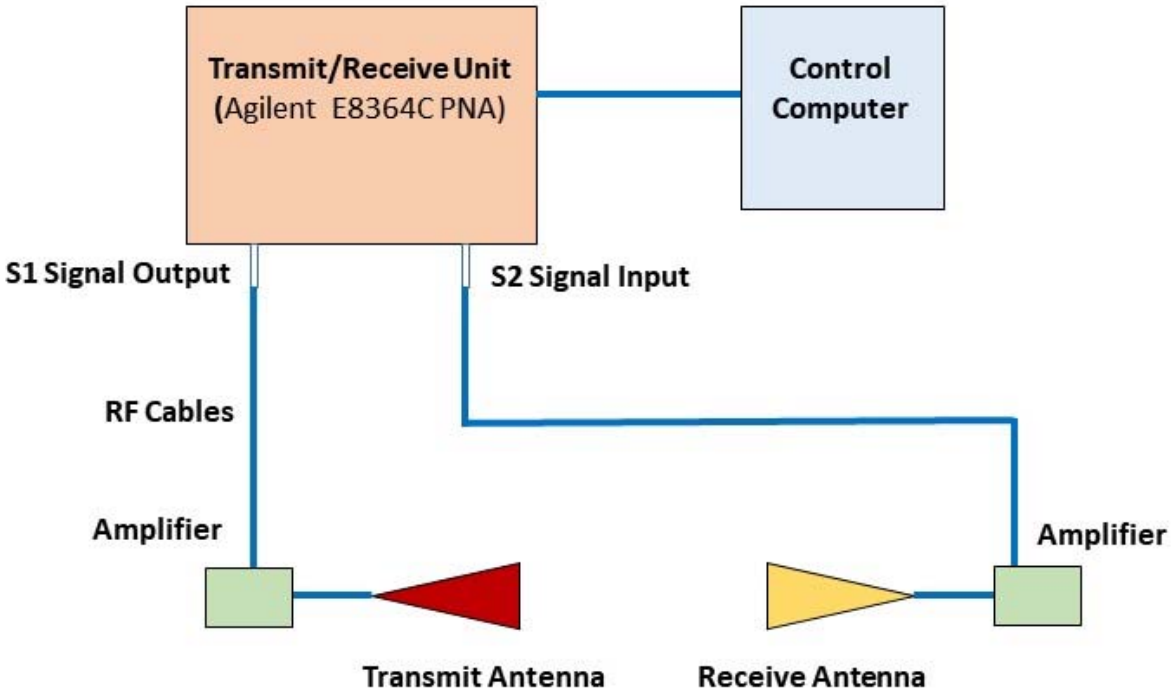

Figure 10. ETR probe RF bistatic configuration.

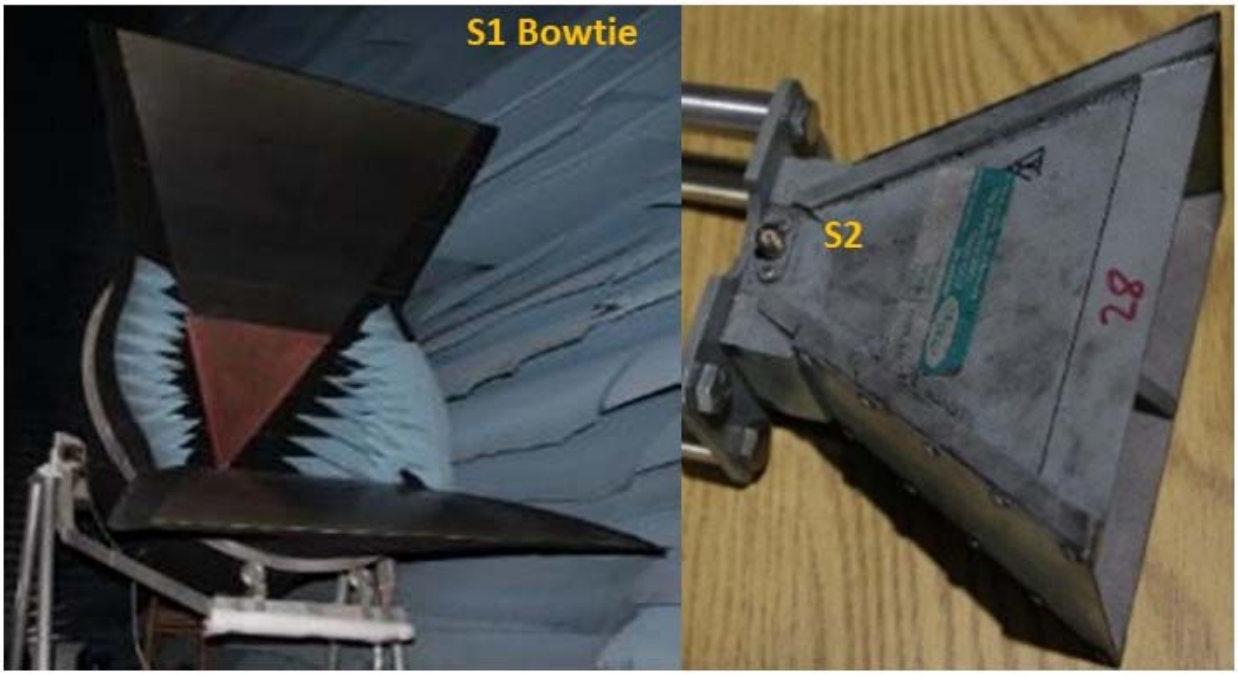

PNA	Frequency Band, GHz	2.0 to 18.0
	Number of data points inband	801
	IF Bandwidth, Hz	700
	Average number of points	8
	Gate Center, ns	-11.86
	Gate Span, ns	1.5
S1	Bowtie Antenna	
S2	AEL H-1498	
	Amplifier	None
Prober	Step size, in.	1.0

Figure 11. Setup for the 2 to 18 GHz probe data..

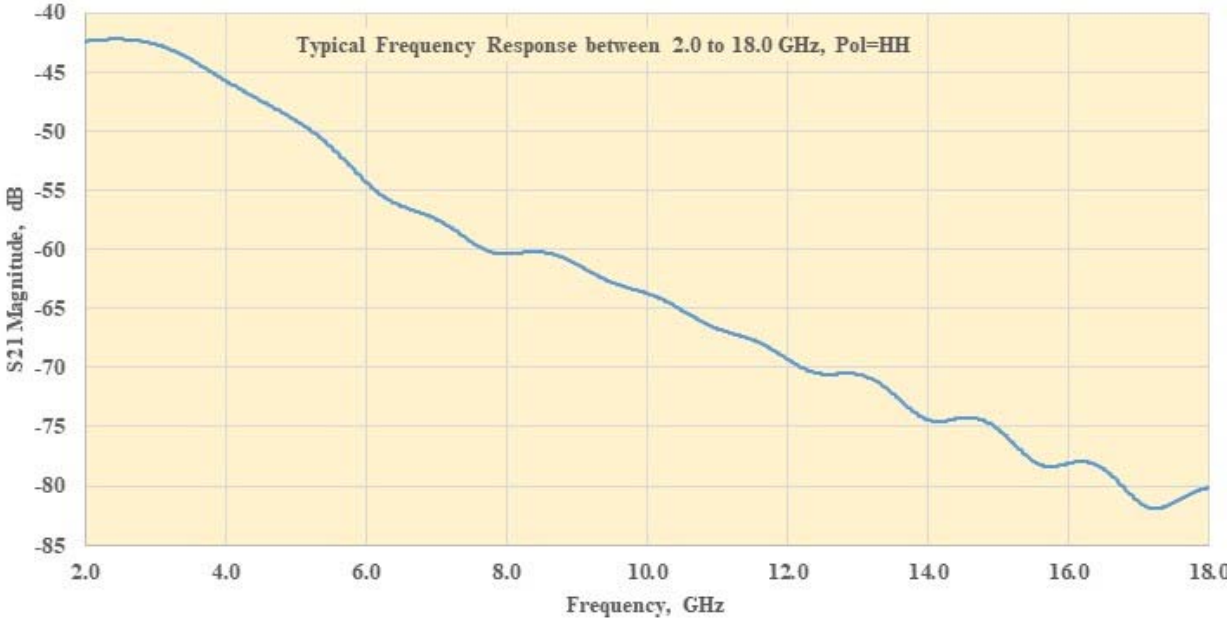

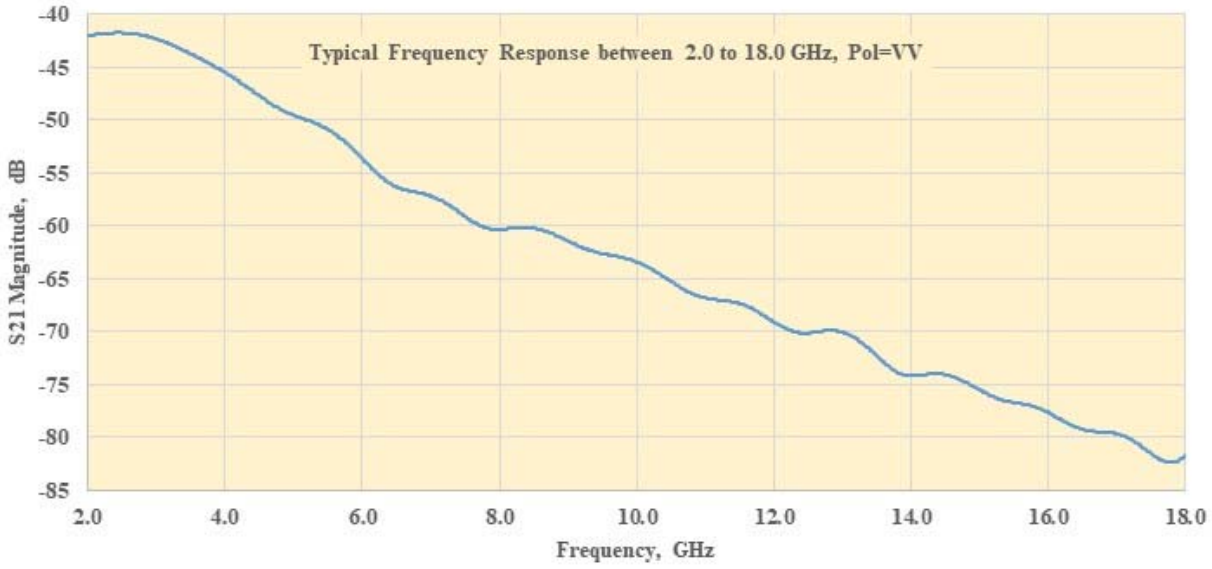

Figure 12. Typical frequency response data for HH and VV for 2- 18 GHz probe data.
Data acquired at probe arm center.

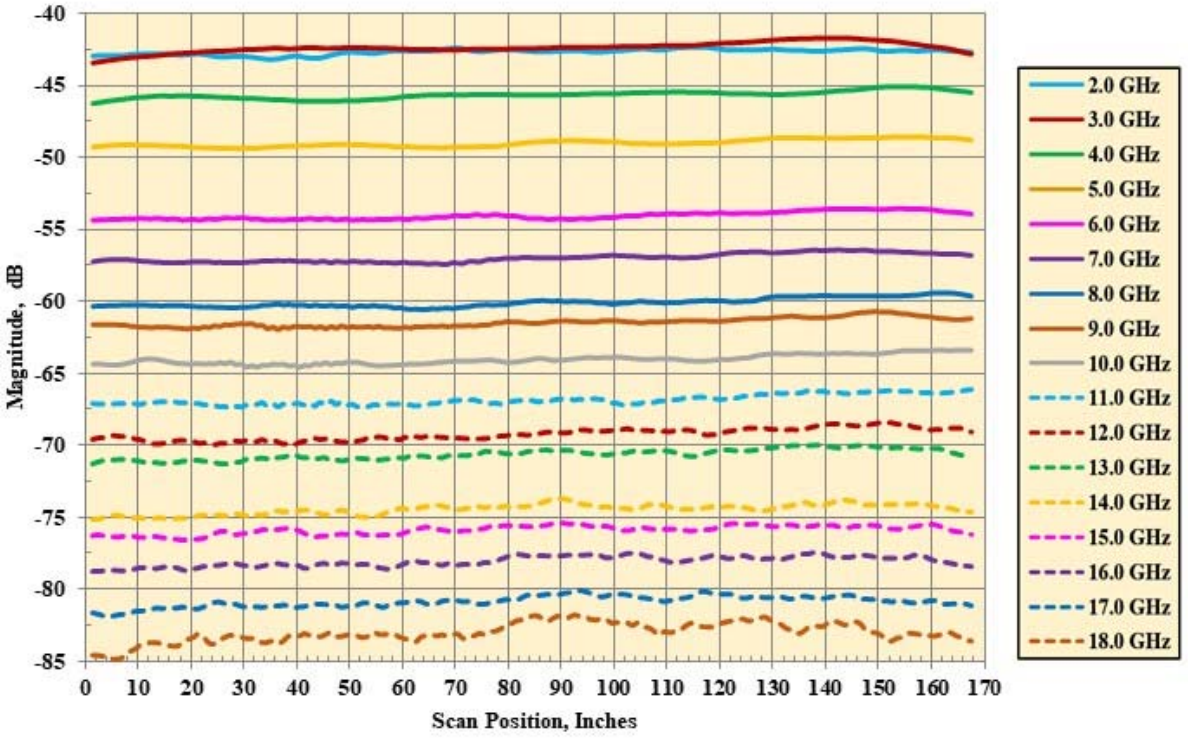

(a) Magnitude probe data, Probe Angle = 0°, Pol HH.

Figure 13. Probe Data at Frequency = 2.0 to 18.0 GHz using the S1 antenna = Bowtie, S2 Antenna = AEL H1734.

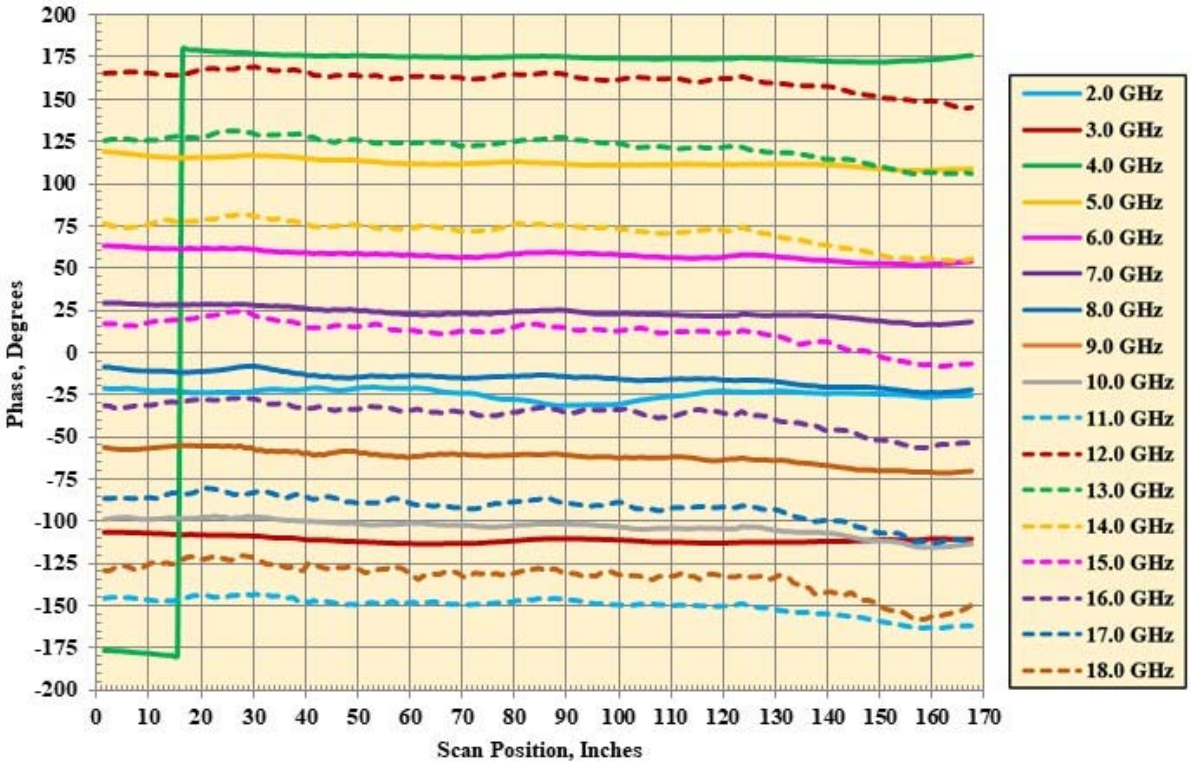

(b) Phase probe data, Probe Angle = 0°, Pol = HH.

Figure 13. Continued.

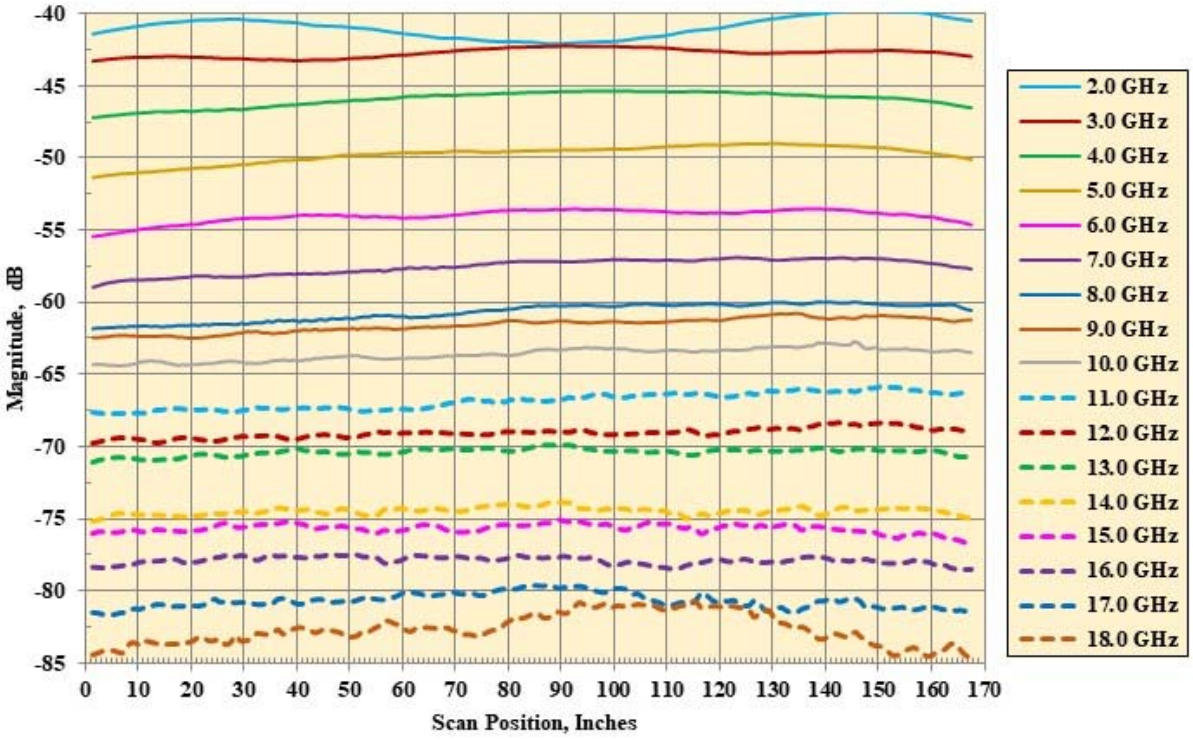

(c) Magnitude probe data, Probe Angle = 0°, Pol VV.
Figure 13. Continued.

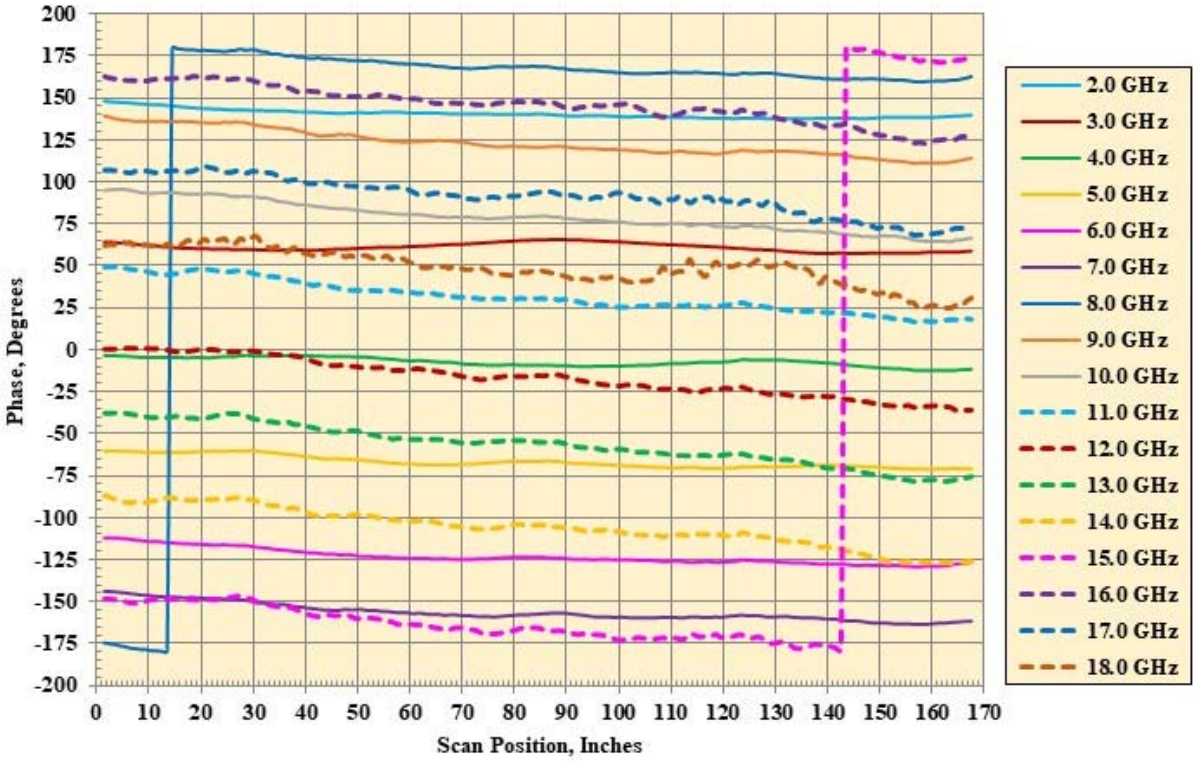

(d) Phase probe data, Probe Angle = 0°, Pol = VV.
Figure 13. Continued.

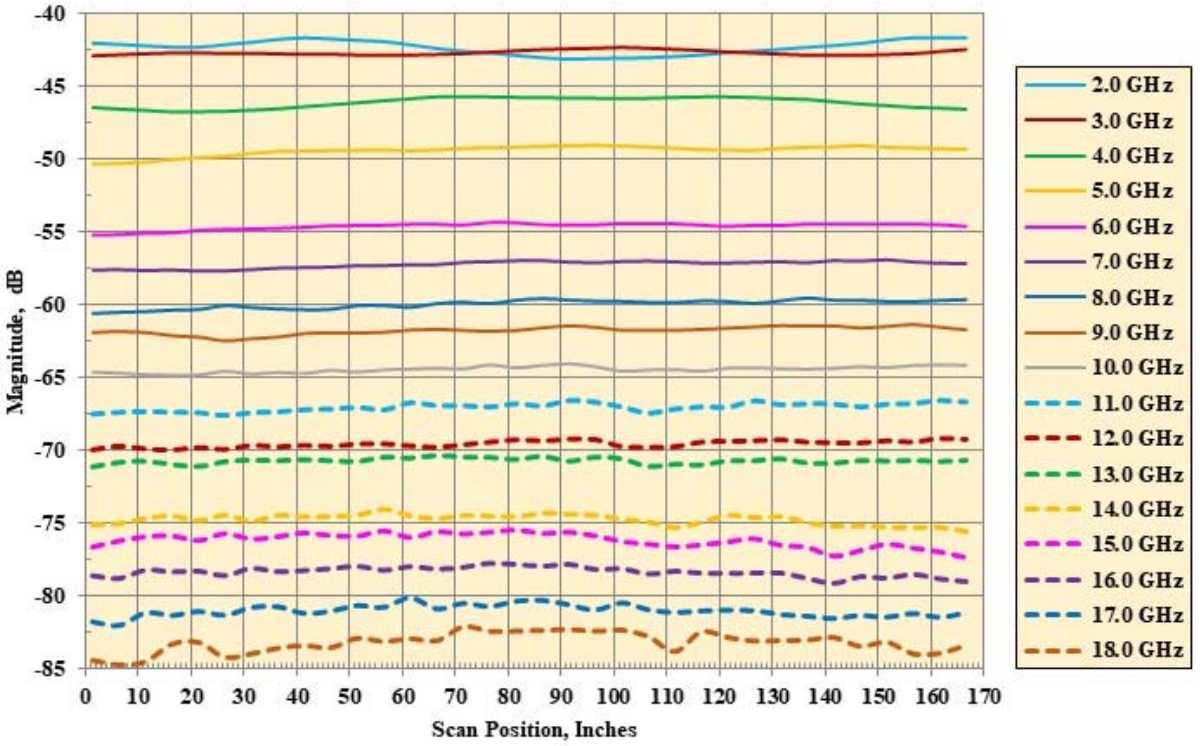

(e) Magnitude probe data, Probe Angle = 45°, Pol HH.
Figure 13. Continued.

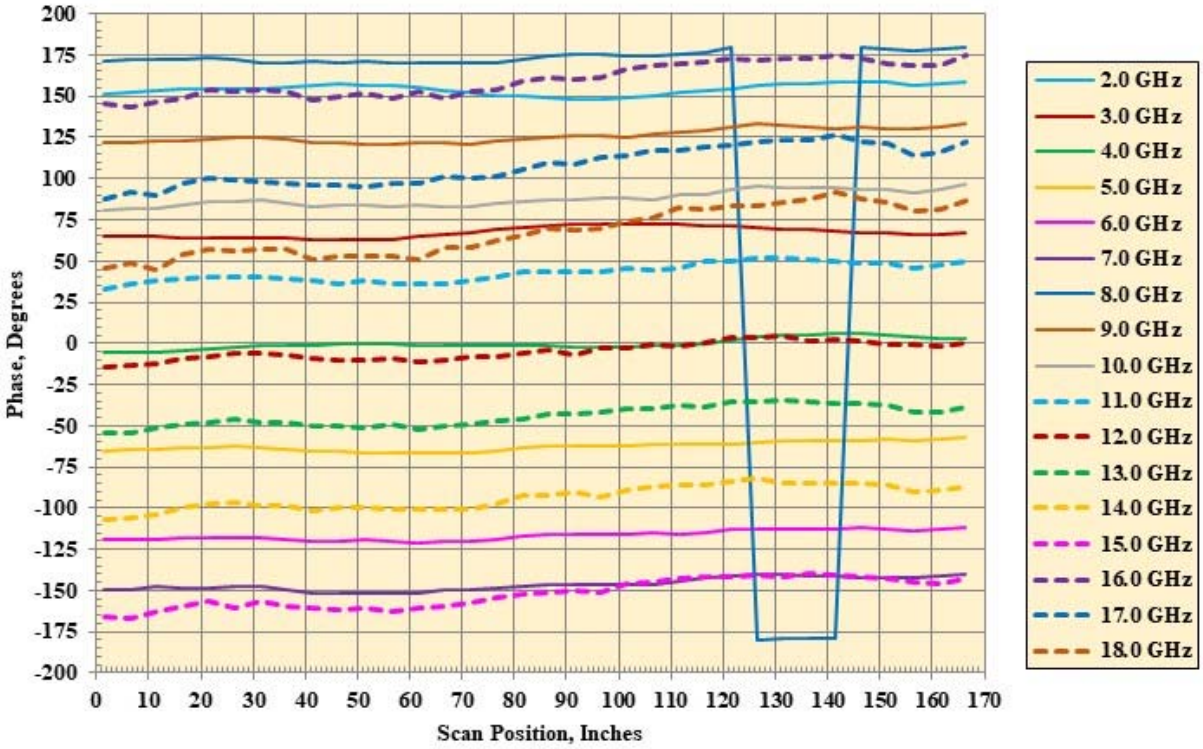

(f) Phase probe data, Probe Angle = 45°, Pol = HH.
Figure 13. Continued.

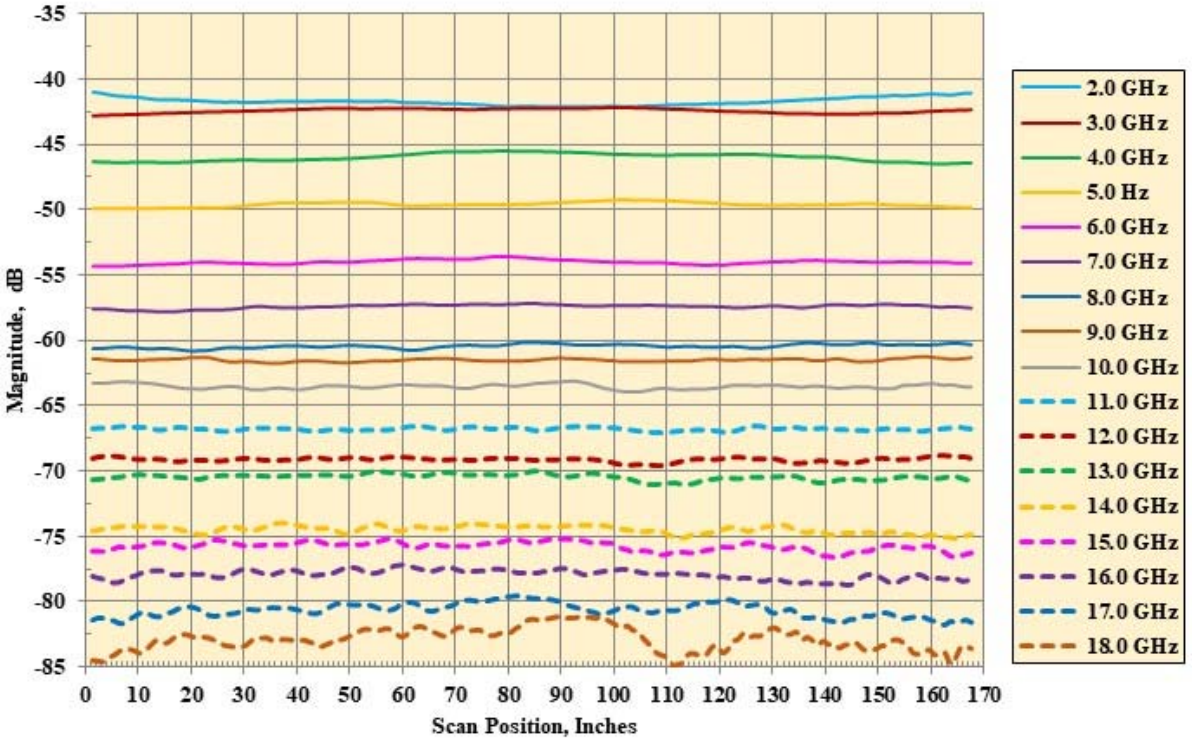

(g) Magnitude probe data, Probe Angle = 45°, Pol VV.
Figure 13. Continued.

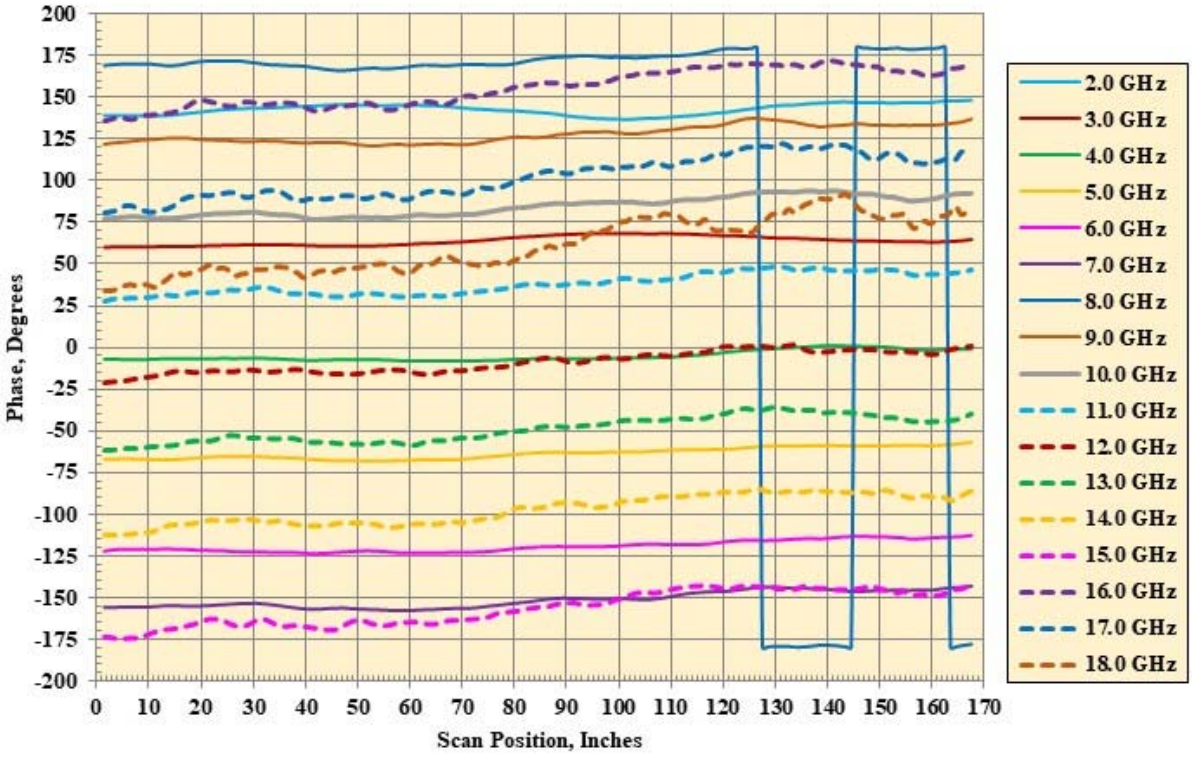

(h) Phase probe data, Probe Angle = 45°, Pol = VV.
Figure 13. Continued.

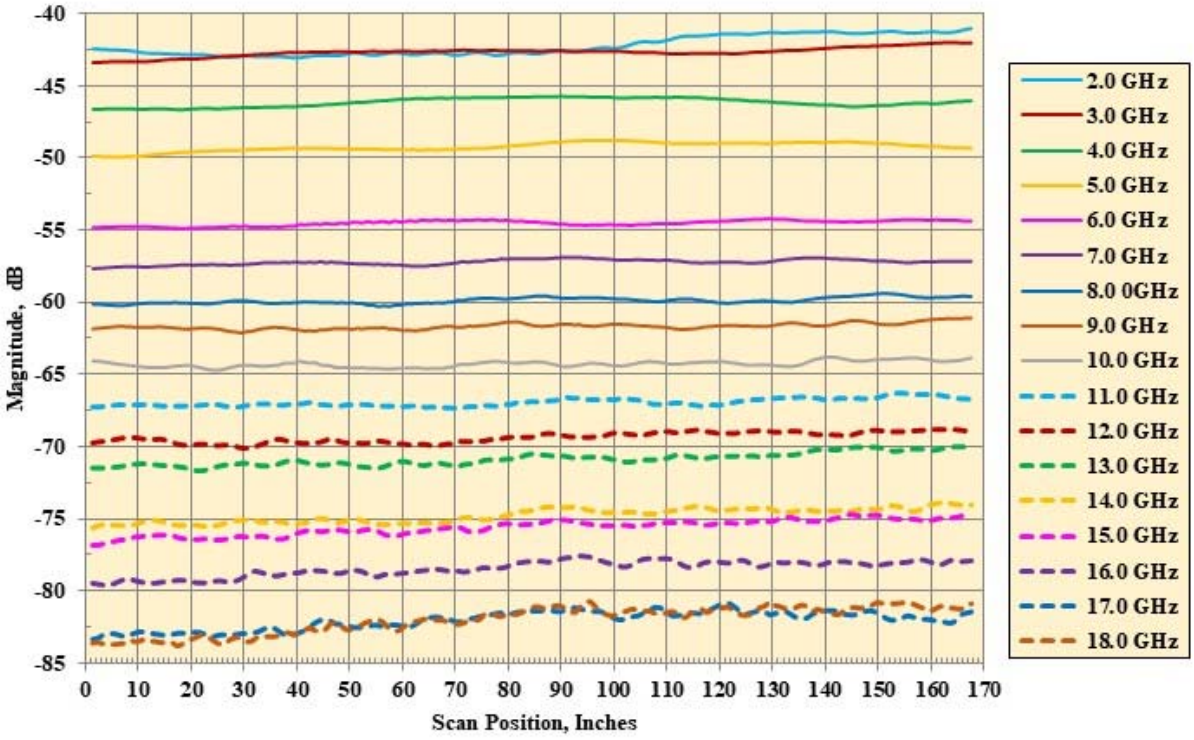

(i) Magnitude probe data, Probe Angle = -45°, Pol HH.
Figure 13. Continued.

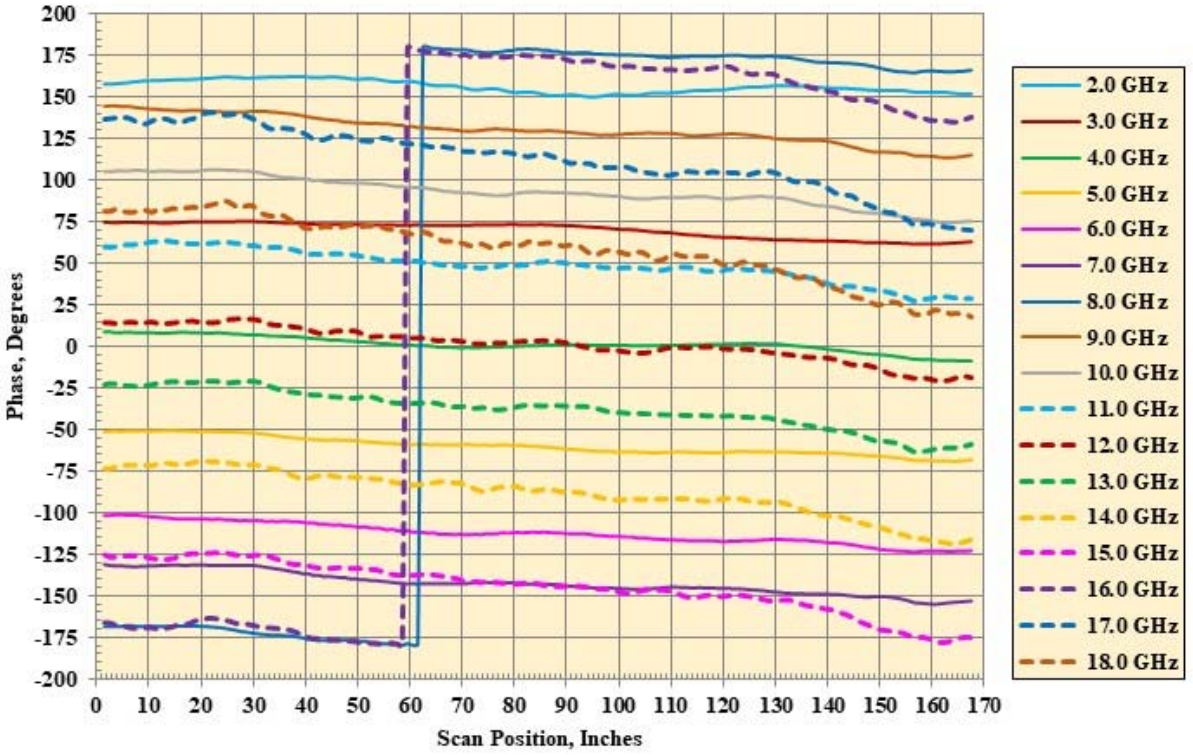

(j) Phase probe data, Probe Angle = -45°, Pol = HH.
Figure 13. Continued.

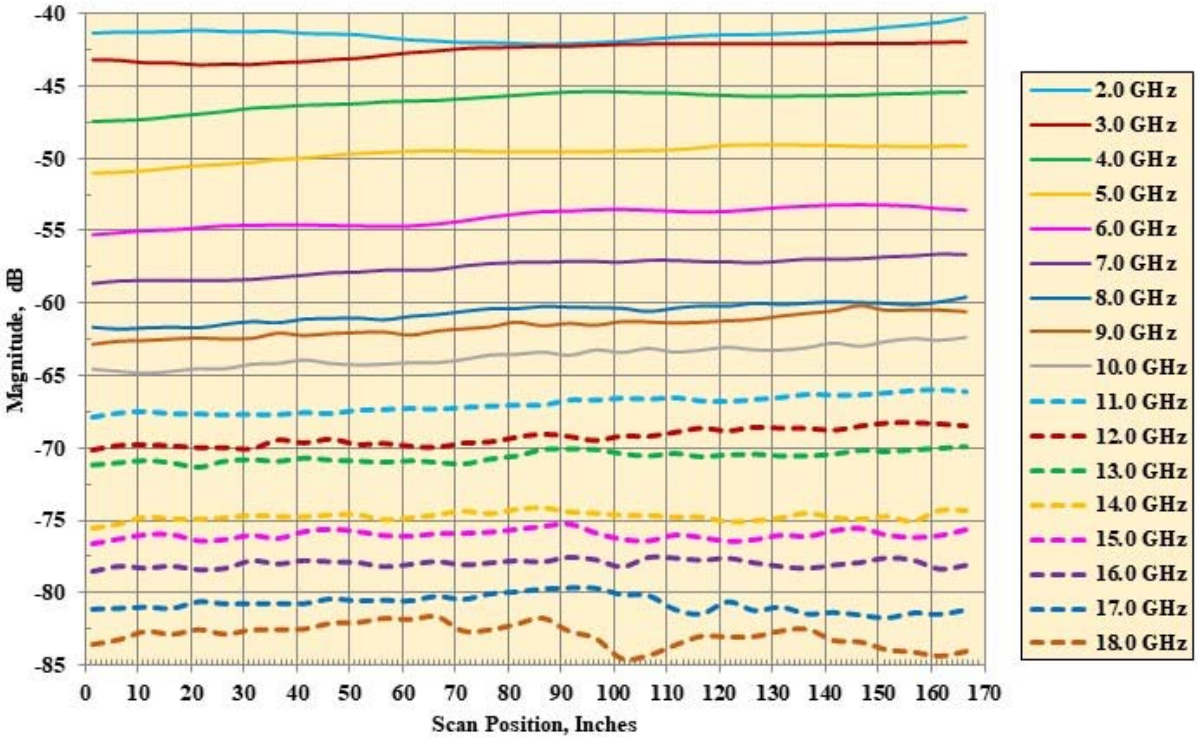

(k) Magnitude probe data, Probe Angle = -45°, Pol VV.
Figure 13. Continued.

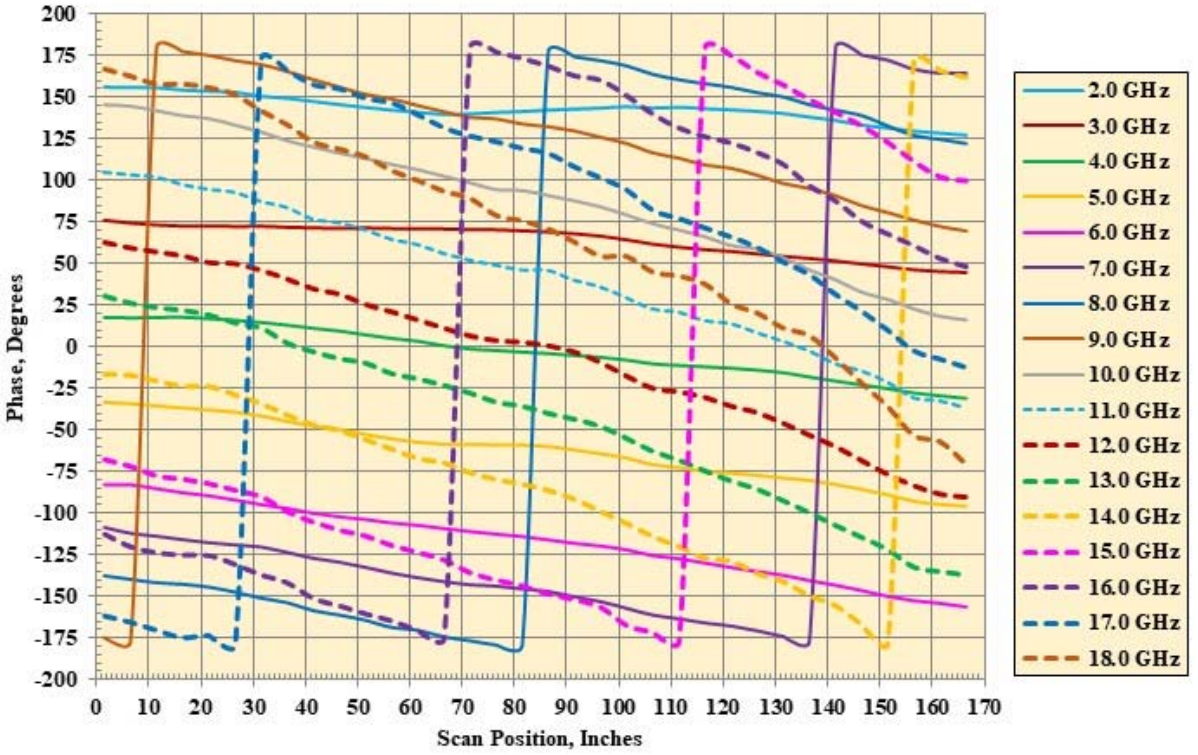

(l) Phase probe data, Probe Angle = -45°, Pol = VV.
Figure 13. Continued.

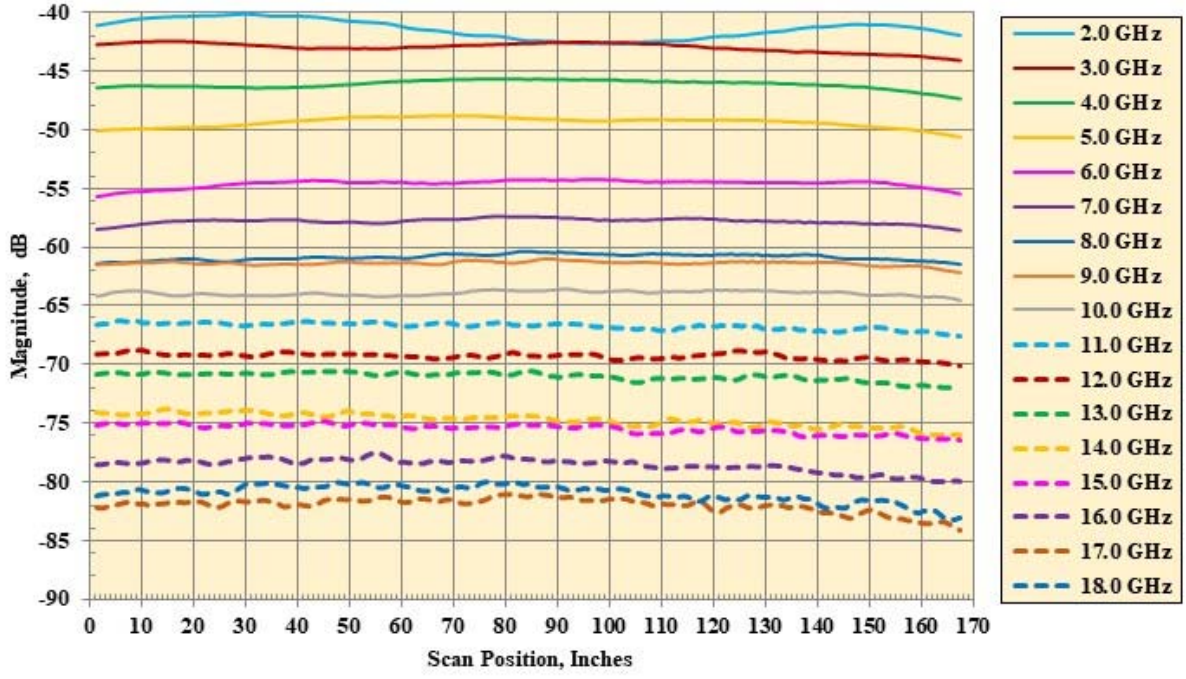

(m) Magnitude probe data, Probe Angle = 90°, Pol HH.
Figure 13. Continued.

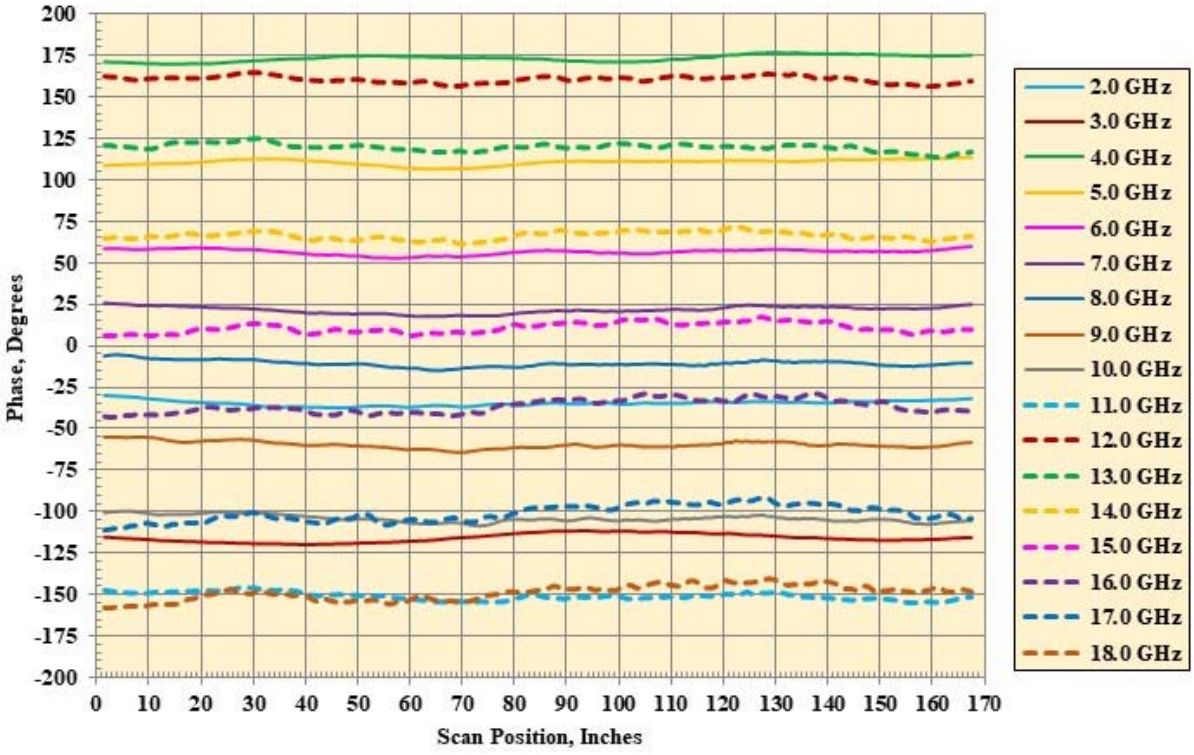

(n) Phase probe data, Probe Angle = 90°, Pol = HH.
Figure 13. Continued.

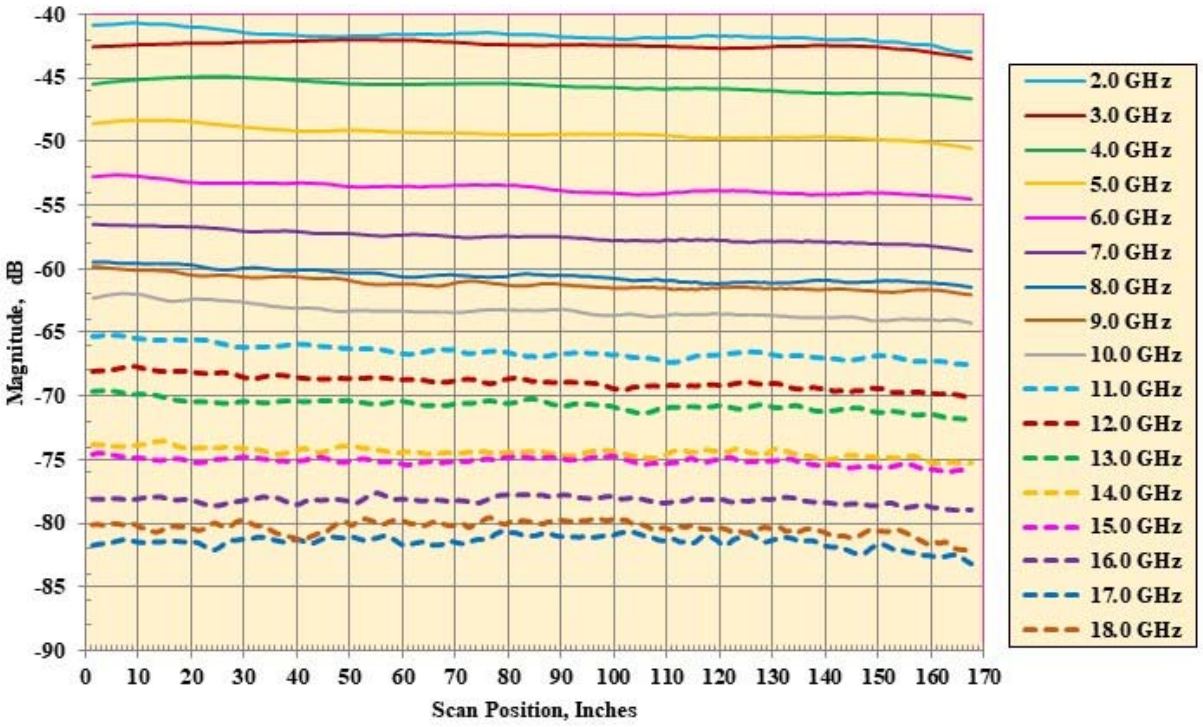

(o) Magnitude probe data, Probe Angle = 90°, Pol VV.
Figure 13. Continued.

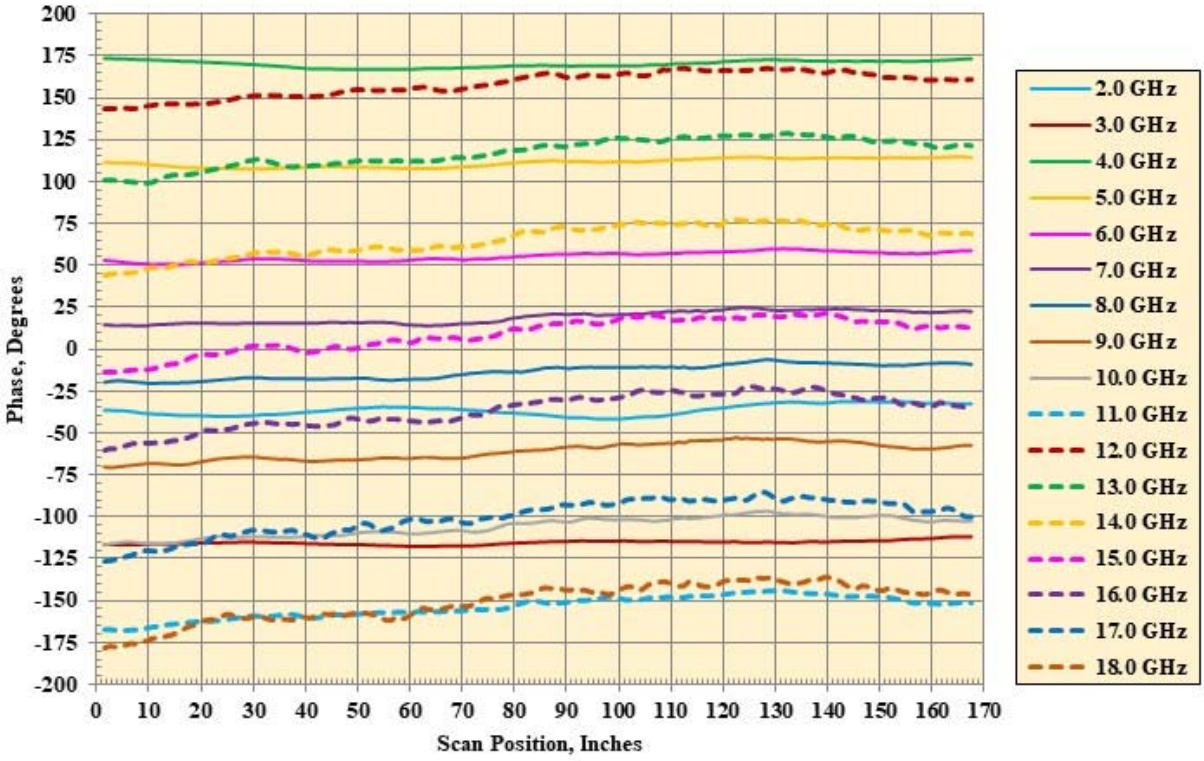

(p) Phase probe data, Probe Angle = 90°, Pol = VV.
Figure 13. Concluded.

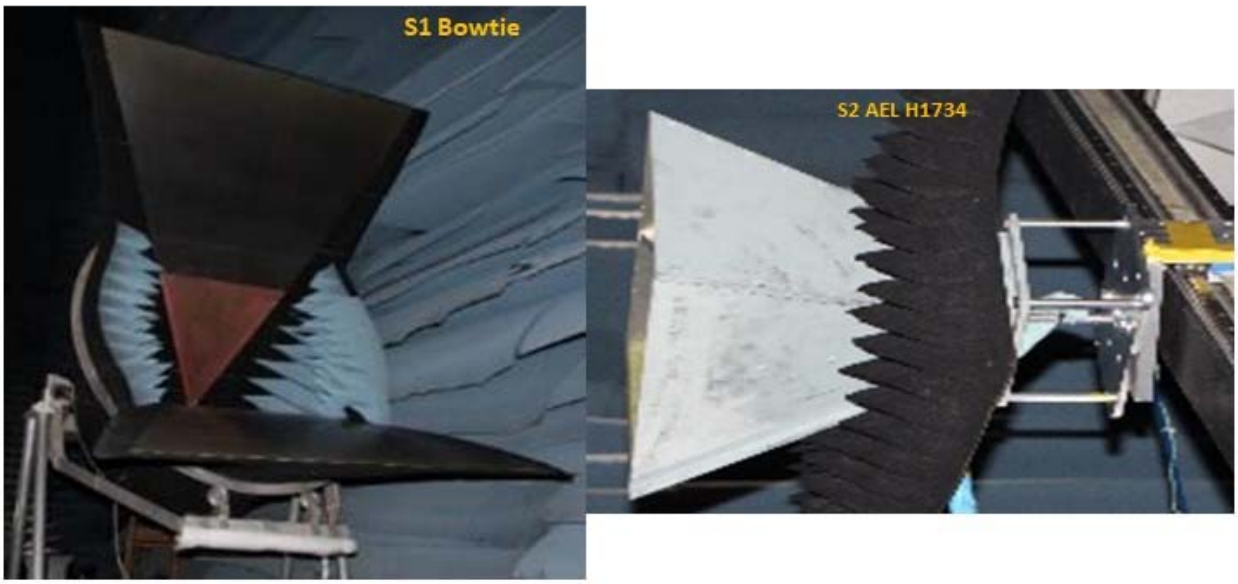

PNA	Frequency Band, GHz	0.3 to 6.0
	Number of data points inband	801
	IF Bandwidth, Hz	700
	Average number of points	8
	Gate Center, ns	-11.852
	Gate Span, ns	1.207
S1	Bowtie Antenna	
S2	AEL H-1734	
	Amplifier	None
Prober	Step size, in.	1.0

Figure 14. Setup for the 0.3 to 6.0 GHz probe data acquisition.

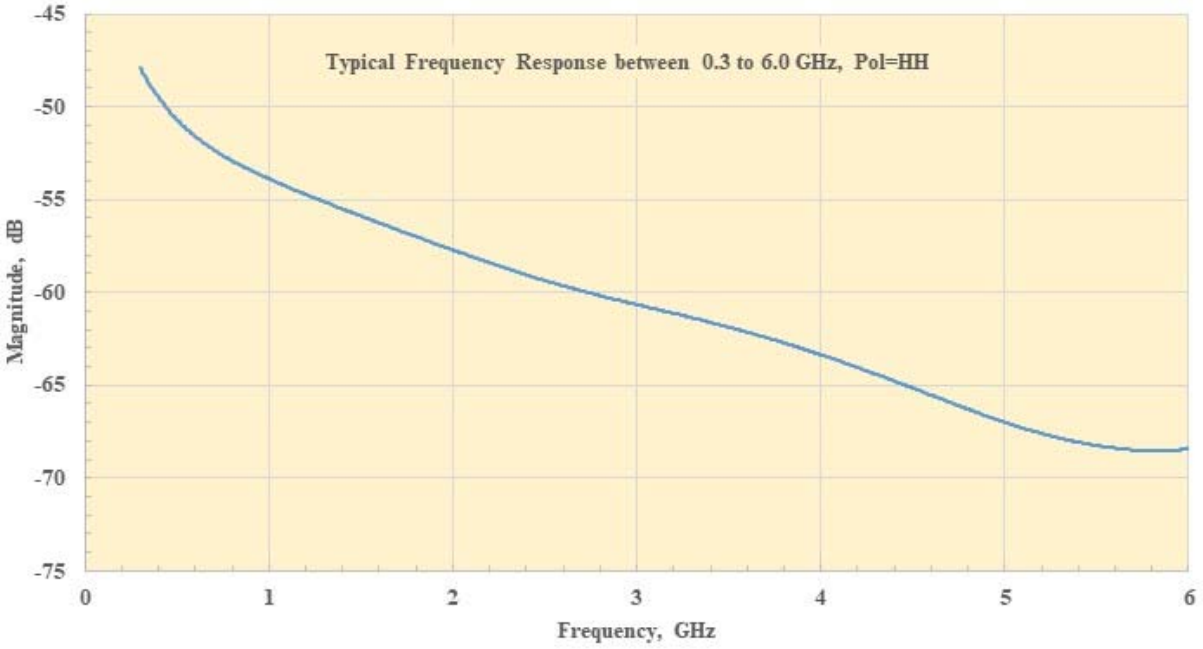

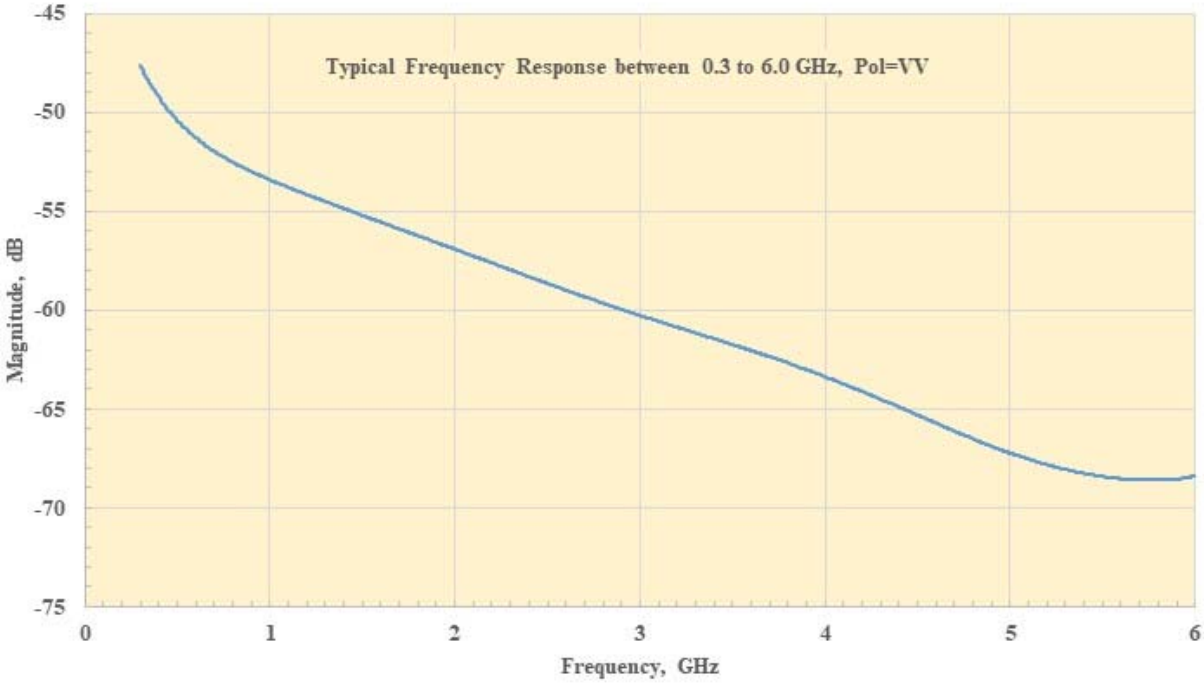

Figure 15. Typical frequency response data for HH and VV for 0.3 – 6.0 GHz probe data.
Data acquired at probe arm center.

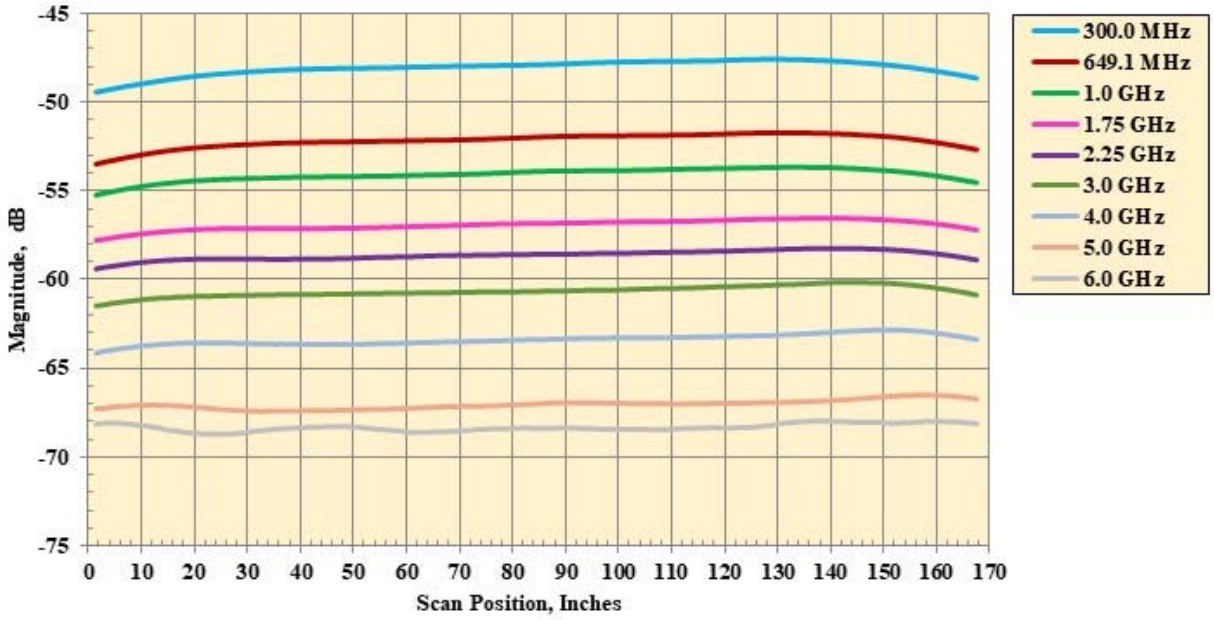

(a) Magnitude probe data, Probe Angle = 0°, Pol = HH.

Figure 16. Probe data at frequency = 0.3 GHz to 6.0 GHz using the S1 antenna = Bowtie, S2 antenna = AEL H1734.

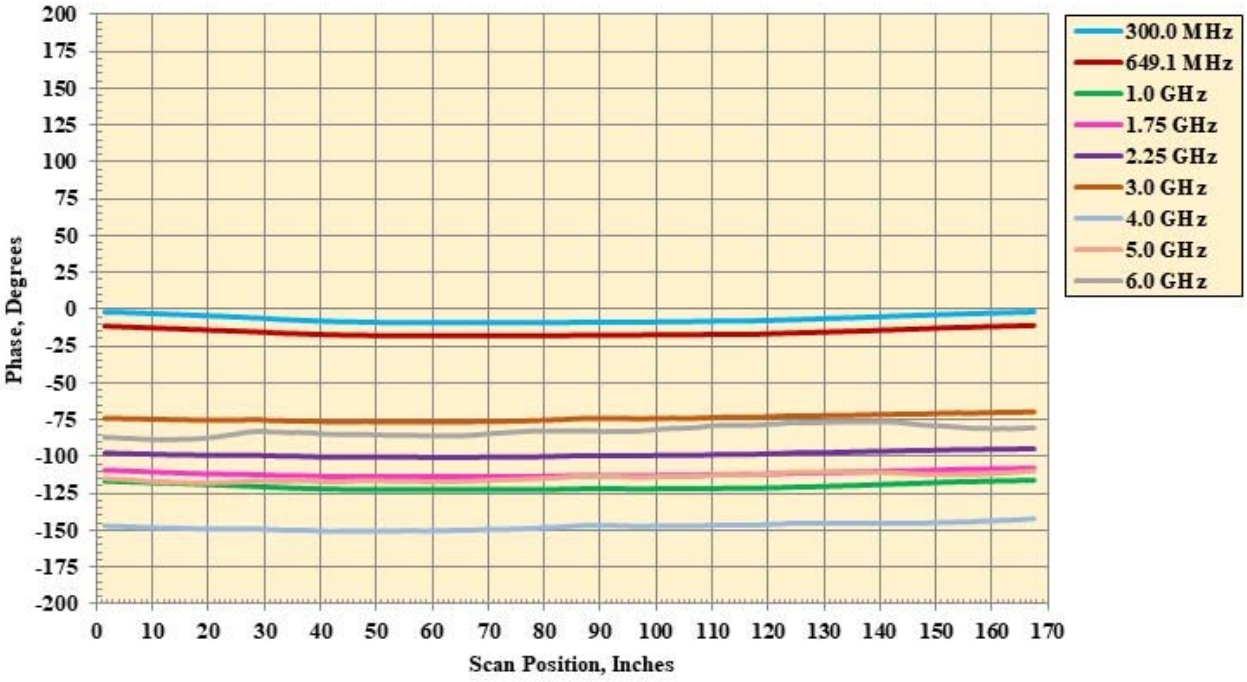

(b) Phase probe data, Probe Angle = 0°, Pol = HH.

Figure16. Continued.

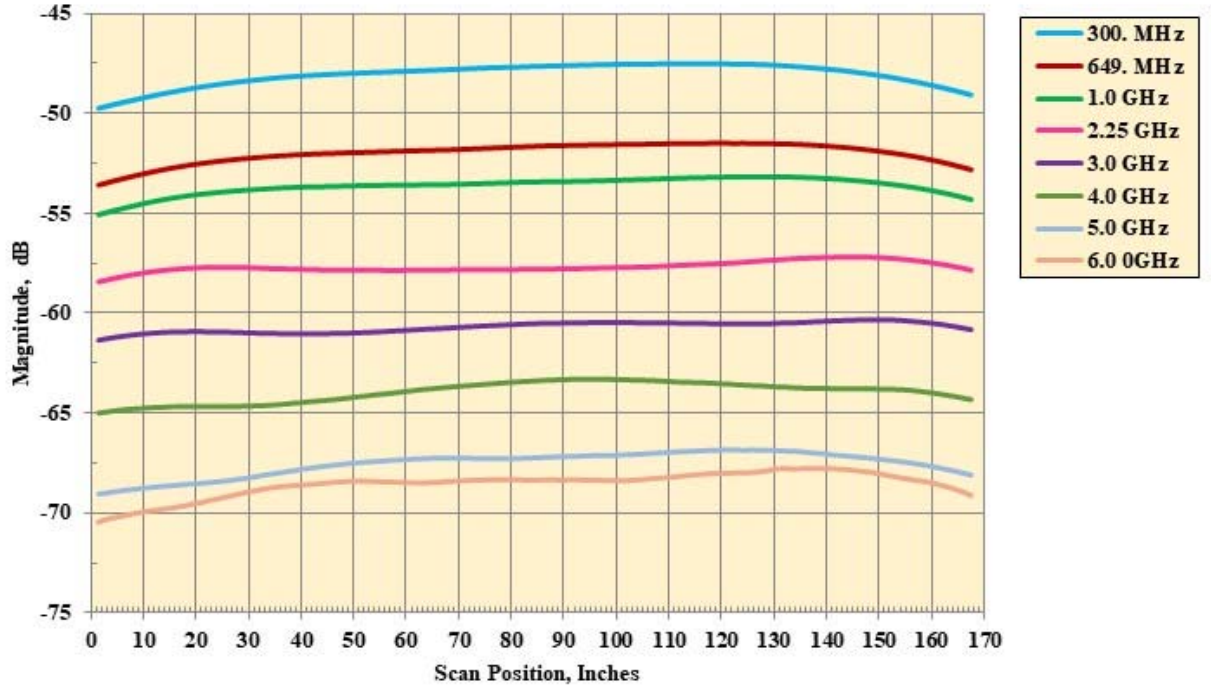

(c) Magnitude probe data, Probe Angle = 0°, Pol = VV.
Figure 16. Continued.

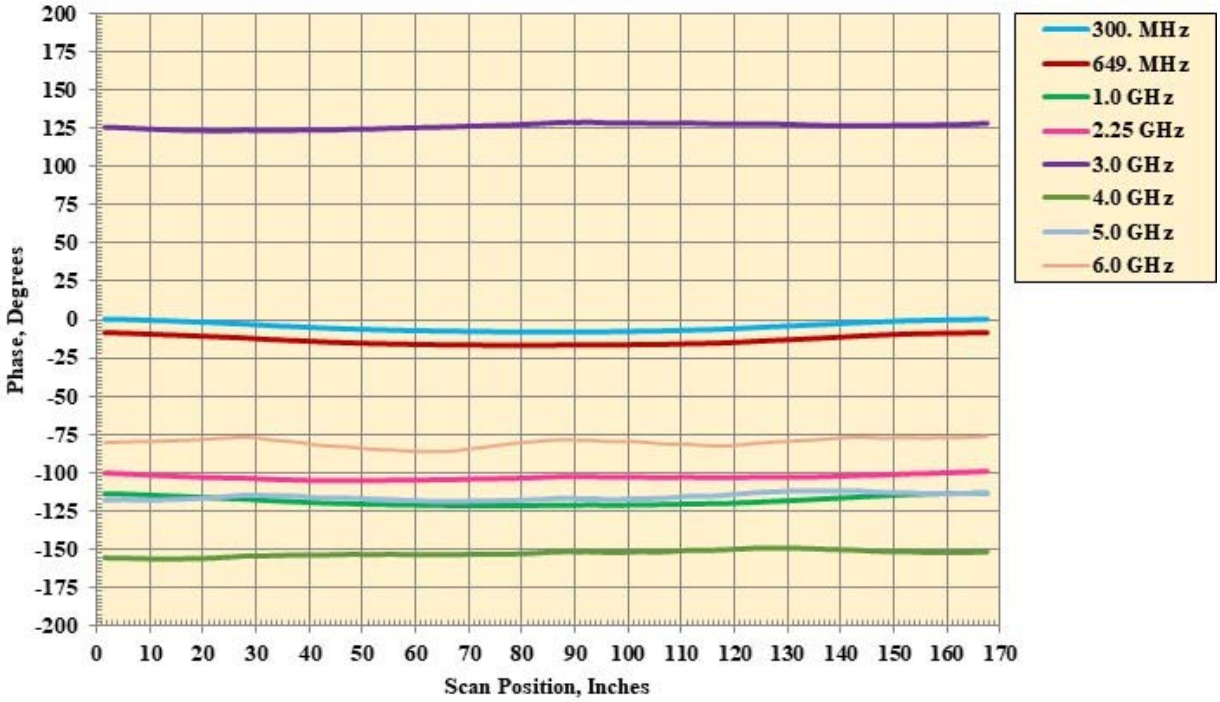

(d) Phase probe data, Probe Angle = 0°, Pol = VV.
Figure 16. Continued.

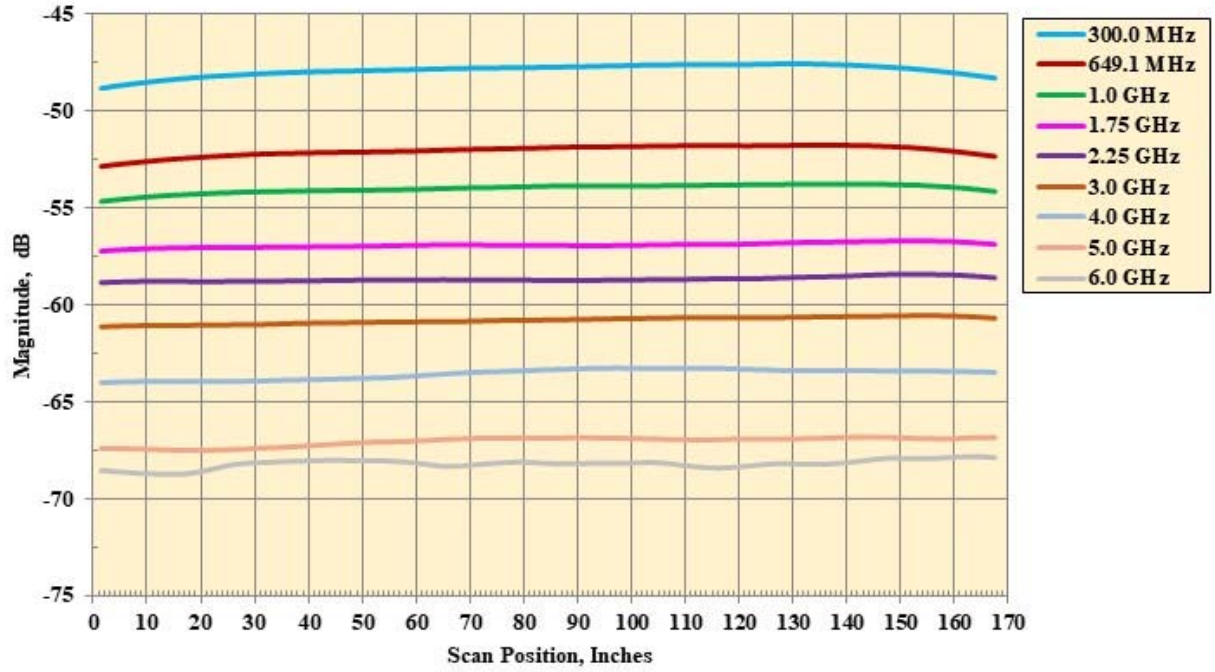

(e) Magnitude probe data, Probe Angle = 30°, Pol = HH.
Figure 16. Continued.

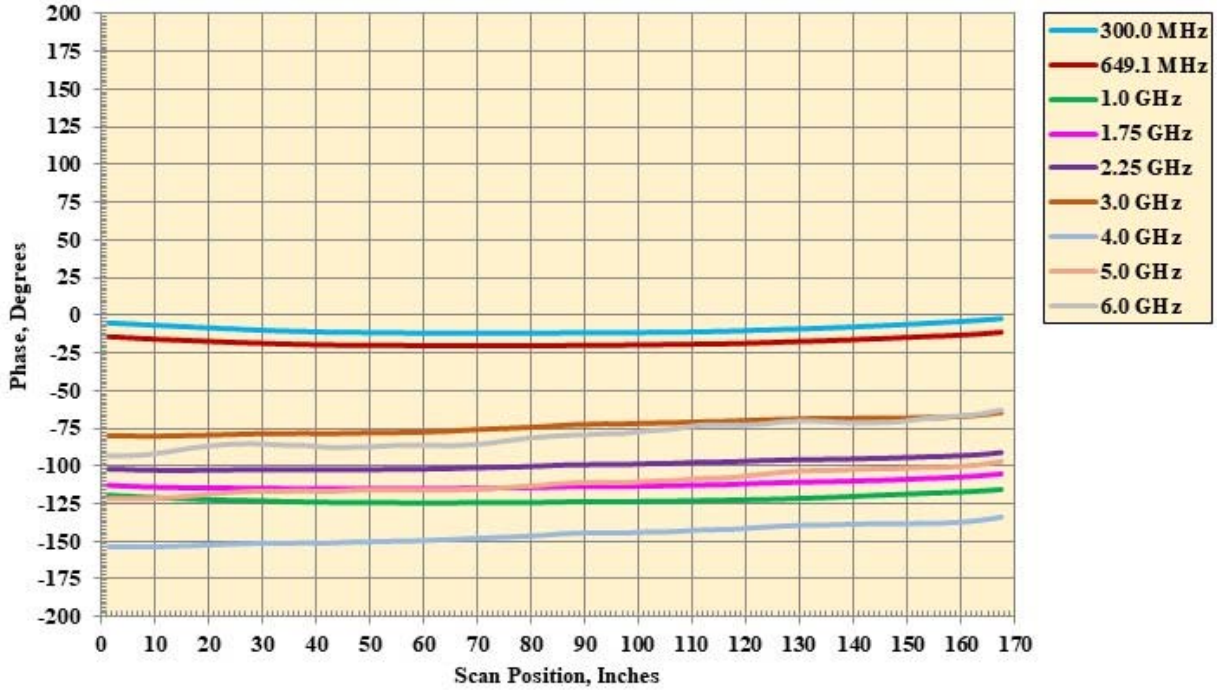

(f) Phase probe data, Probe Angle = 30°, Pol = HH.
Figure 16. Continued.

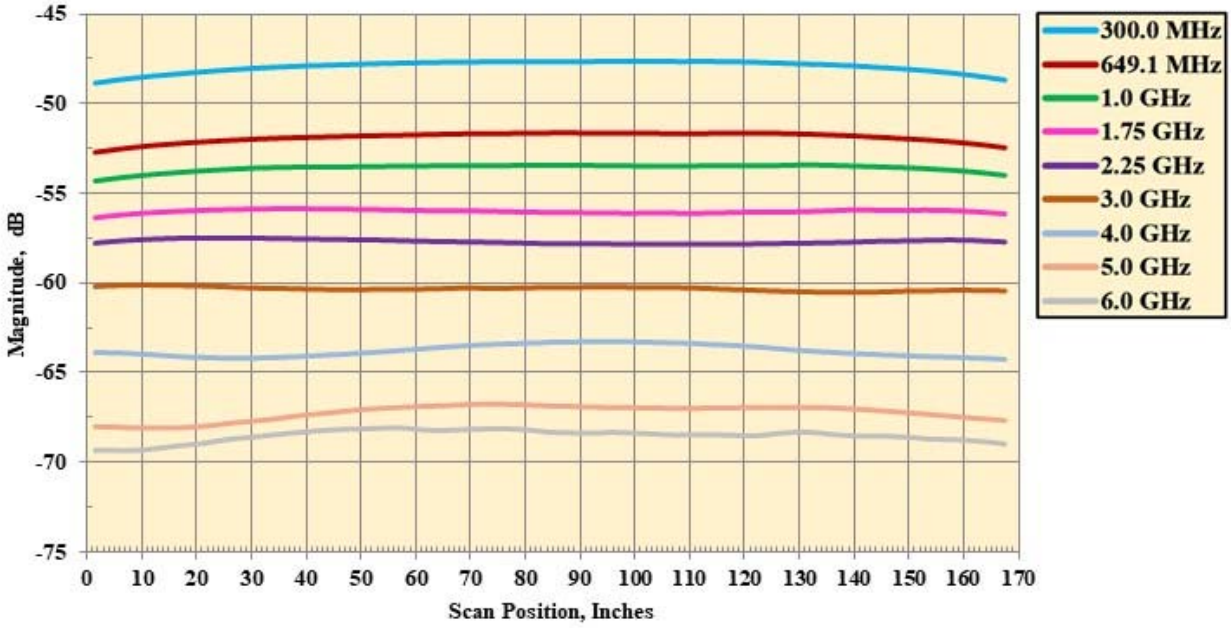

(g) Magnitude probe data, Probe Angle = 60°, Pol = HH.
Figure 16. Continued.

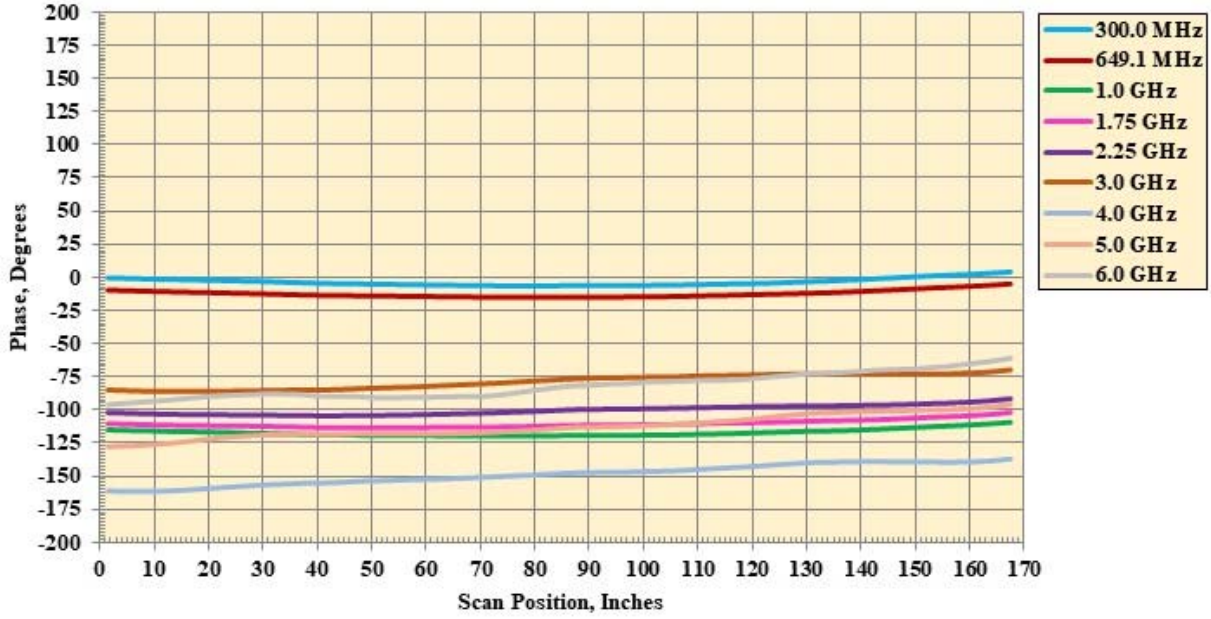

(h) Phase probe data, Probe Angle = 60°, Pol = HH.
Figure 16. Continued.

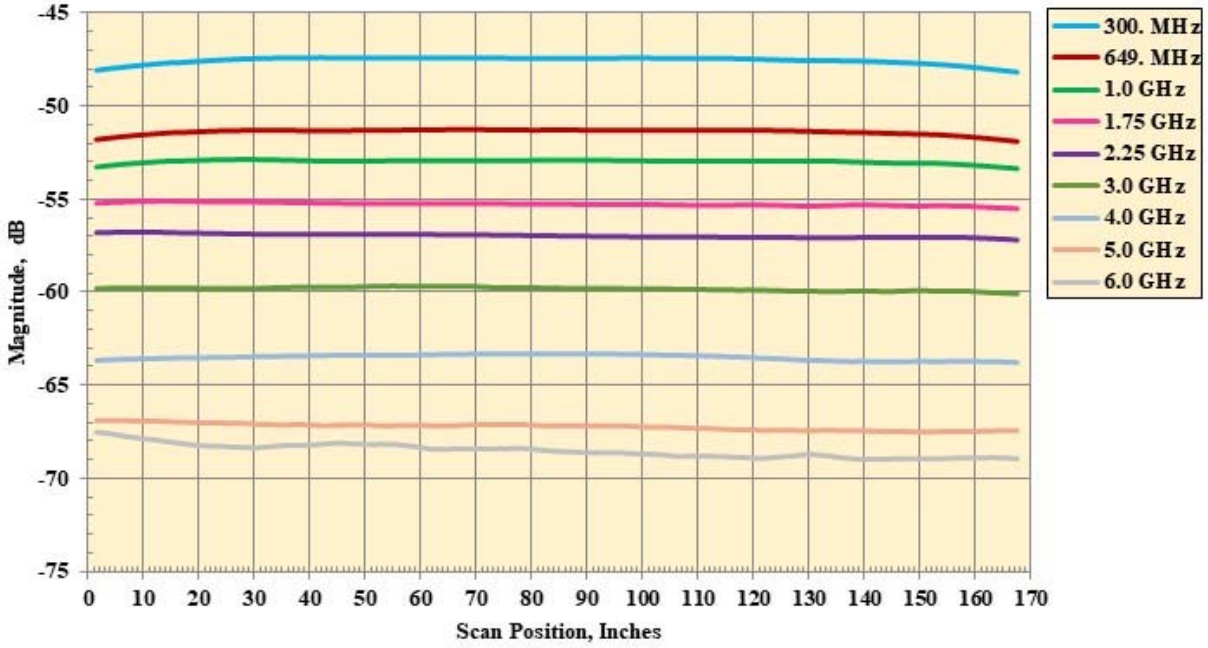

(i) Magnitude probe data, Probe Angle = 60°, Pol = VV.
Figure 16. Continued.

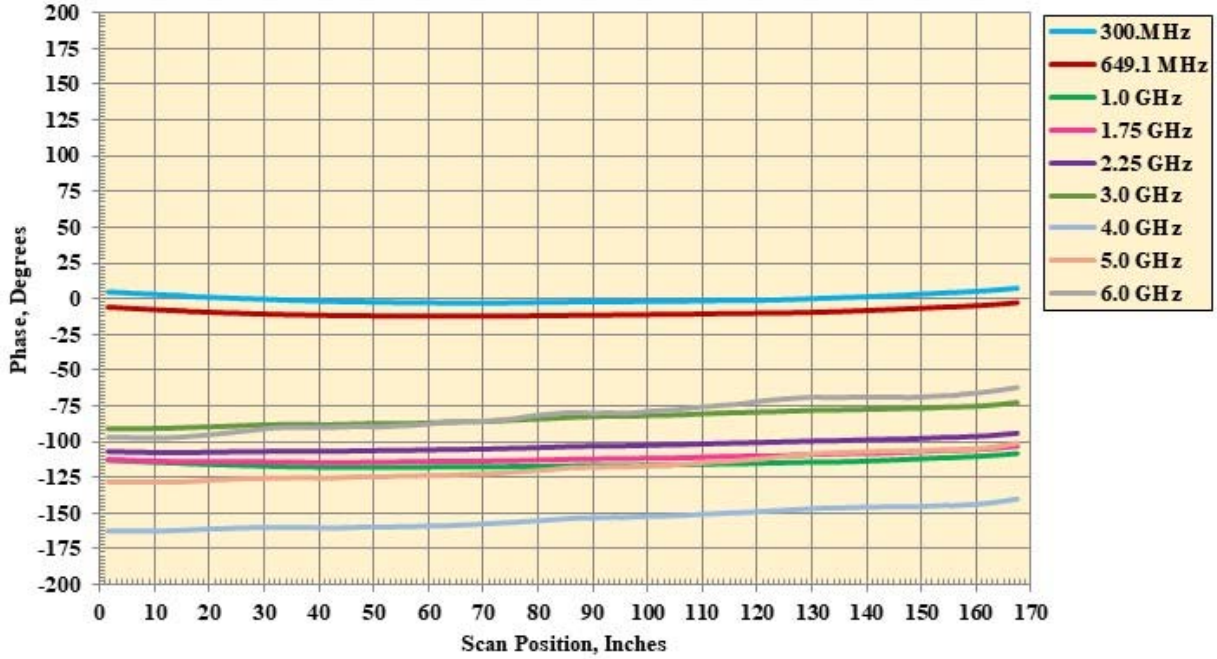

(j) Phase probe data, Probe Angle = 60°, Pol = VV.
Figure 16. Continued.

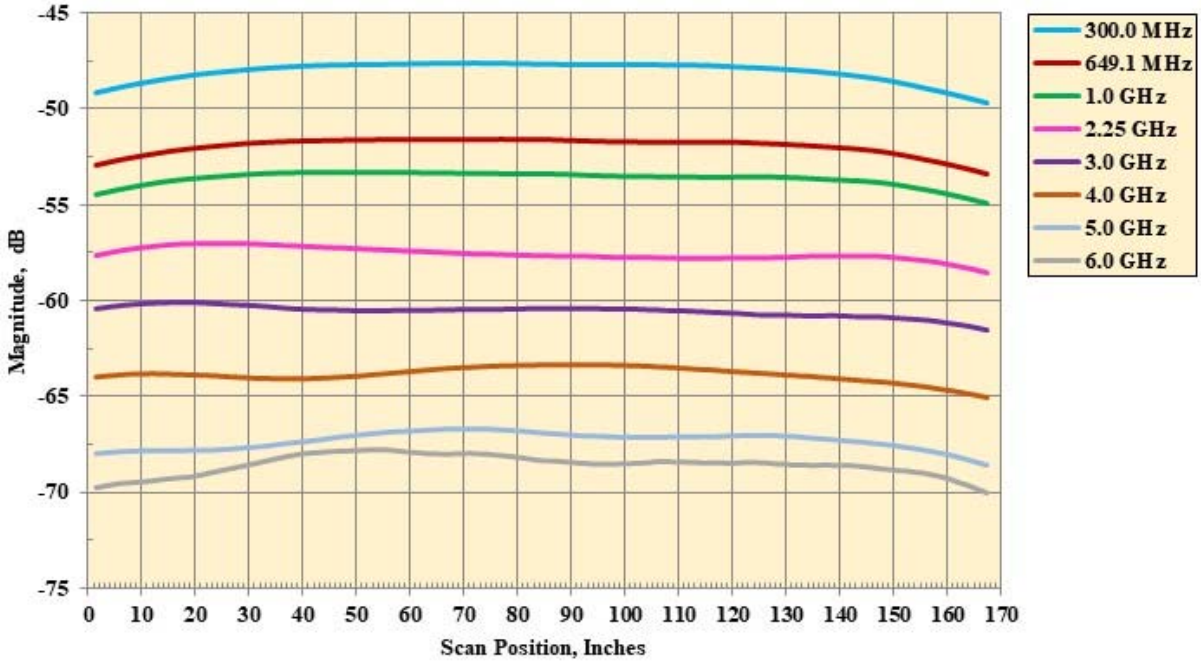

(k) Magnitude probe data, Probe Angle = 90°, Pol = HH.
Figure 16. Continued.

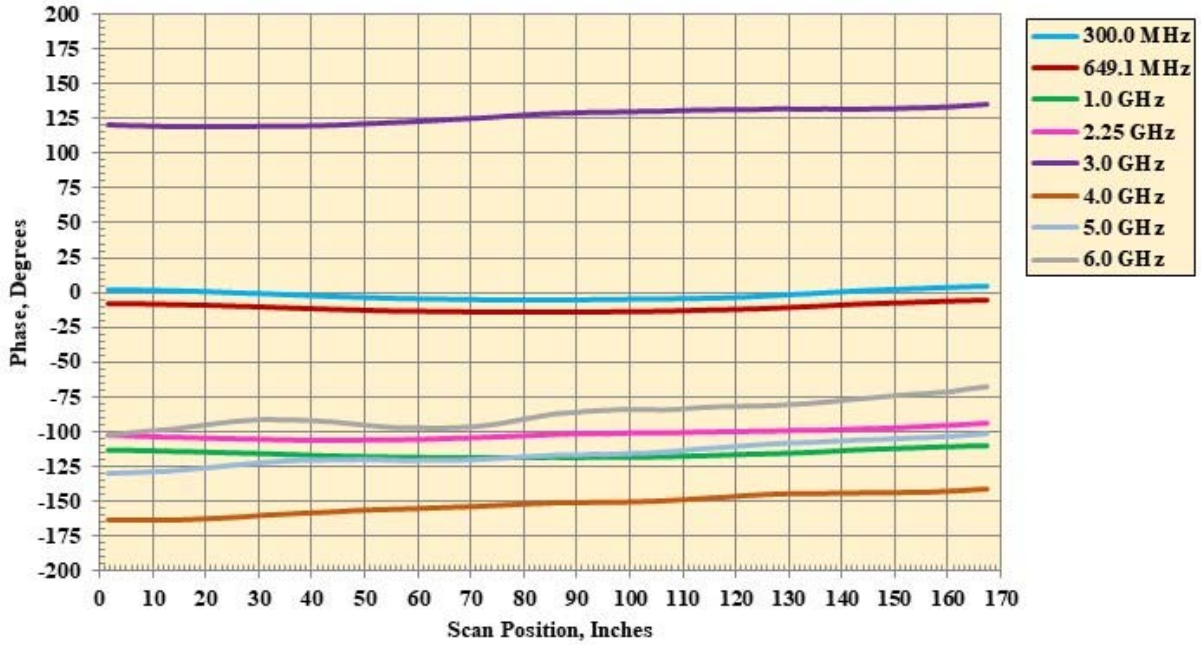

(l) Phase probe data, Probe Angle = 90°, Pol = HH.
Figure 16. Continued.

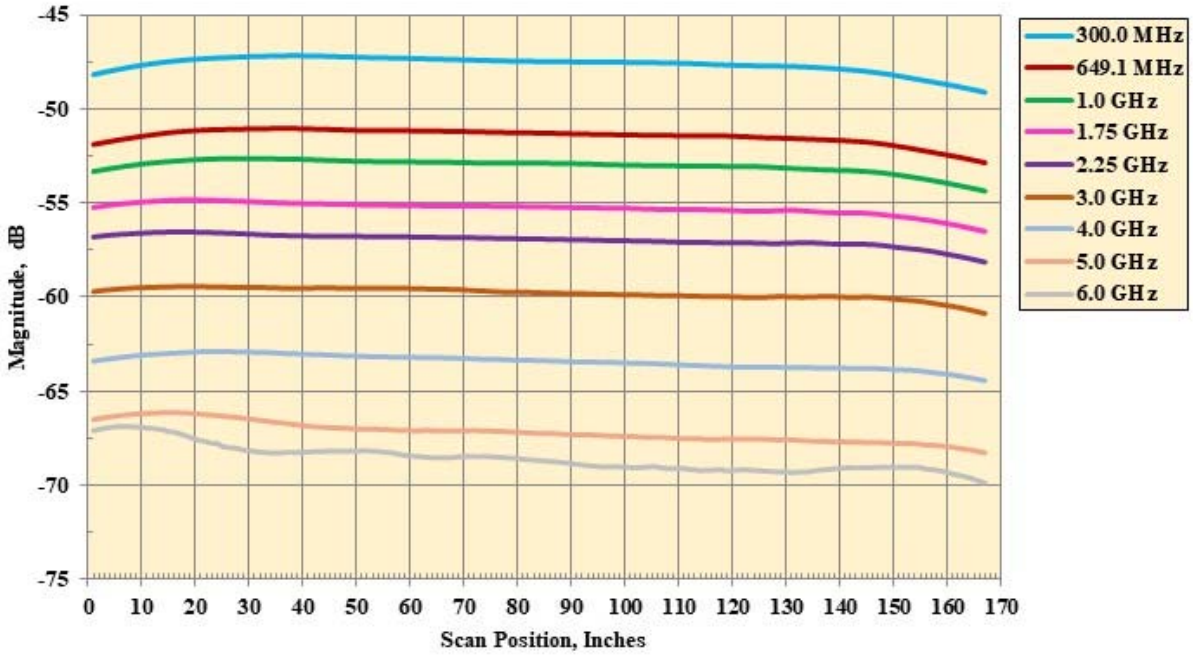

(m) Magnitude probe data, Probe Angle = 90°, Pol = VV.
Figure 16. Continued.

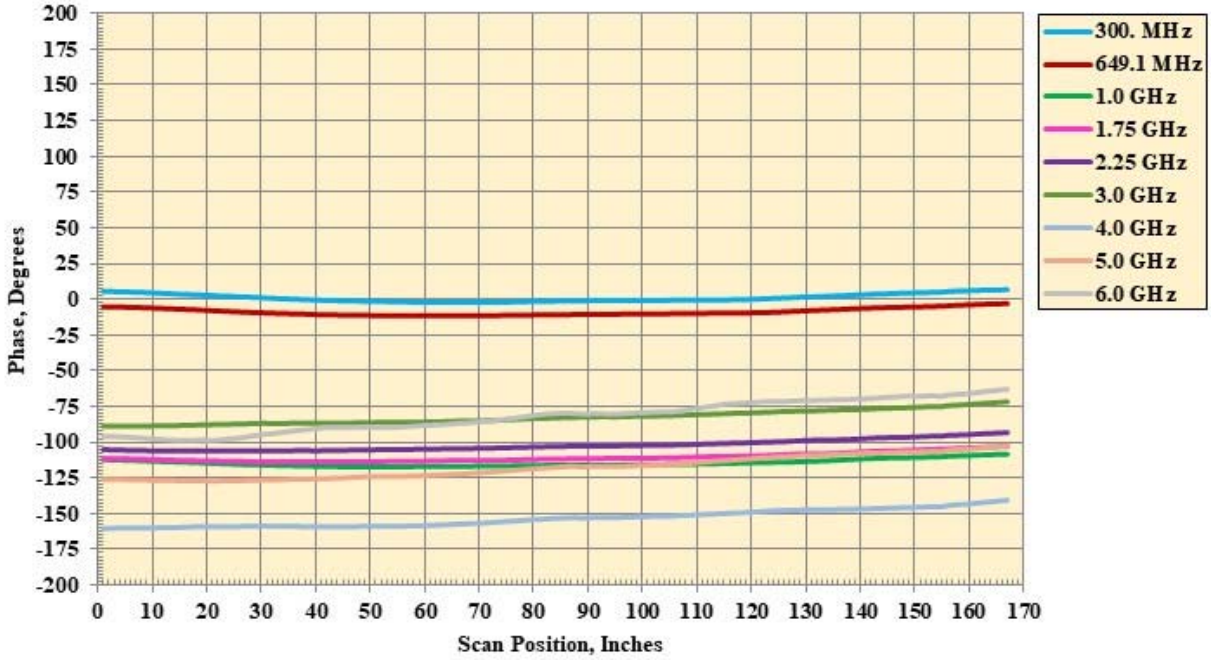

(n) Phase probe data, Probe Angle = 90°, Pol = VV.
Figure 16. Continued.

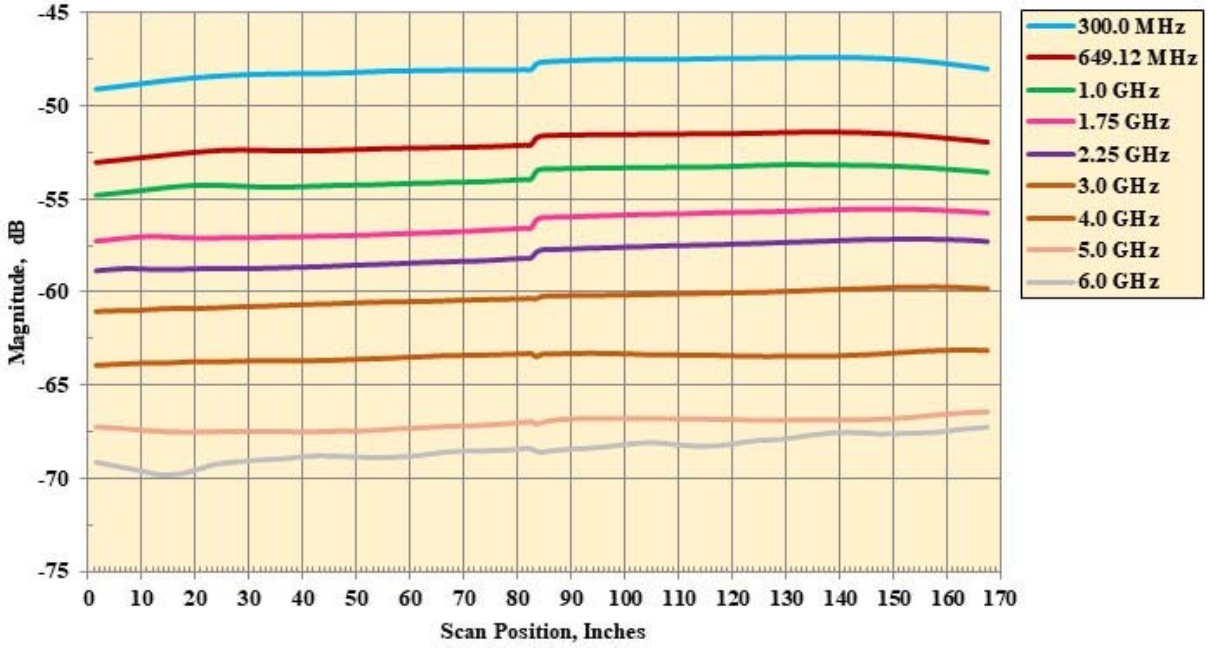

(o) Magnitude probe data, Probe Angle = -30°, Pol = HH.
Figure 16. Continued.

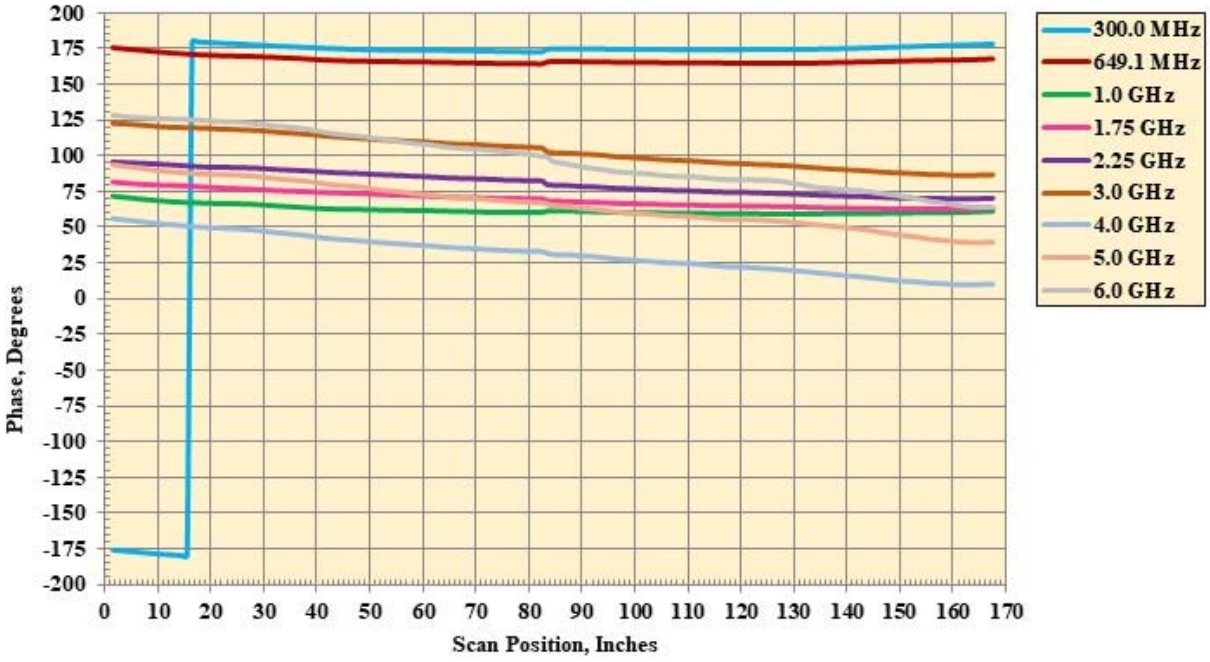

(p) Phase probe data, Probe Angle = -30°, Pol = HH.
Figure 16. Continued.

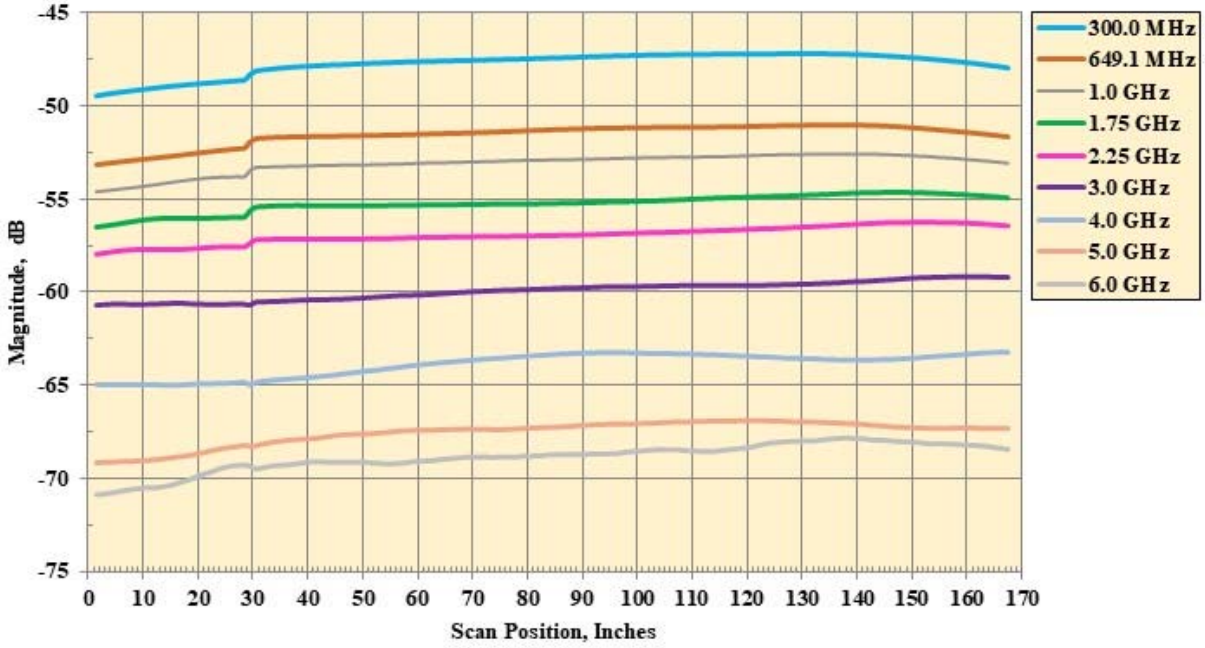

(q) Magnitude probe data, Probe Angle = -30°, Pol = VV.
Figure 16. Continued.

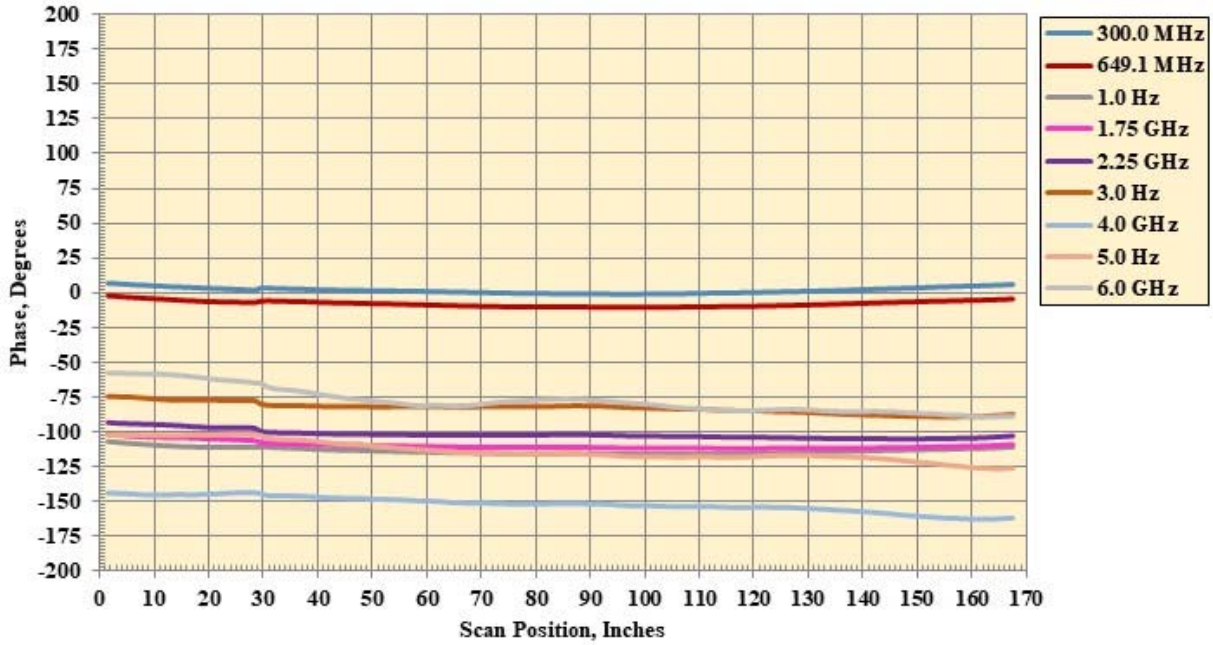

(r) Phase probe data, Probe Angle = -30°, Pol = VV.
Figure 16. Continued.

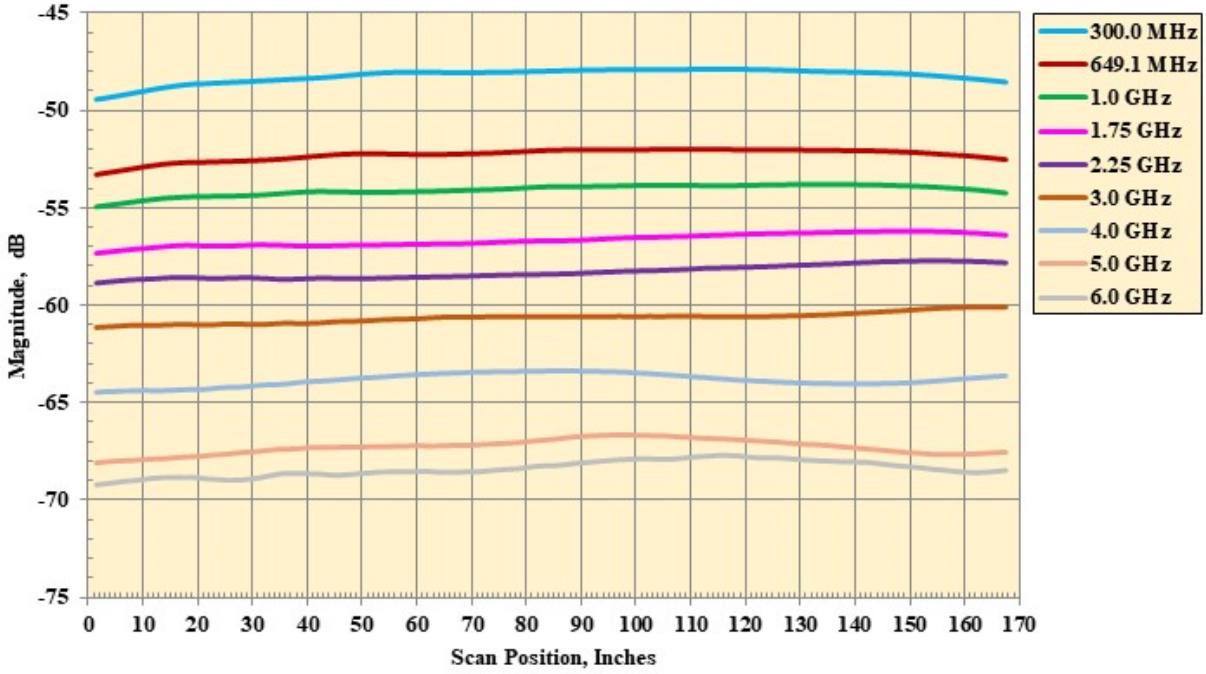

(s) Magnitude probe data, Probe Angle = -60°, Pol = HH.
Figure 16. Continued.

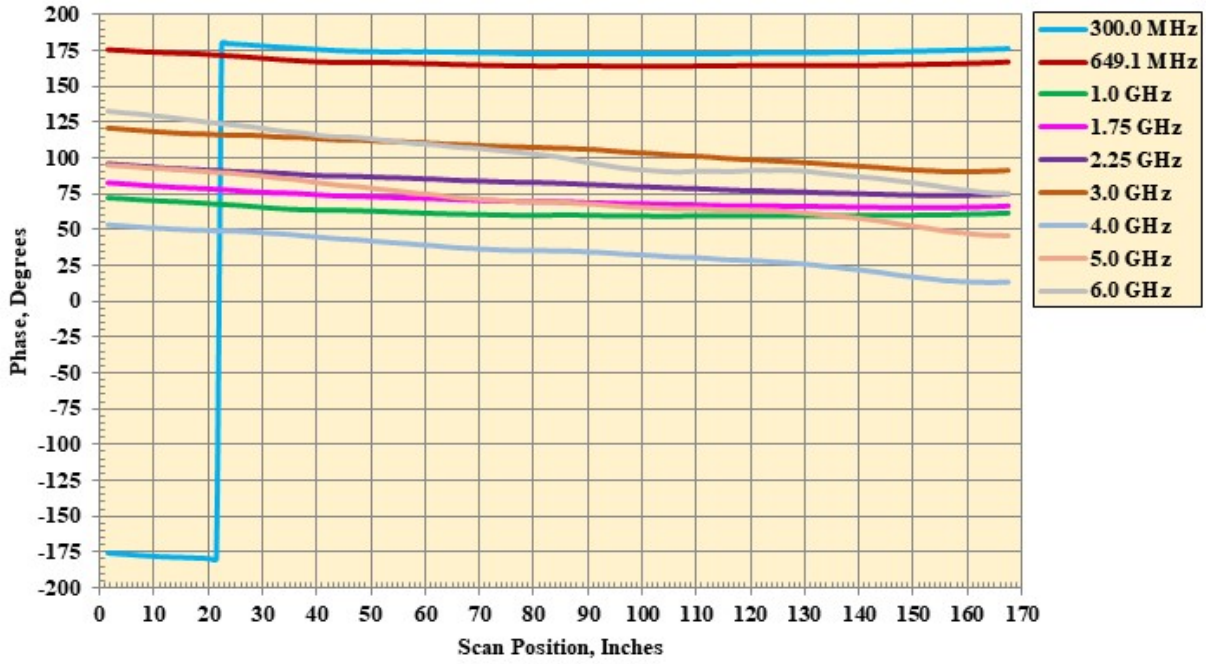

(t) Phase probe data, Probe Angle = -60°, Pol = HH.
Figure 16. Continued.

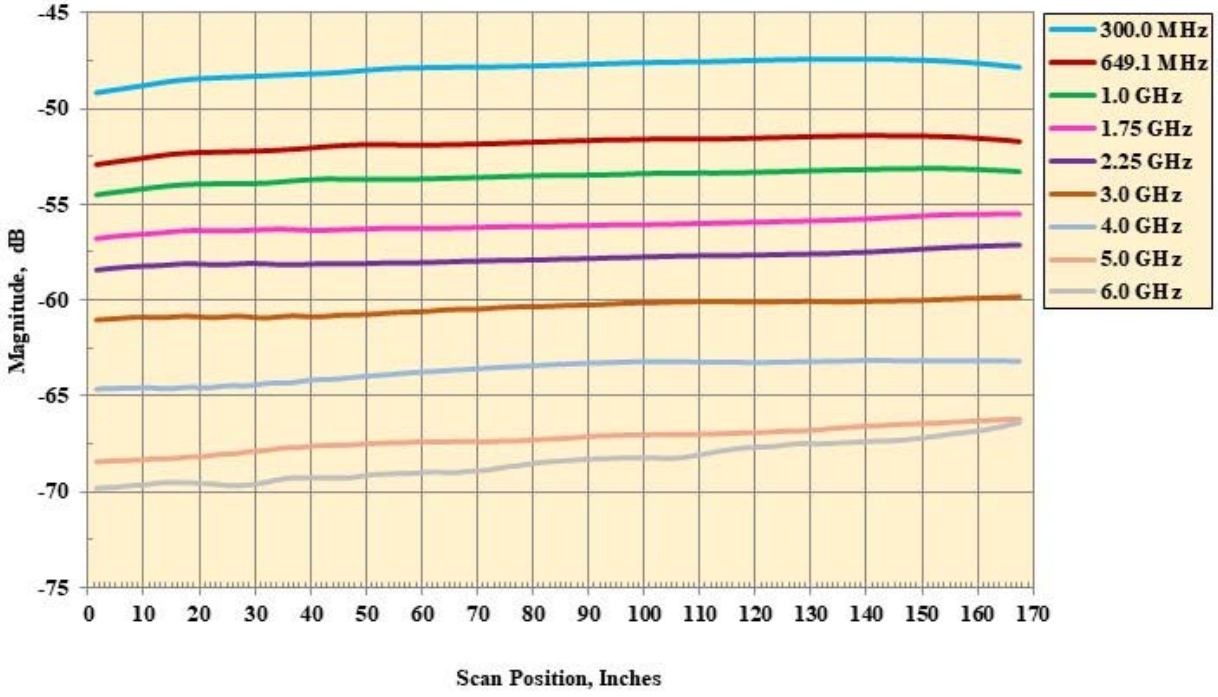

(u) Magnitude probe data, Probe Angle = -60°, Pol = VV.
Figure 16. Continued.

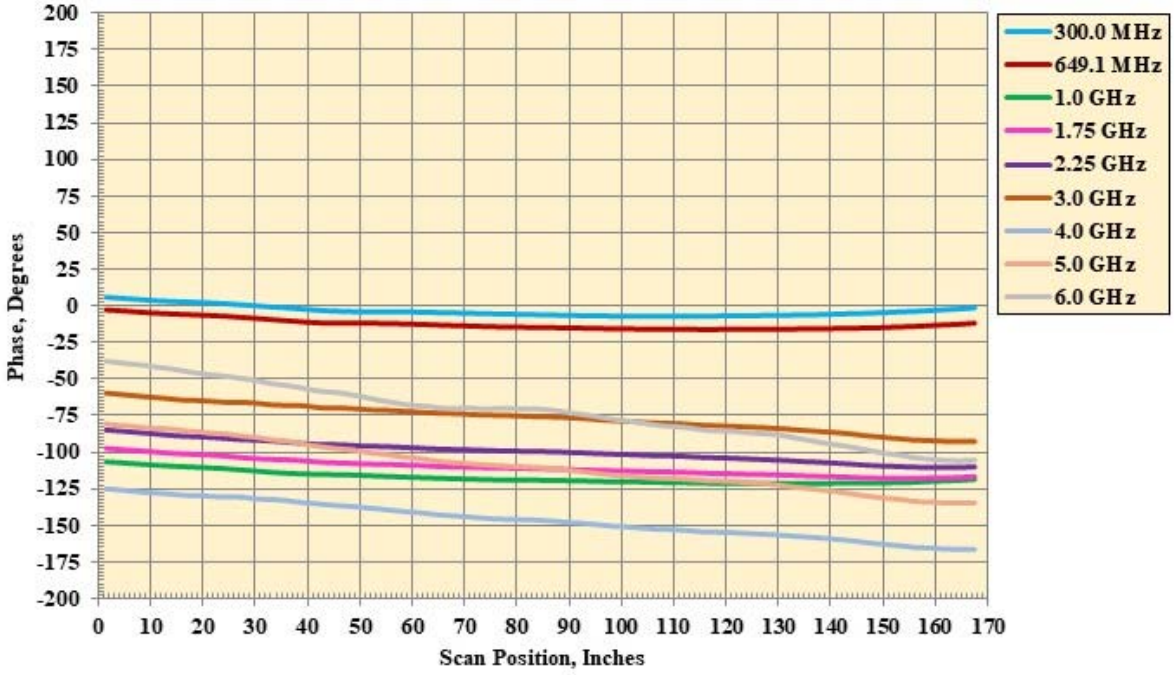

(v) Phase probe data, Probe Angle = -60°, Pol = VV.
Figure 16. Concluded.

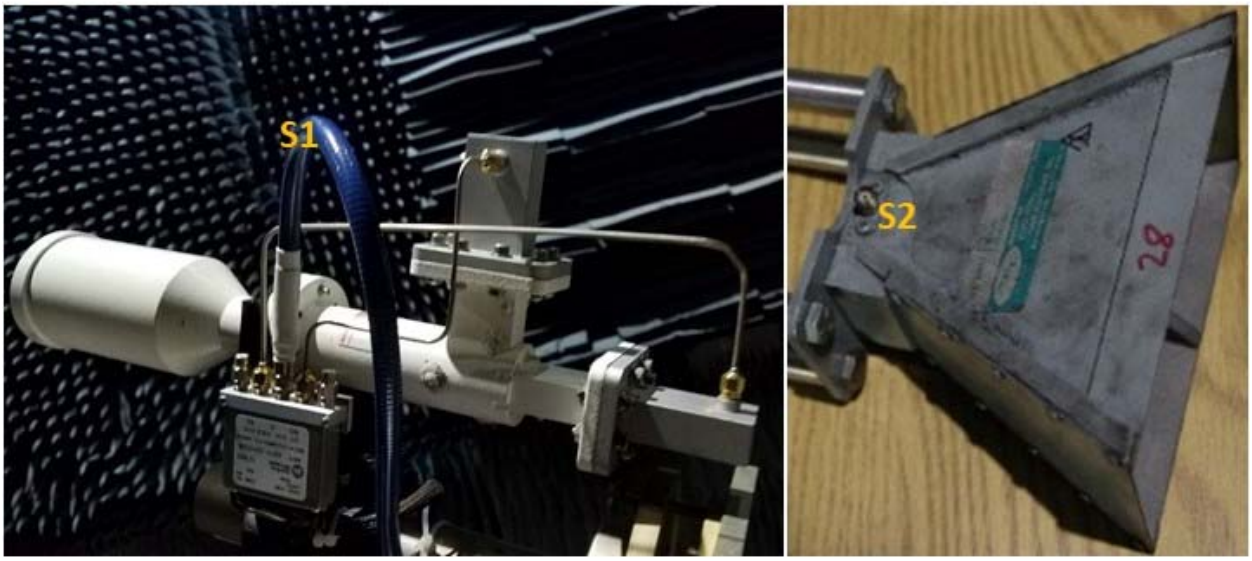

PNA	Frequency Band, GHz	7.0 to 9.0
	Number of data points inband	201
	IF Bandwidth, Hz	700
	Average number of points	4
HH	Gate Center, ns	-18.14
HH	Gate Span, ns	2.34
VV	Gate Center, ns	-17.22
VV	Gate Span, ns	2.25
S1	Seavey OSA-77C	
S2	AEL H-1498	
S1	Amplifier Keysight Model 83017	Yes
S2	Amplifier	None
Prober	Step size, in.	0.2

Figure 17. Setup for the 7.0 to 9.0 GHz probe data acquisition.

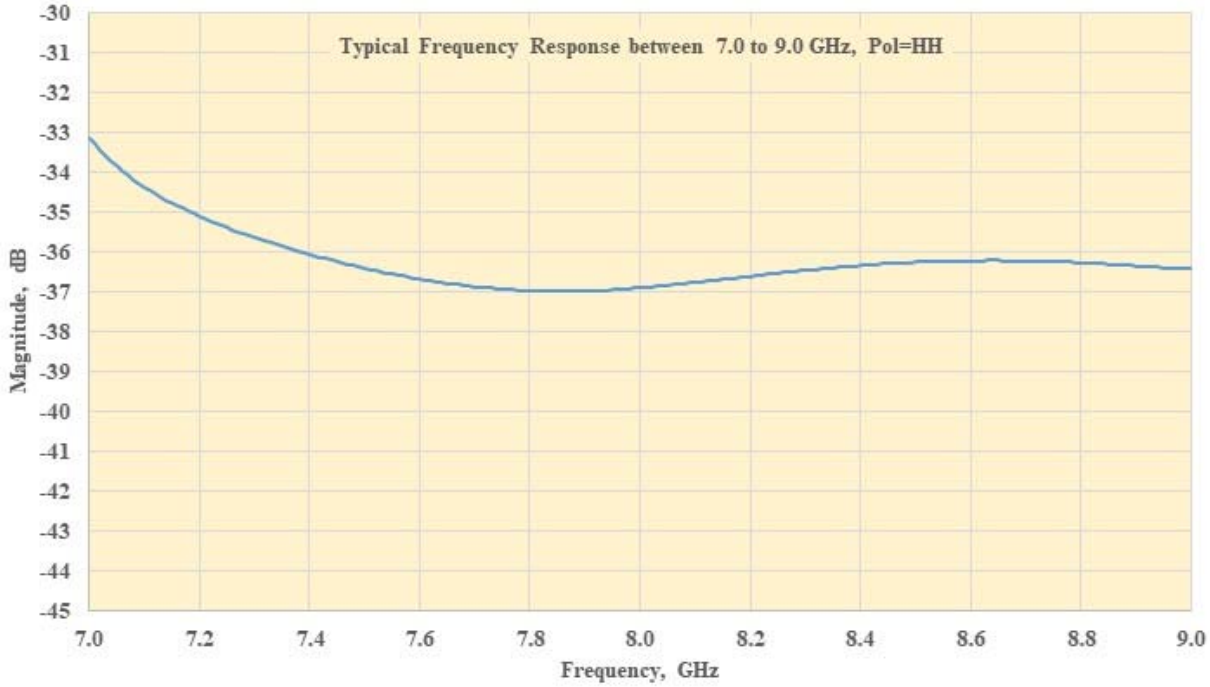

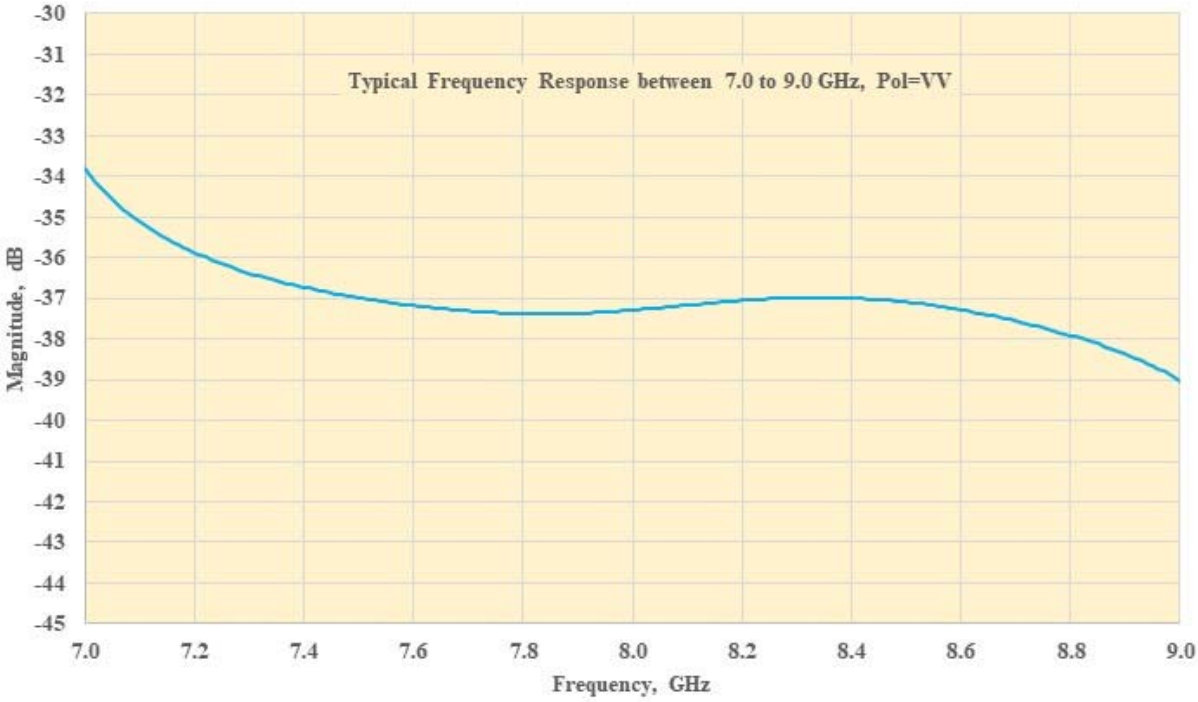

Figure 18. Typical frequency response data for HH and VV for 7.0 – 9.0 GHz probe data.
Data acquired at probe arm center.

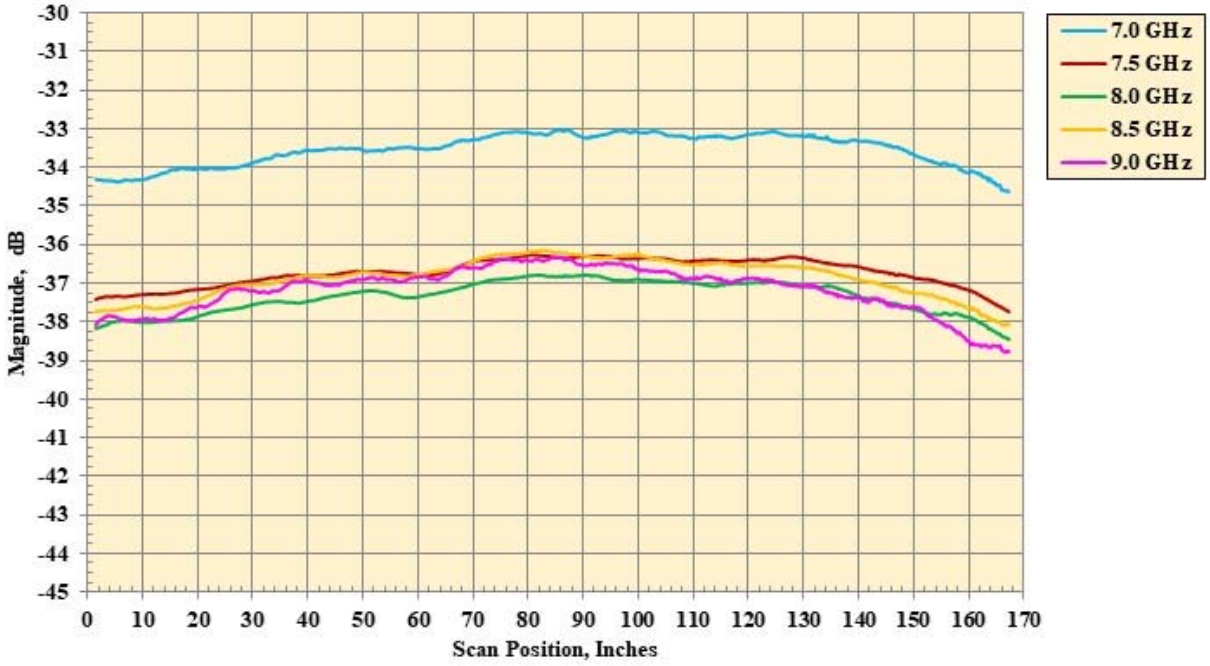

(a) Magnitude probe data, Probe Angle = 0°, Pol = HH.

Figure 19. Probe data at frequency = 7.0 GHz to 9.0 GHz using the S1 antenna = Seavey OSA-77C , S2 antenna = AEL H1498

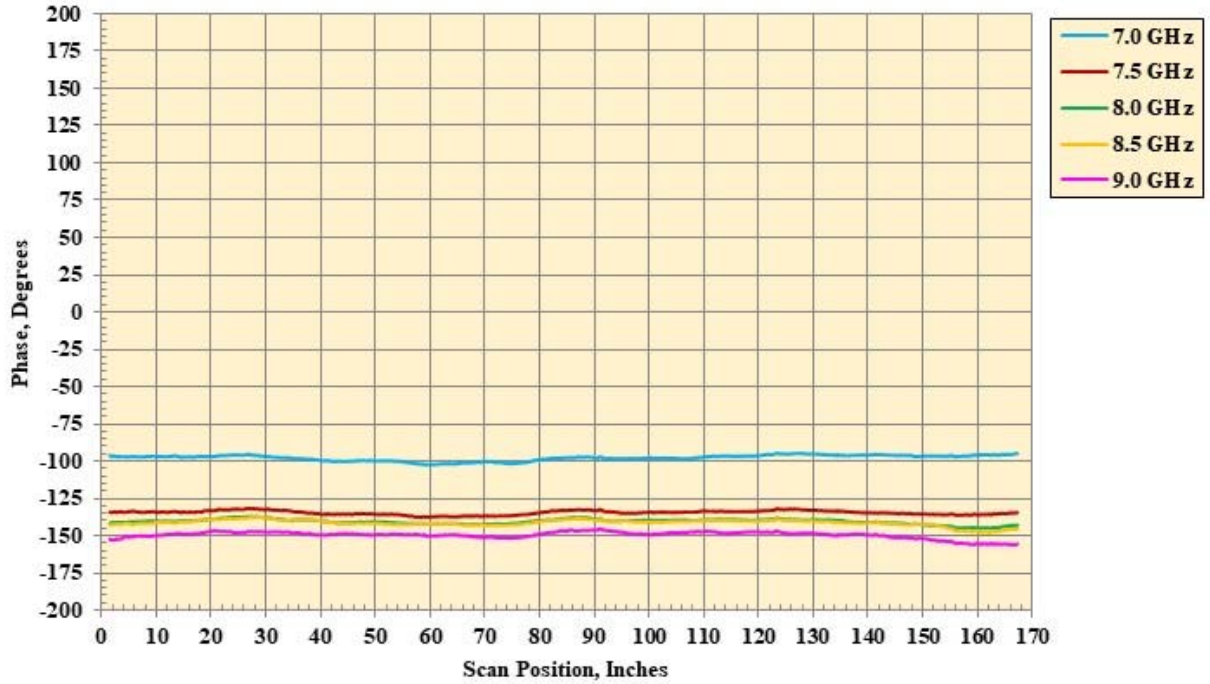

(b) Phase probe data, Probe Angle = 0°, Pol = HH.

Figure 19. Continued.

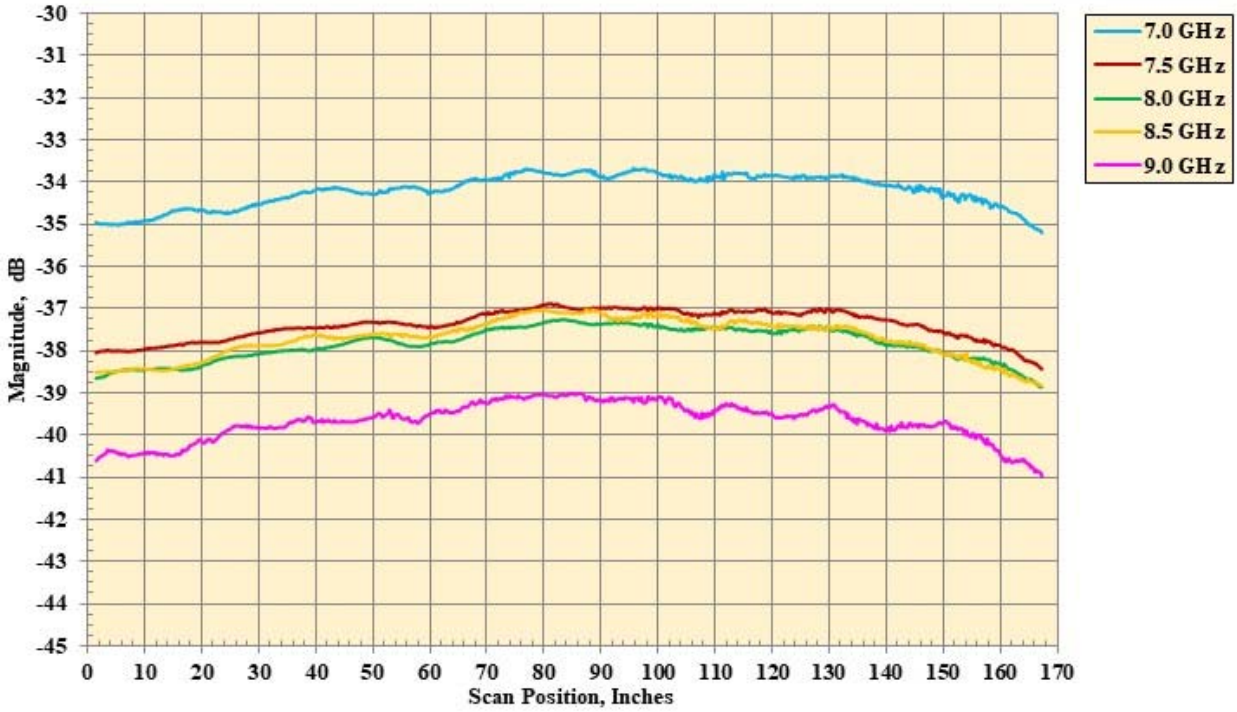

(c) Magnitude probe data, Probe Angle = 0°, Pol = VV.
Figure 19. Continued.

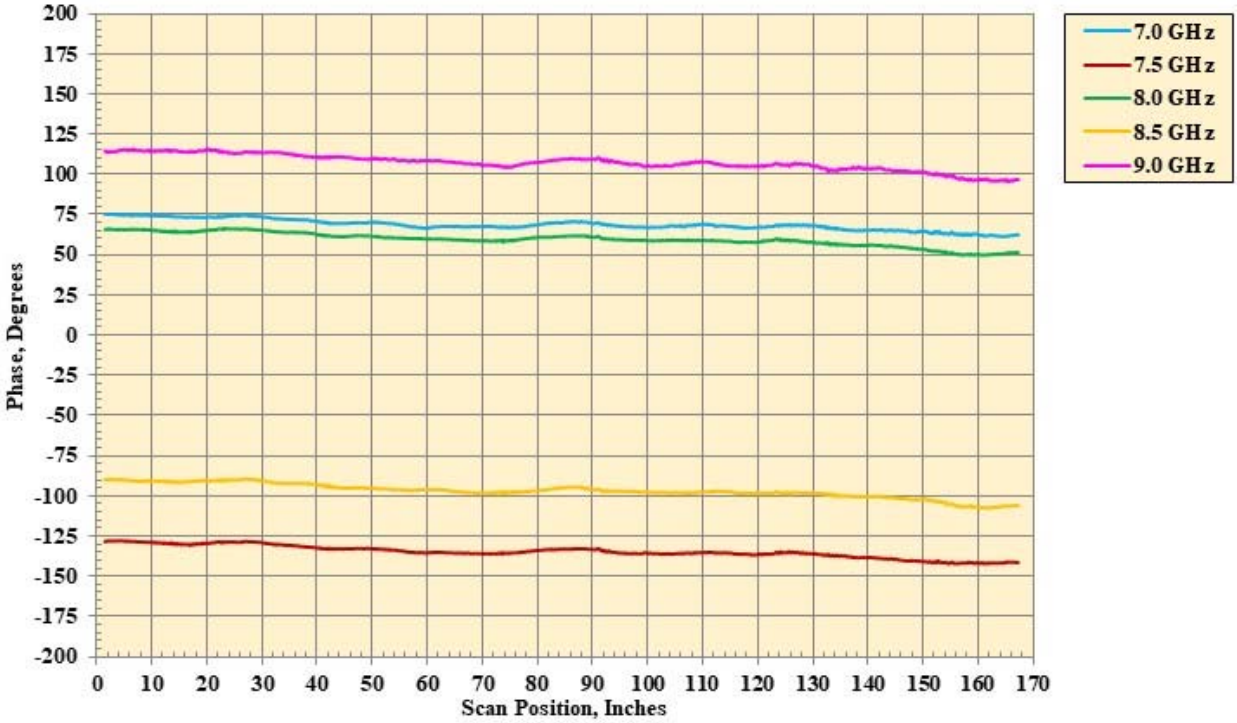

(d) Phase probe data, Probe Angle = 0°, Pol = VV.
Figure 19. Continued.

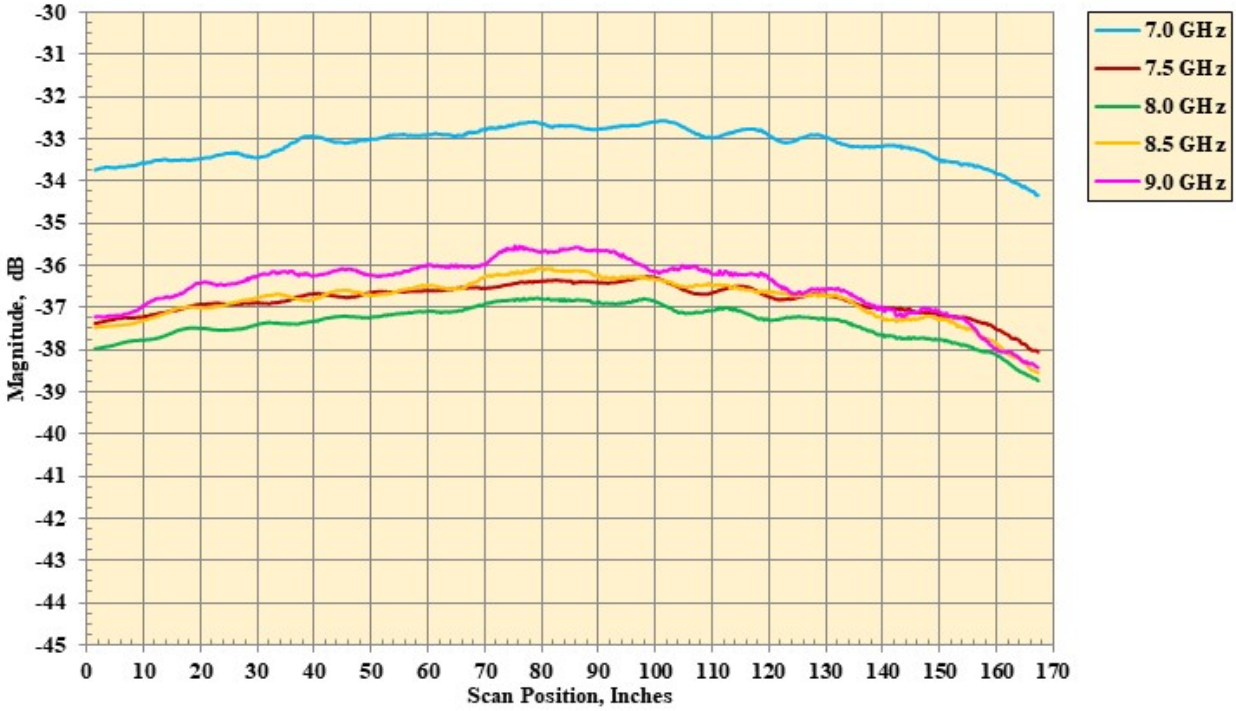

(e) Magnitude probe data, Probe Angle = 15°, Pol = HH.
Figure 19. Continued.

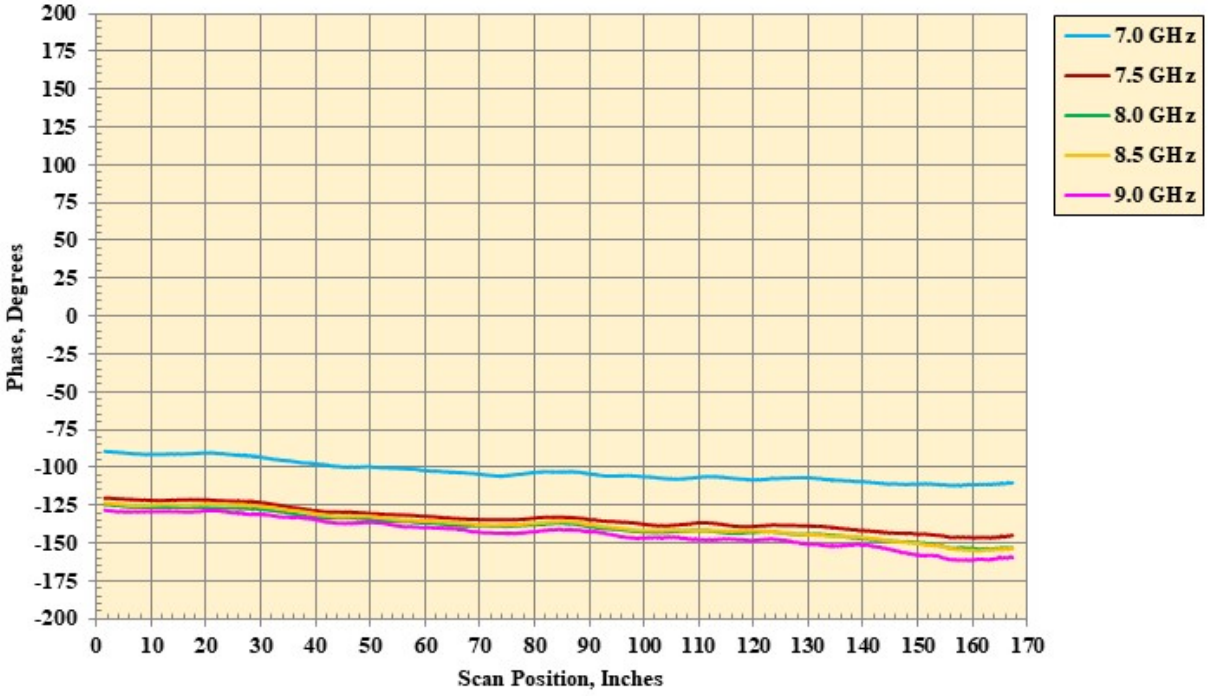

(f) Phase probe data, Probe Angle = 15°, Pol = HH.
Figure 19. Continued.

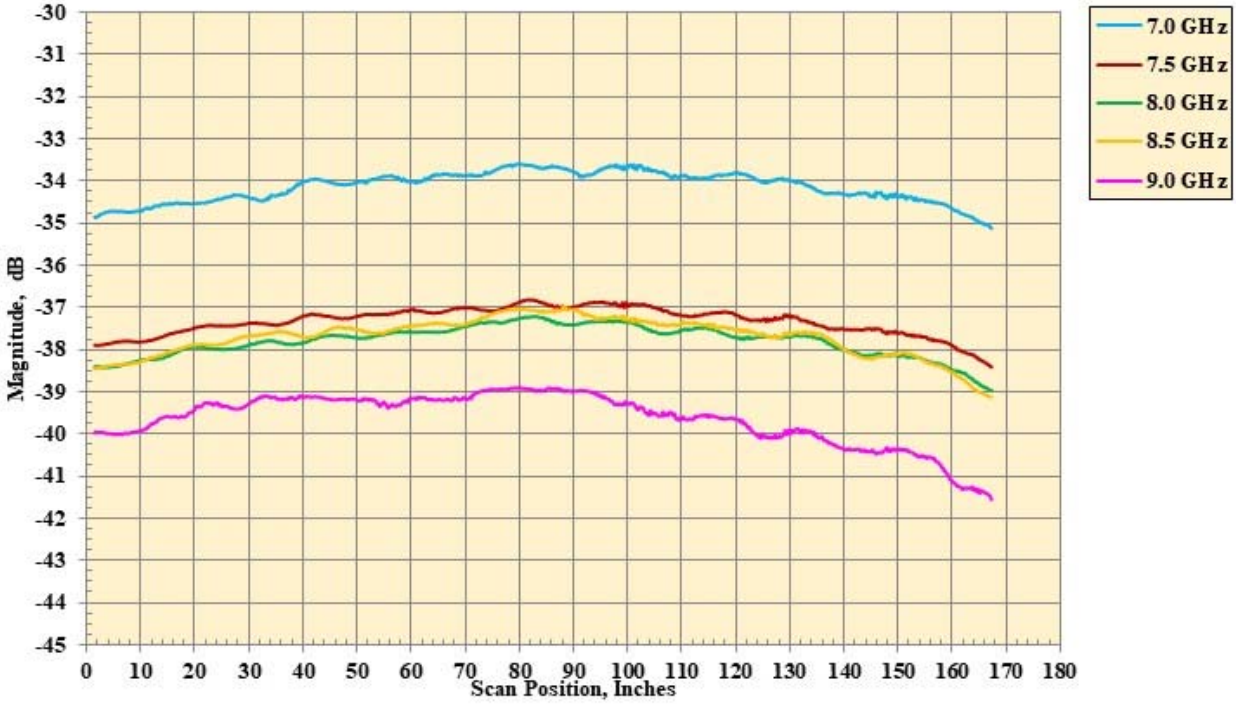

(g) Magnitude probe data, Probe Angle = 15°, Pol = VV.
Figure 19. Continued.

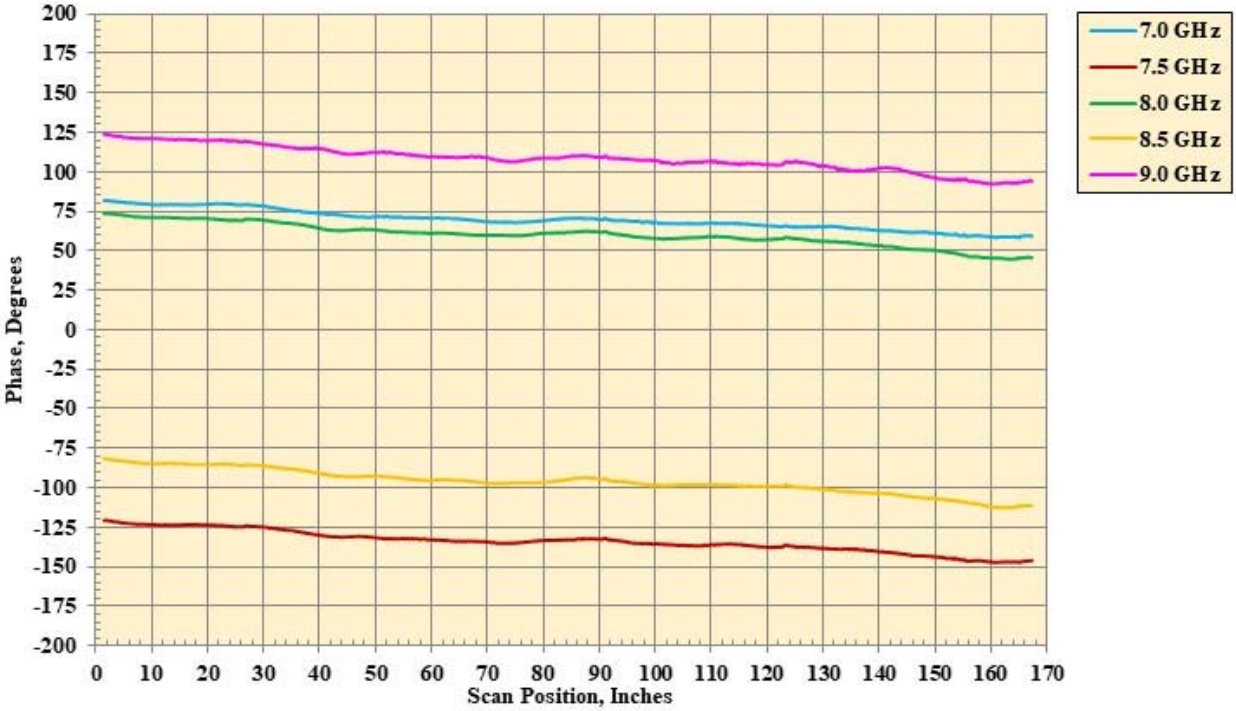

(h) Phase probe data, Probe Angle = 15°, Pol = VV.
Figure 19. Continued.

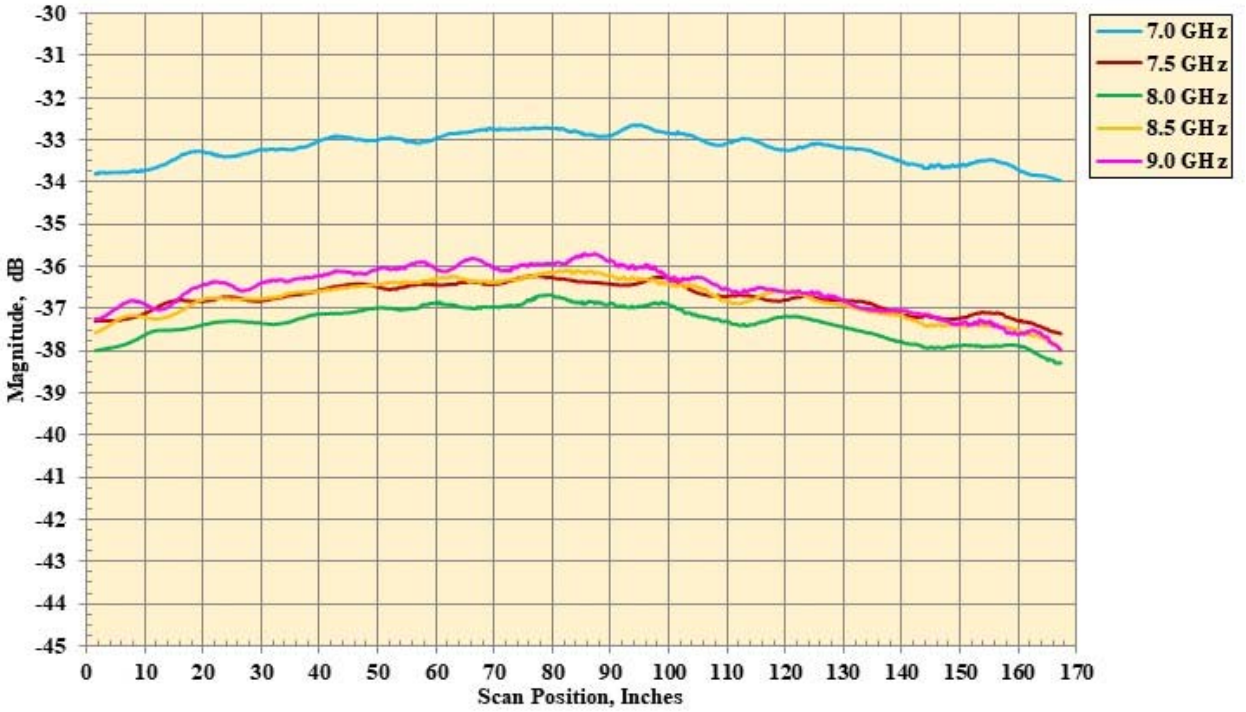

(i) Magnitude probe data, Probe Angle = 30°, Pol = HH.
Figure 19. Continued.

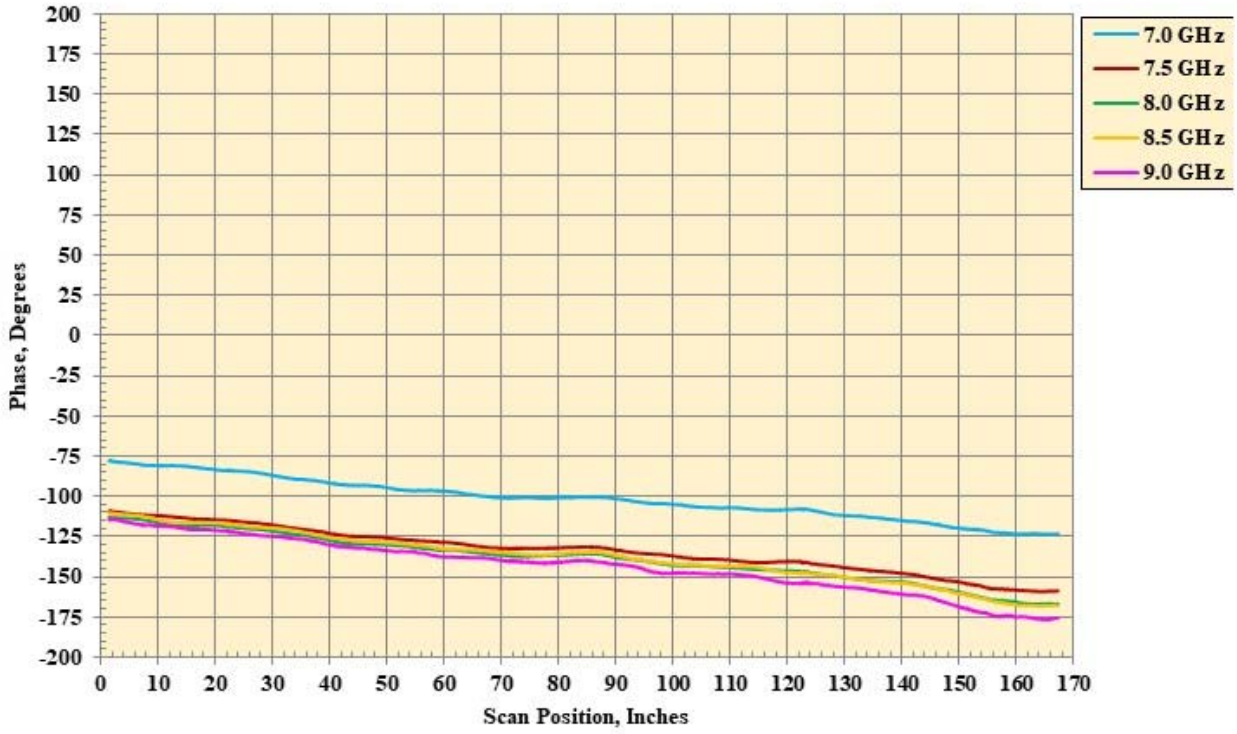

(j) Phase probe data, Probe Angle = 30°, Pol = HH.
Figure 19. Continued.

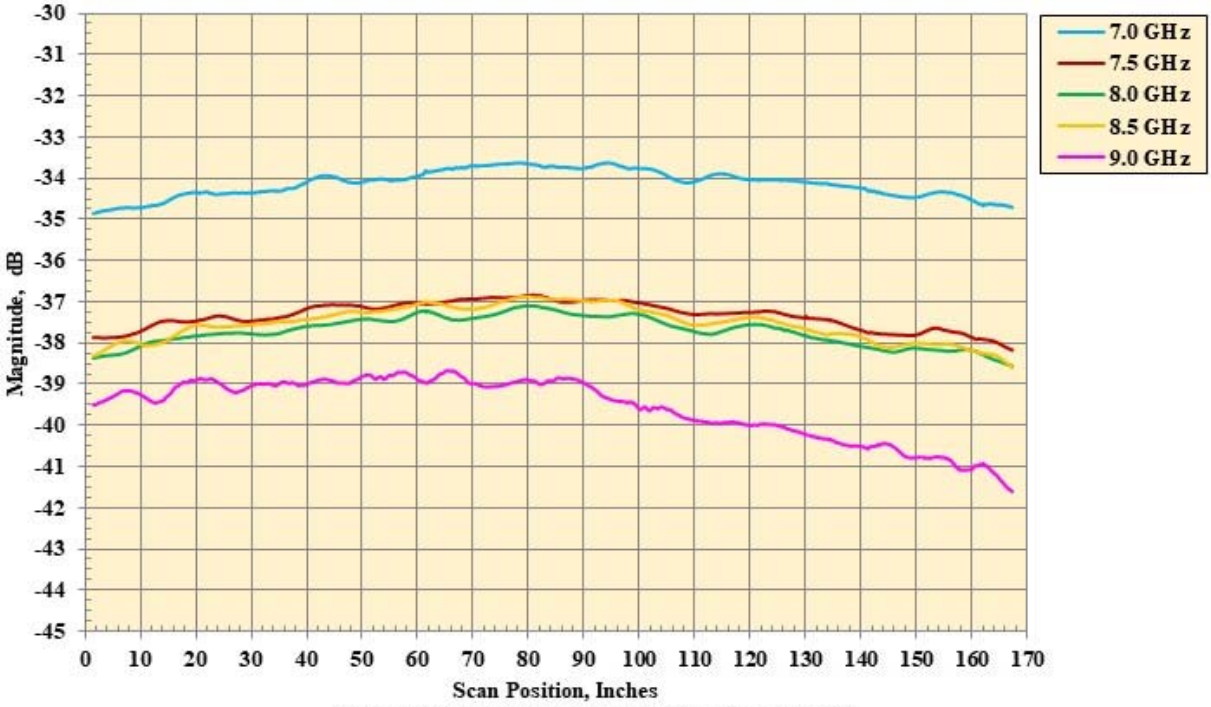

(k) Magnitude probe data, Probe Angle = 30°, Pol = VV.
Figure 19. Continued.

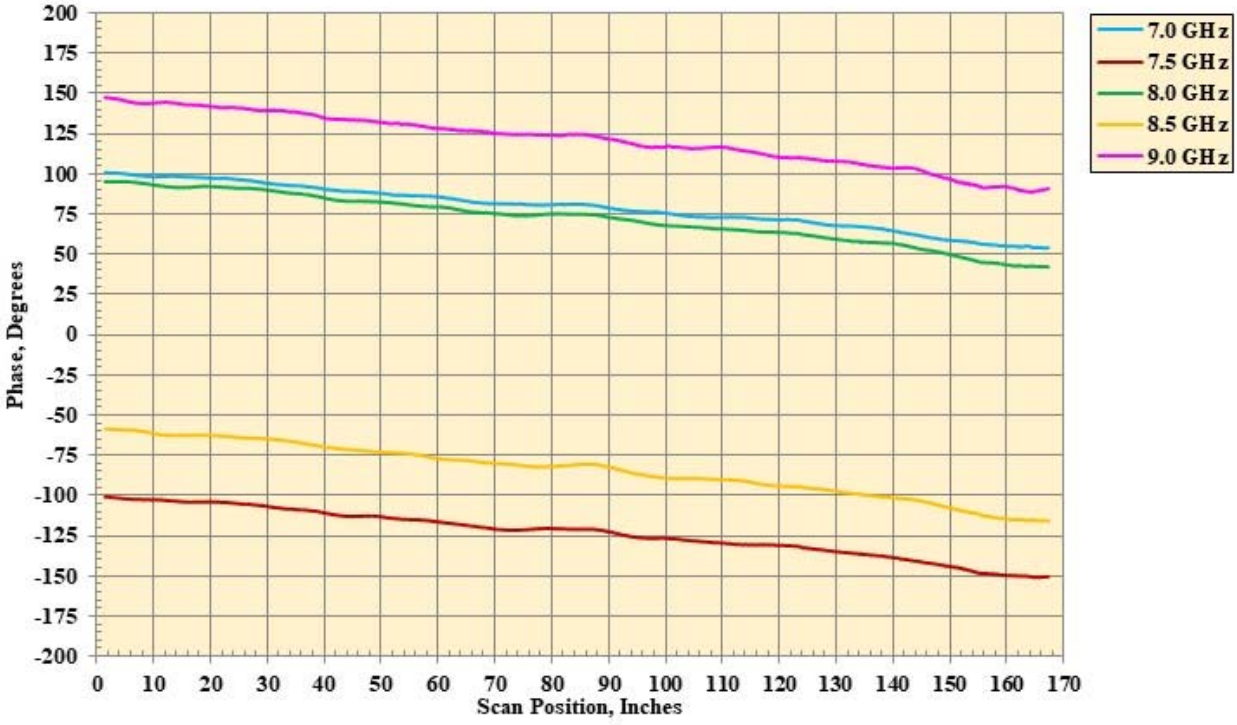

(l) Phase probe data, Probe Angle = 30°, Pol = VV.
Figure19. Continued.

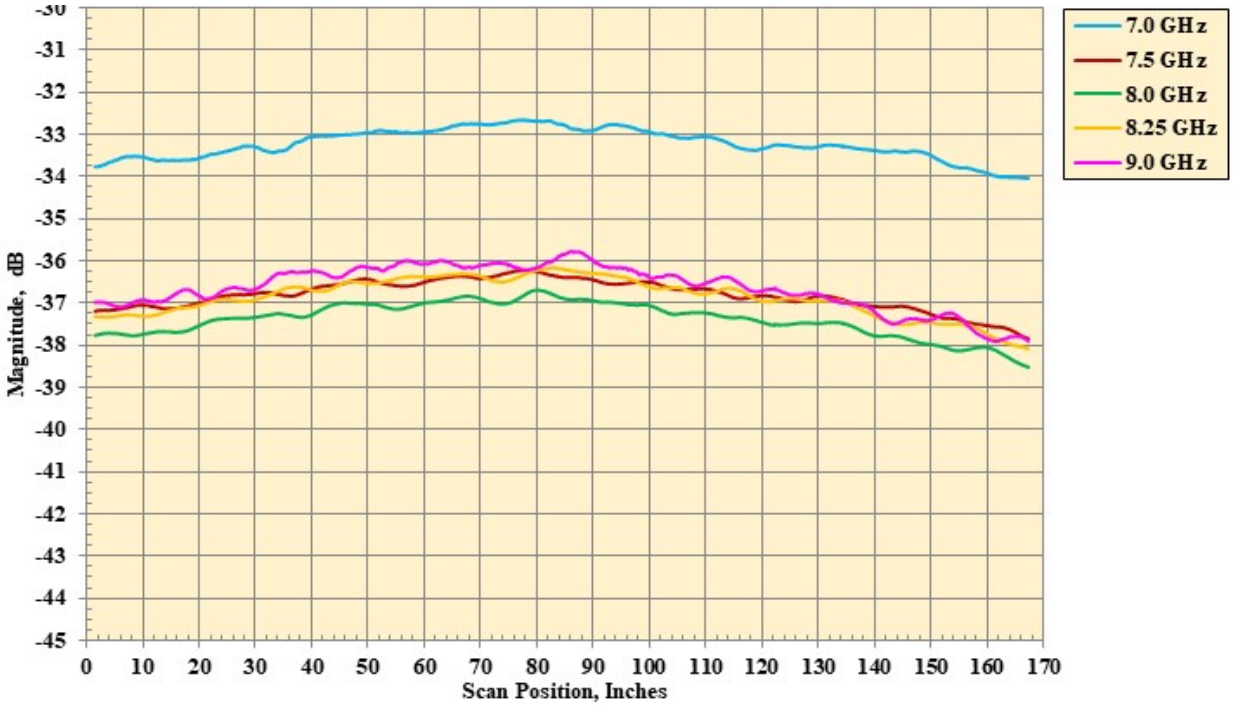

(m) Magnitude probe data, Probe Angle = 45°, Pol = HH.
Figure 19. Continued.

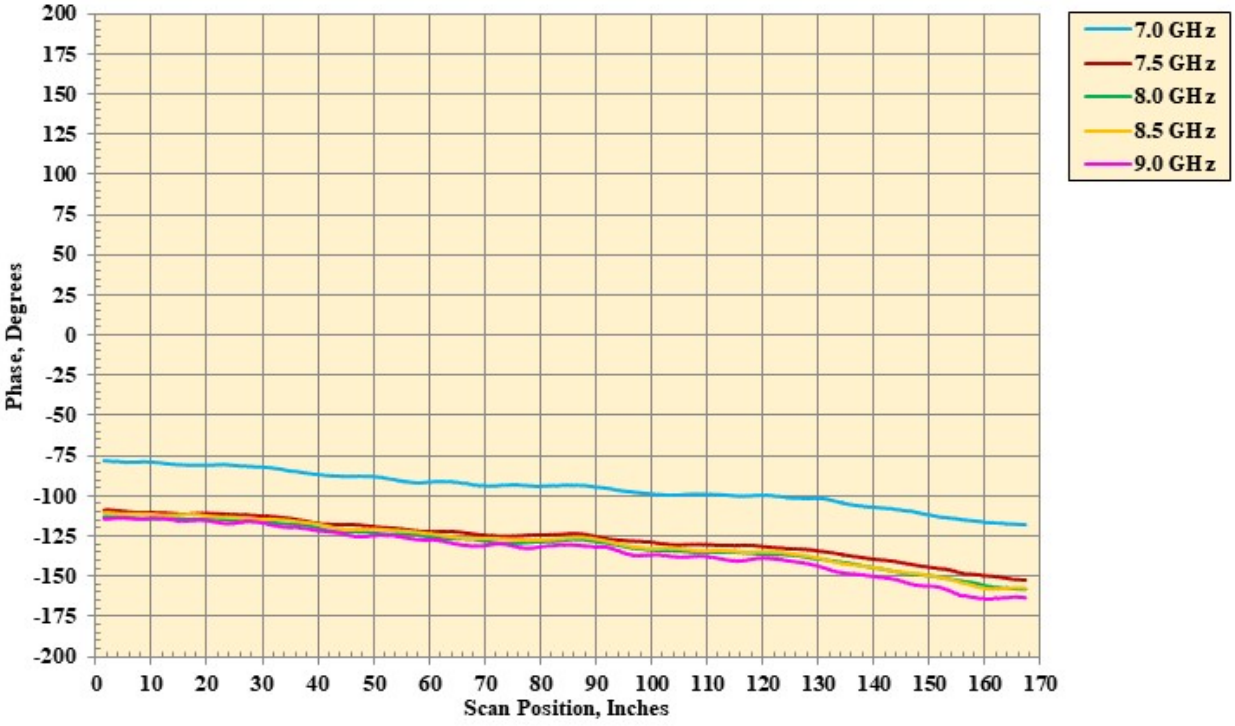

(n) Phase probe data, Probe Angle = 45°, Pol = HH.
Figure 19. Continued.

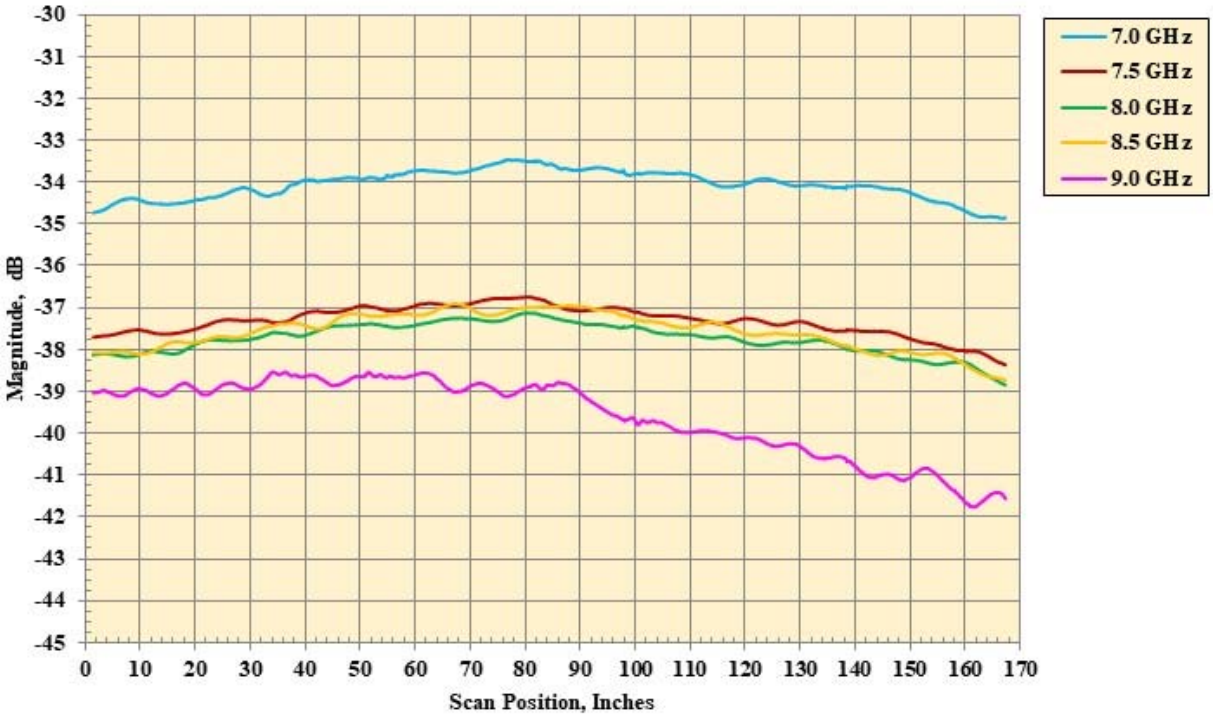

(o) Magnitude probe data, Probe Angle = 45°, Pol = VV.
Figure 19. Continued.

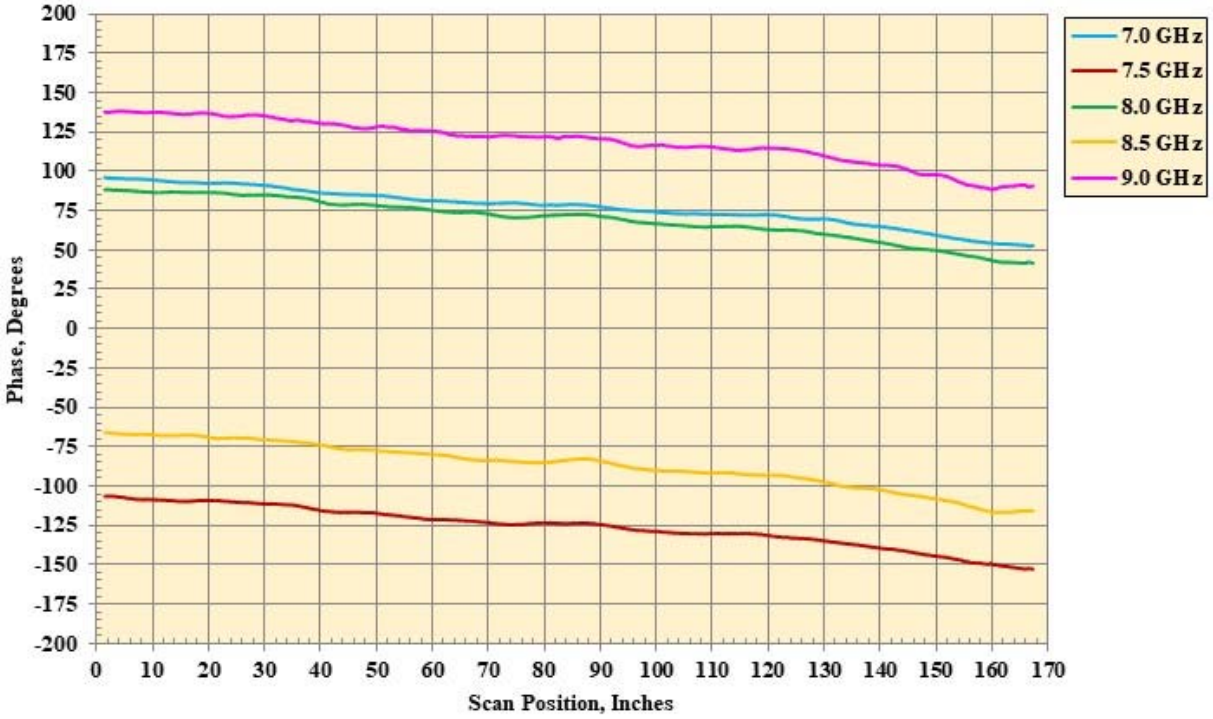

(p) Phase probe data, Probe Angle = 45°, Pol = VV.
Figure 19. Continued.

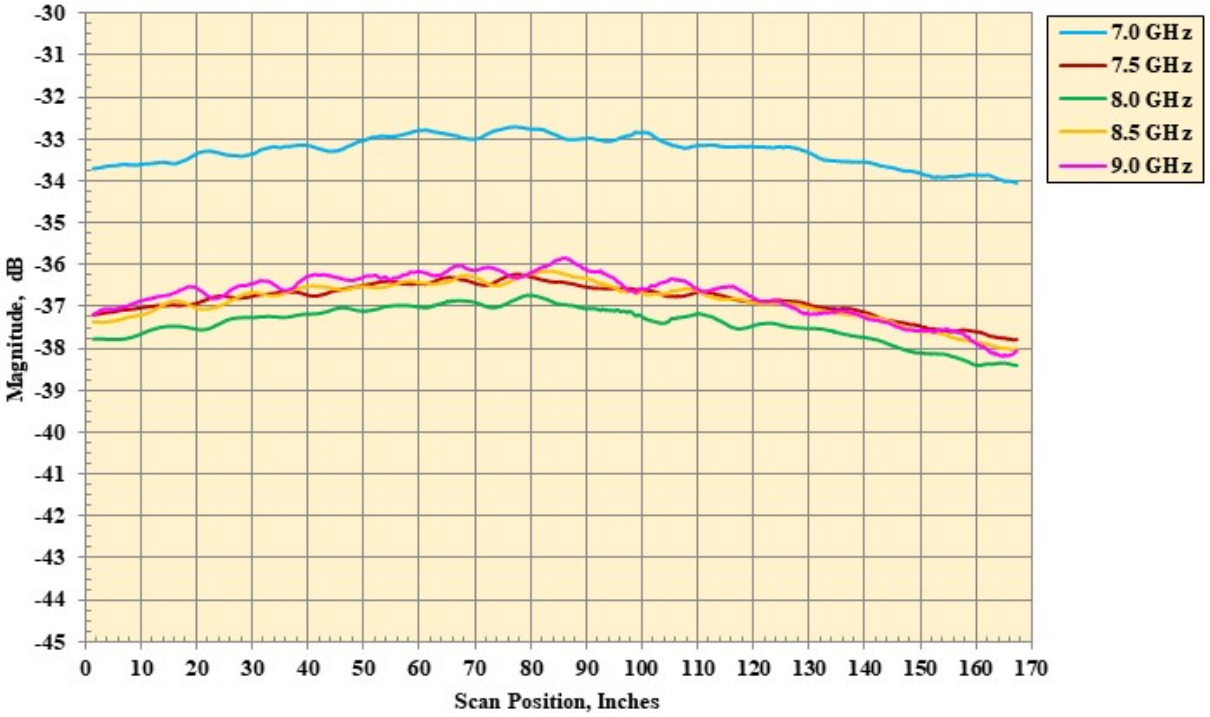

(q) Magnitude probe data, Probe Angle =60°, Pol = HH.
Figure 19. Continued.

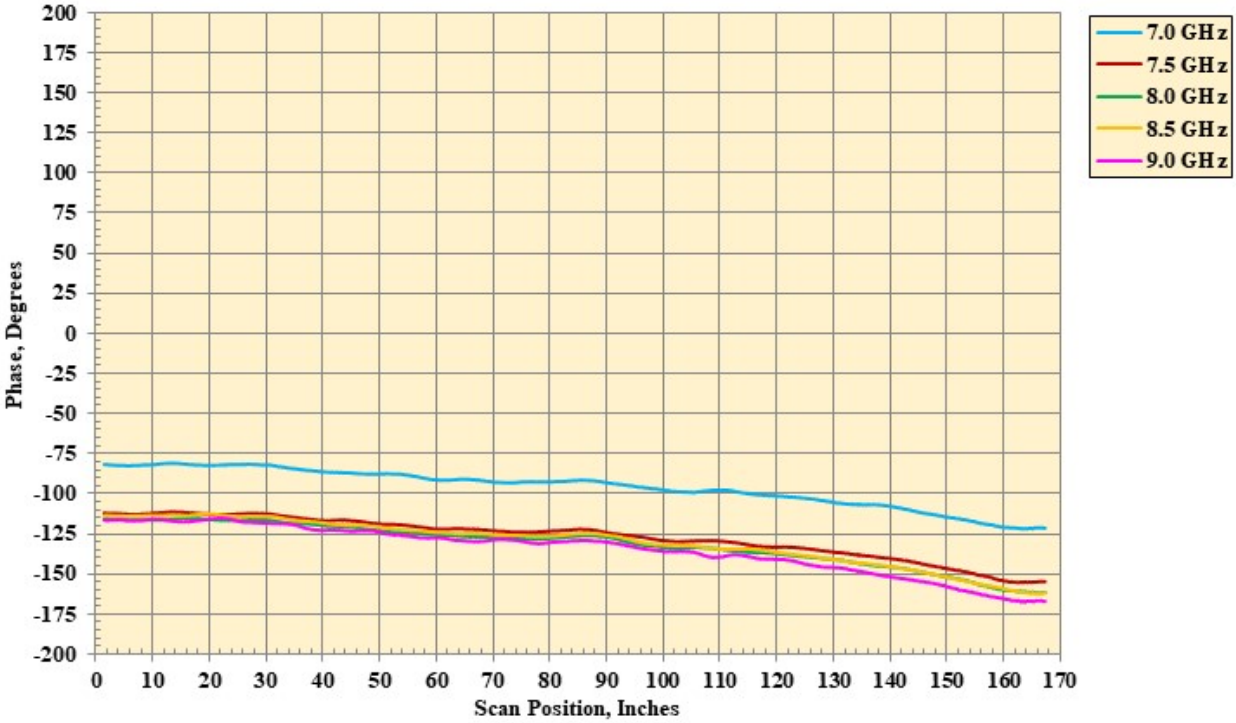

(r) Phase probe data, Probe Angle = 60°, Pol = HH.
Figure 19. Continued.

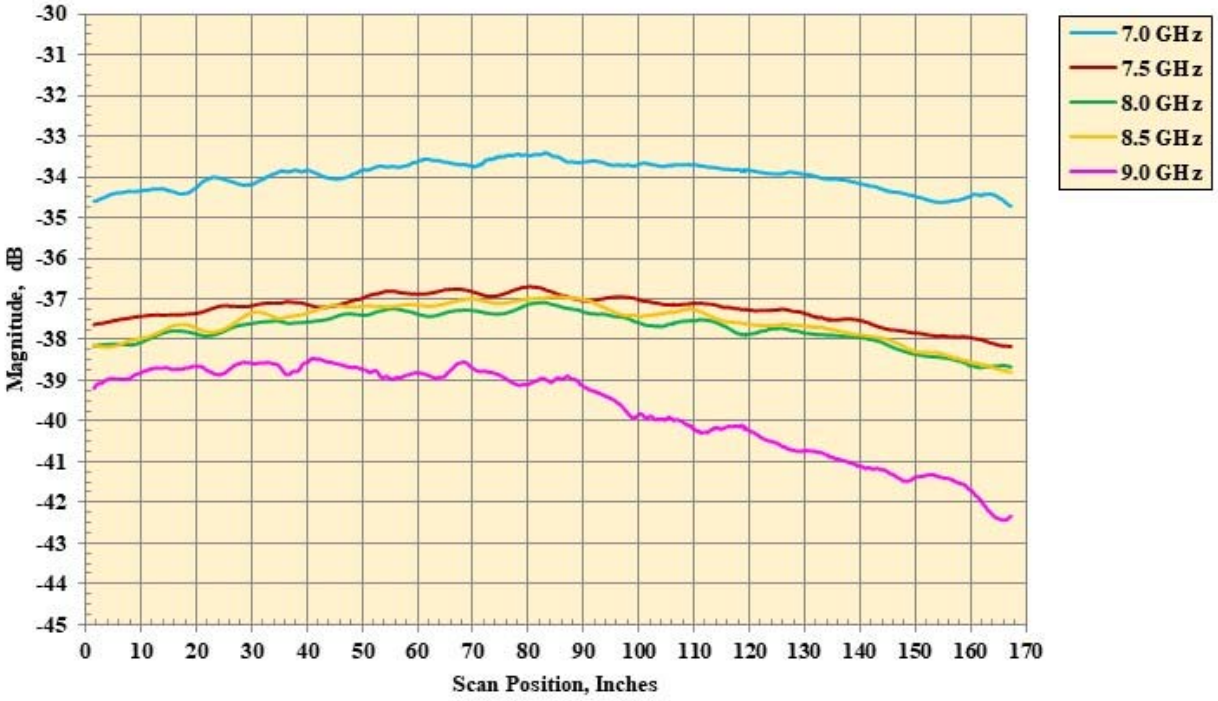

(s) Magnitude probe data, Probe Angle =60°, Pol = VV.
Figure 19. Continued.

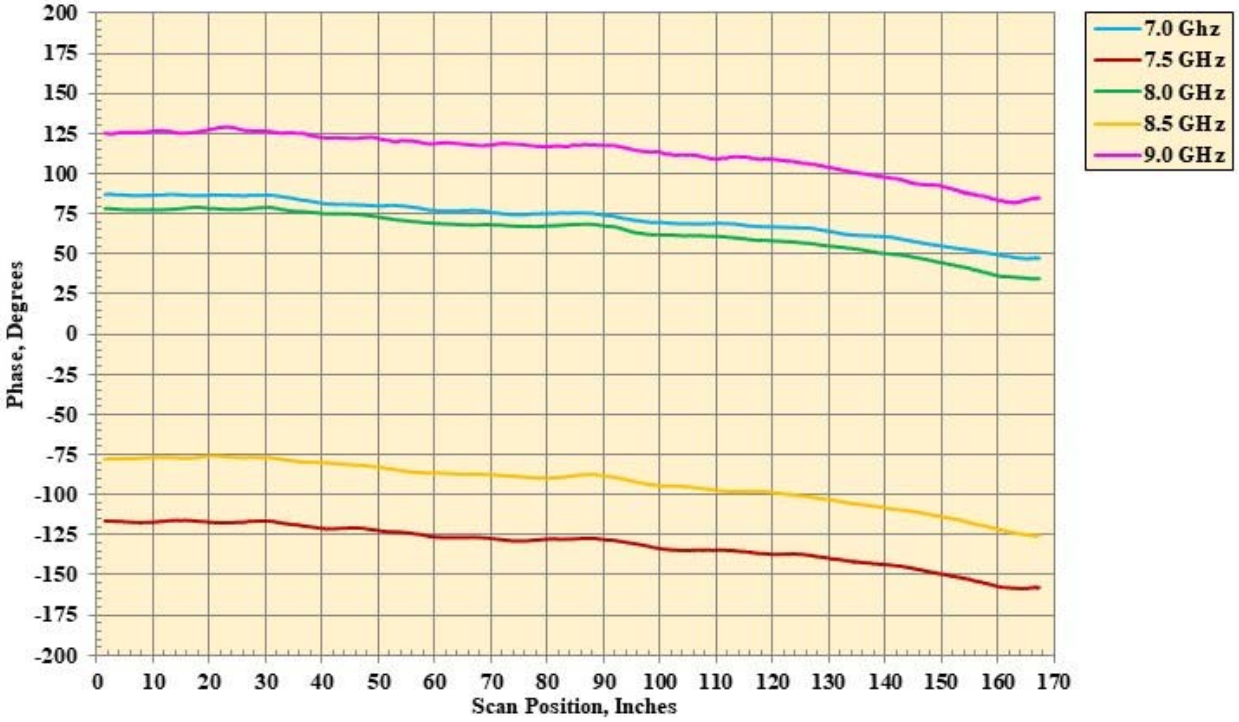

(t) Phase probe data, Probe Angle = 60°, Pol = VV.
Figure 19. Continued.

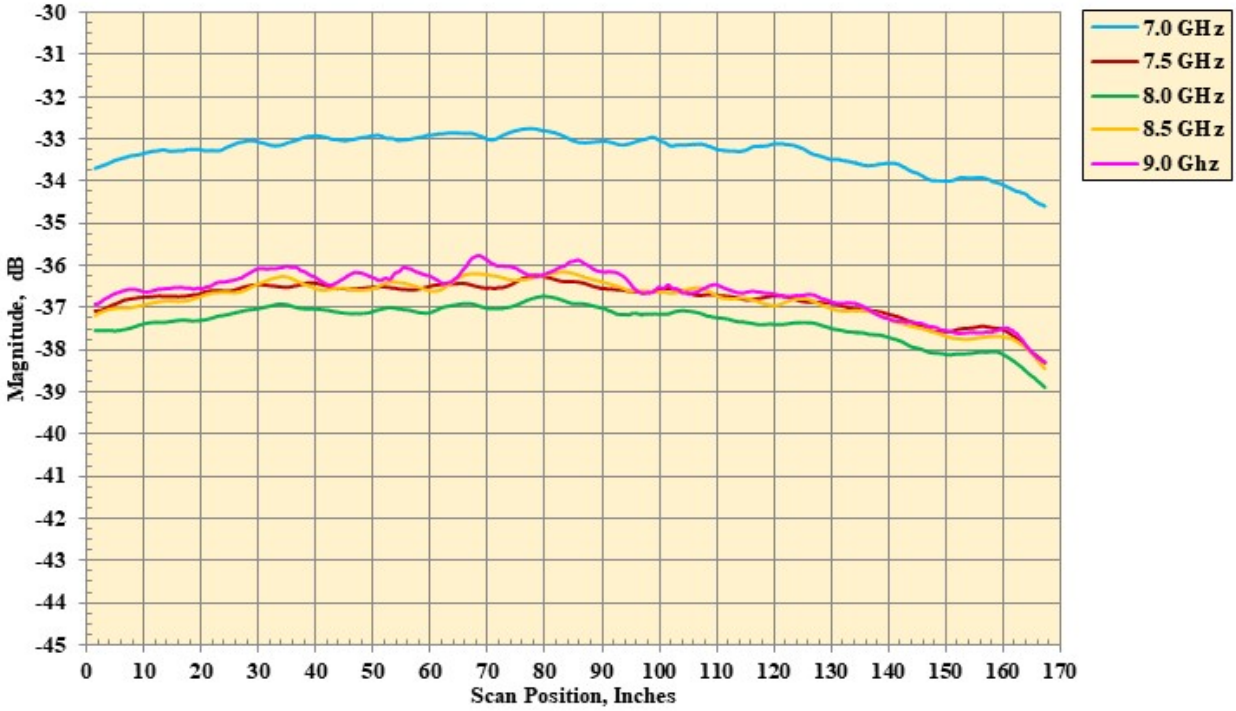

(u) Magnitude probe data, Probe Angle =75°, Pol = HH.
Figure 19. Continued.

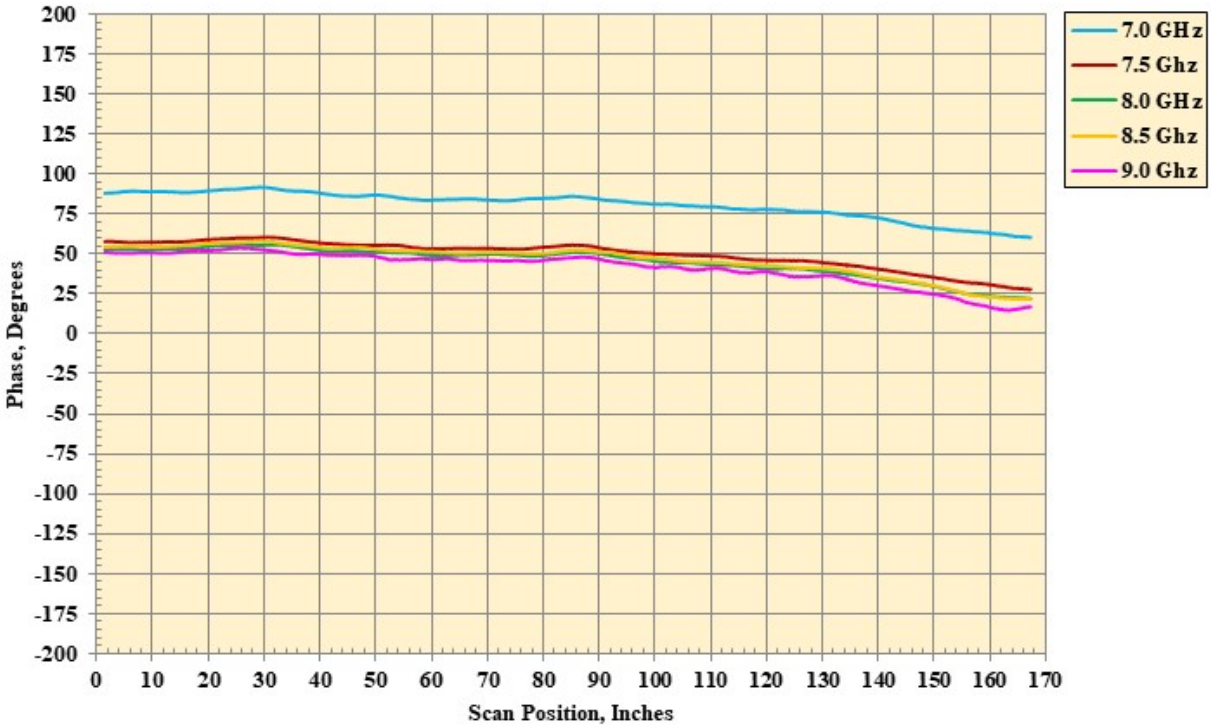

(v) Phase probe data, Probe Angle = 75°, Pol = HH.
Figure 19. Continued.

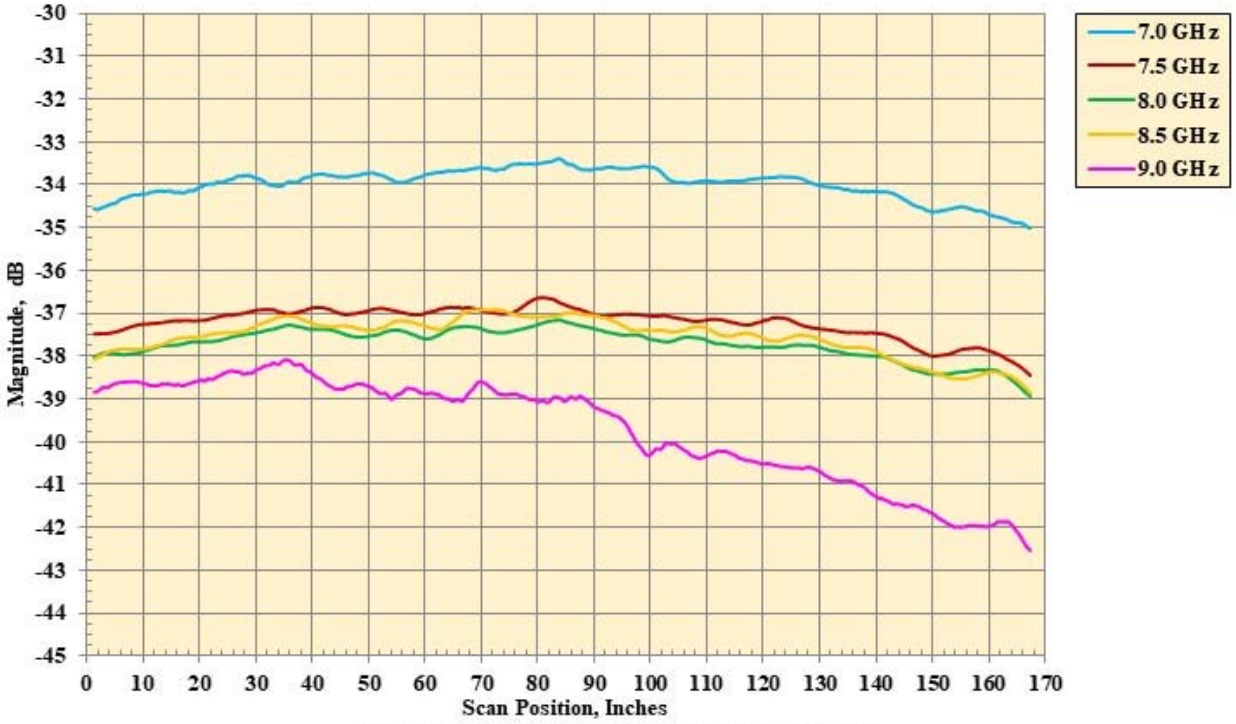

(w) Magnitude probe data, Probe Angle =75°, Pol = VV.
Figure 19. Continued.

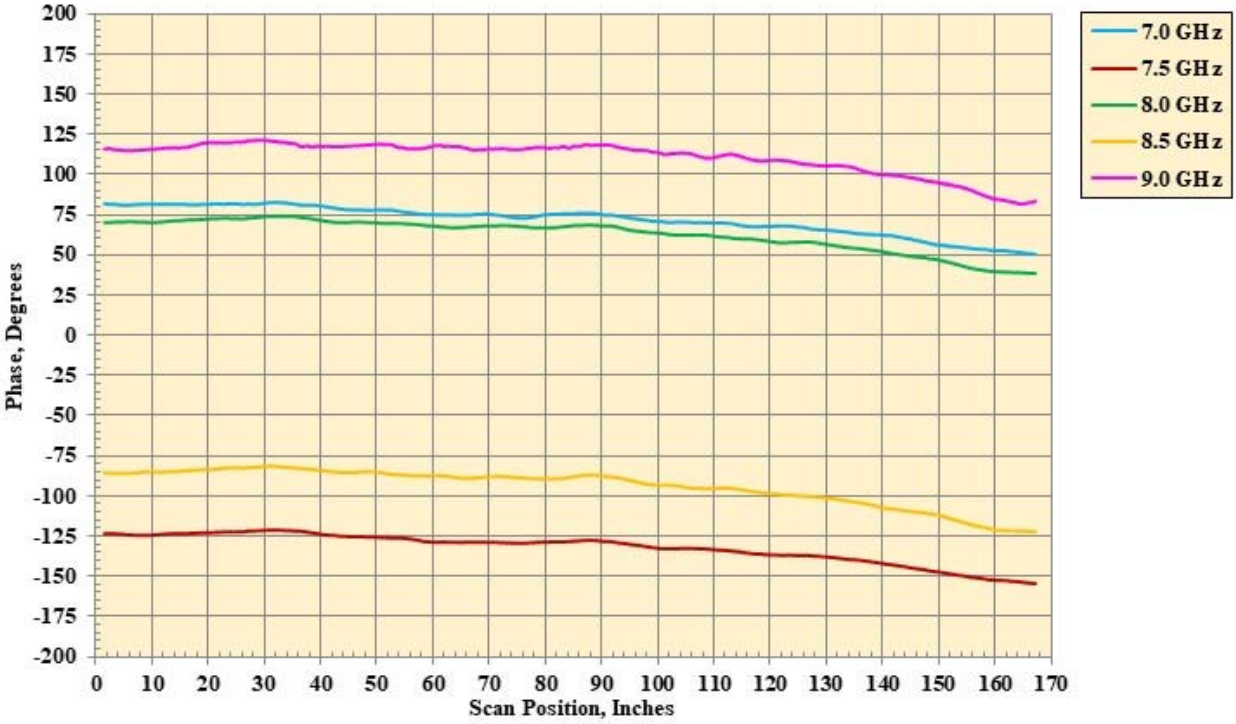

(x) Phase probe data, Probe Angle = 75°, Pol = VV.
Figure 19. Continued.

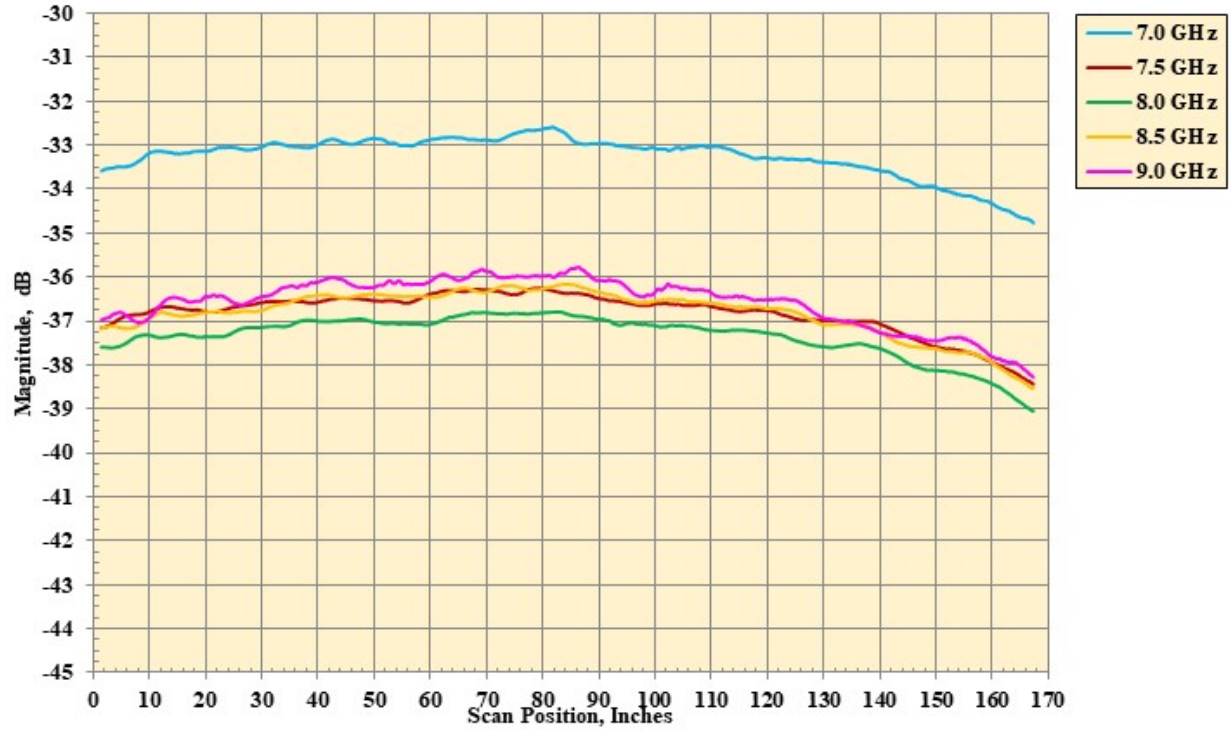

(y) Magnitude probe data, Probe Angle = 90°, Pol = HH.
Figure 19. Continued.

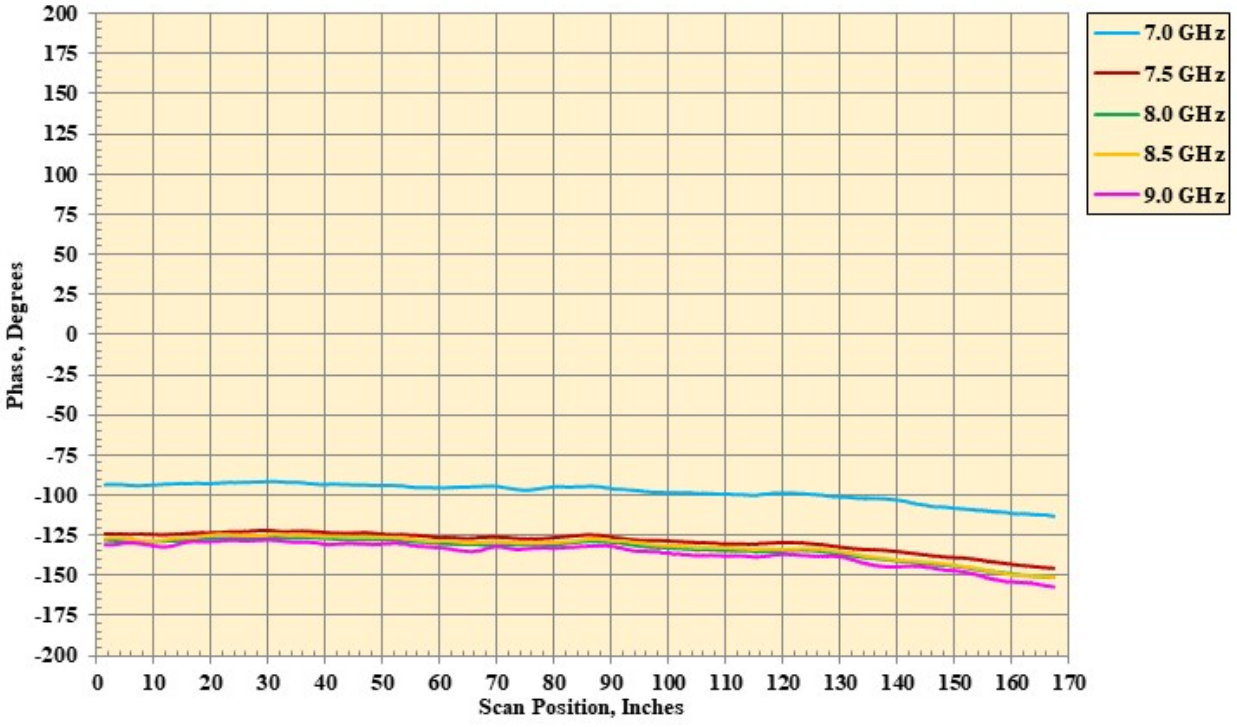

(z) Phase probe data, Probe Angle = 90°, Pol = HH.
Figure 19. Continued.

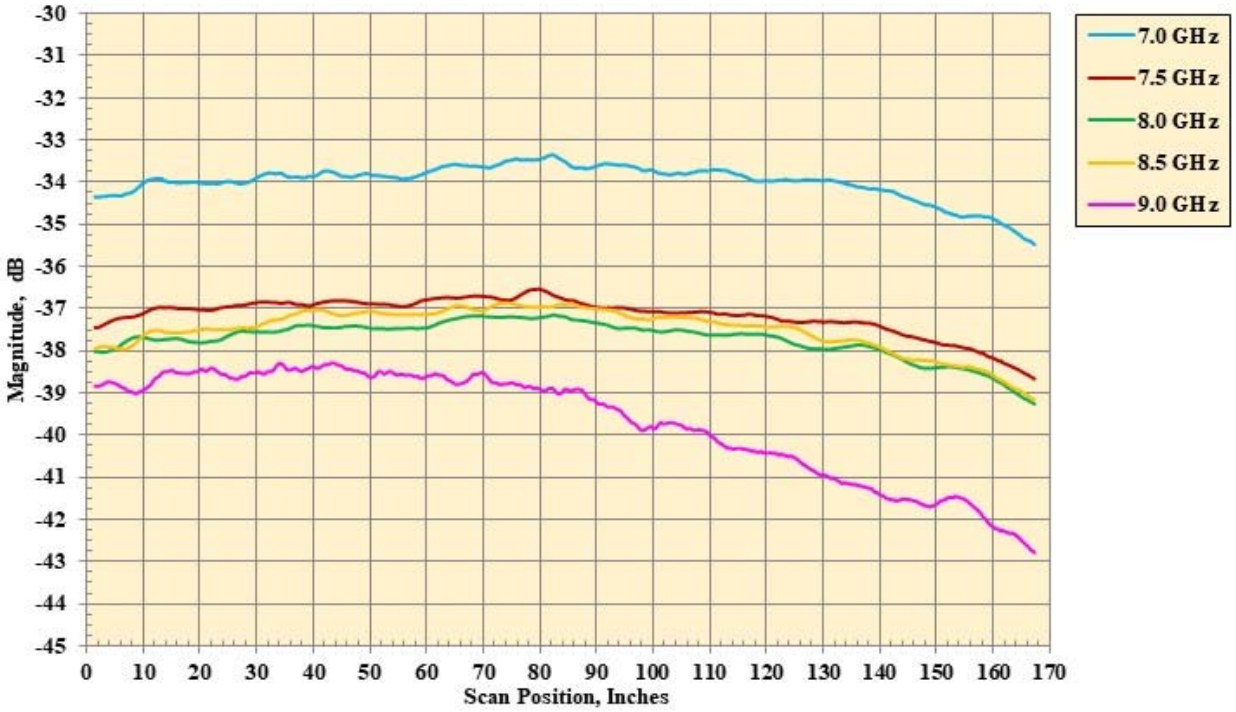

(aa) Magnitude probe data, Probe Angle = 90°, Pol = VV.
Figure 19. Continued.

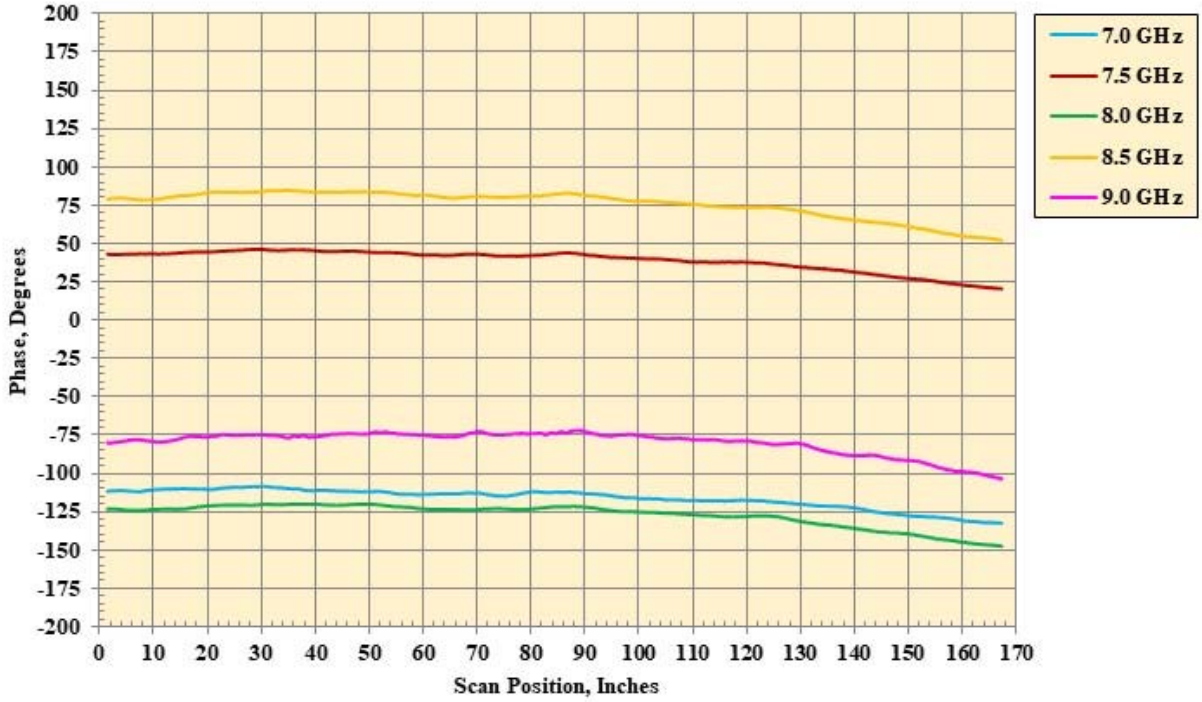

(bb) Phase probe data, Probe Angle = 90°, Pol = VV.
Figure 19. Continued.

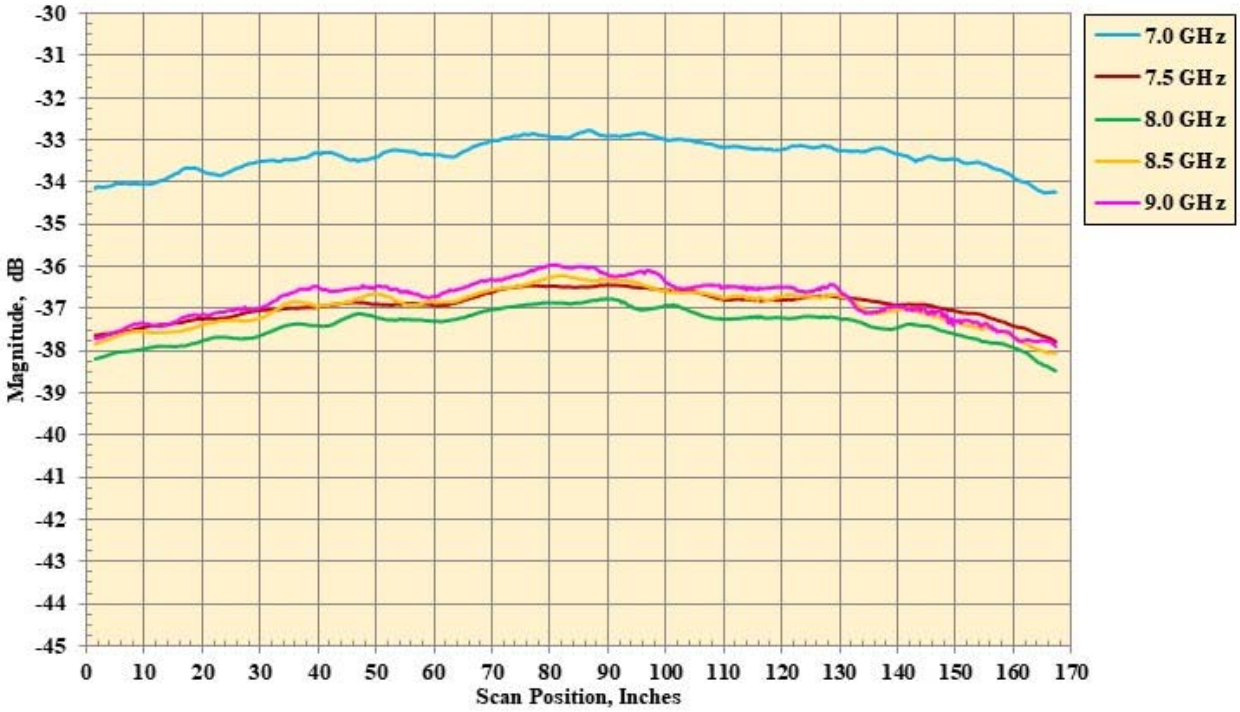

(cc) Magnitude probe data, Probe Angle = -15°, Pol = HH.
Figure 19. Continued.

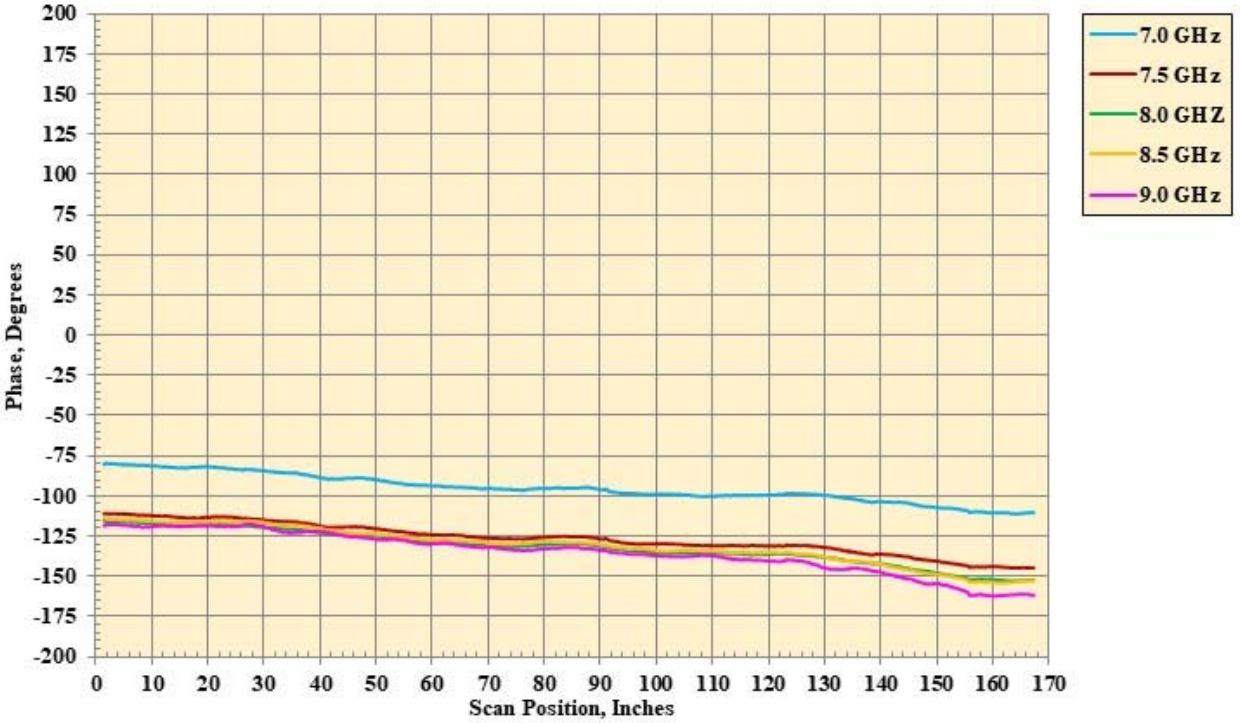

(dd) Phase probe data, Probe Angle = -15°, Pol = HH.
Figure 19. Continued.

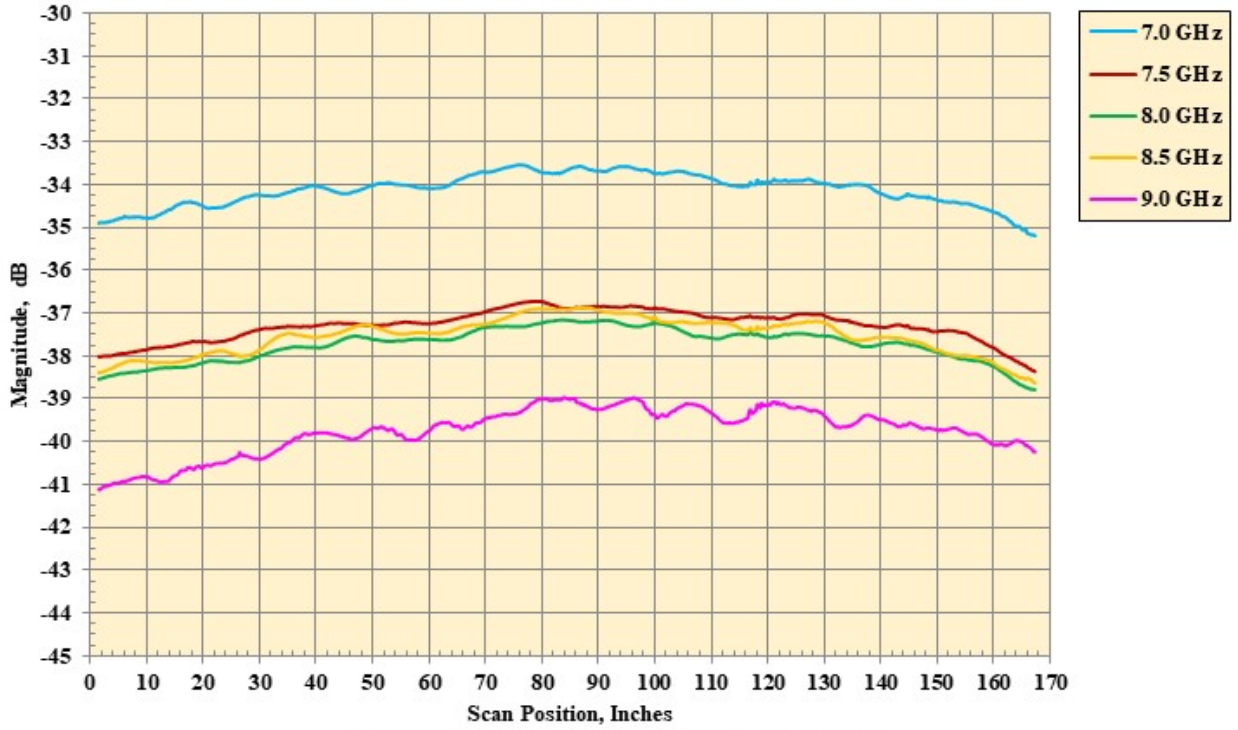

(ee) Magnitude probe data, Probe Angle = -15°, Pol = VV.
Figure 19. Continued.

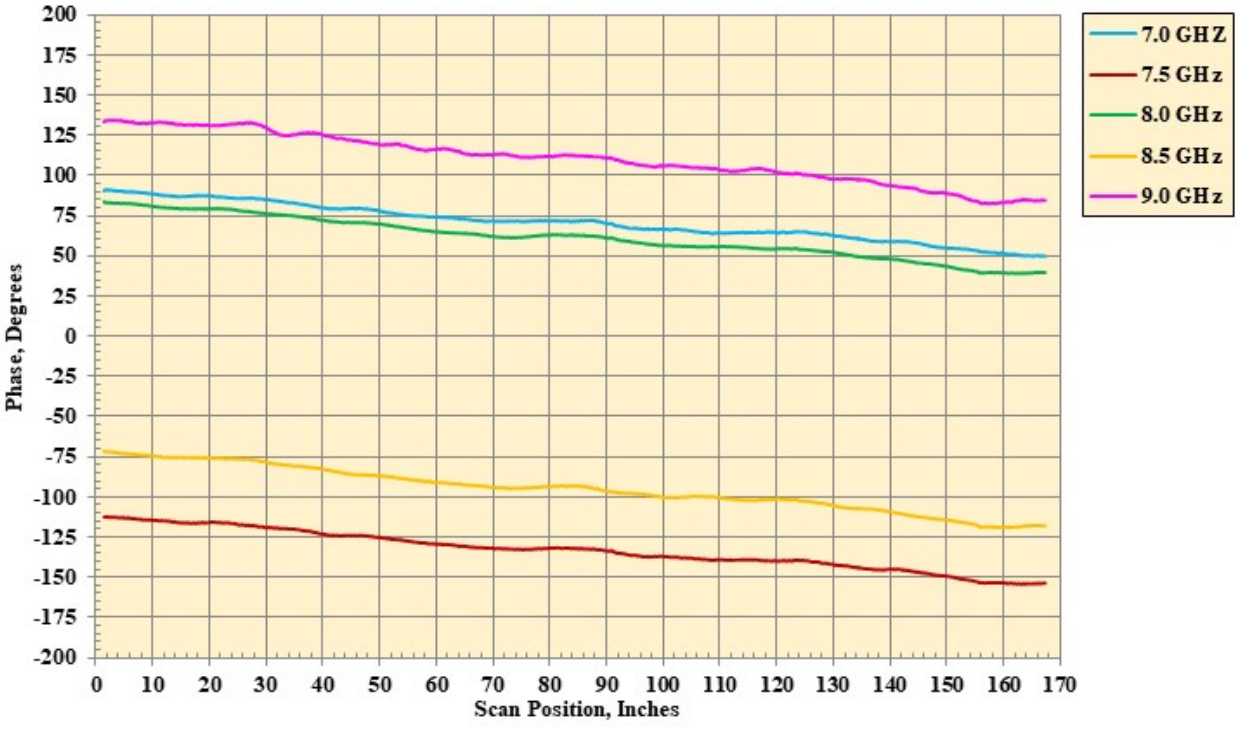

(ff) Phase probe data, Probe Angle = -15°, Pol = VV.
Figure 19. Continued.

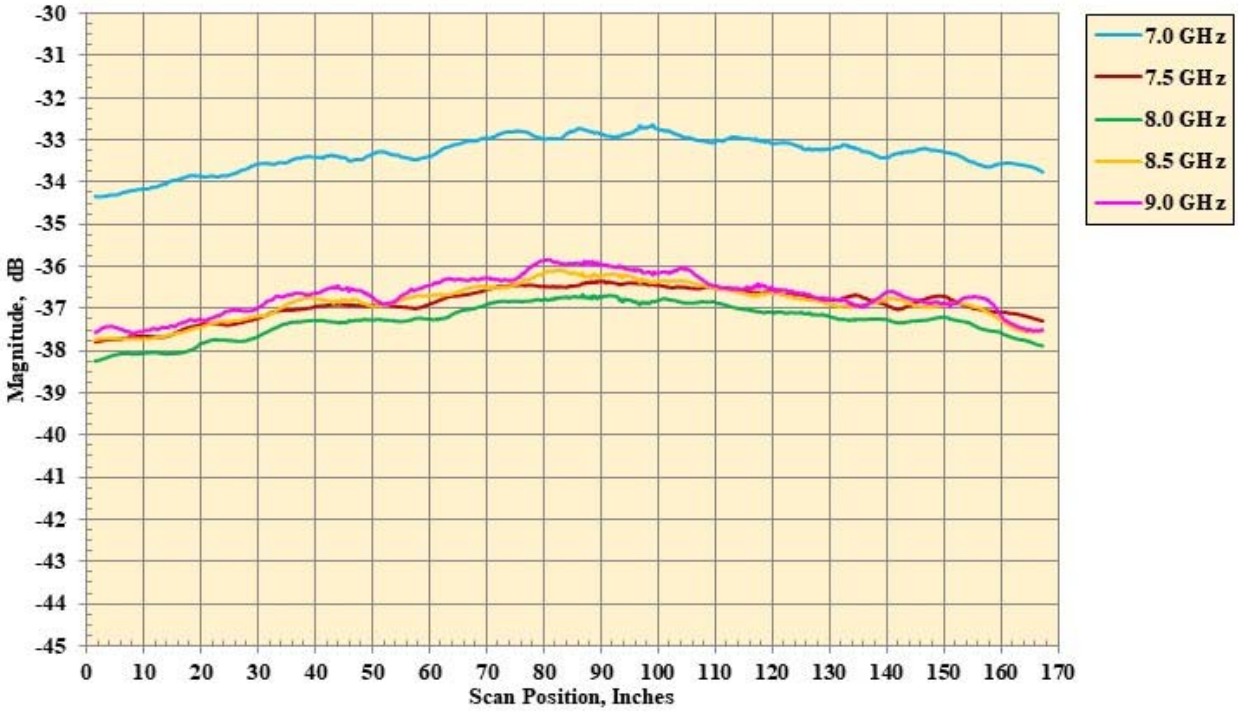

(gg) Magnitude probe data, Probe Angle = -30°, Pol = HH.
Figure 19. Continued.

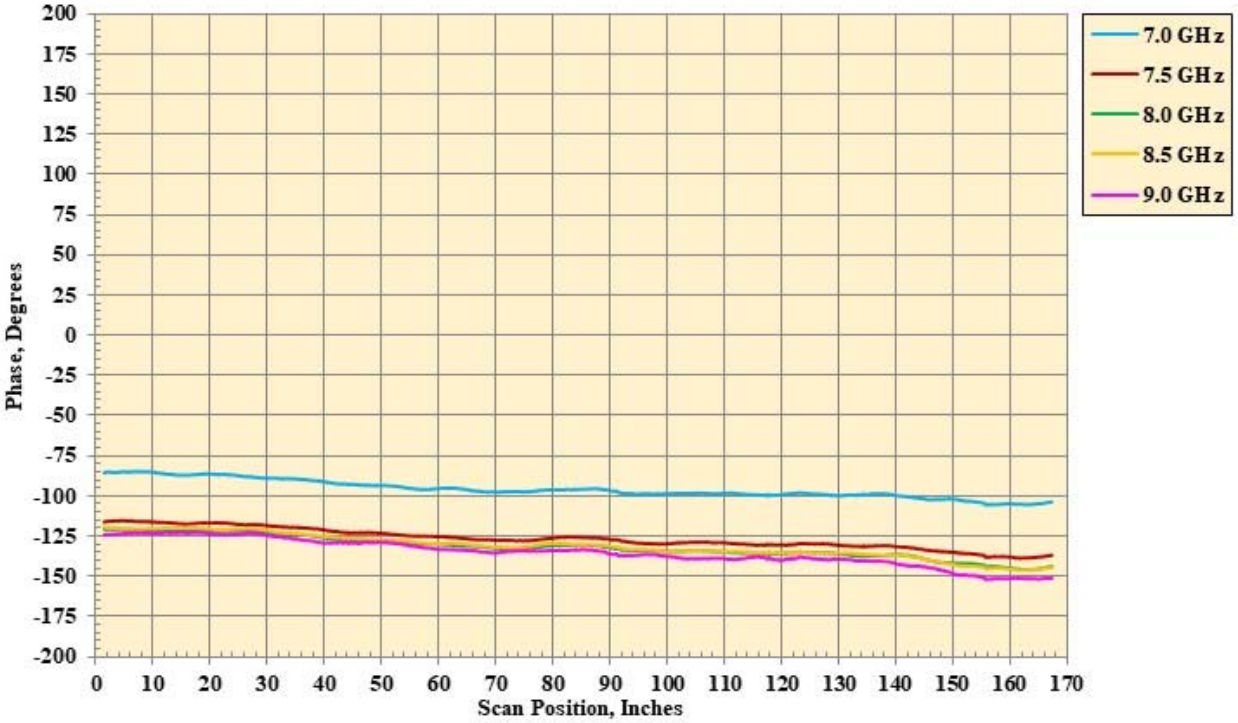

(hh) Phase probe data, Probe Angle = -30°, Pol = HH.
Figure 19. Continued.

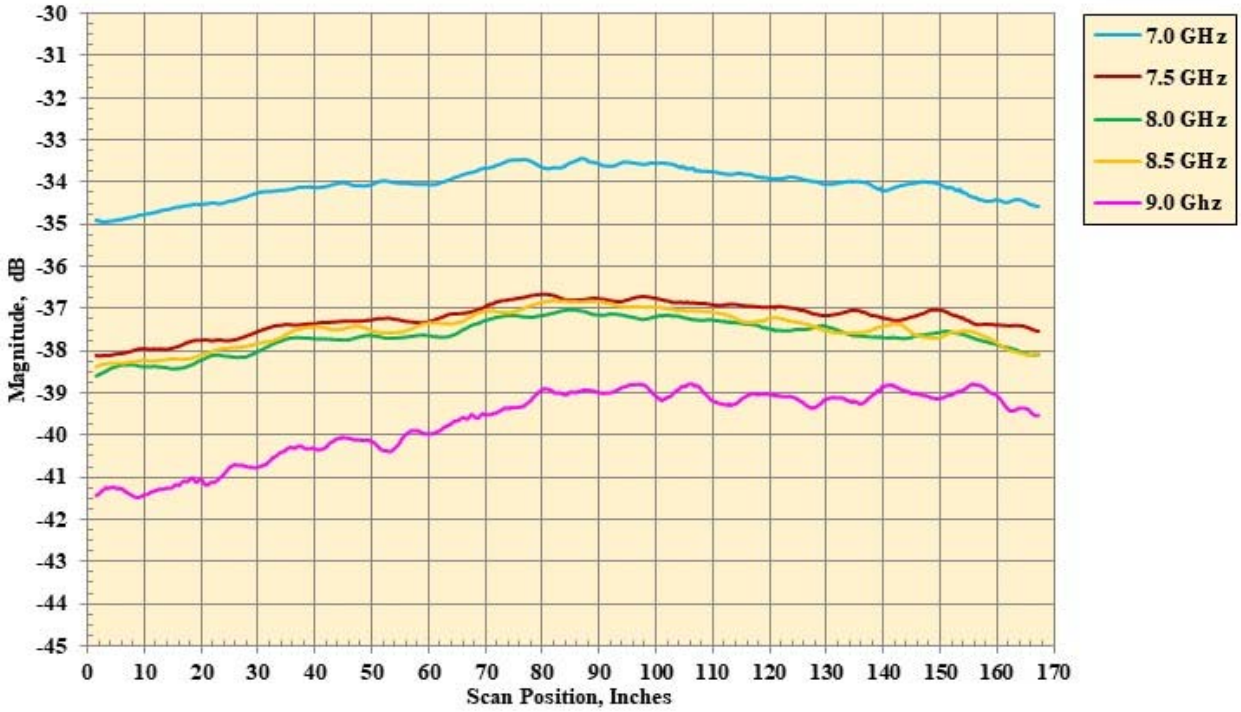

(ii) Magnitude probe data, Probe Angle = -30°, Pol = VV.
Figure 19. Continued.

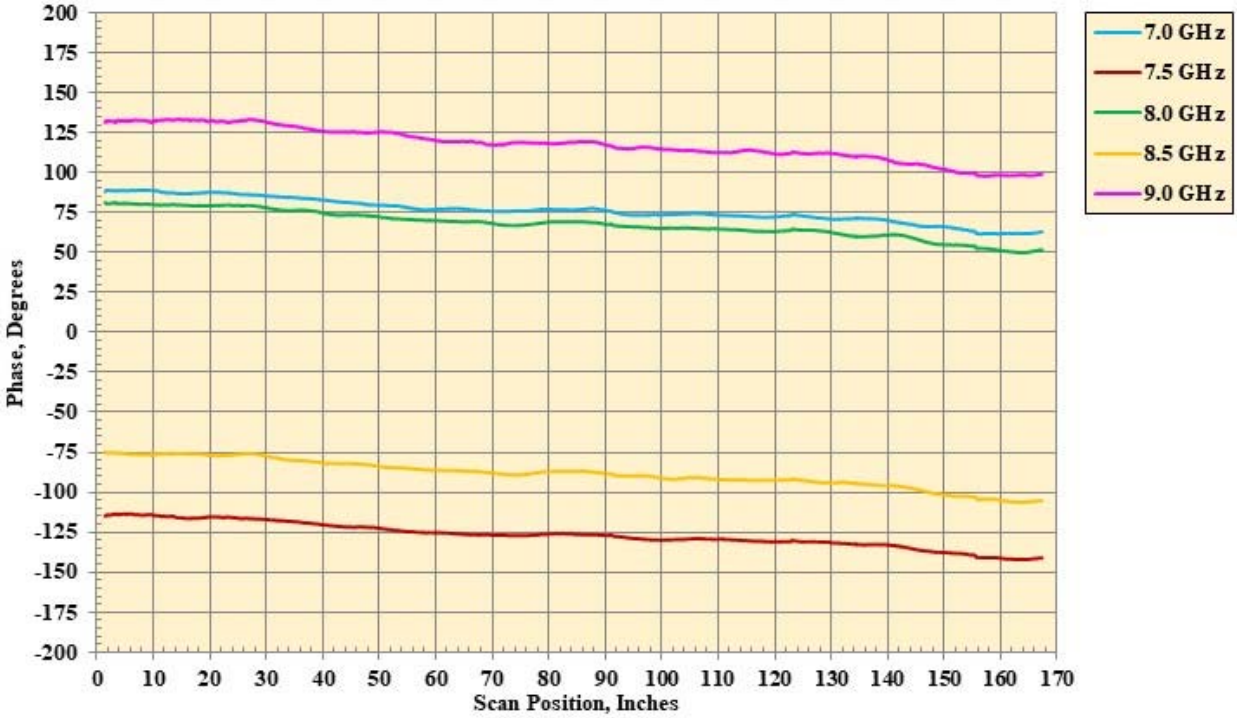

(jj) Phase probe data, Probe Angle = -30°, Pol =VV.
Figure 19. Continued.

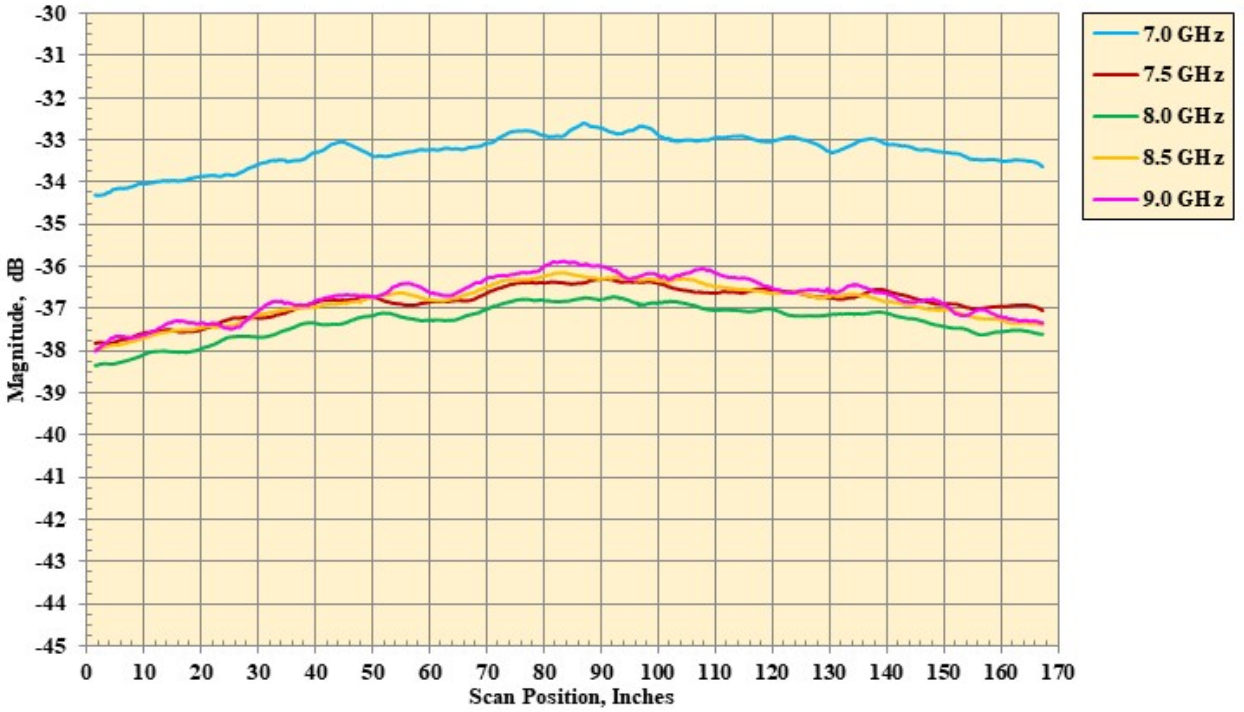

(ll) Magnitude probe data, Probe Angle = -45°, Pol = HH.
Figure 19. Continued.

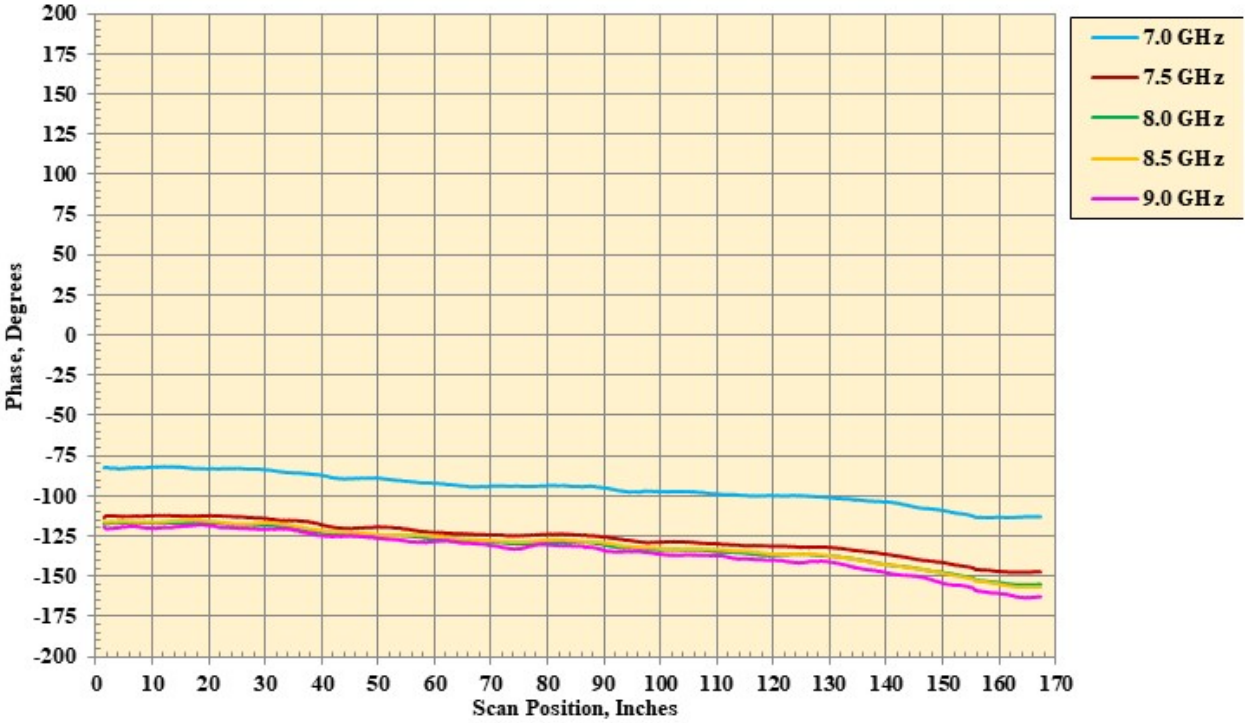

(mm) Phase probe data, Probe Angle = -45°, Pol = HH.
Figure 19. Continued.

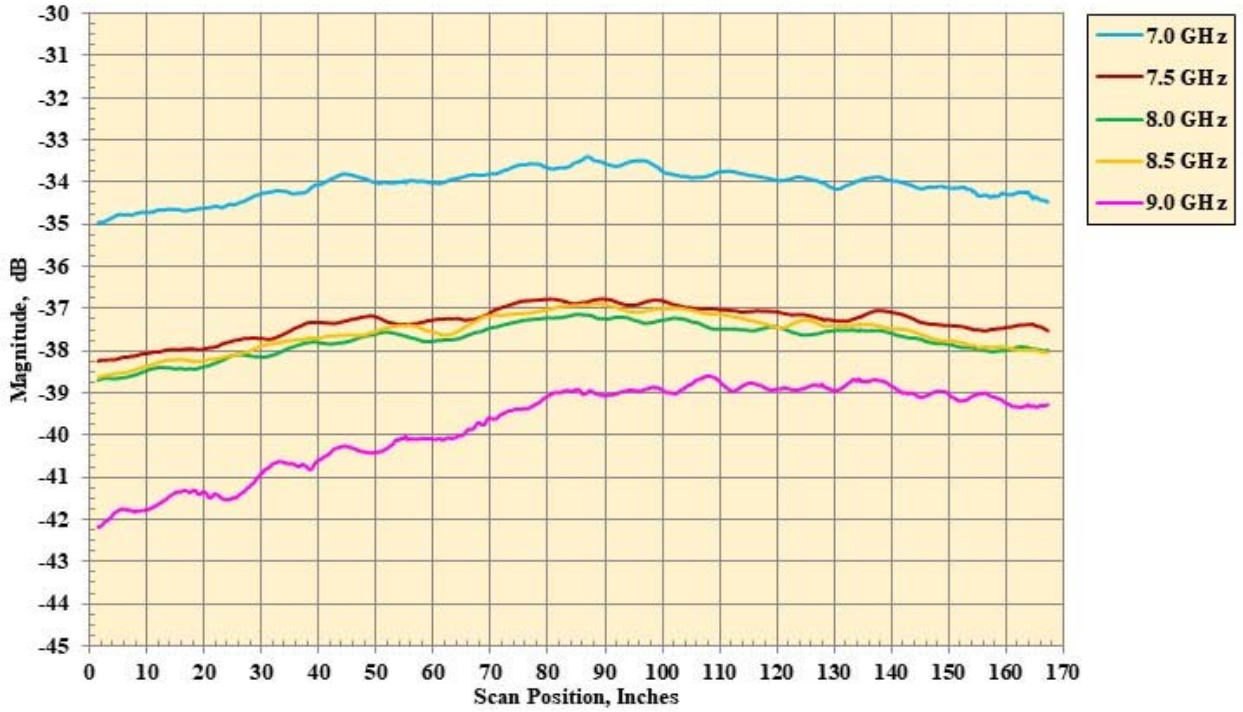

(oo) Magnitude probe data, Probe Angle = -45°, Pol = VV.
Figure 19. Continued.

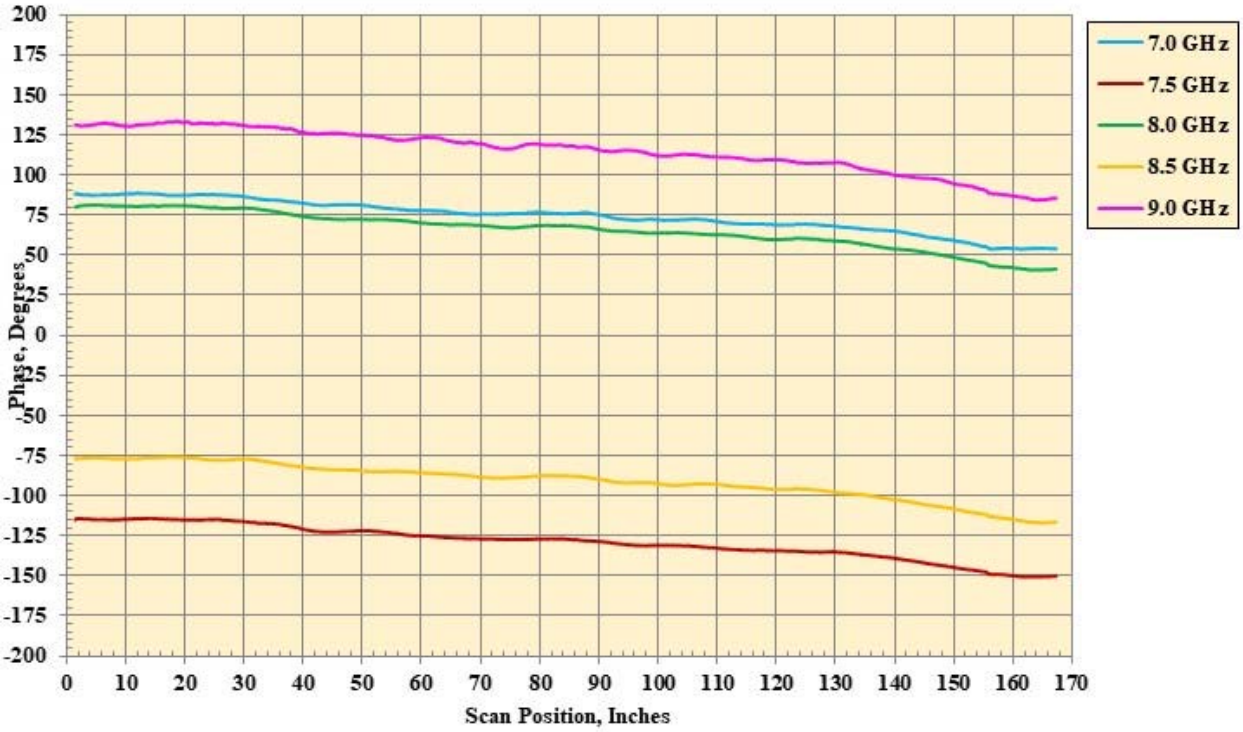

(pp) Phase probe data, Probe Angle = -45°, Pol = VV.
Figure 19. Continued.

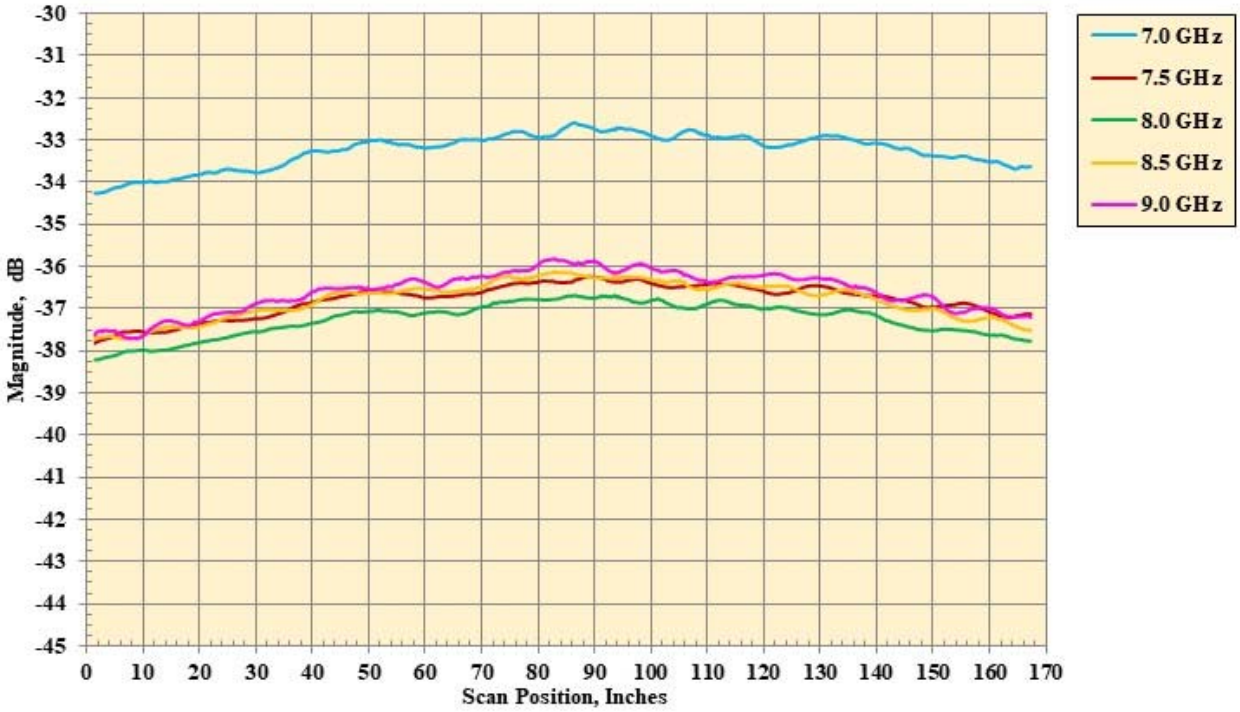

(qq) Magnitude probe data, Probe Angle = -60°, Pol = HH.
Figure 19. Continued.

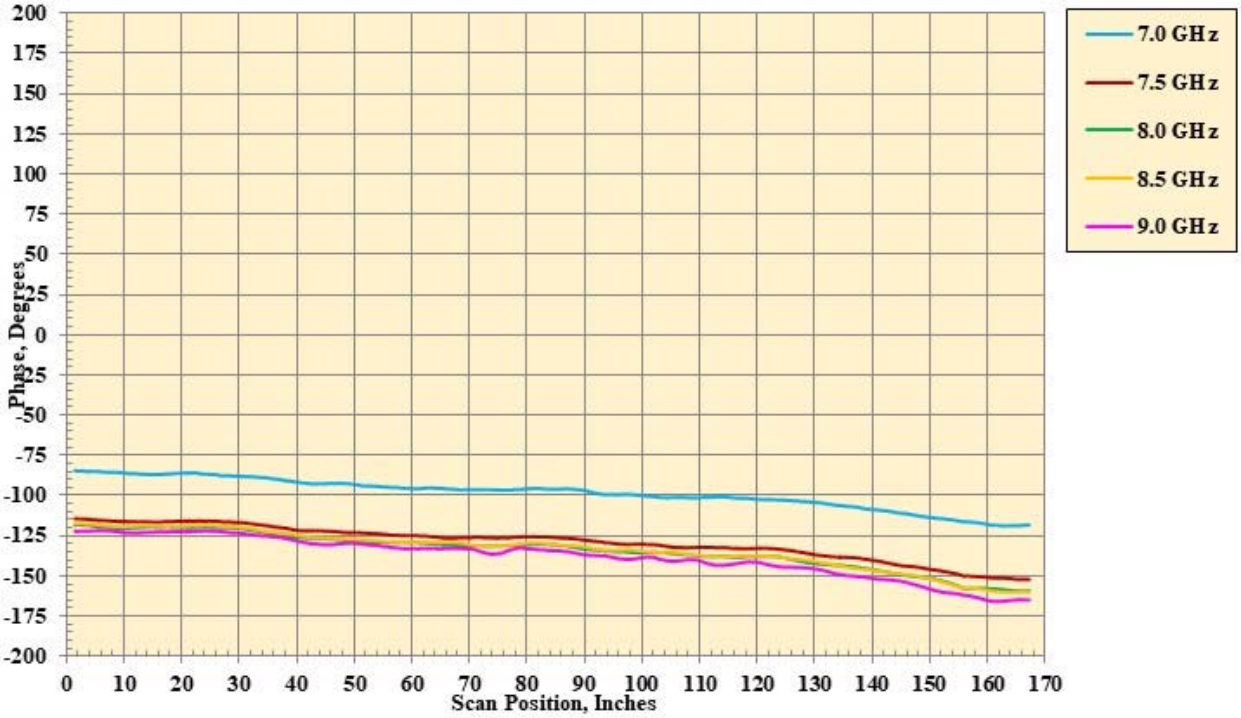

(rr) Phase probe data, Probe Angle = -60°, Pol = HH.
Figure 19. Continued.

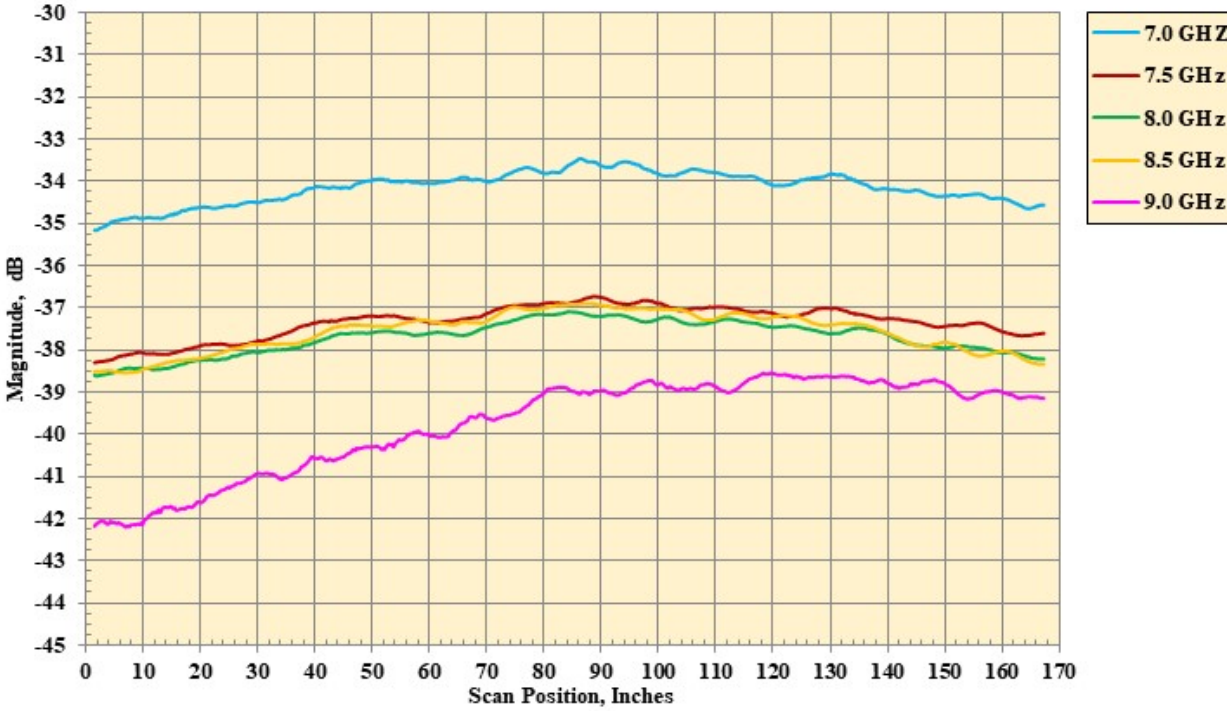

(ss) Magnitude probe data, Probe Angle = -60°, Pol = VV.
Figure 19. Continued.

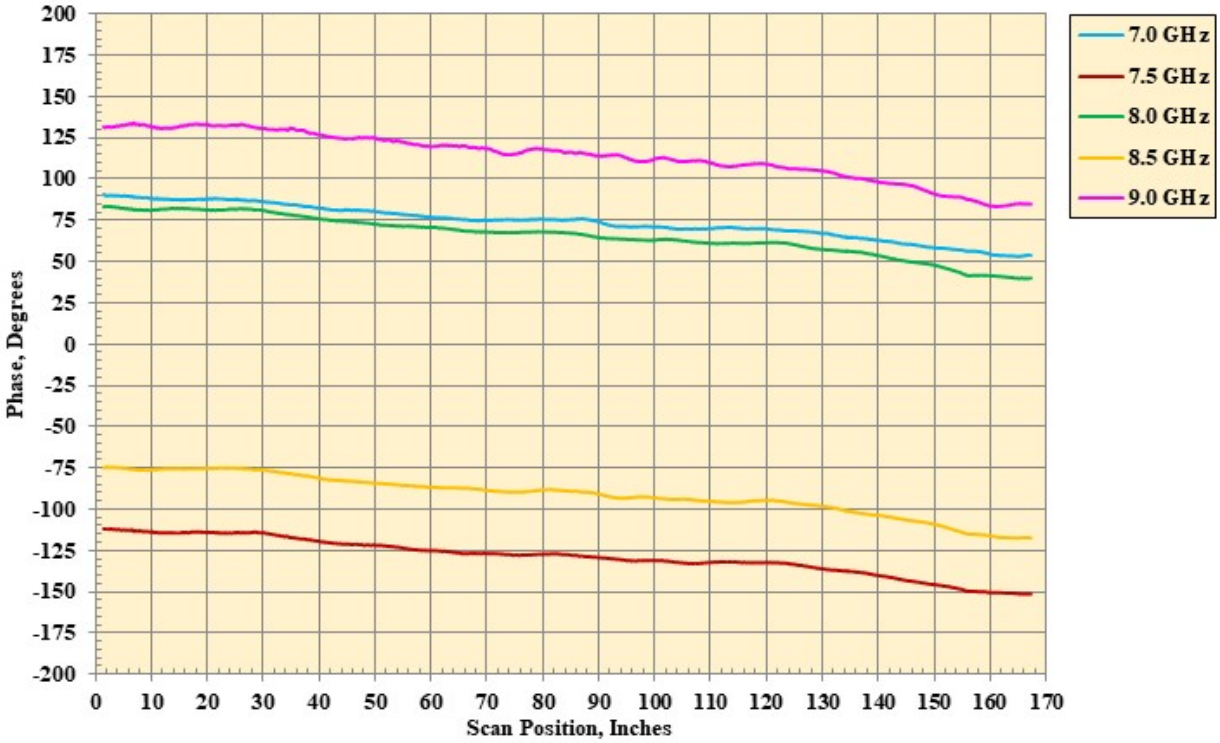

(tt) Phase probe data, Probe Angle = -60°, Pol = VV.
Figure 19. Continued.

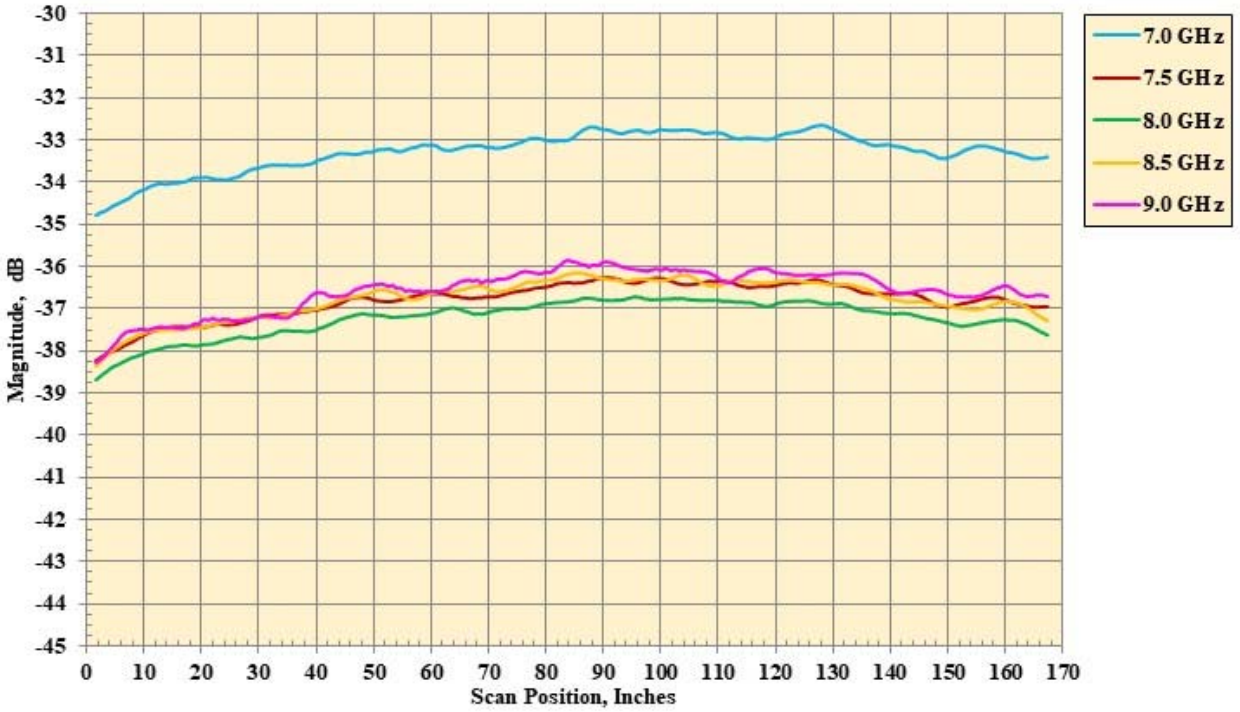

(uu) Magnitude probe data, Probe Angle = -75°, Pol = HH.
Figure19. Continued.

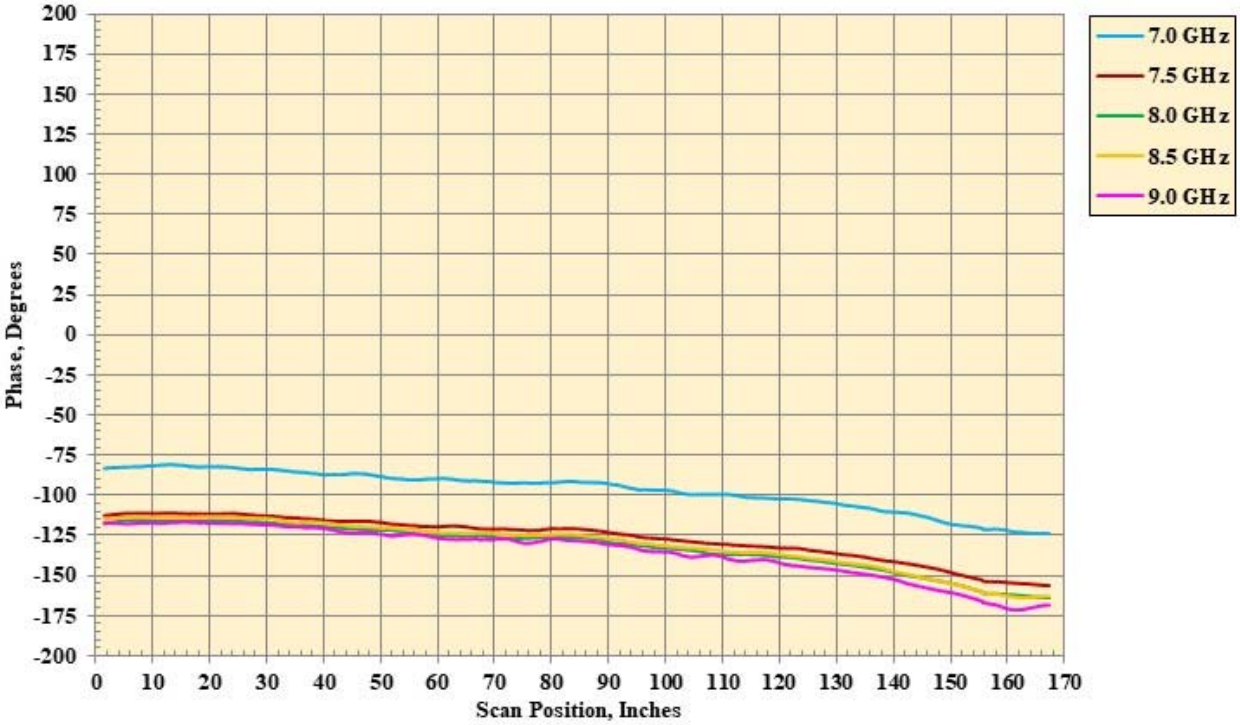

(vv) Phase probe data, Probe Angle = -75°, Pol = HH.
Figure 19. Continued.

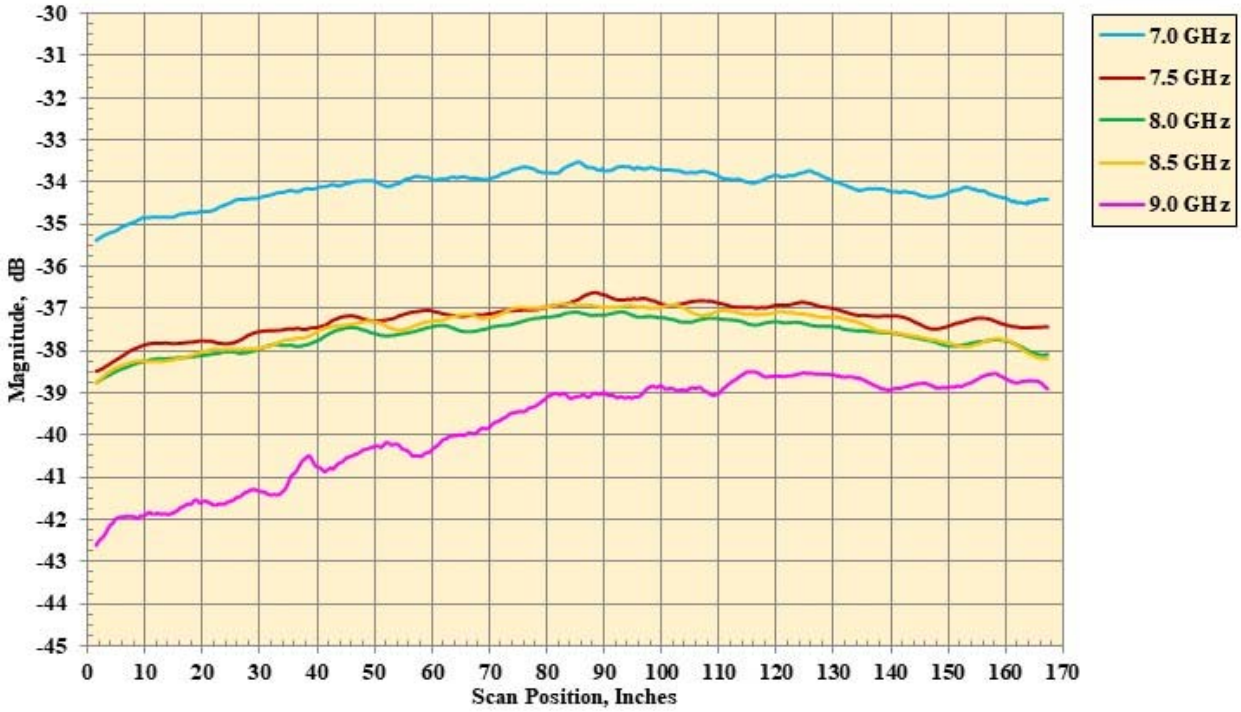

(ww) Magnitude probe data, Probe Angle = -75°, Pol = VV.
Figure 19. Continued.

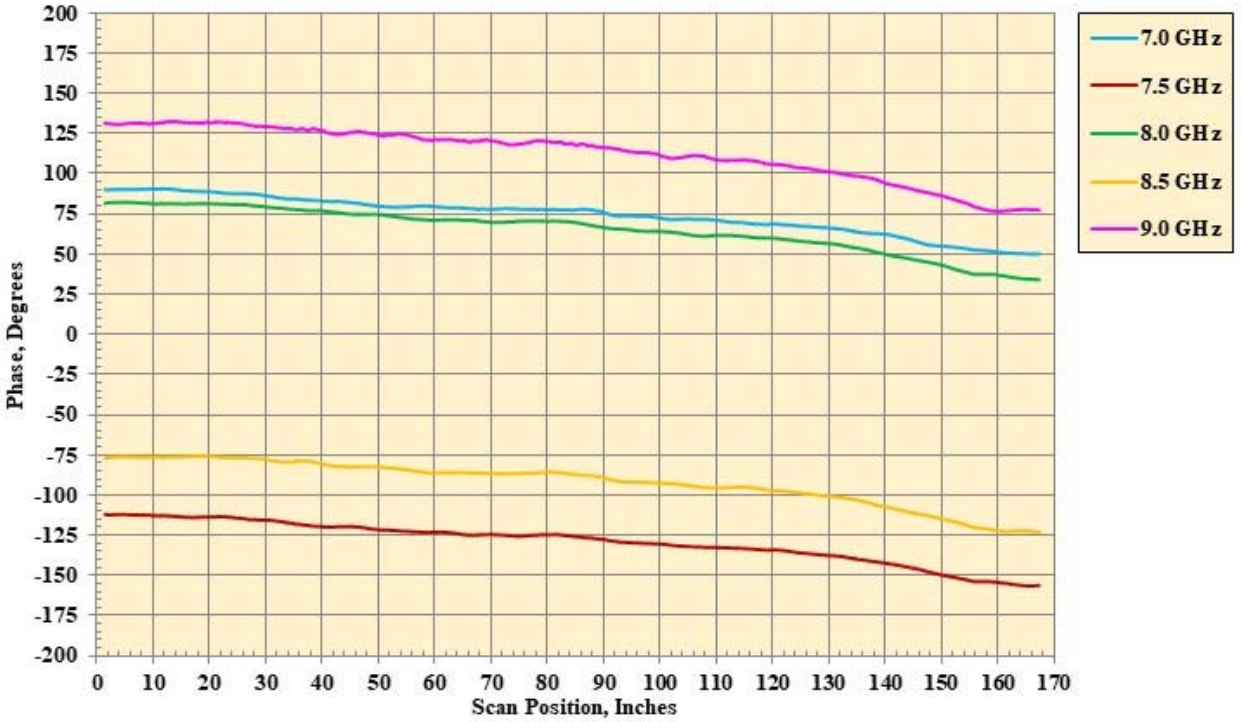

(xx) Phase probe data, Probe Angle = -75°, Pol = VV.
Figure 19. Continued.

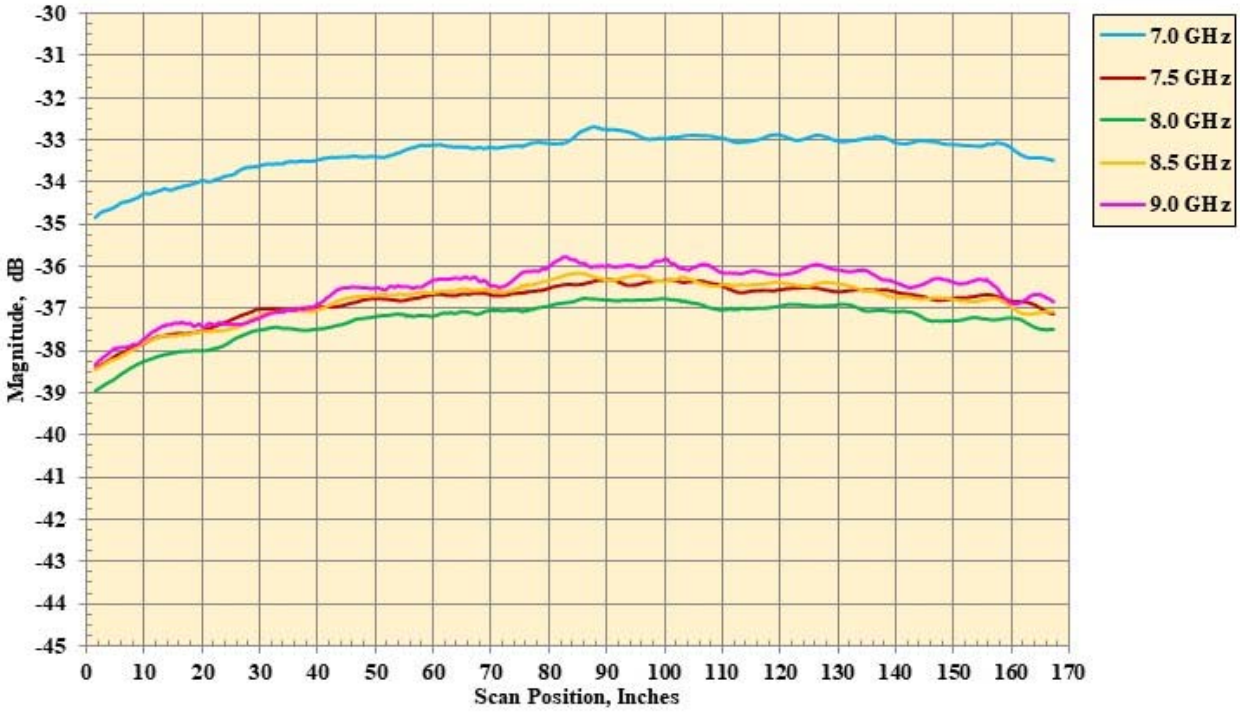

(yy) Magnitude probe data, Probe Angle = -90°, Pol = HH.
Figure 19. Continued.

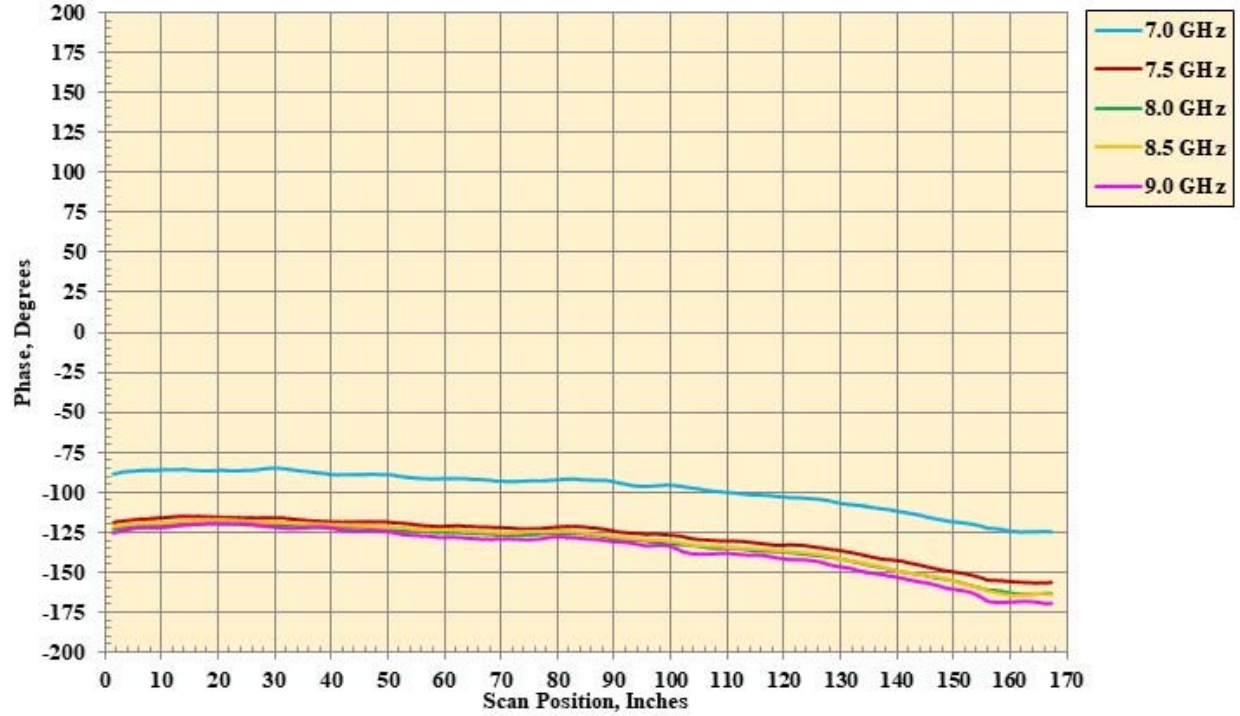

(zz) Phase probe data, Probe Angle = -90°, Pol = HH.
Figure 19. Continued.

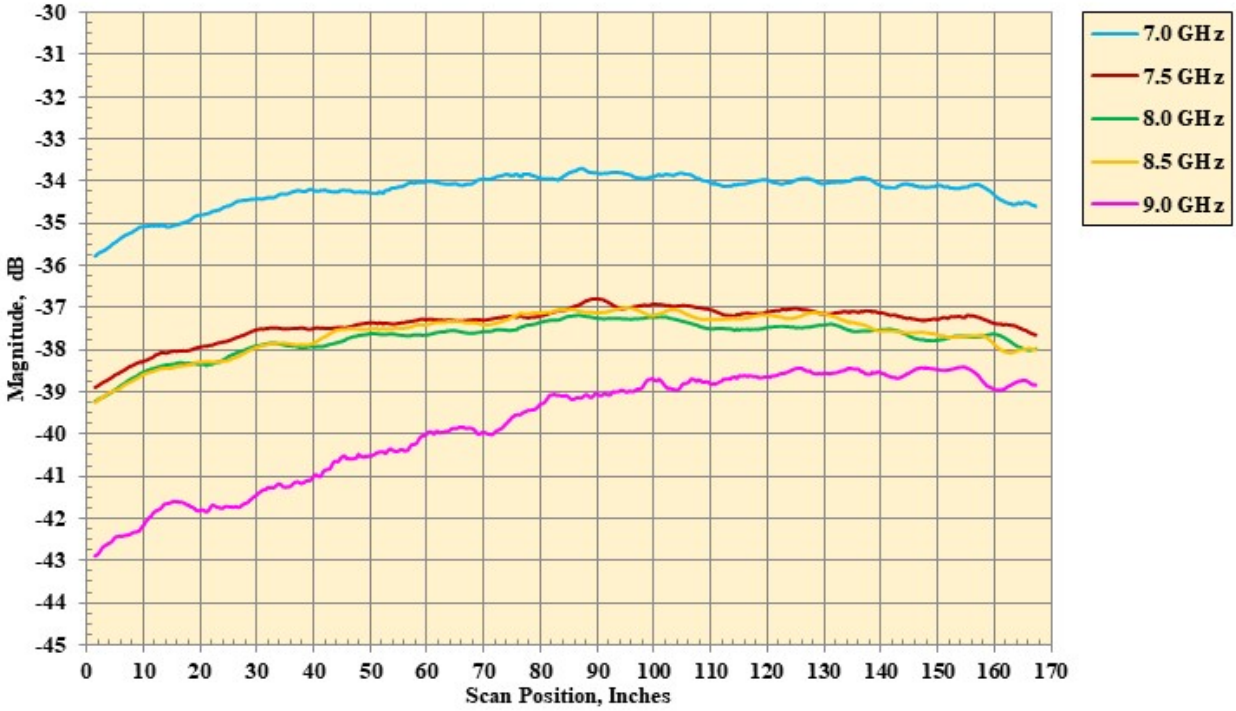

(aaa) Magnitude probe data, Probe Angle = -90°, Po l= VV.
Figure 19. Continued.

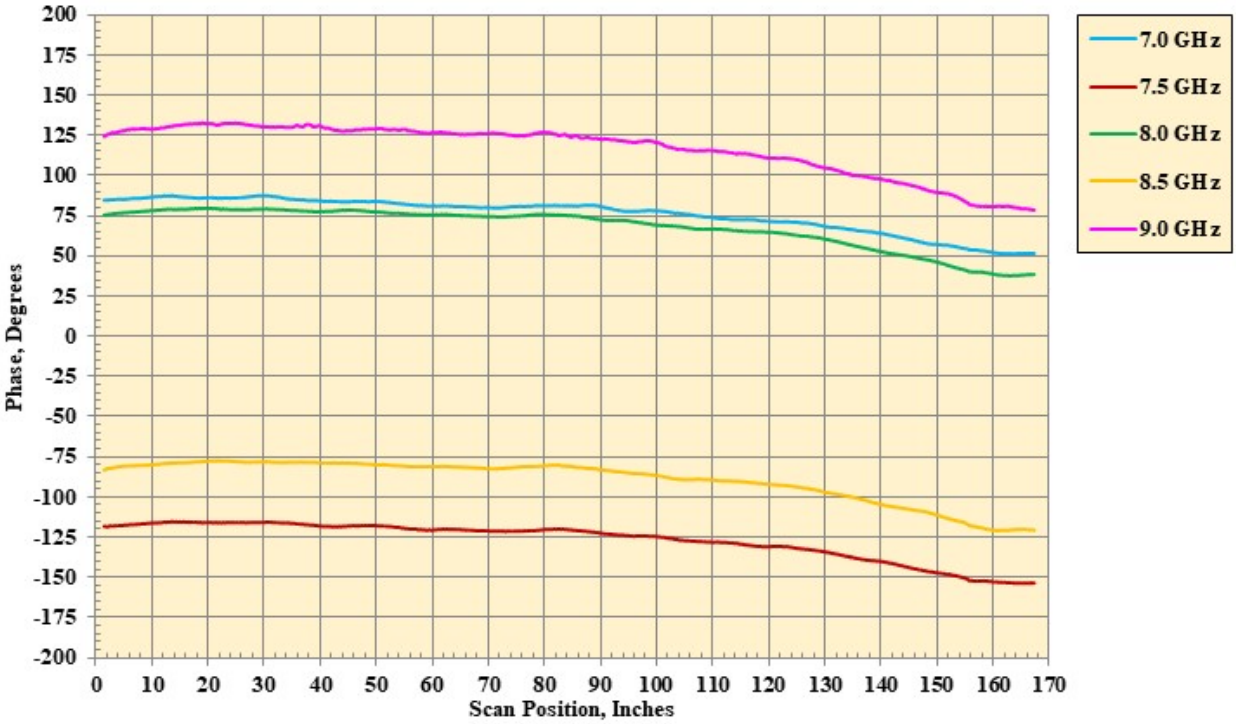

(bbb) Phase probe data, Probe Angle = -90°, Pol = VV.
Figure 19. Concluded.

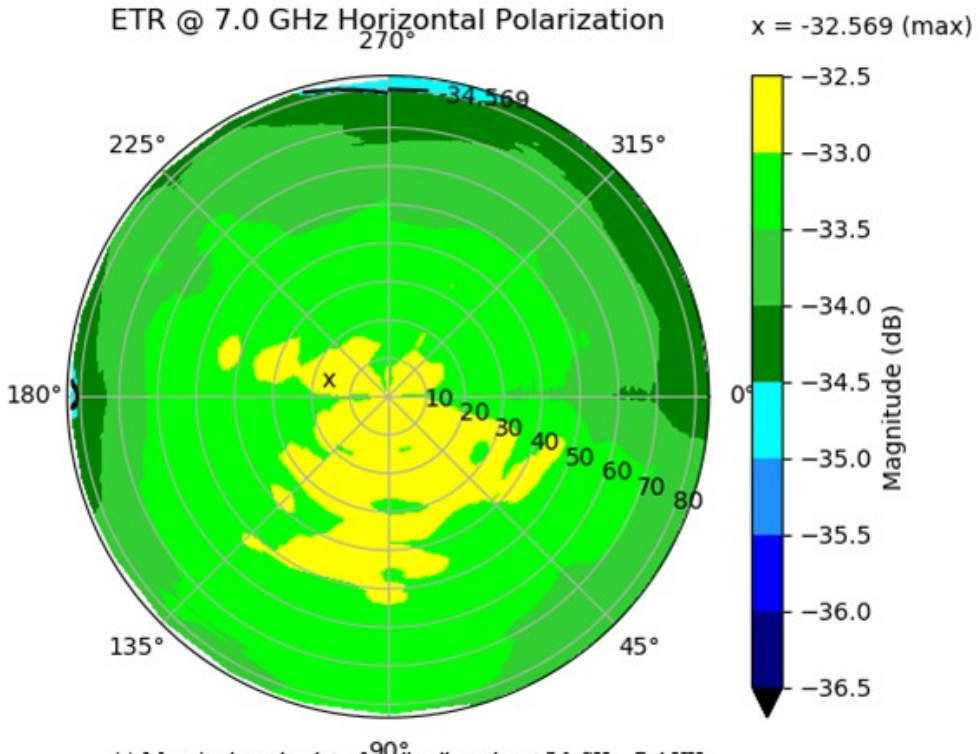

(a) Magnitude probe data, for all roll angles at 7.0 GHz, Pol HH.

Figure 20. Combined summary of all scan data at all roll angle for frequencies from 7 GHz to 9 GHz.

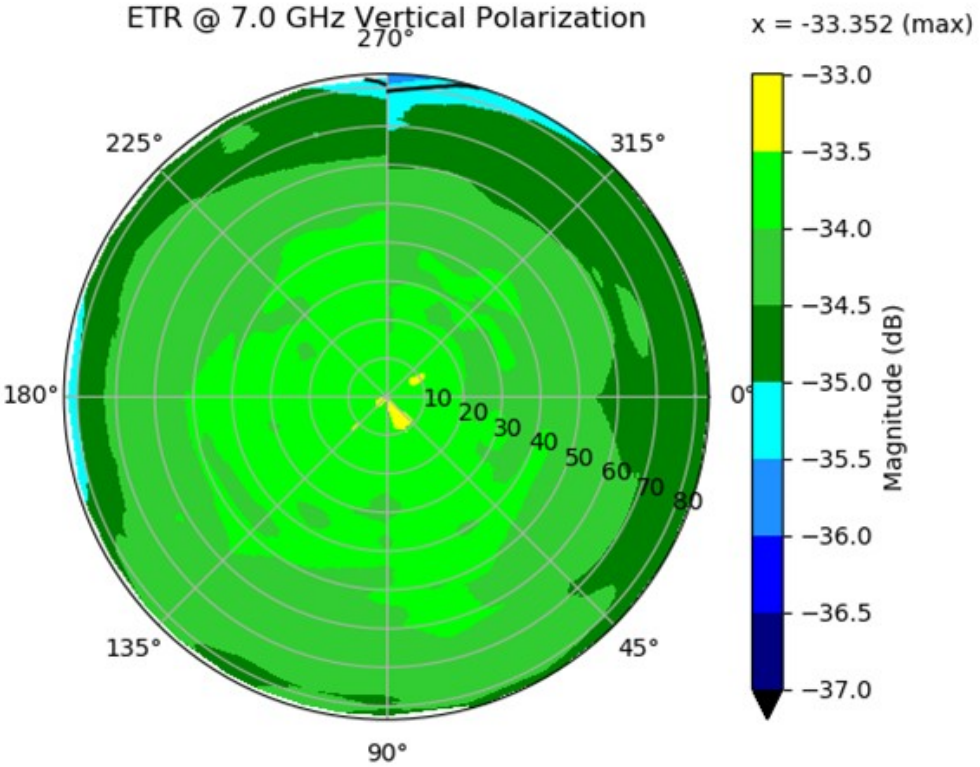

(b) Magnitude probe data, for all roll angles at 7.0 GHz, Pol VV.

Figure 20. Continued.

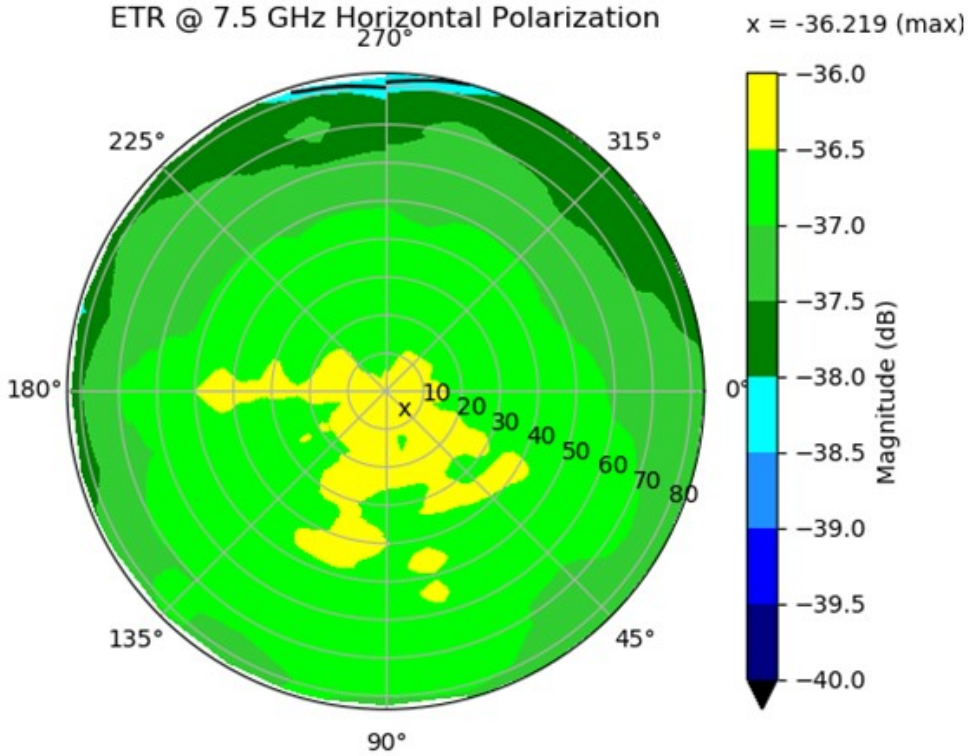

(c) Magnitude probe data, for all roll angles at 7.5 GHz, Pol HH.
Figure 20. Continued.

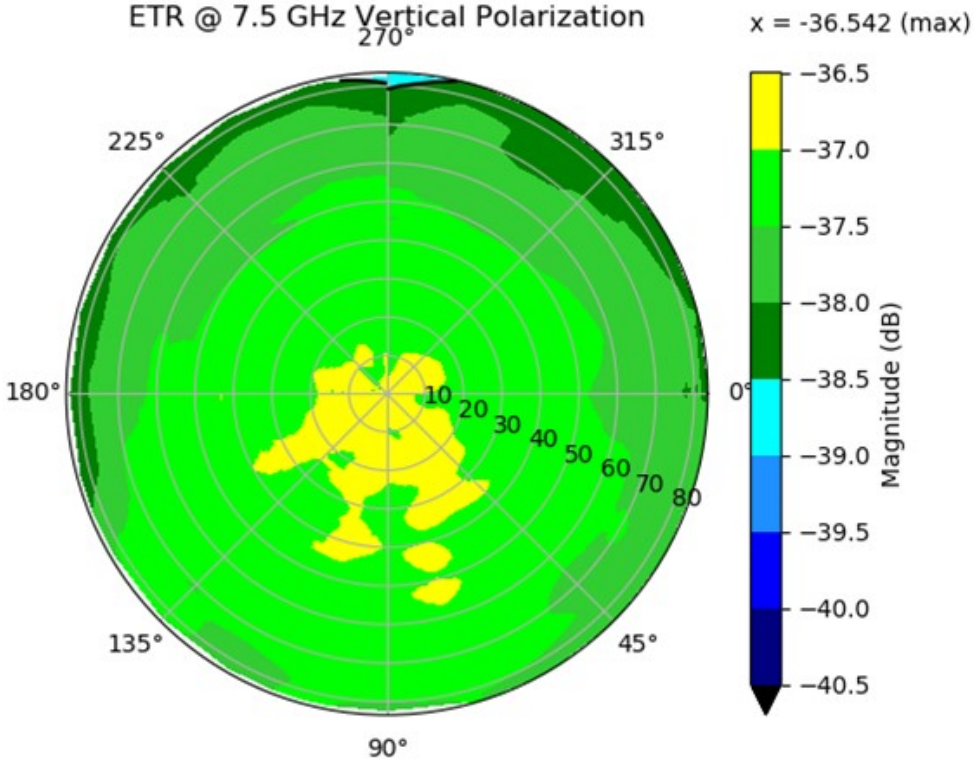

(d) Magnitude probe data, for all roll angles at 7.5 GHz, Pol VV.
Figure 20. Continued.

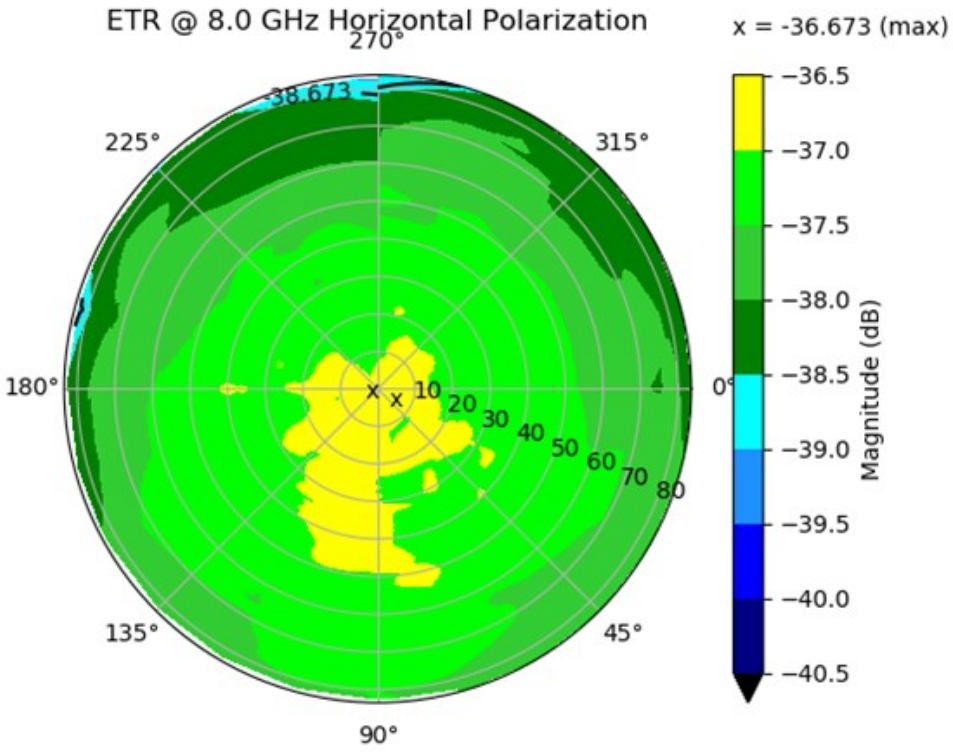

(e) Magnitude probe data, for all roll angles at 8.0 GHz, Pol HH.
Figure 20. Continued.

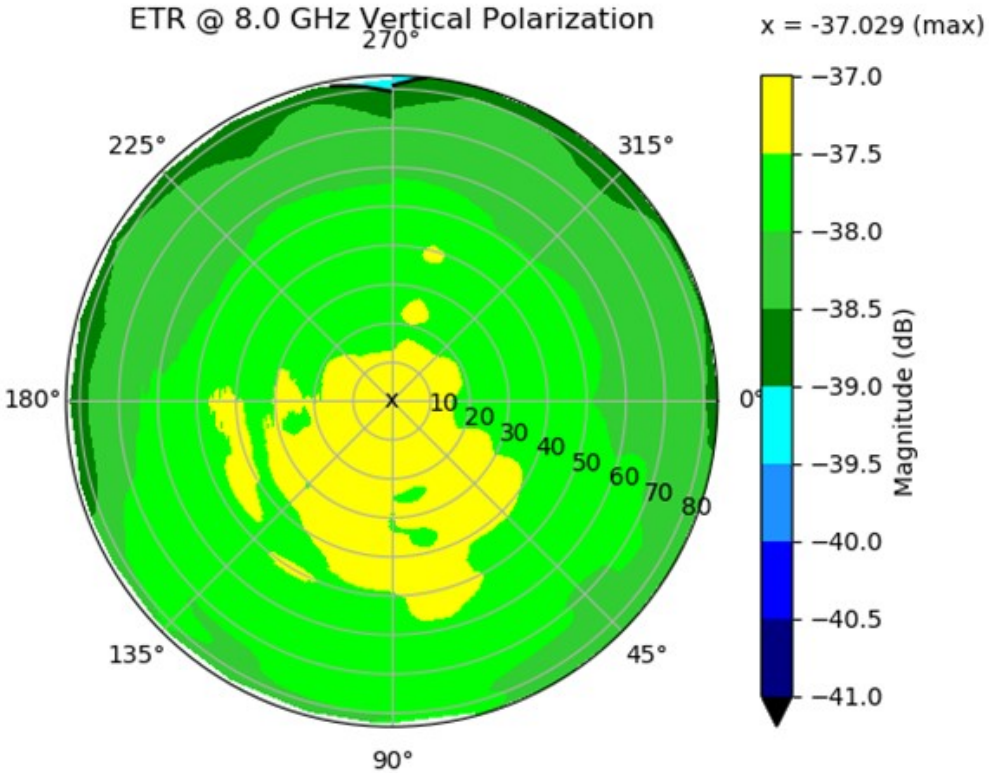

(f) Magnitude probe data, for all roll angles at 8.0 GHz, Pol VV.
Figure 20. Continued.

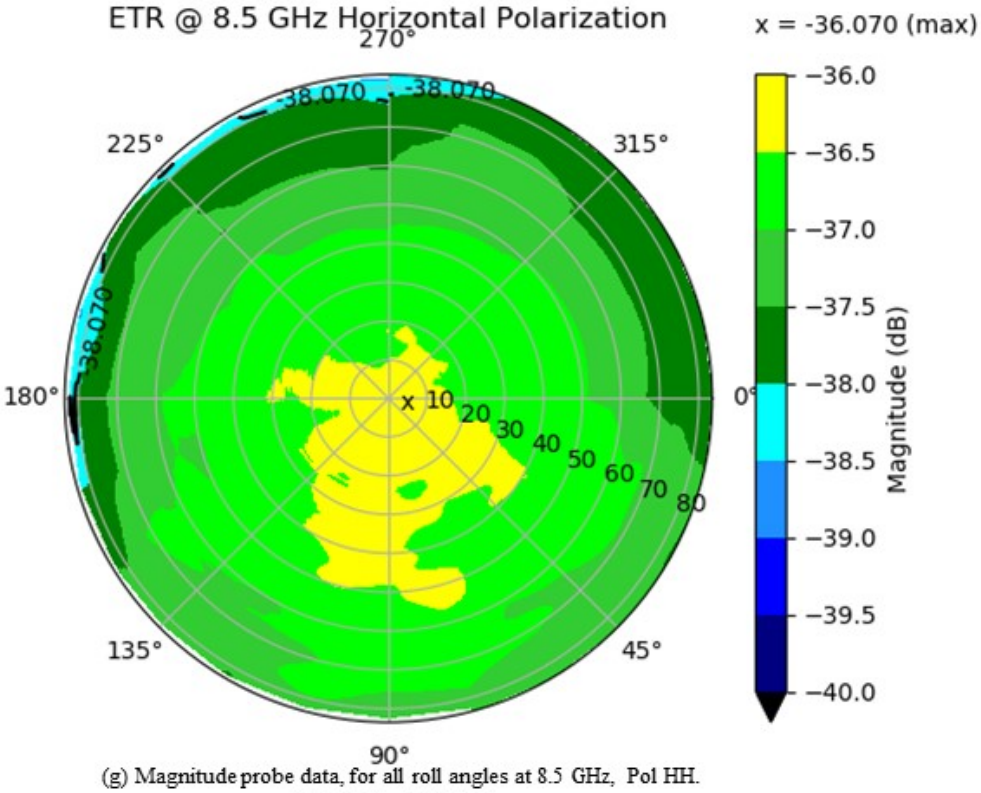

(g) Magnitude probe data, for all roll angles at 8.5 GHz, Pol HH.
Figure 20. Continued.

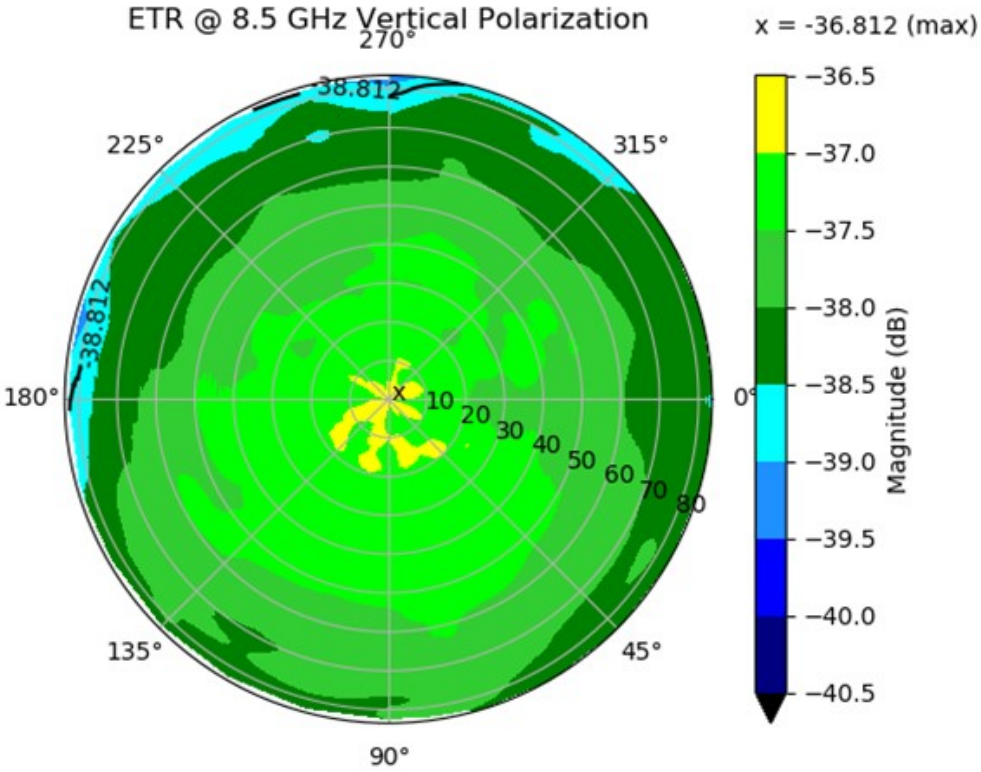

(h) Magnitude probe data, for all roll angles at 8.5 GHz, Pol VV.
Figure 20. Continued.

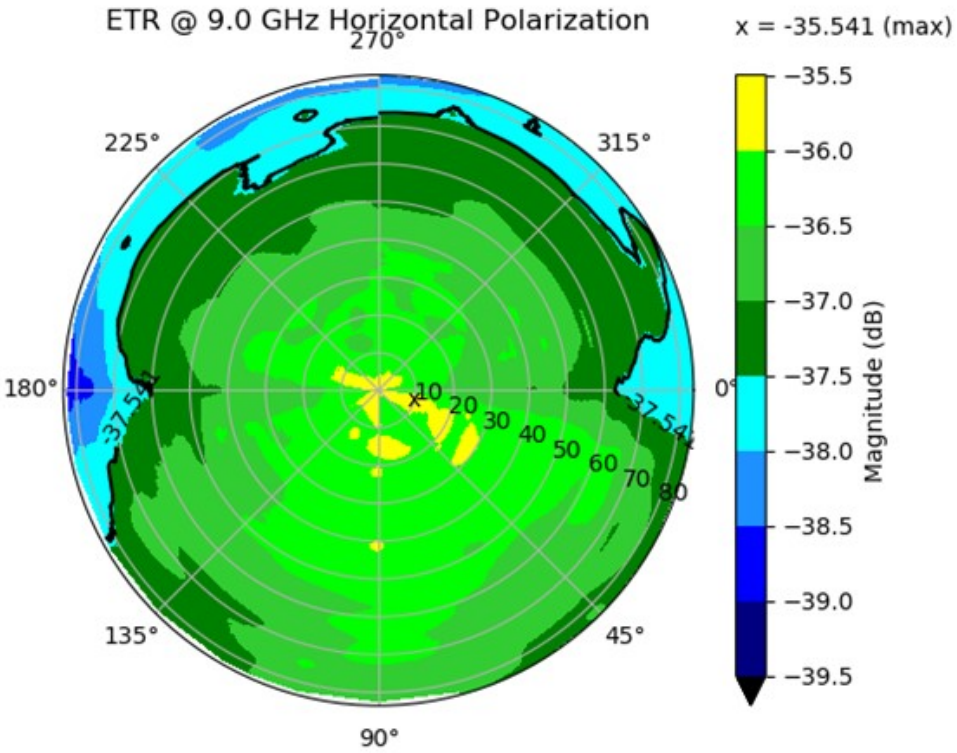

(i) Magnitude probe data, for all roll angles at 9.0 GHz, Pol HH.
Figure 20. Continued.

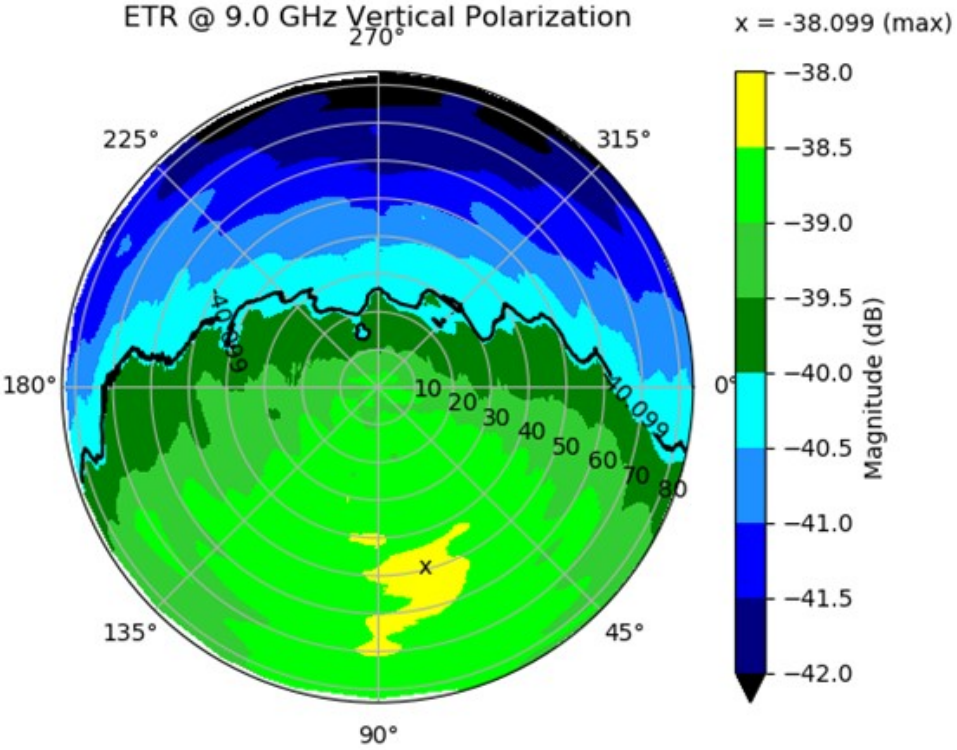

(j) Magnitude probe data, for all roll angles at 9.0 GHz, Pol VV.
Figure 20. Concluded.

PNA	Frequency Band, GHz	31.0 to 33.0
	Number of data points inband	201
	IF Bandwidth, Hz	700
	Average number of points	32
HH	Gate Center, ns	-22.515
HH	Gate Span, ns	2.28
VV	Gate Center, ns	-22.515
VV	Gate Span, ns	2.28
S1	Milltech SFH-28-R31560N A17503	
S2	DRG SAS-574	
S1	Amplifier RF-Lambda RLNA16G32G	Yes
S2	Amplifier	None
Prober	Step size, in.	0.2

Figure 21. Setup for the 31.0 to 33.0 GHz probe data acquisition.

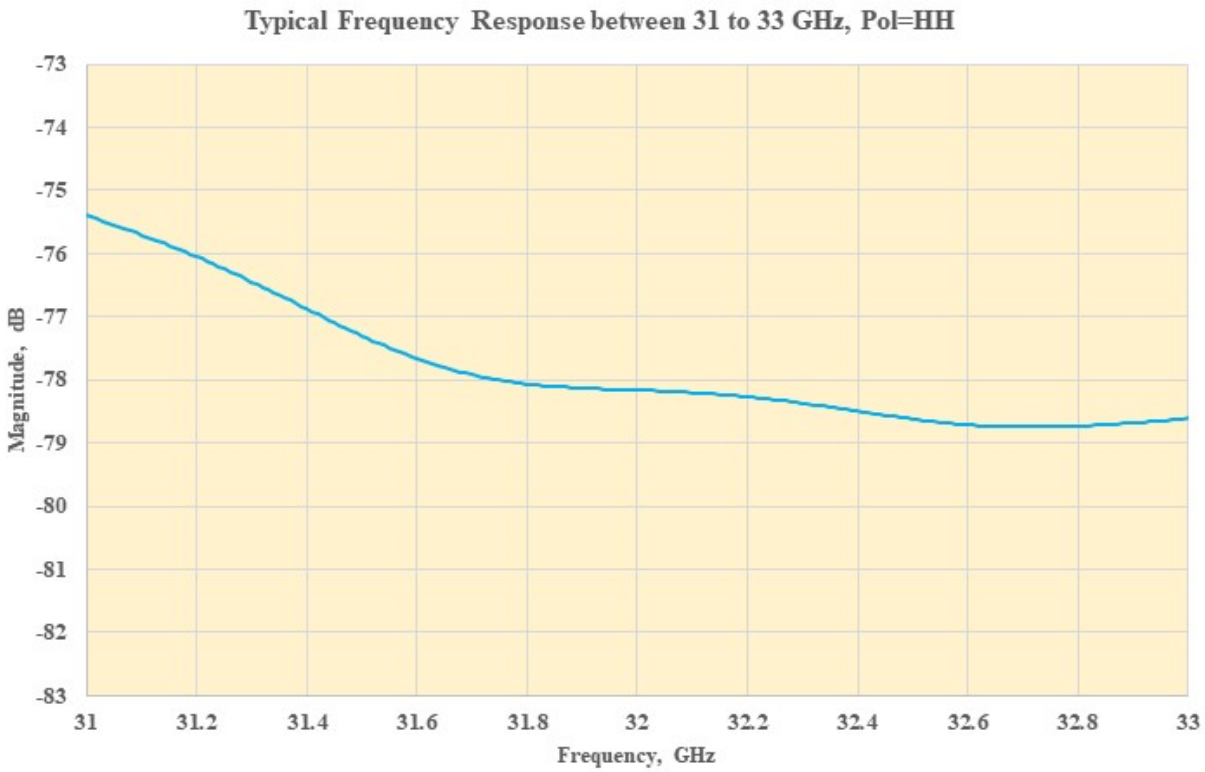

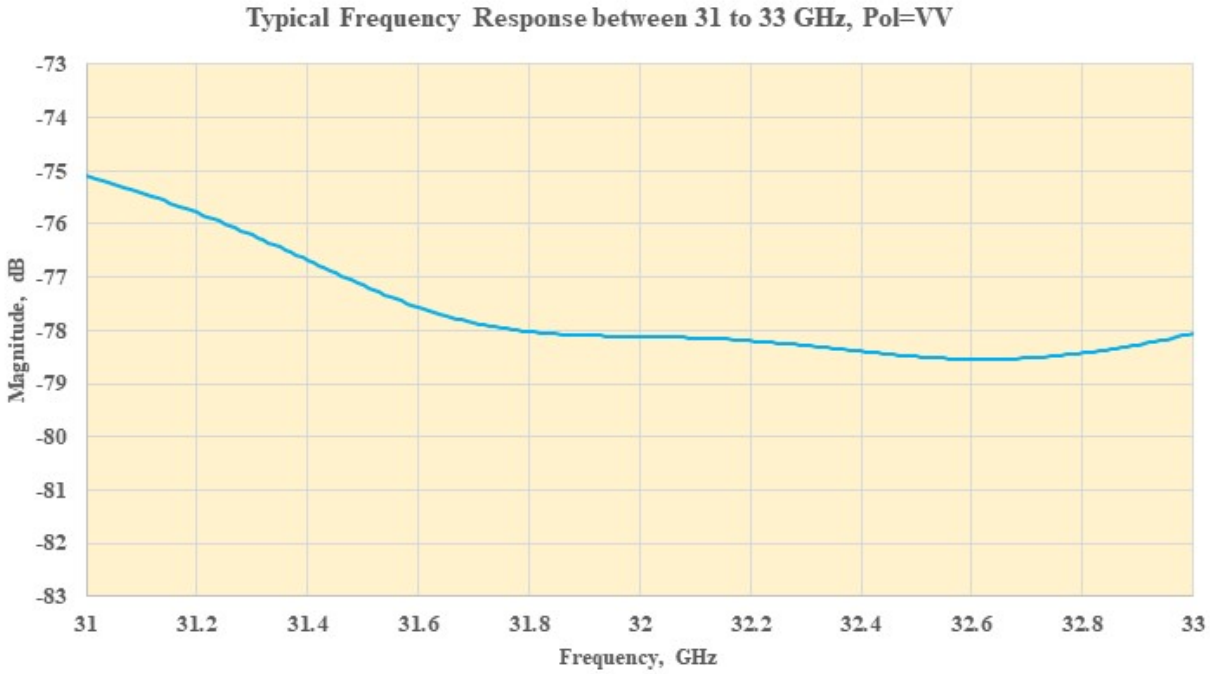

Figure 22. Typical frequency response data for HH and VV for 31.0 – 33.0 GHz probe data. Data acquired at probe arm center.

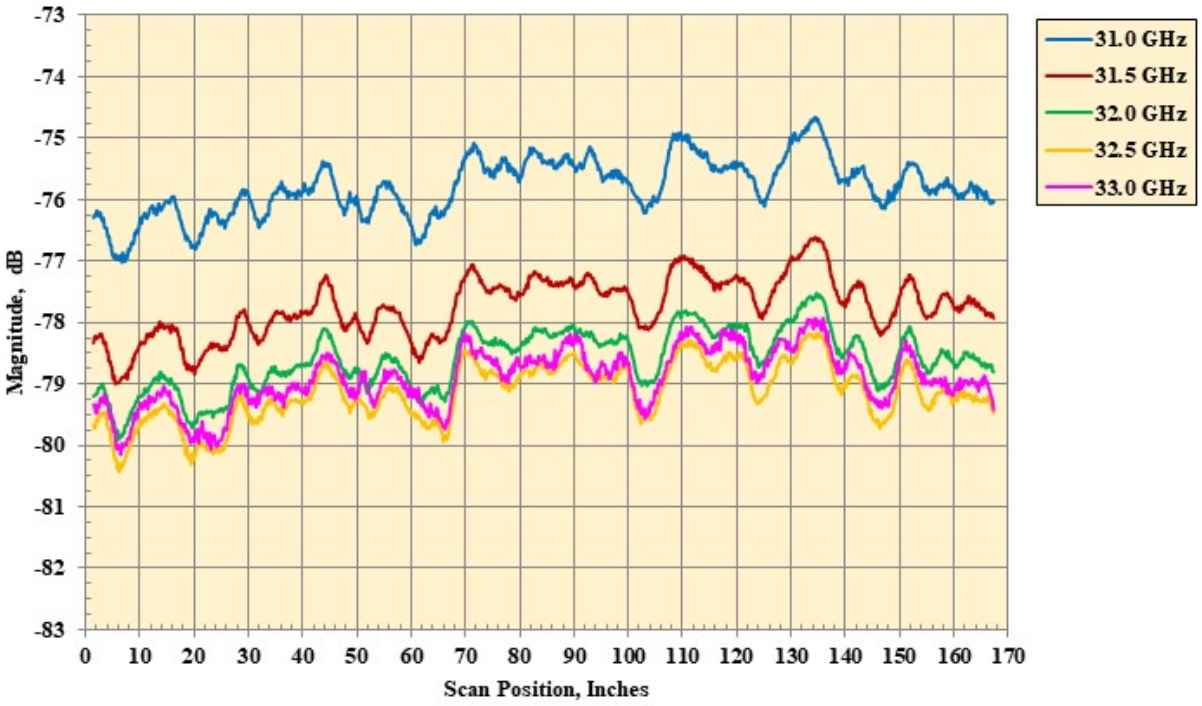

(a) Magnitude probe data, Probe Angle = 0°, Pol = HH.

Figure 23. Probe data at frequency = 31.0 GHz to 33.0 GHz using the S1 antenna = Milltech SFH-28-R31560N A17503 , S2 antenna = DRG SAS-574

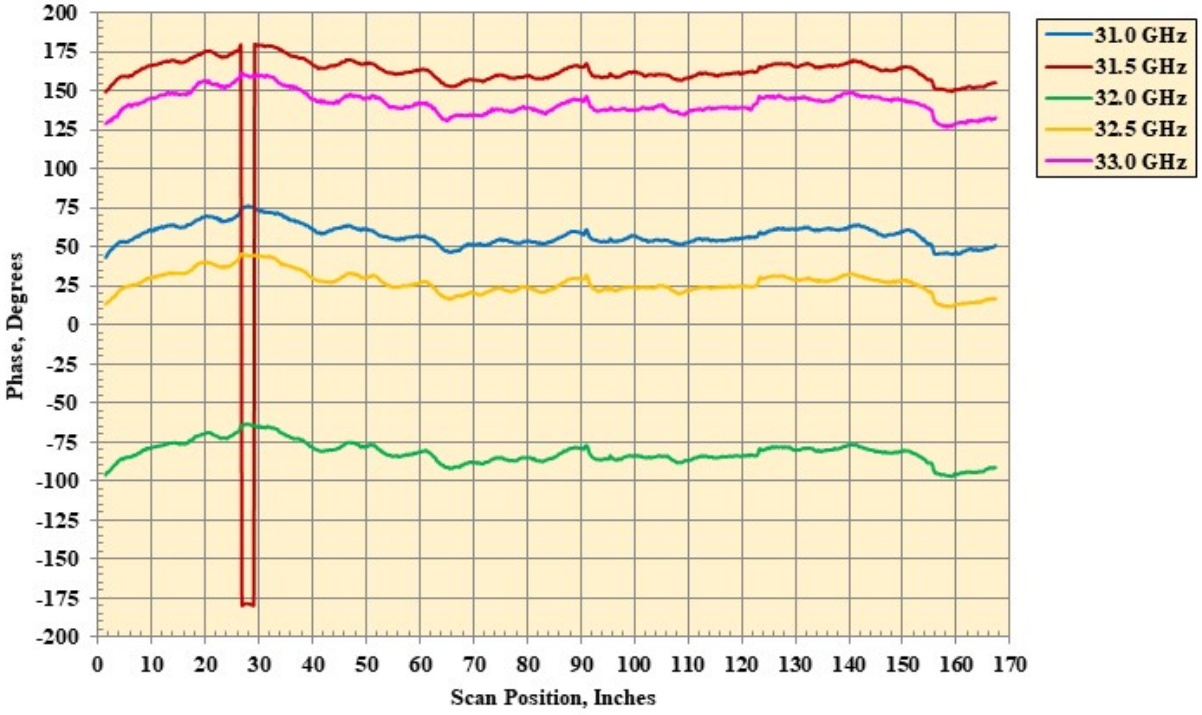

(b) Phase probe data, Probe Angle = 0°, Pol = HH.

Figure 23. Continued.

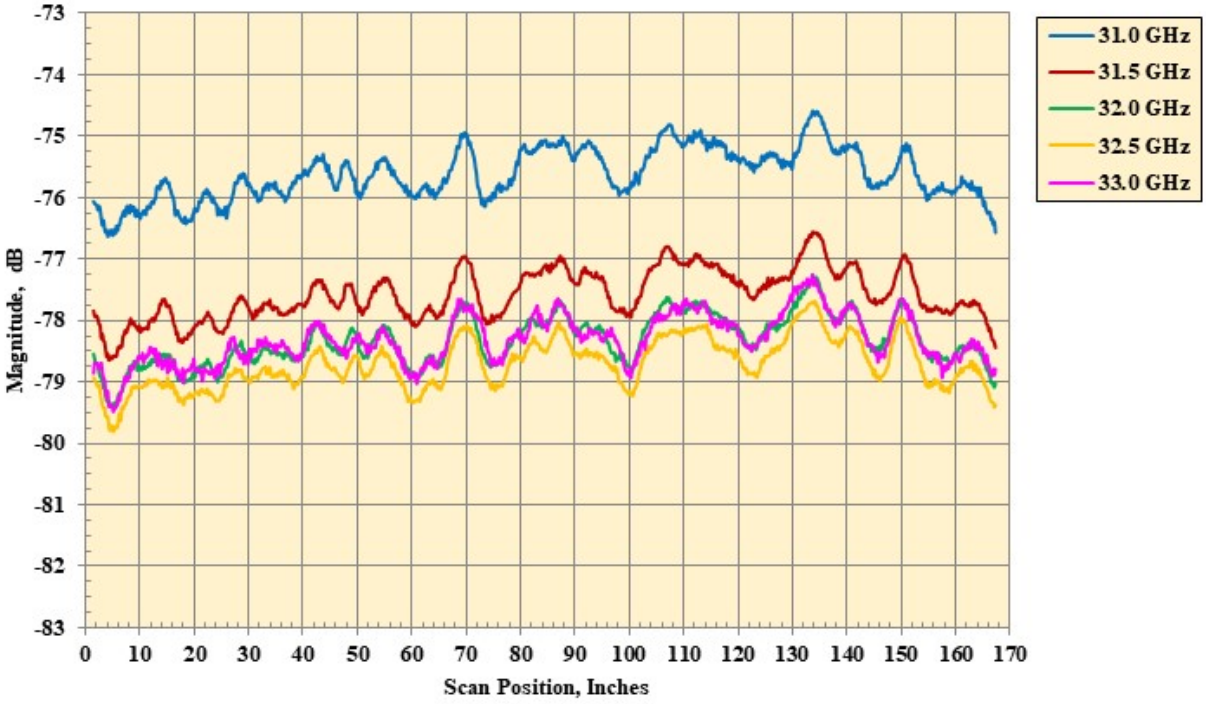

(c) Magnitude probe data, Probe Angle = 0°, Pol = VV.
Figure 23. Continued.

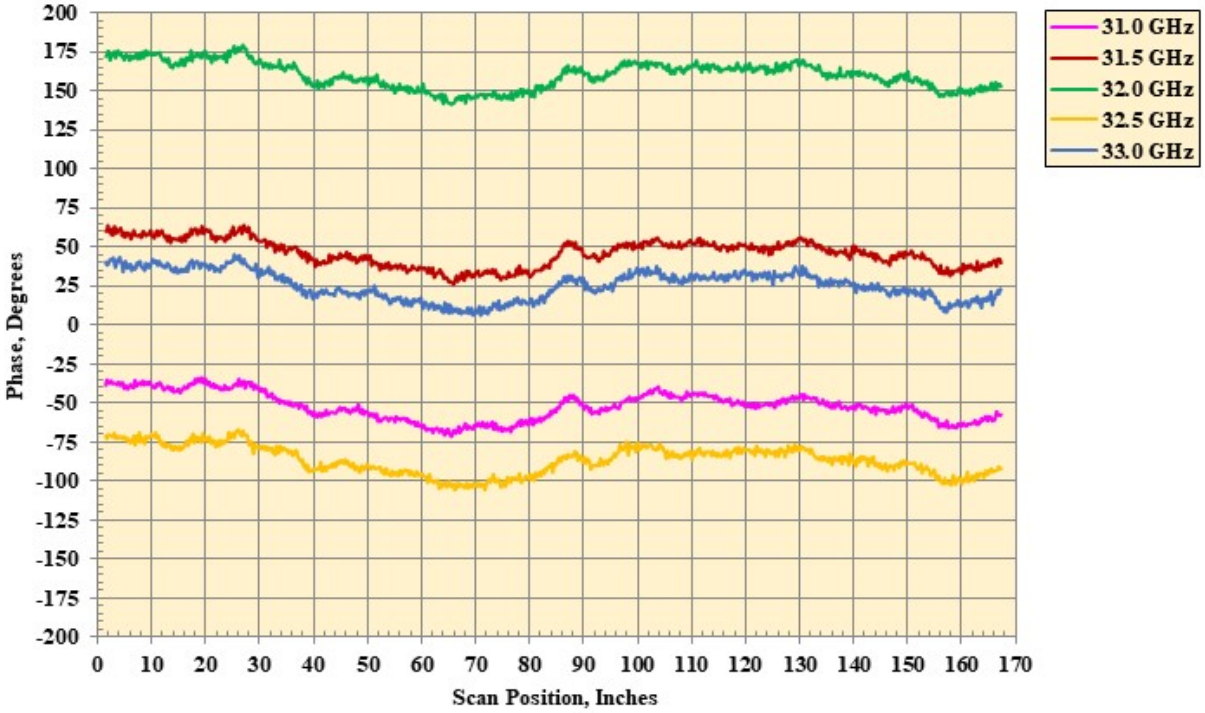

(d) Phase probe data, Probe Angle = 0°, Pol = VV.
Figure 23. Continued.

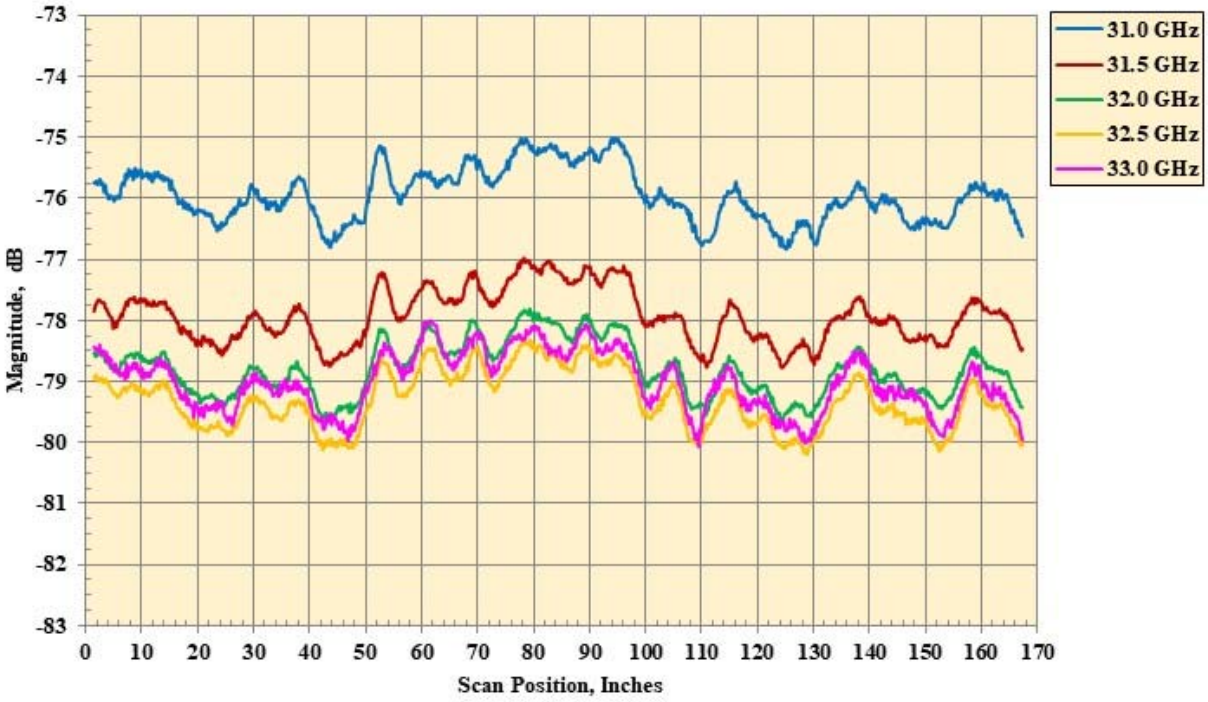

(e) Magnitude probe data, Probe Angle = 15°, Pol = HH.
Figure 23. Continued.

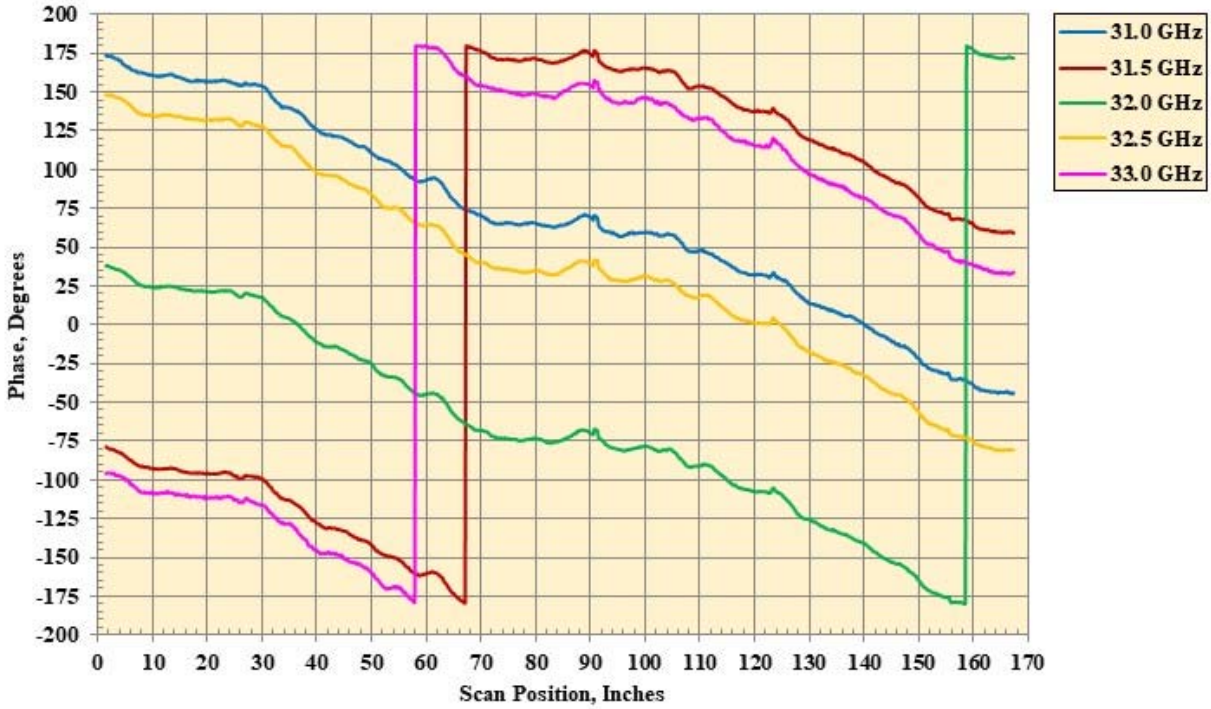

(f) Phase probe data, Probe Angle = 15°, Pol = HH.
Figure 23. Continued.

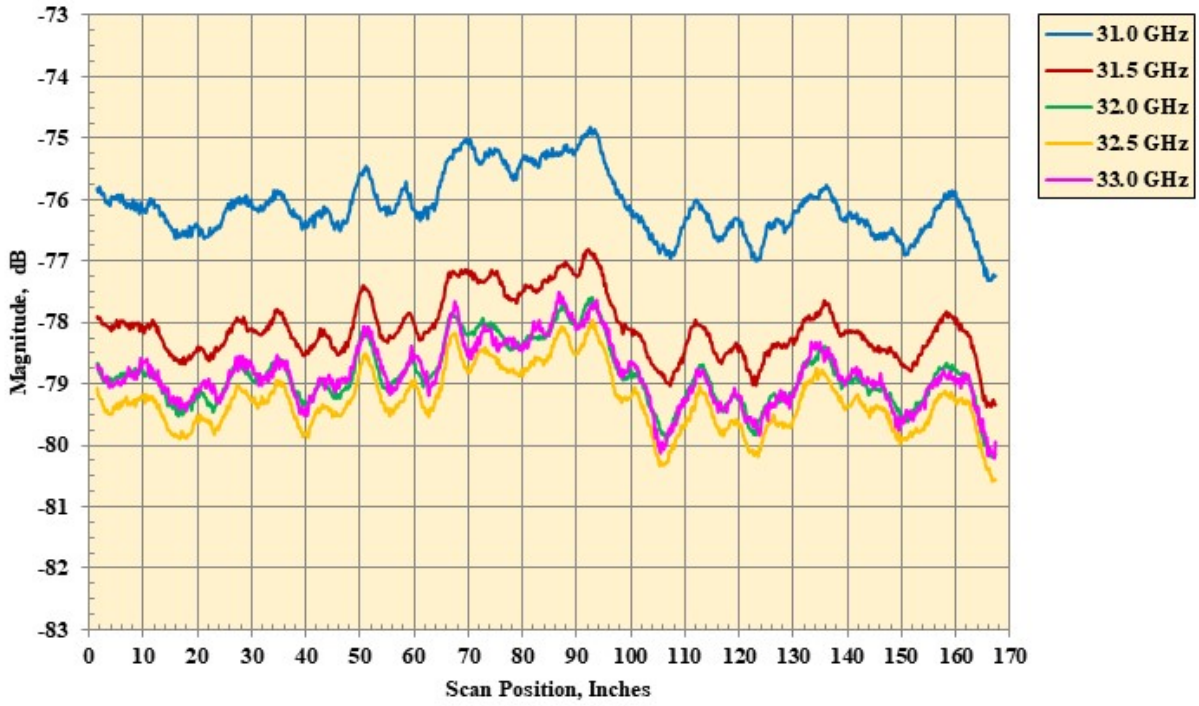

(g) Magnitude probe data, Probe Angle = 15°, Pol = VV.
Figure 23. Continued.

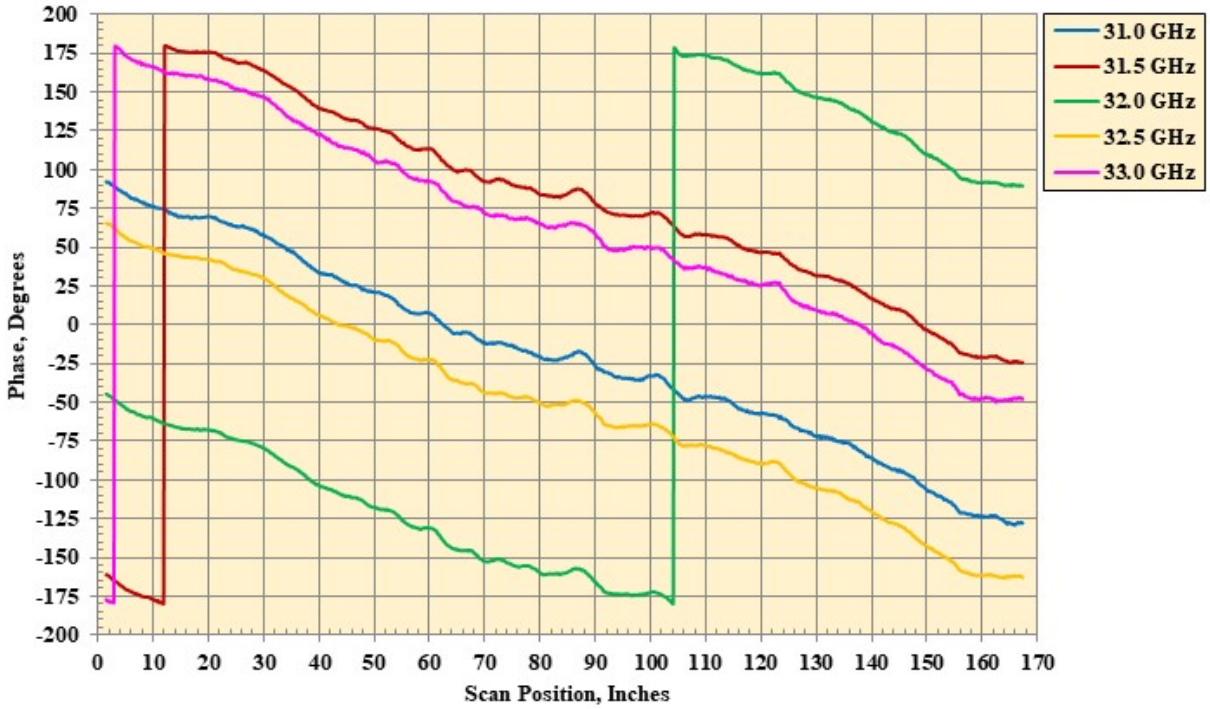

(h) Phase probe data, Probe Angle = 15°, Pol = VV.
Figure 23. Continued.

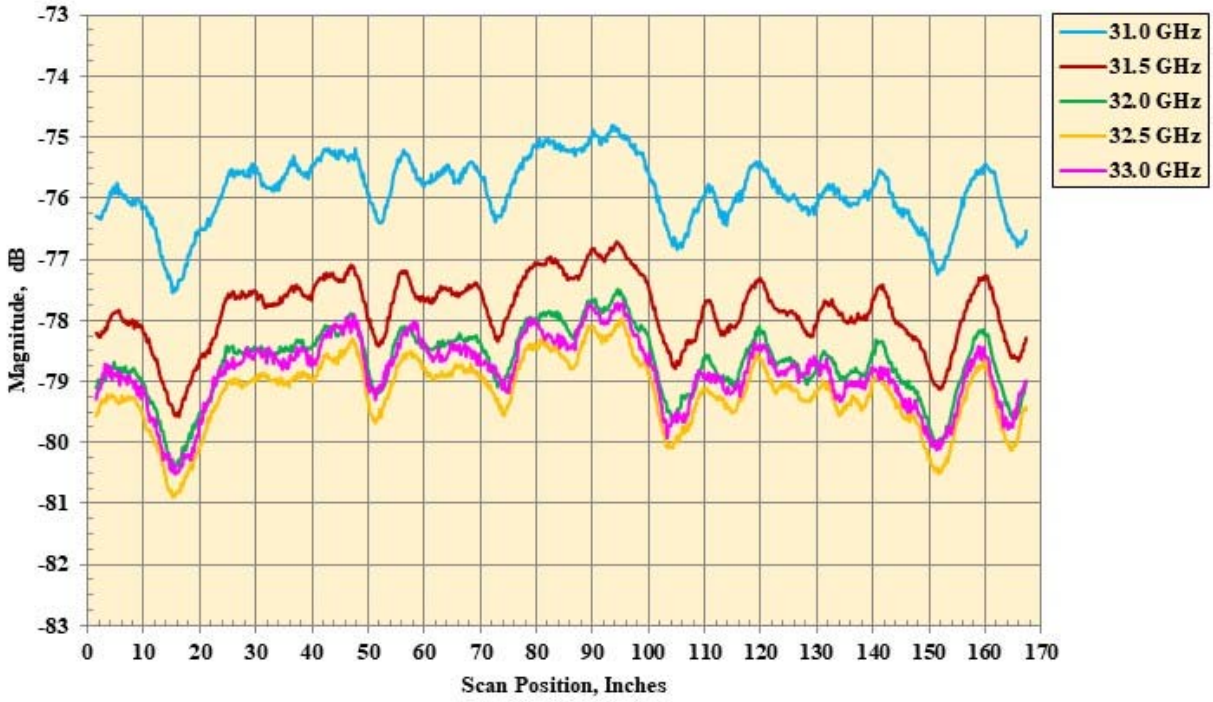

(i) Magnitude probe data, Probe Angle = 30°, Pol = HH.
Figure 23. Continued.

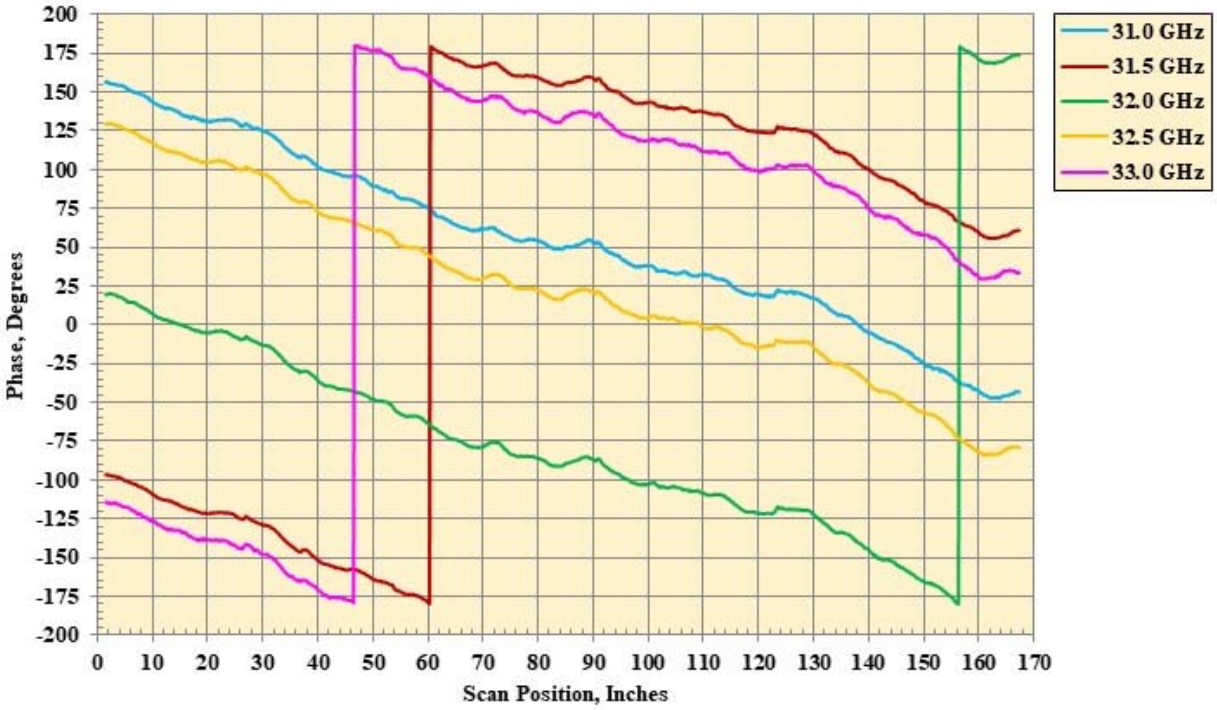

(j) Phase probe data, Probe Angle = 30°, Pol = HH.
Figure 23. Continued.

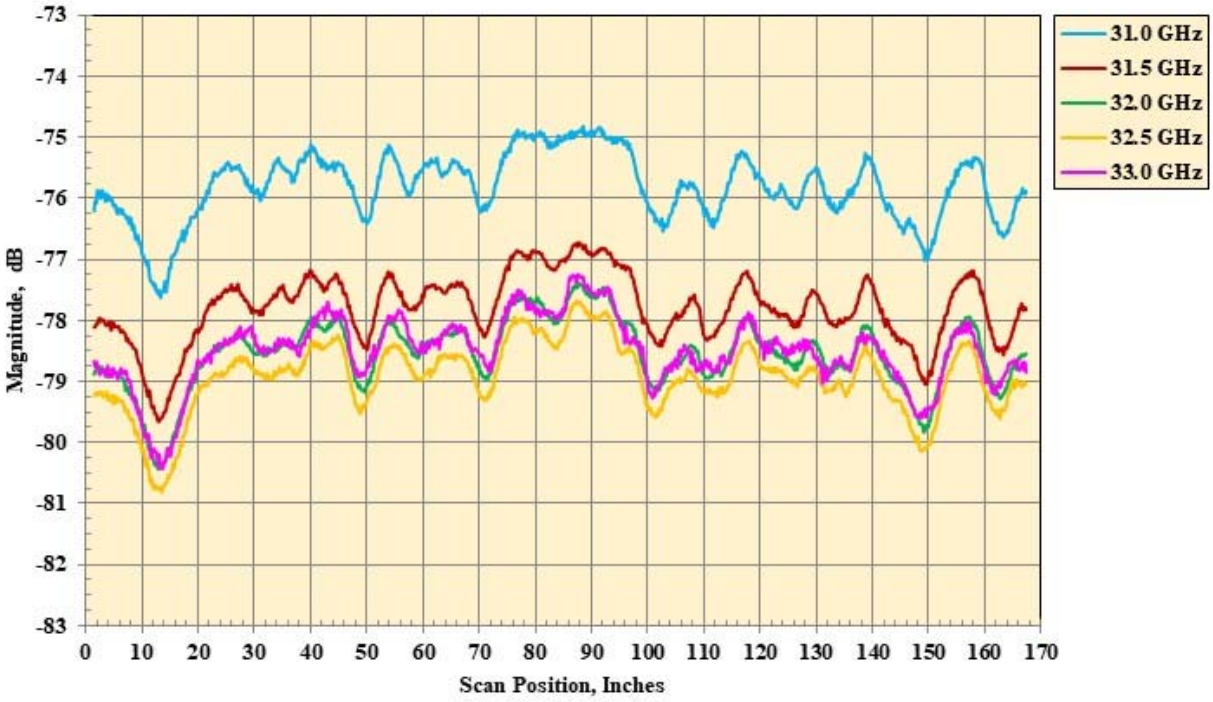

(k) Magnitude probe data, Probe Angle = 30°, Pol = VV.
Figure 23. Continued.

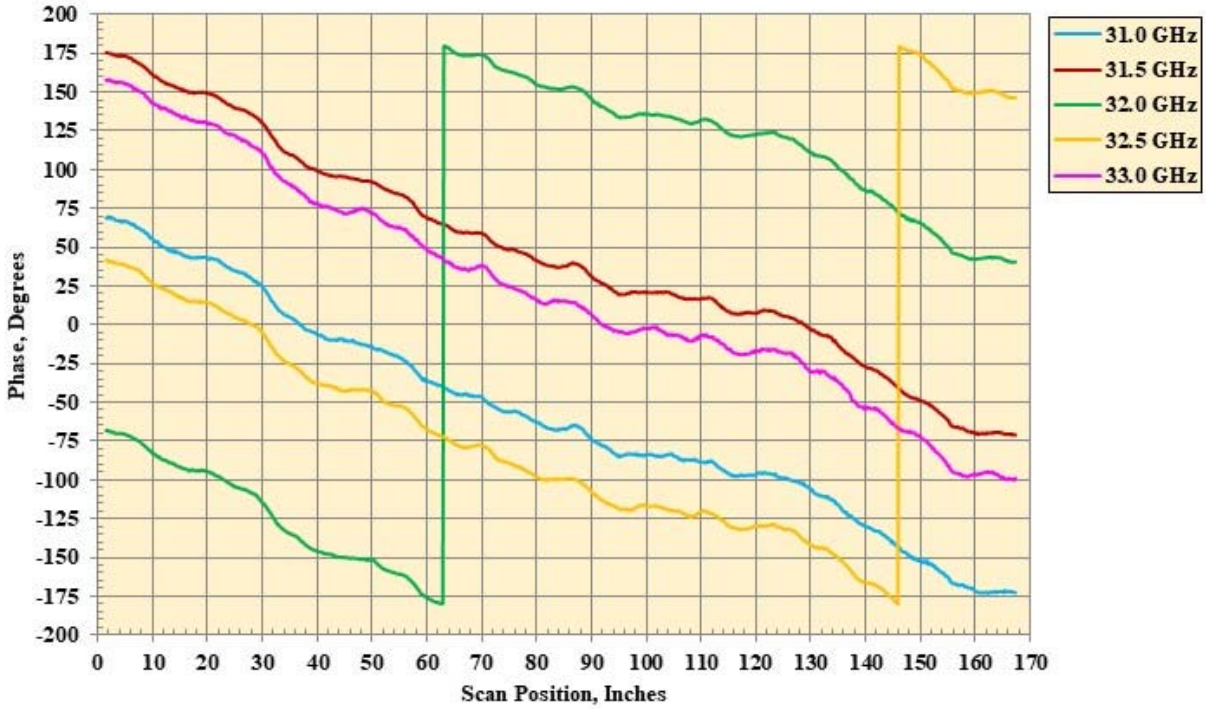

(l) Phase probe data, Probe Angle = 30°, Pol = VV.
Figure 23. Continued.

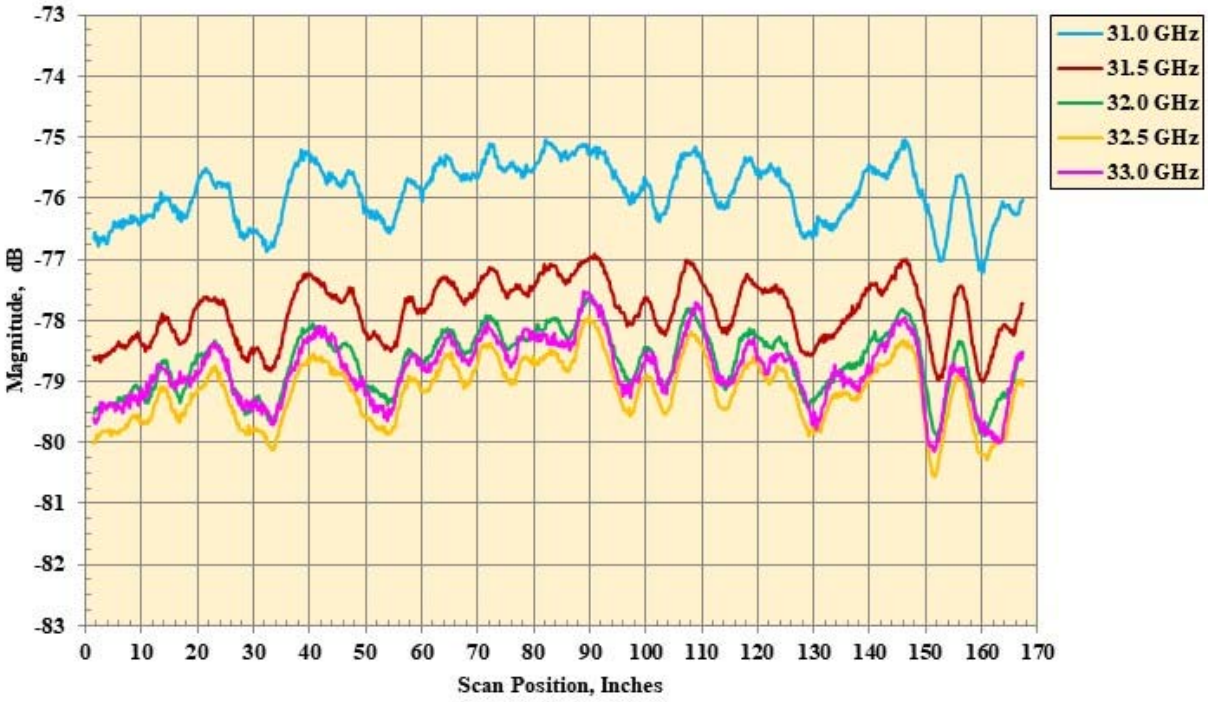

(m) Magnitude probe data, Probe Angle = 45°, Pol = HH.
Figure 23. Continued.

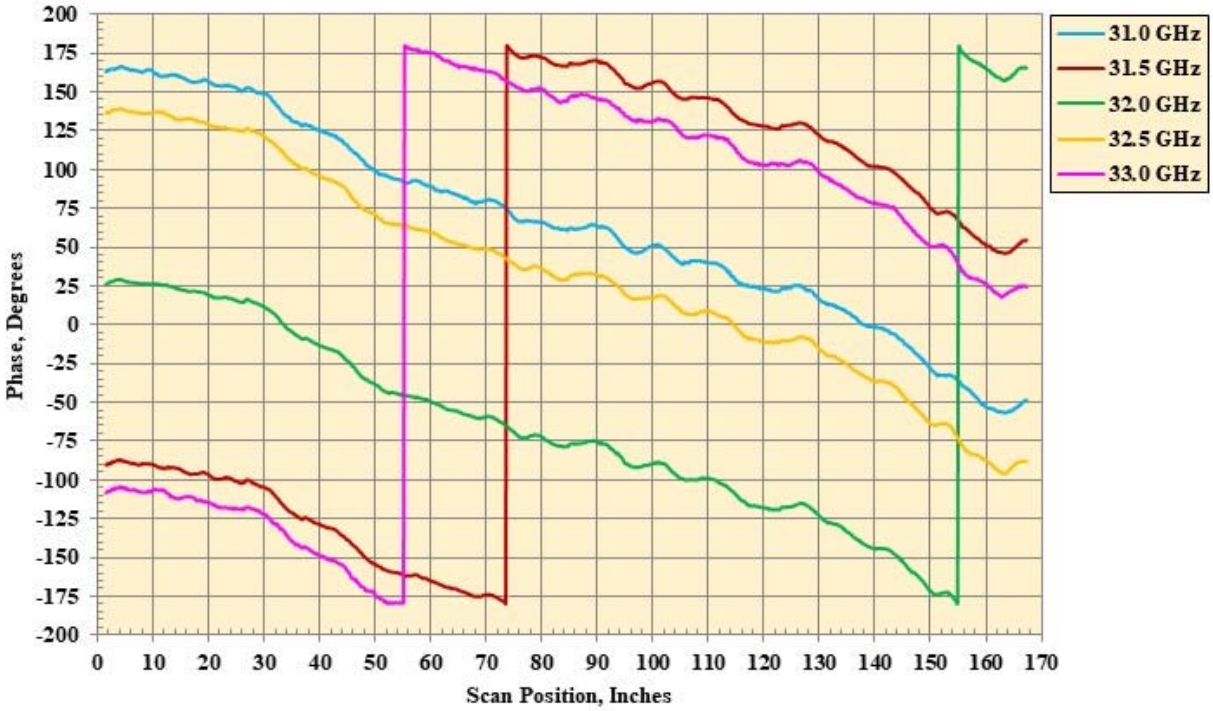

(n) Phase probe data, Probe Angle = 45°, Pol = HH.
Figure 23. Continued.

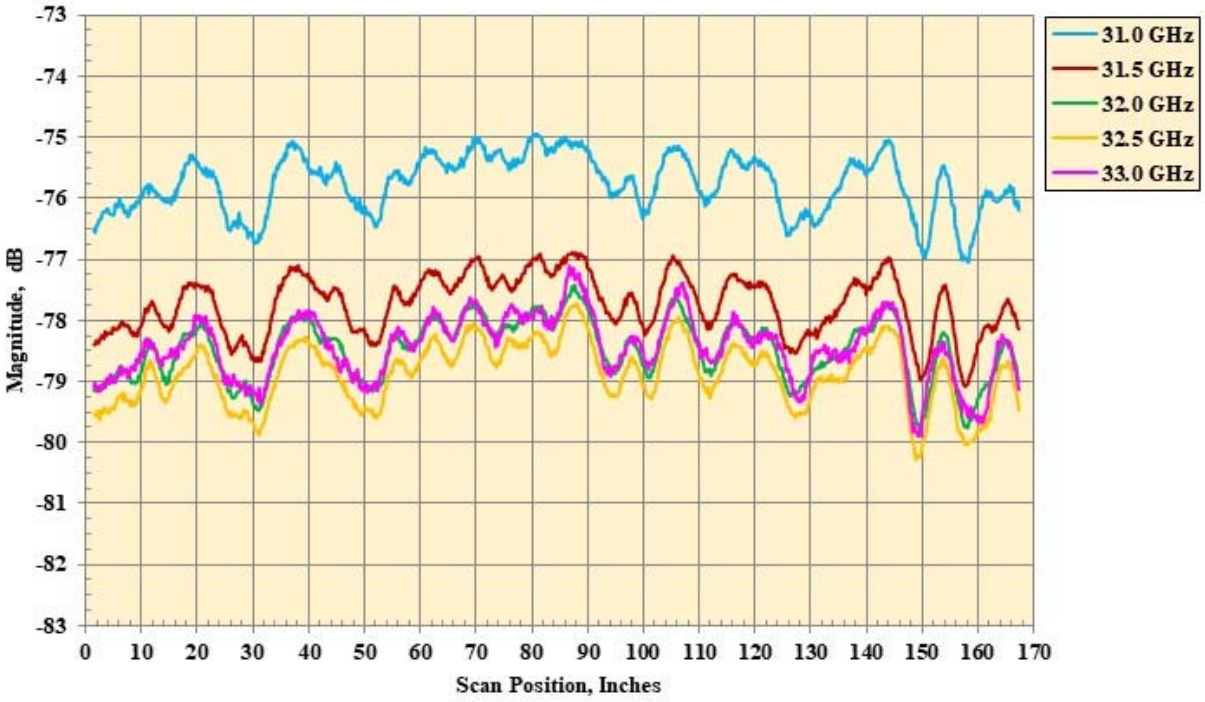

(o) Magnitude probe data, Probe Angle = 45°, Pol = VV.
Figure 23. Continued.

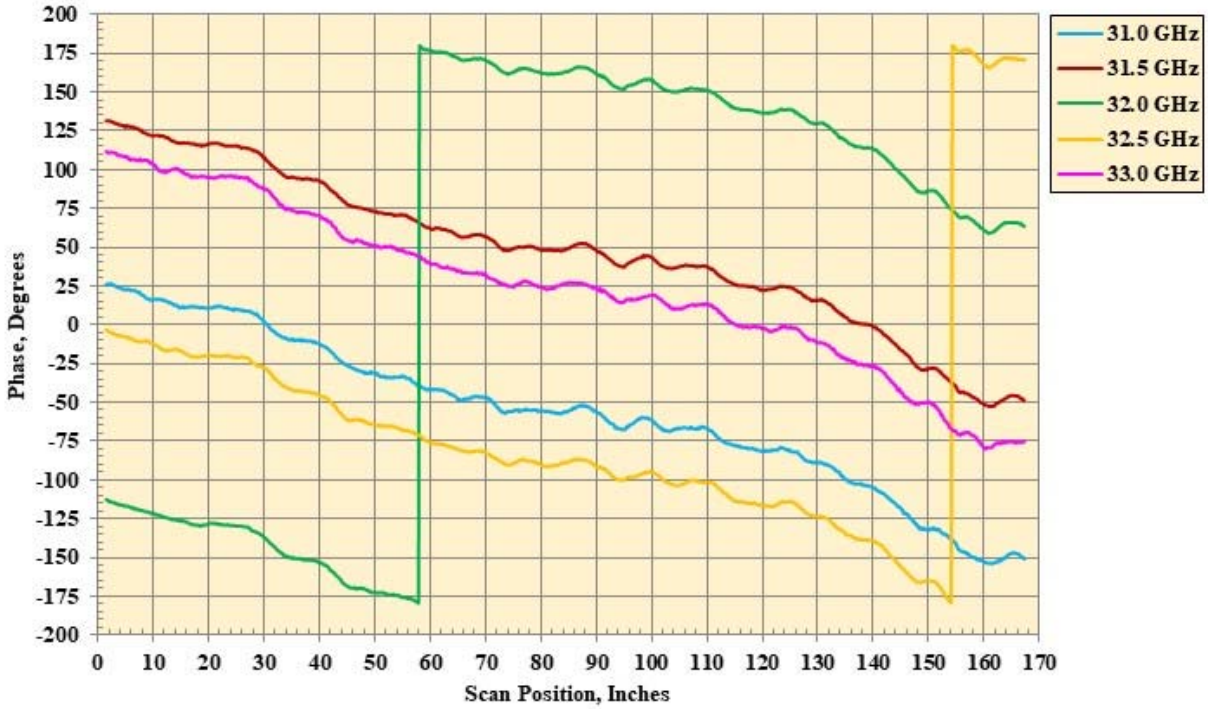

(p) Phase probe data, Probe Angle = 45°, Pol = VV.
Figure 23. Continued.

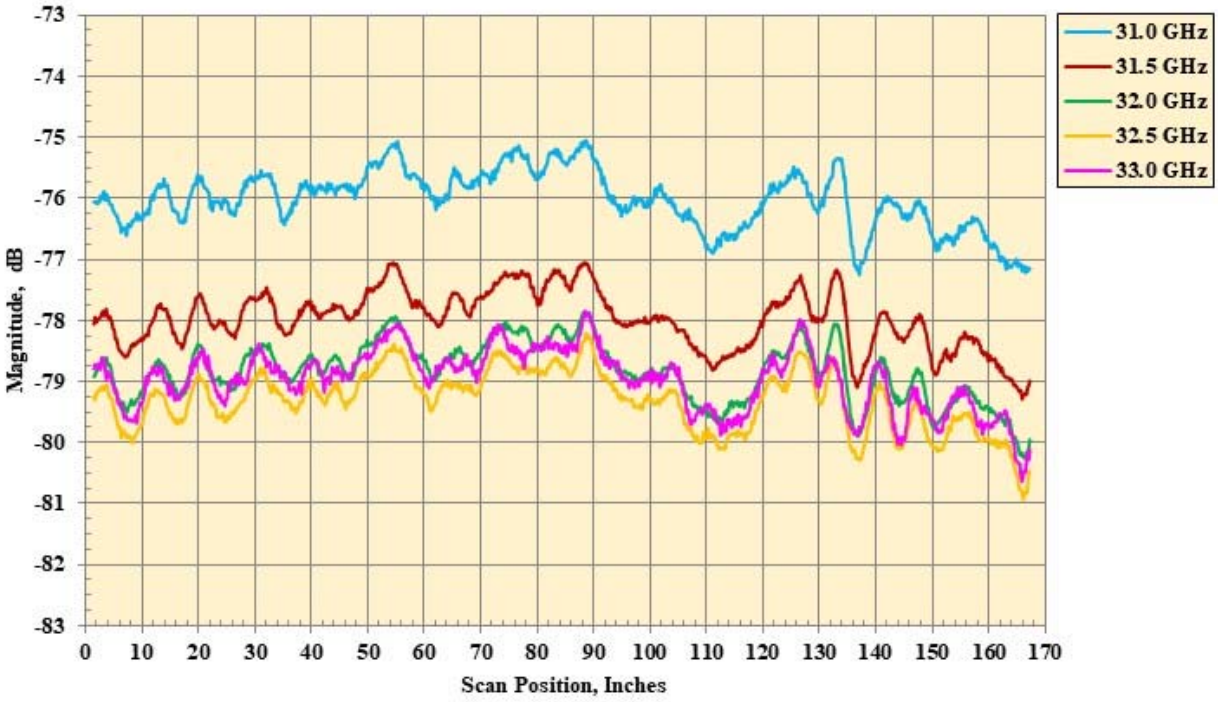

(q) Magnitude probe data, Probe Angle = 60°, Pol = HH.
Figure 23. Continued.

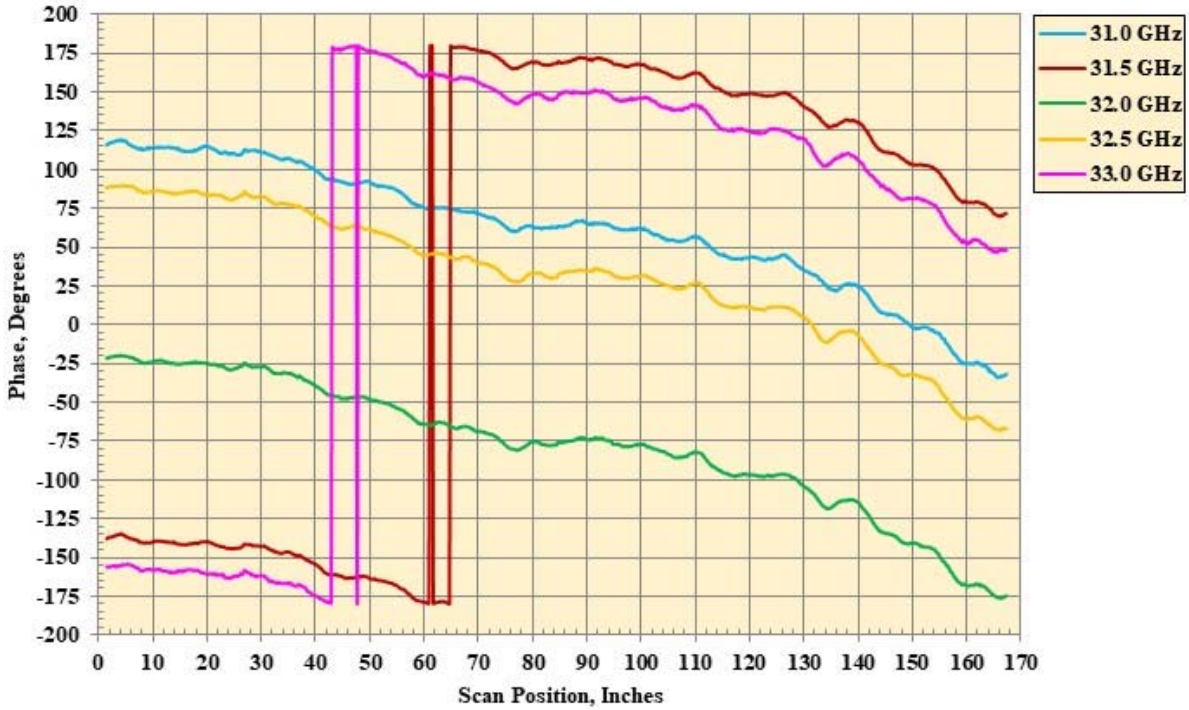

(r) Phase probe data, Probe Angle = 60°, Pol = HH.
Figure 23. Continued

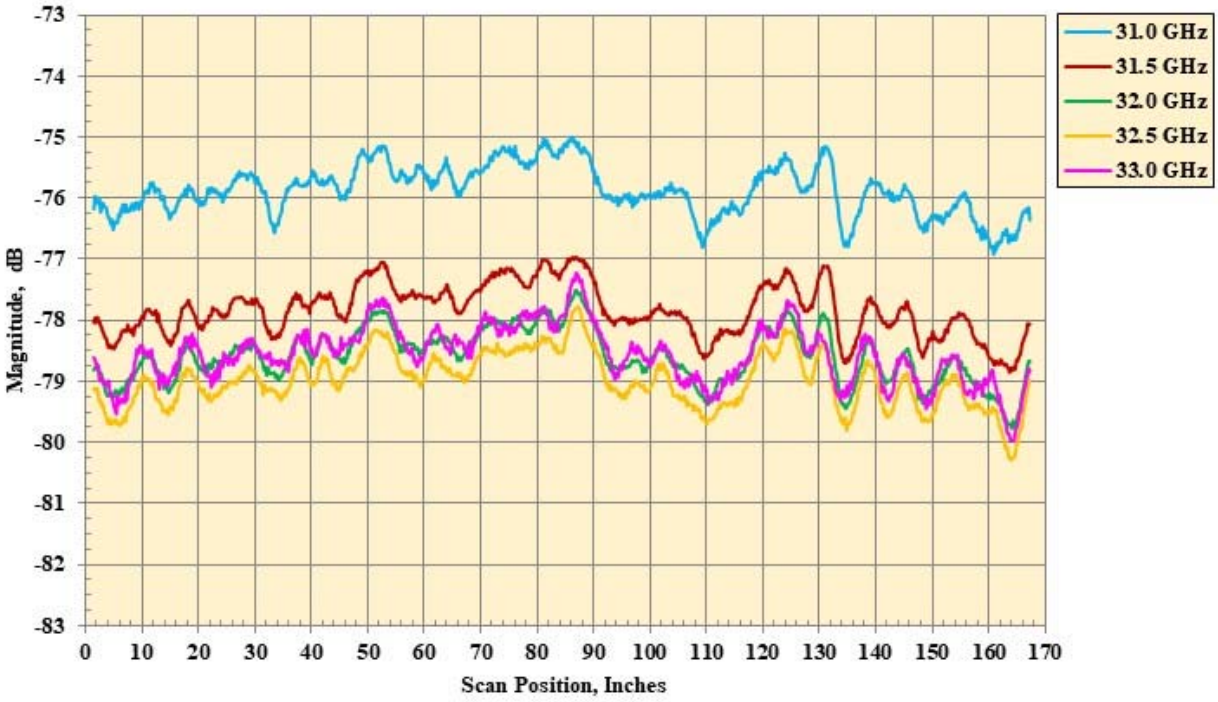

(s) Magnitude probe data, Probe Angle = 60°, Pol = VV.
Figure 23. Continued.

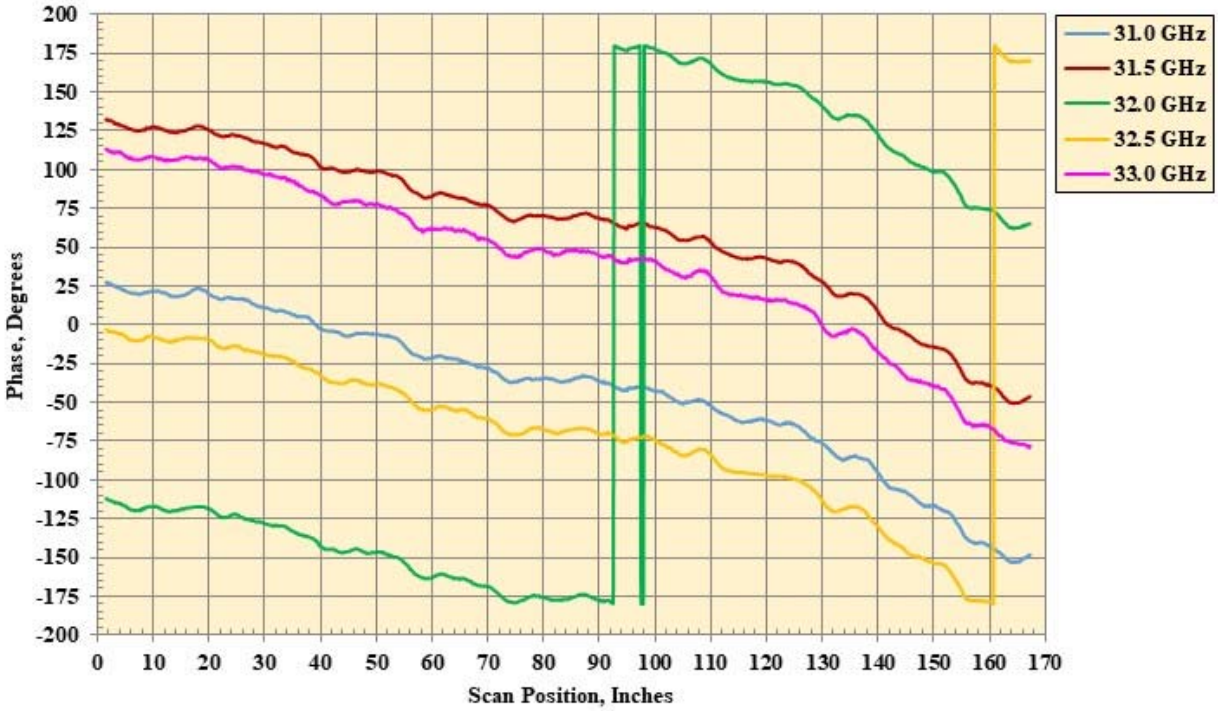

(t) Phase probe data, Probe Angle = 60°, Pol = VV.
Figure 23. Continued.

(u) Magnitude probe data, Probe Angle = 75°, Pol = HH.
Figure 23. Continued.

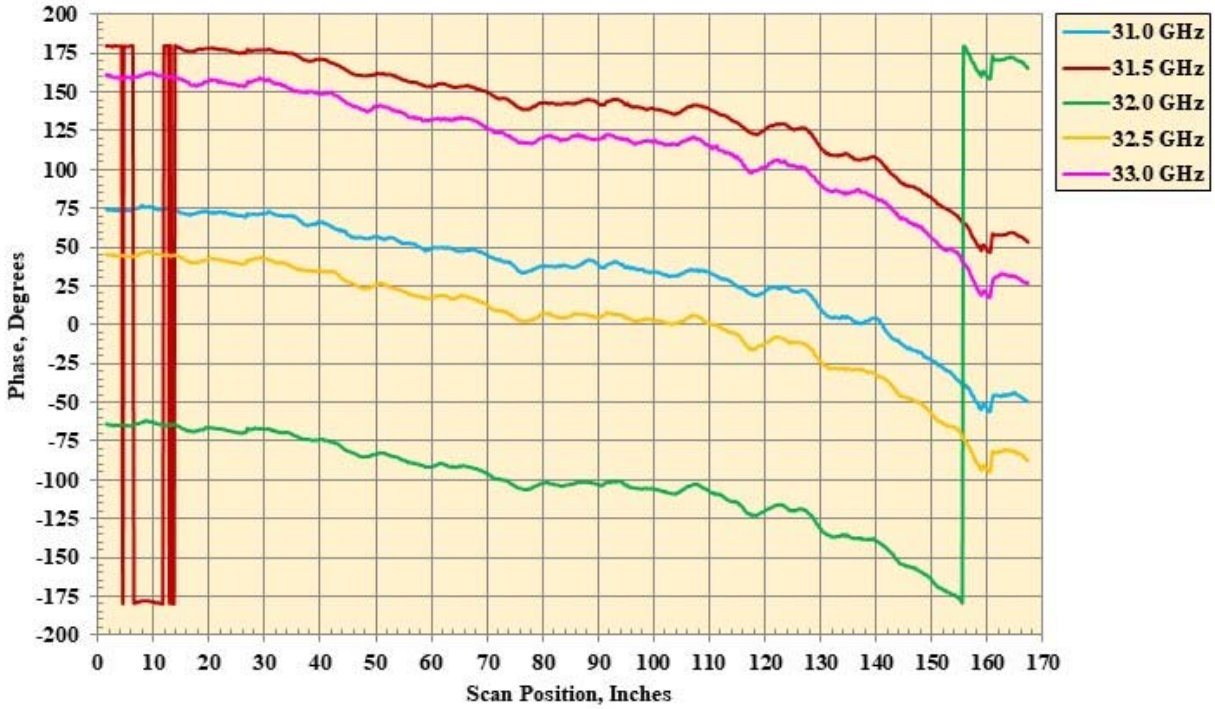

(v) Phase probe data, Probe Angle = 75°, Pol = HH.
Figure 23. Continued.

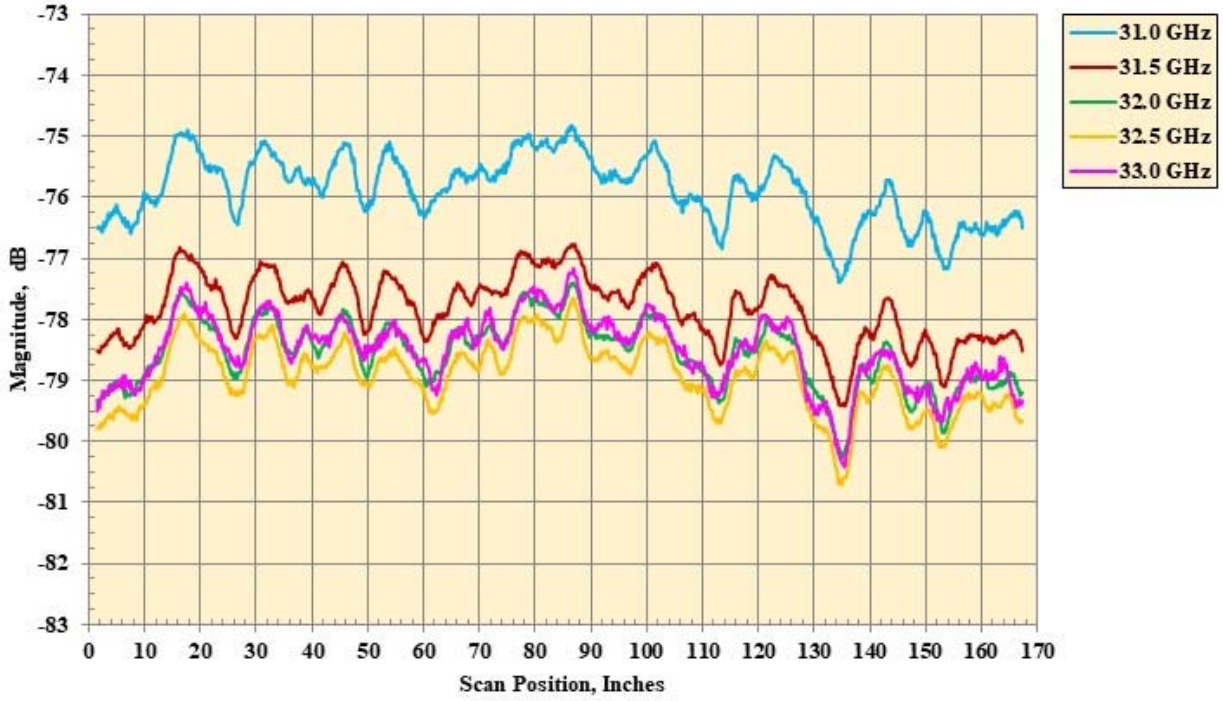

(w) Magnitude probe data, Probe Angle = 75°, Pol = VV.
Figure 23. Continued.

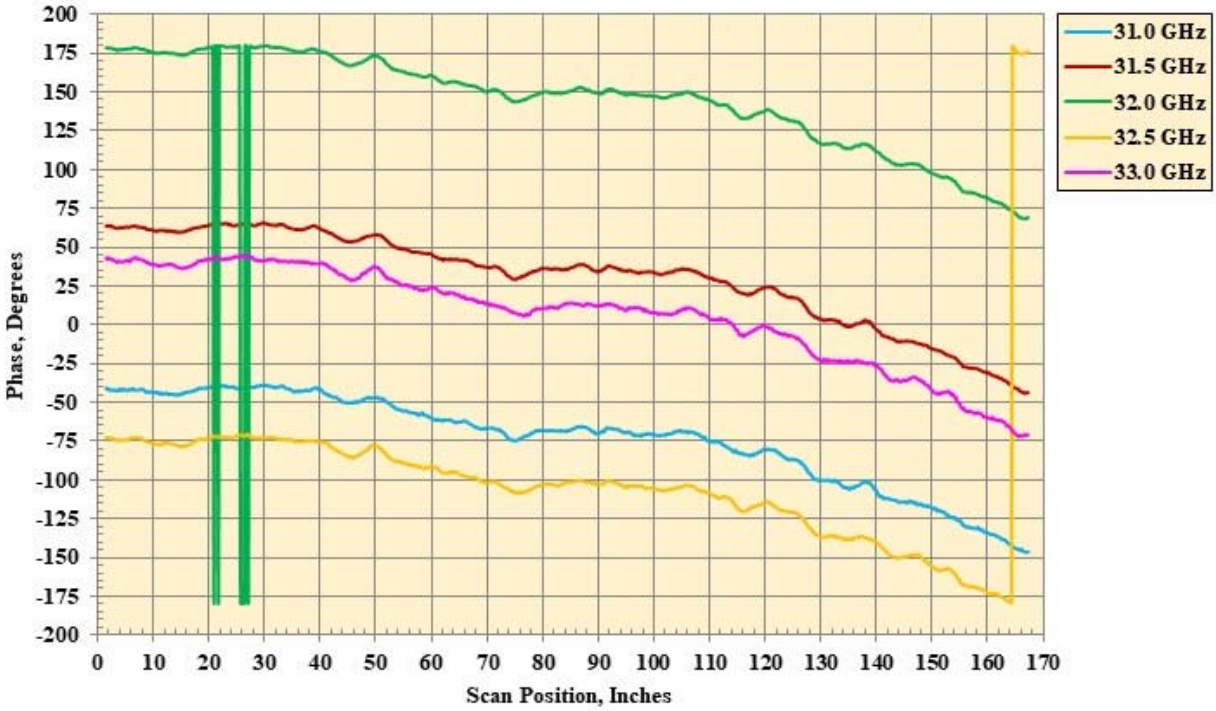

(x) Phase probe data, Probe Angle = 75°, Pol = VV.
Figure 23. Continued.

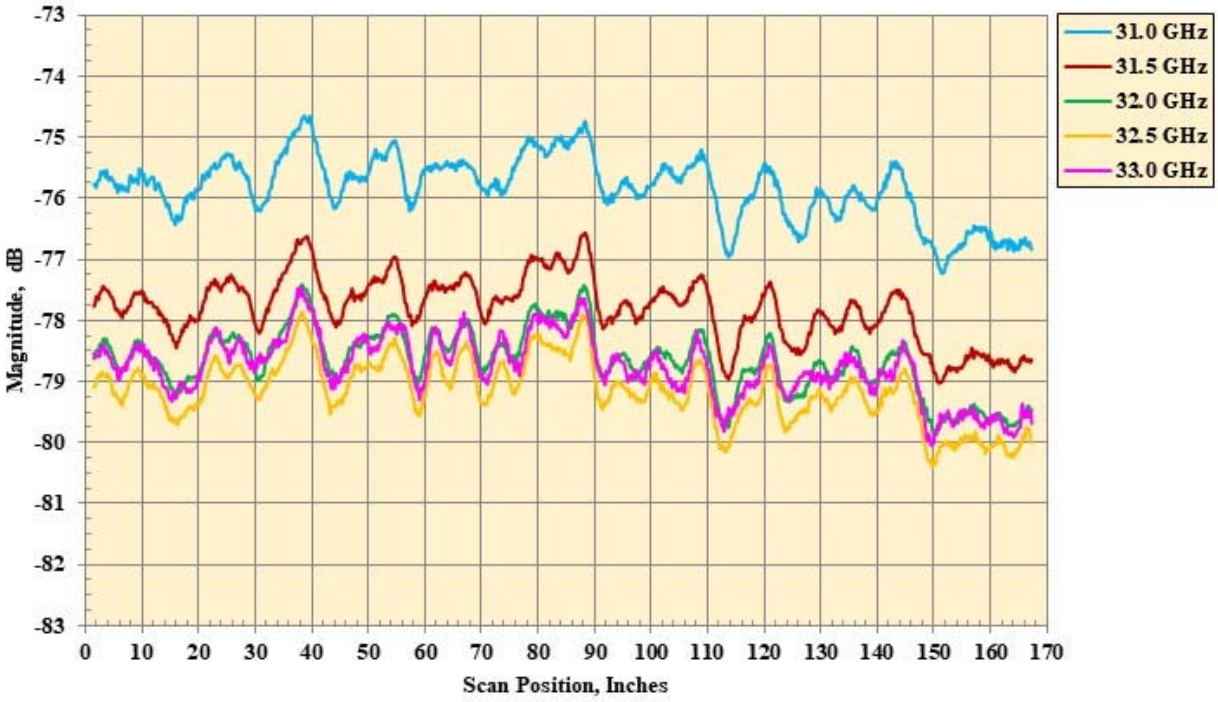

(y) Magnitude probe data, Probe Angle = 90°, Pol = HH.
Figure 23. Continued.

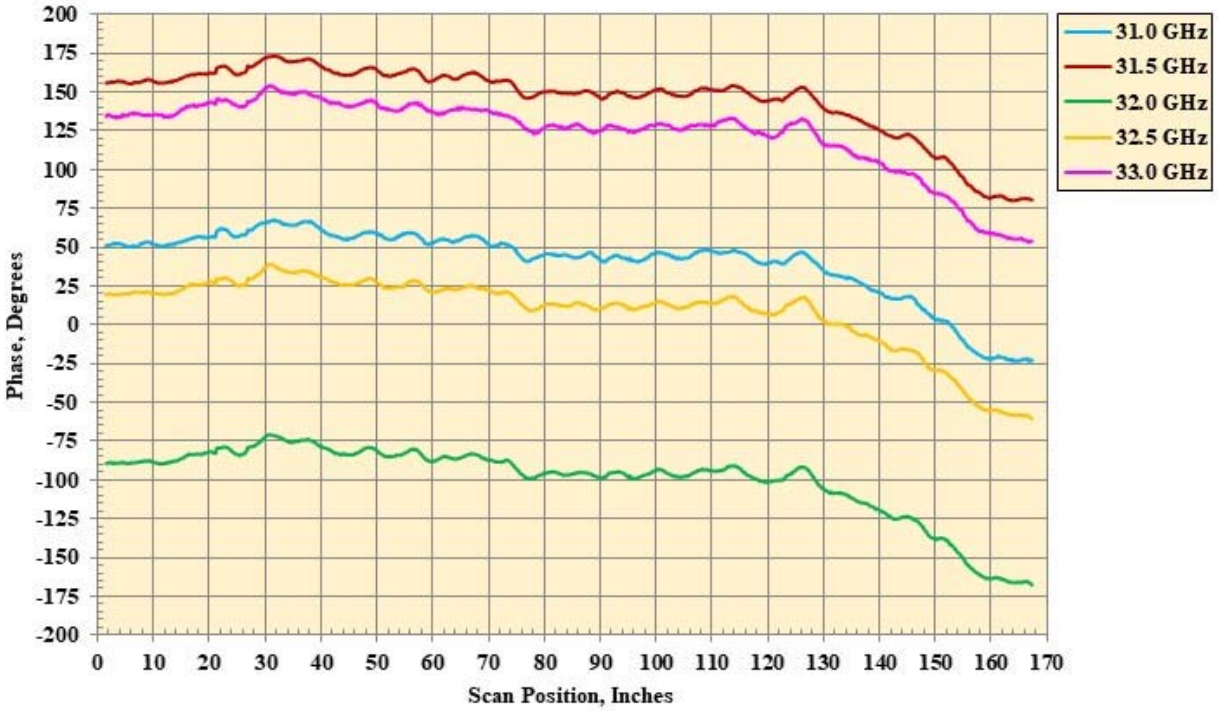

(z) Phase probe data, Probe Angle = 90°, Pol = HH.
Figure 23. Continued.

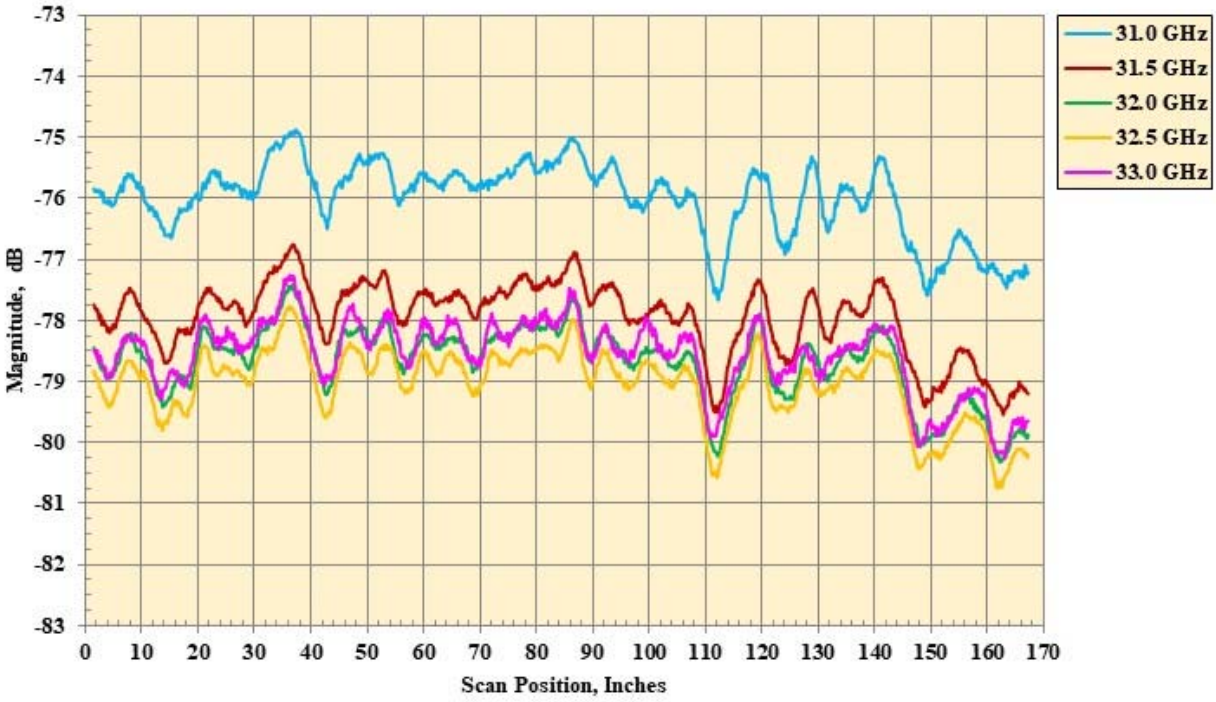

(aa) Magnitude probe data, Probe Angle = 90°, Pol = VV.
Figure 23. Continued.

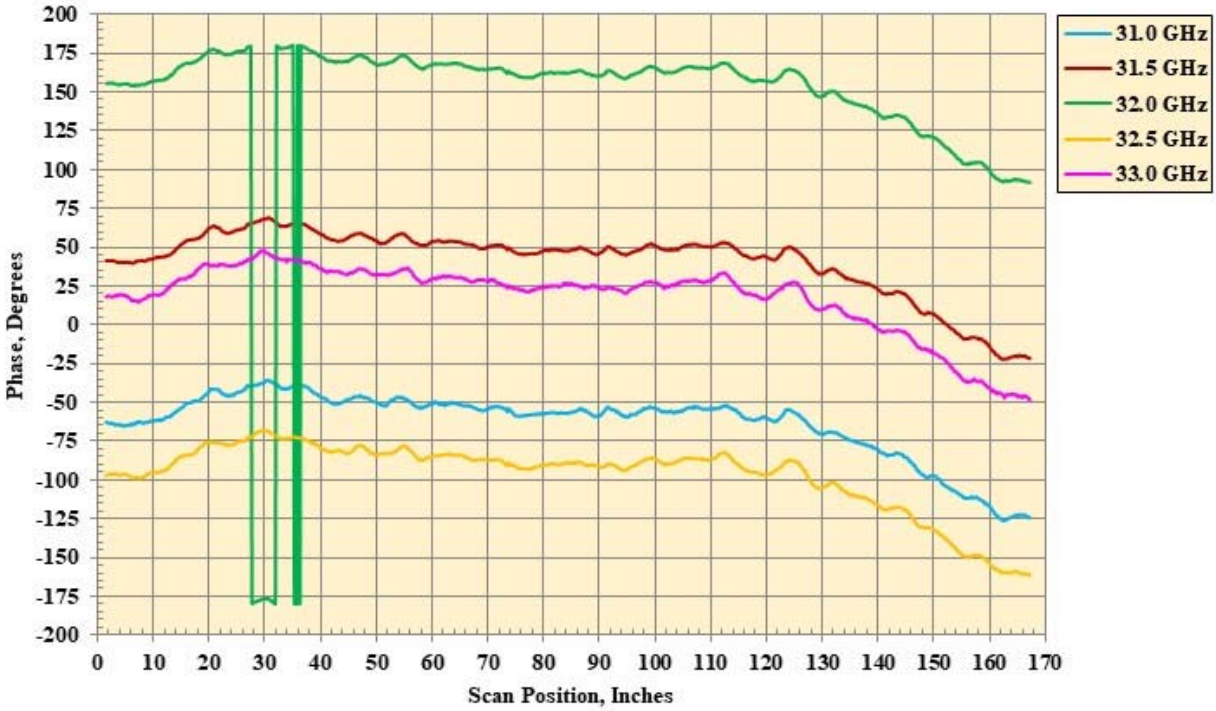

(bb) Phase probe data, Probe Angle = 90°, Pol = VV.
Figure 23. Continued.

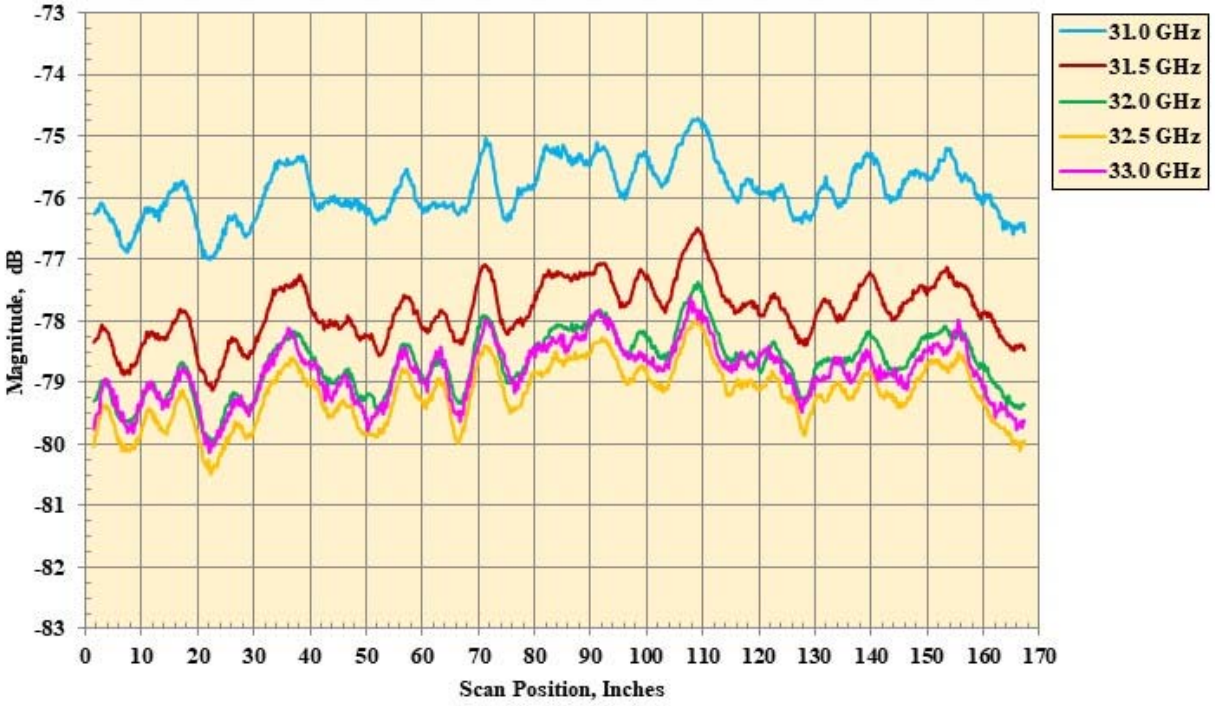

(cc) Magnitude probe data, Probe Angle = -15°, Pol = HH.
Figure 23. Continued.

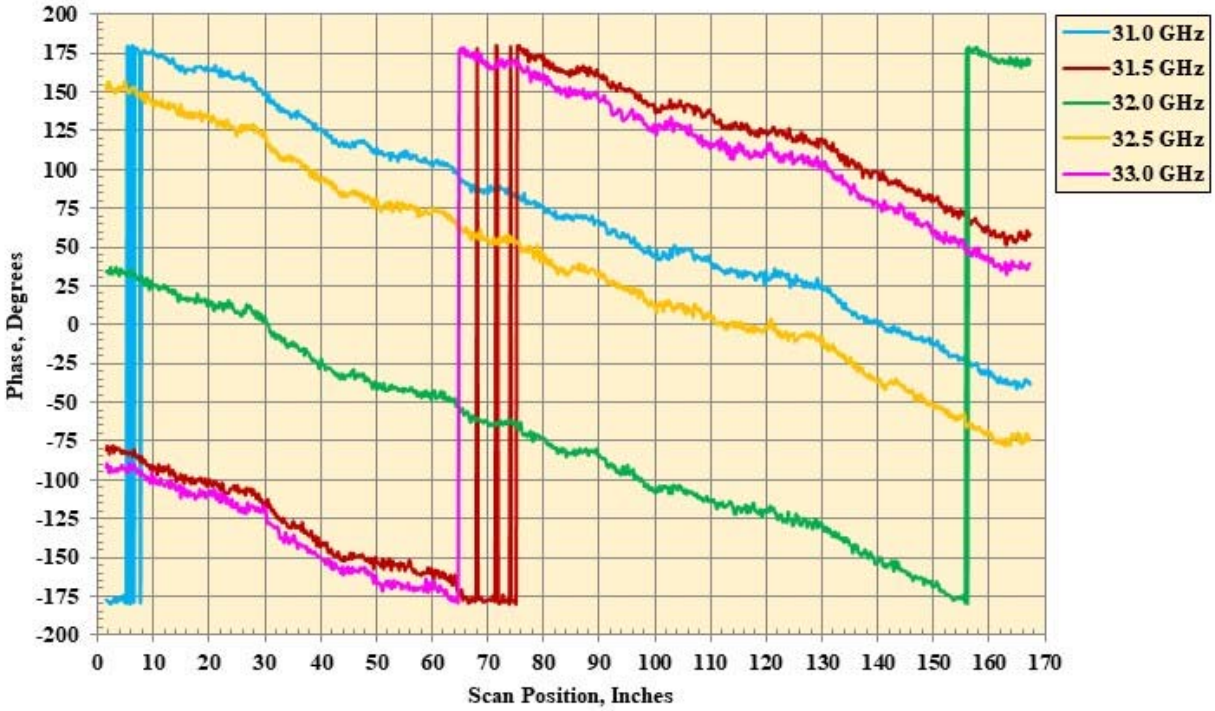

(dd) Phase probe data, Probe Angle = -15°, Pol = HH.
Figure 23. Continued.

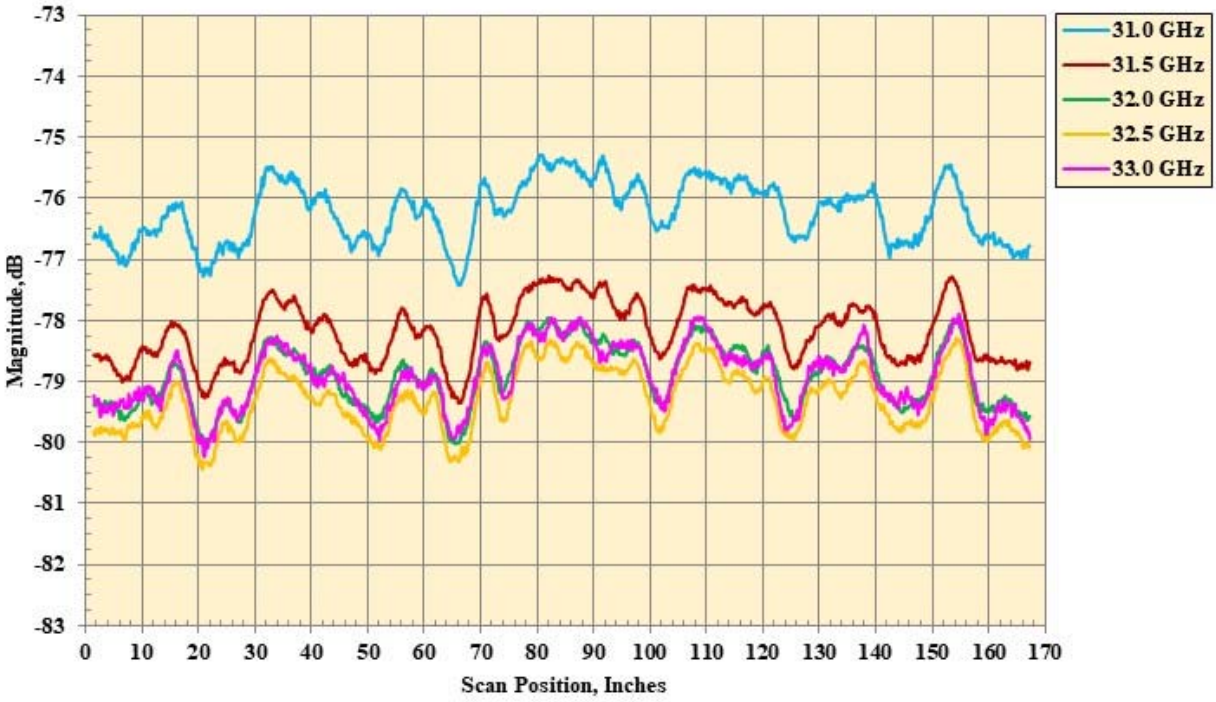

(ee) Magnitude probe data, Probe Angle = -15°, Pol = VV.
Figure 23. Continued.

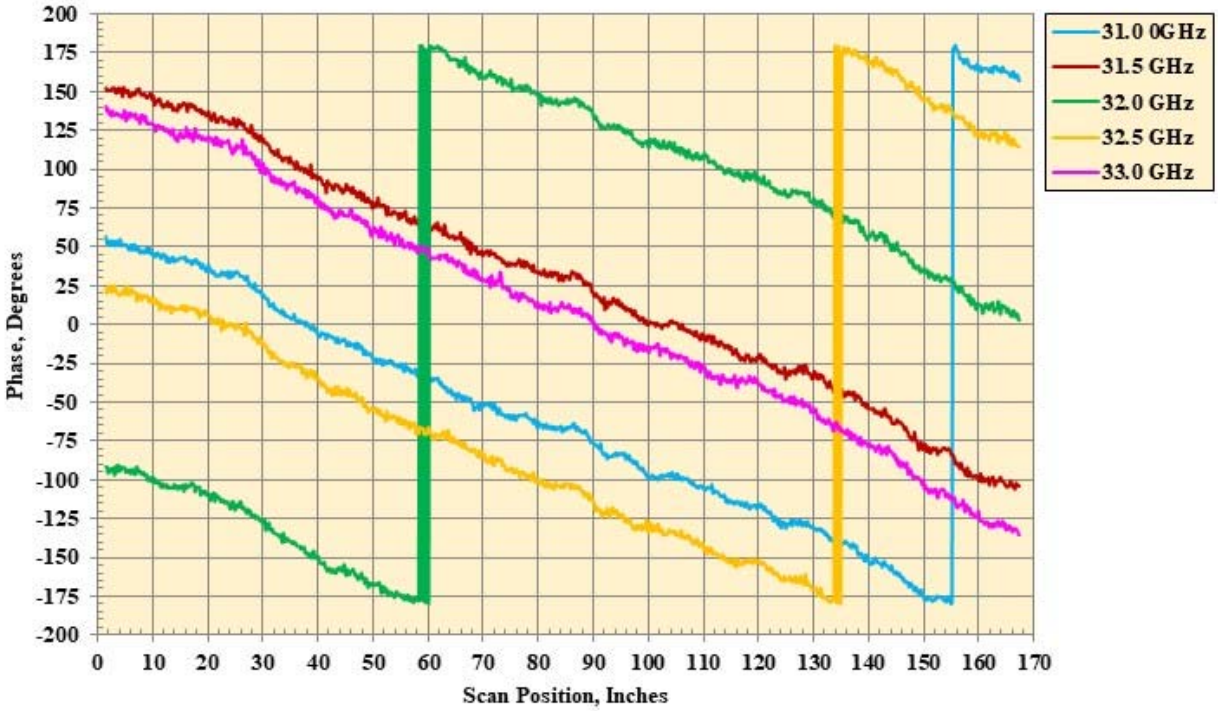

(ff) Phase probe data, Probe Angle = -15°, Pol = VV.
Figure 23. Continued.

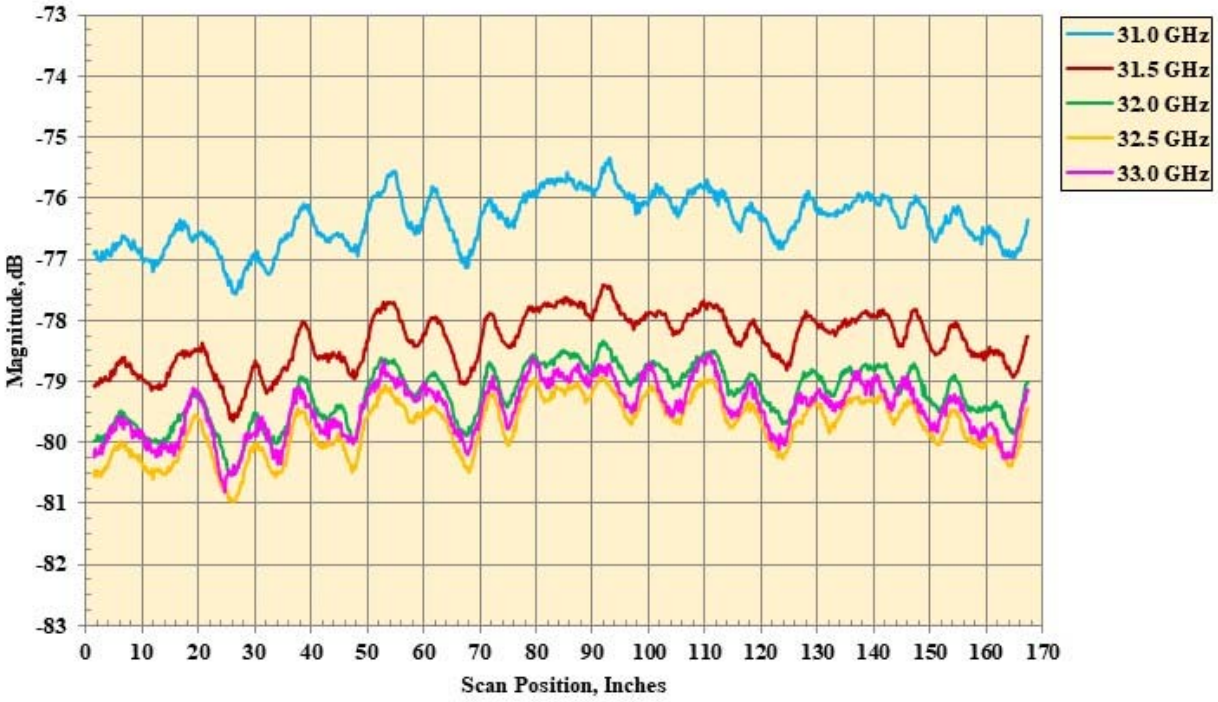

(gg) Magnitude probe data, Probe Angle = -30°, Pol = HH.
Figure 23. Continued.

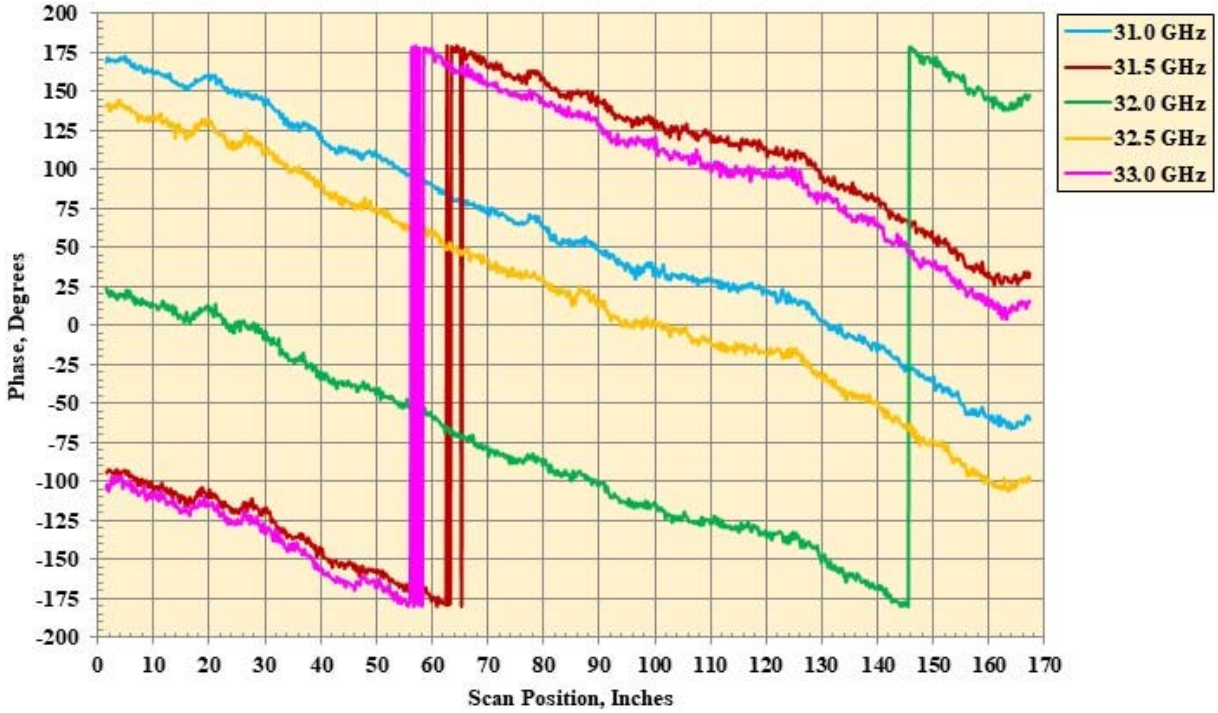

(hh) Phase probe data, Probe Angle = -30°, Pol = HH.
Figure 23. Continued.

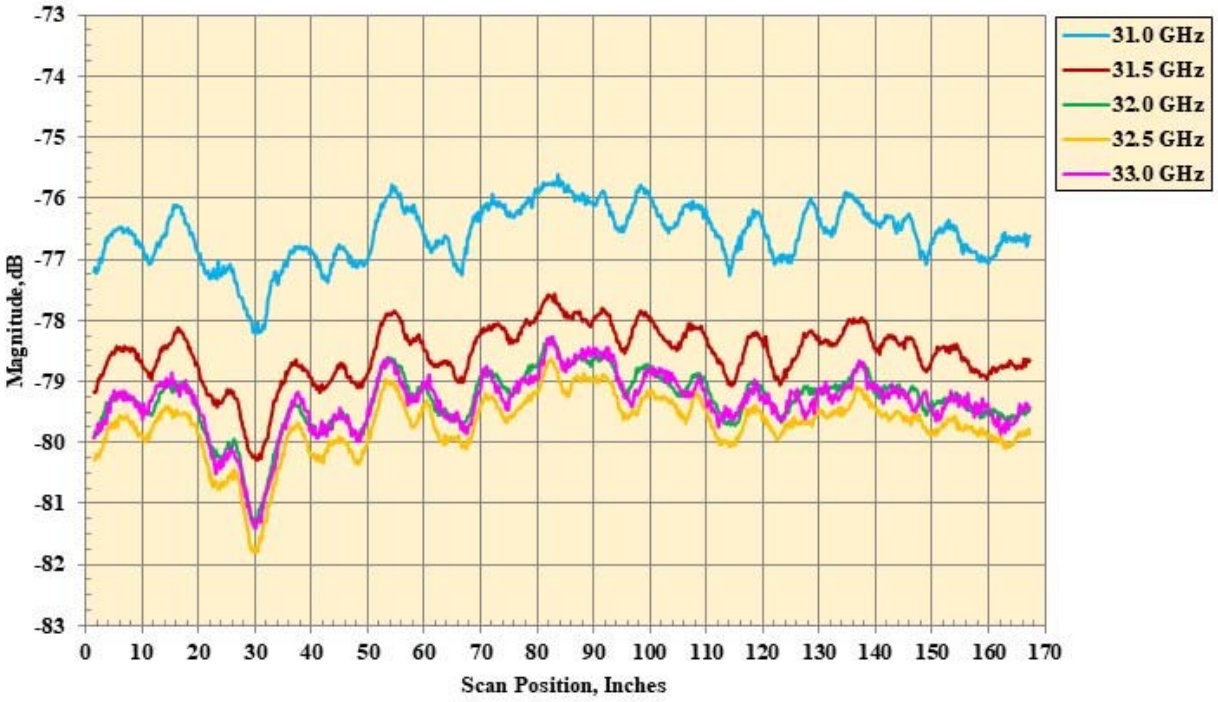

(ii) Magnitude probe data, Probe Angle = -30°, Pol = VV.
Figure 23. Continued.

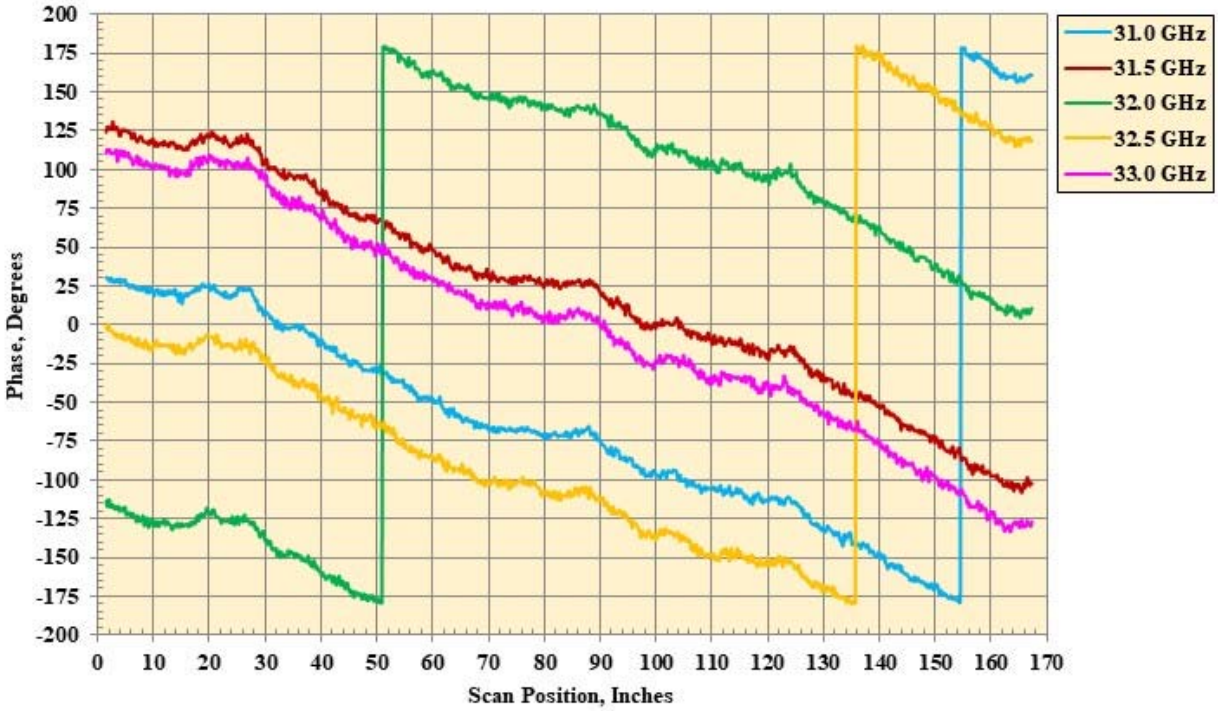

(jj) Phase probe data, Probe Angle = -30°, Pol = VV.
Figure 23. Continued.

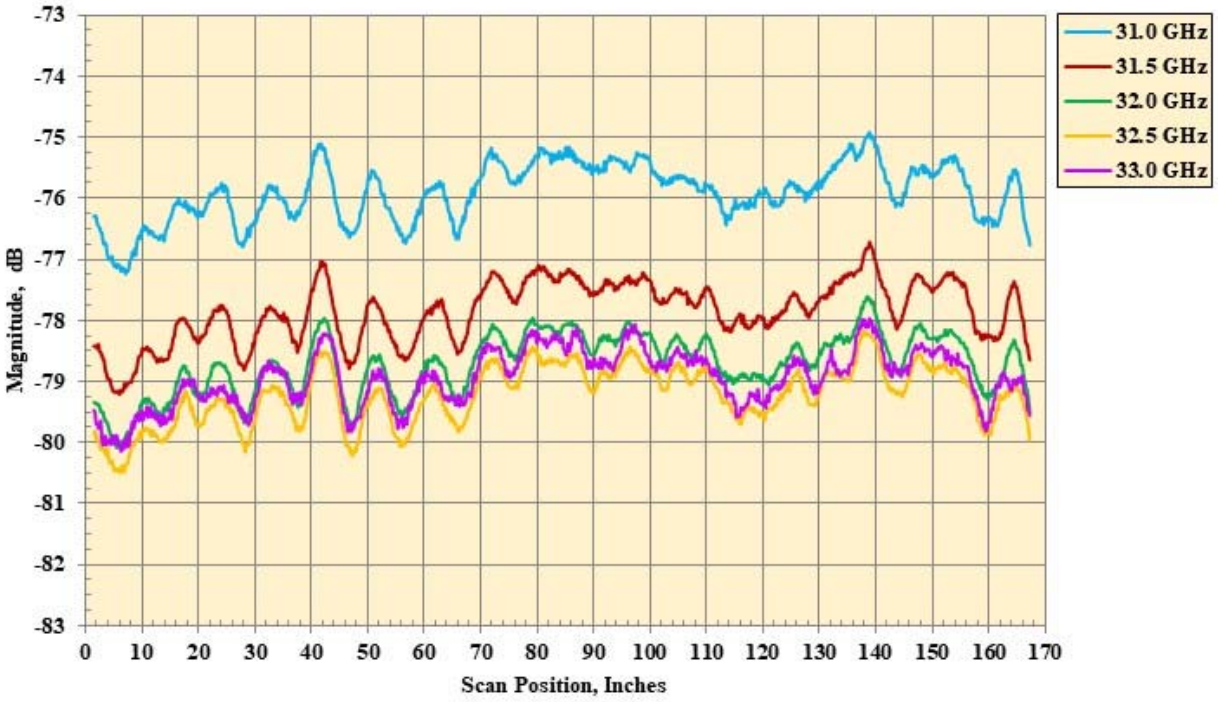

(kk) Magnitude probe data, Probe Angle = -45°, Pol HH.
Figure 23. Continued.

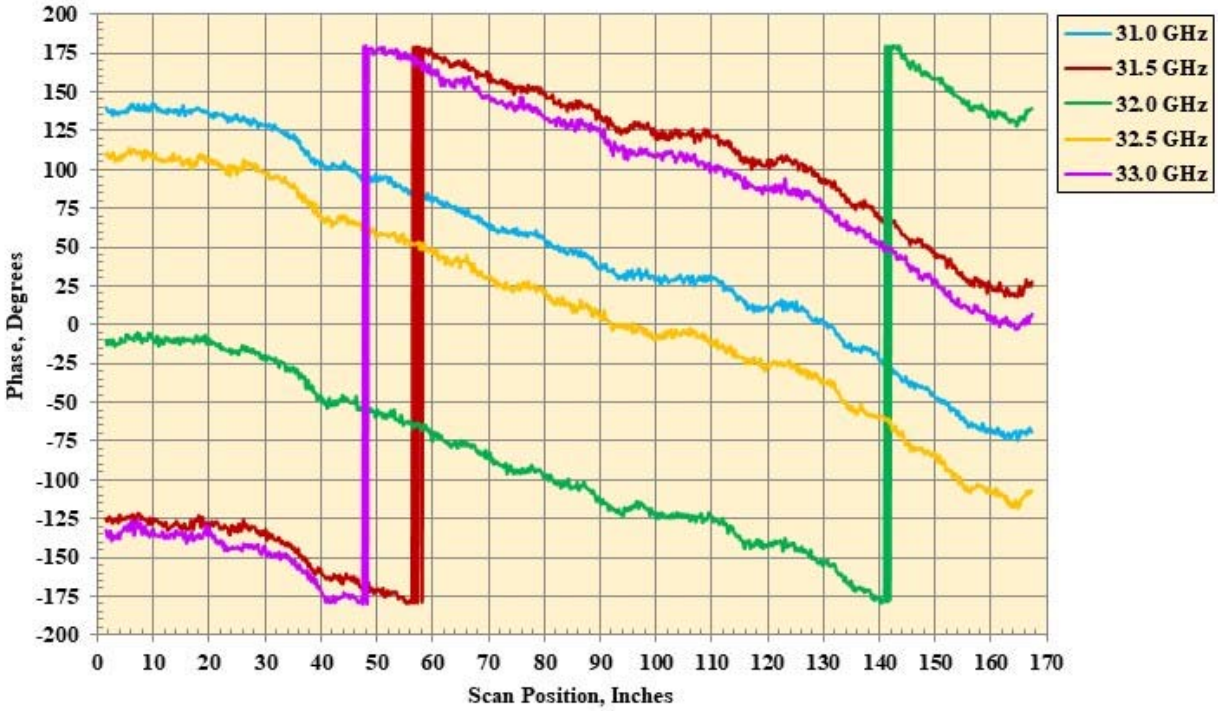

(ll) Phase probe data, Probe Angle = -45°, Pol = HH.
Figure 23. Continued.

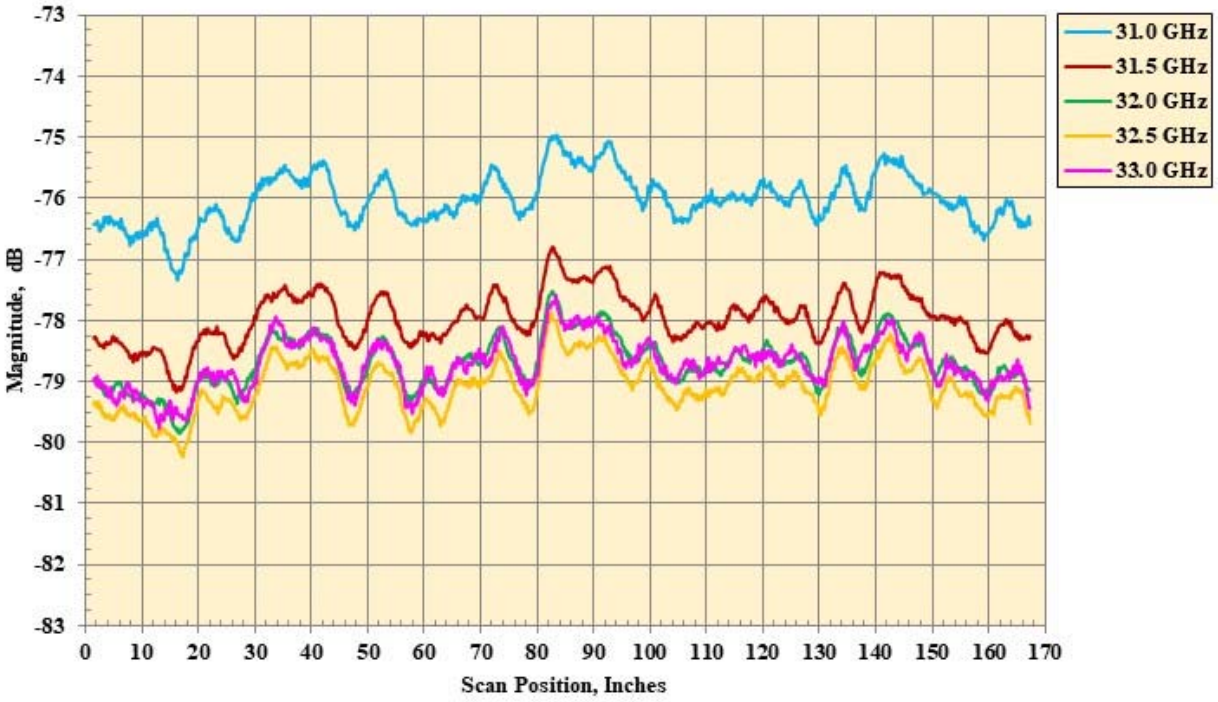

(mm) Magnitude probe data, Probe Angle = -45°, Pol = VV.
Figure 23. Continued.

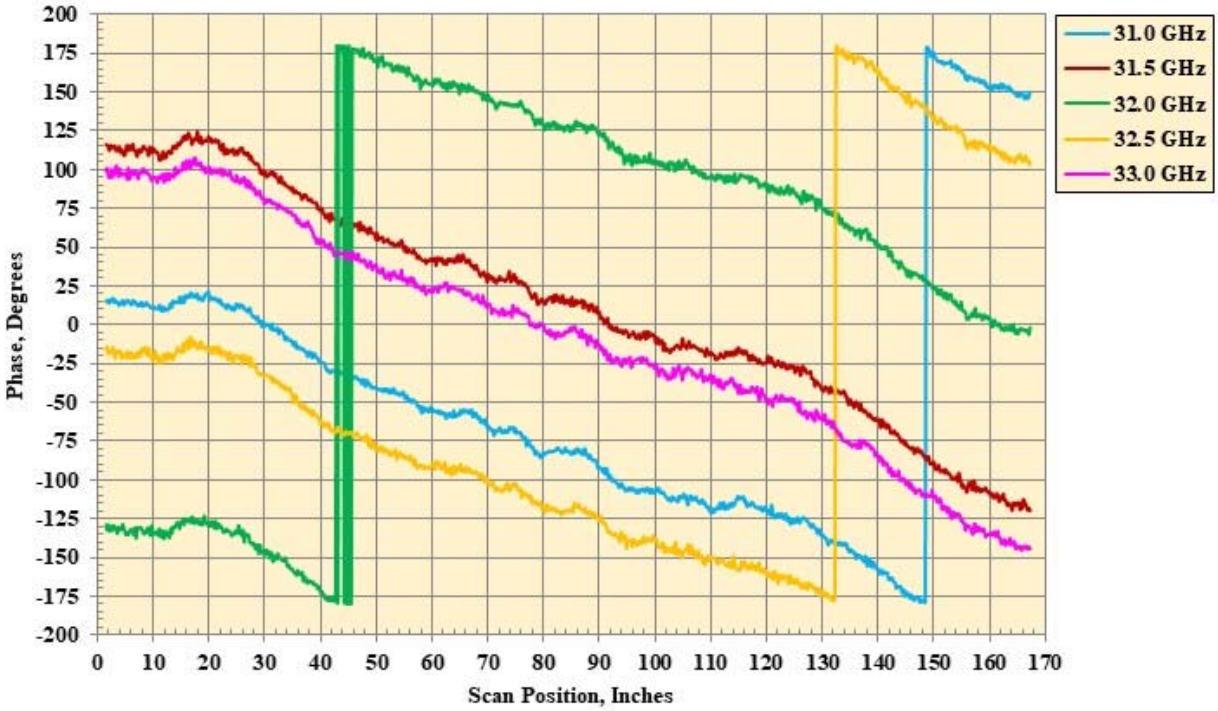

(nn) Phase probe data, Probe Angle = -45°, Pol = VV.
Figure 23. Continued.

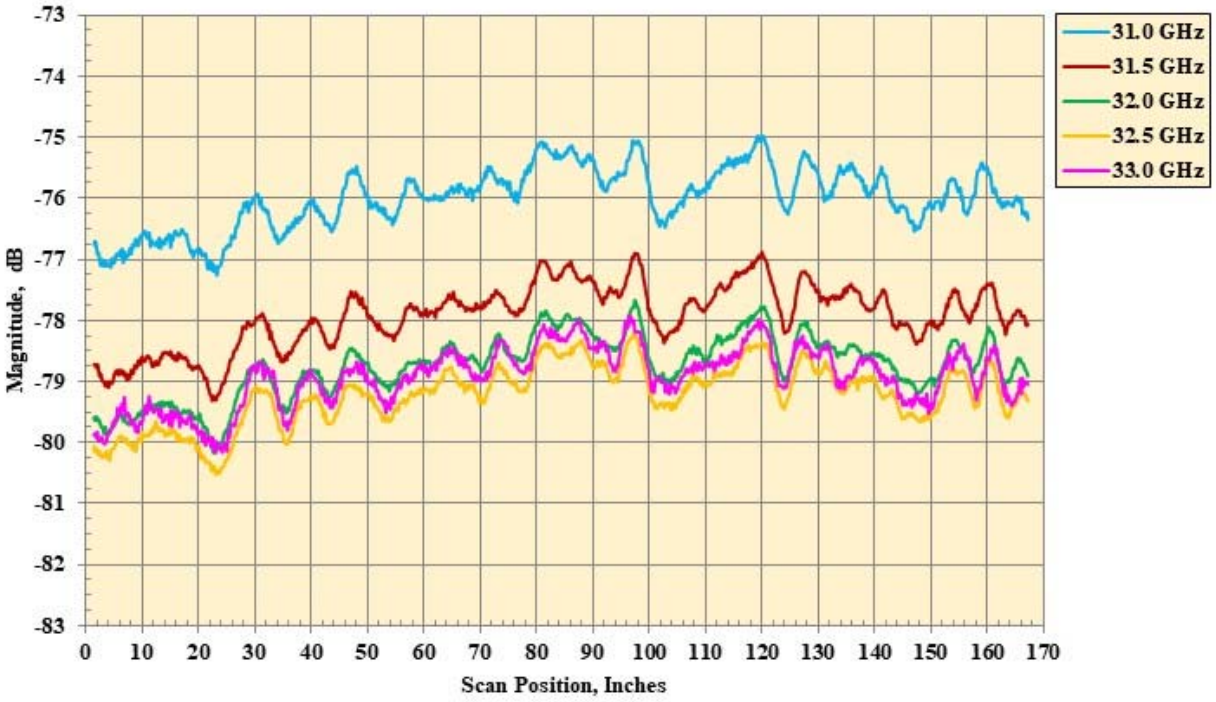

(oo) Magnitude probe data, Probe Angle = -60°, Pol = HH.
Figure 23. Continued.

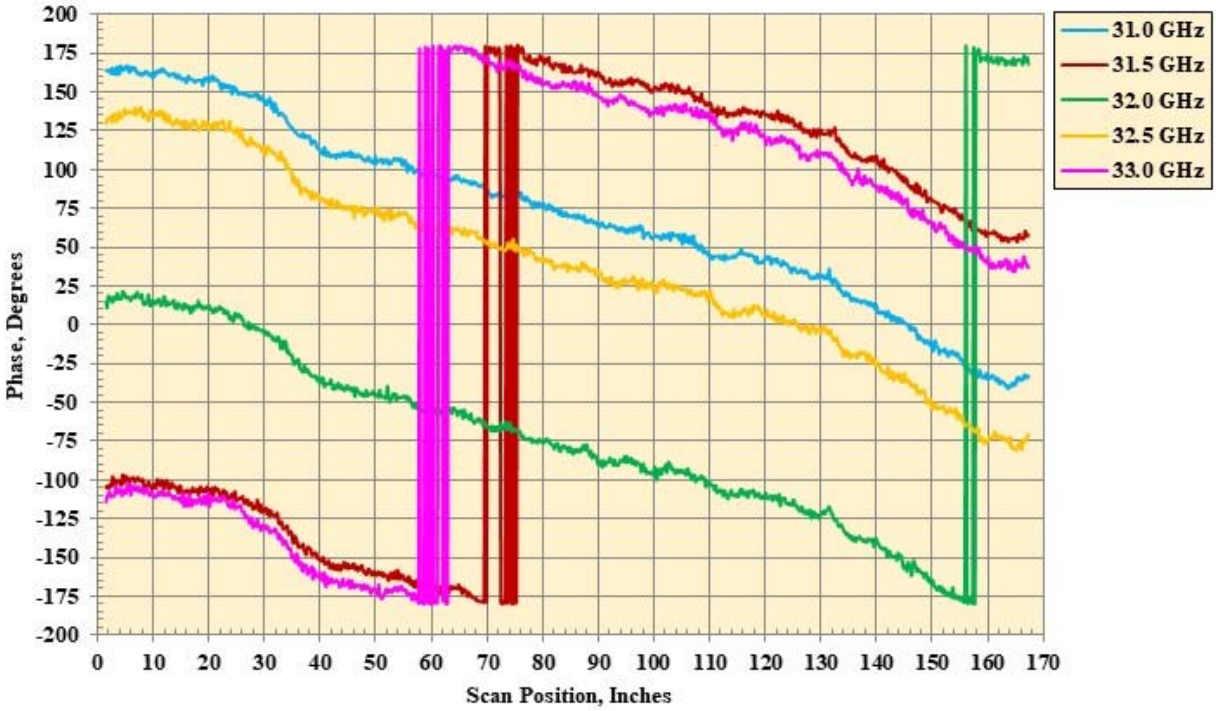

(pp) Phase probe data, Probe Angle = -60°, Pol = HH.
Figure 23. Continued.

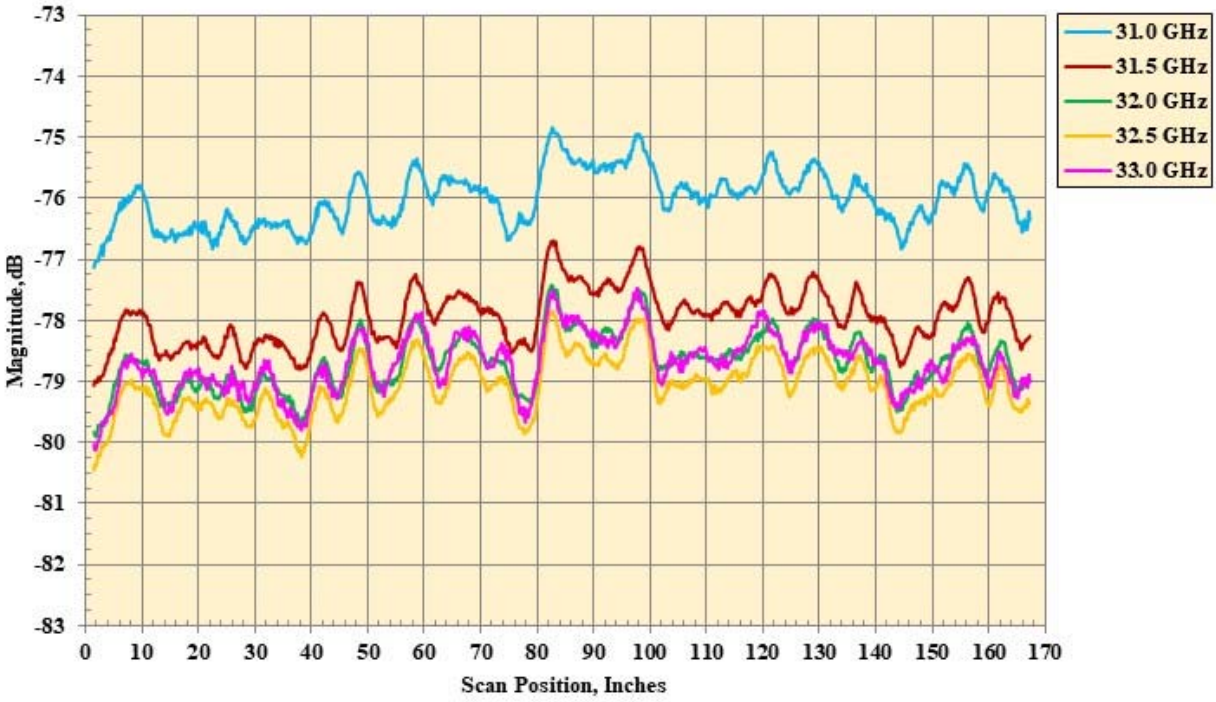

(qq) Magnitude probe data, Probe Angle = -60°, Pol = VV.
Figure 23. Continued.

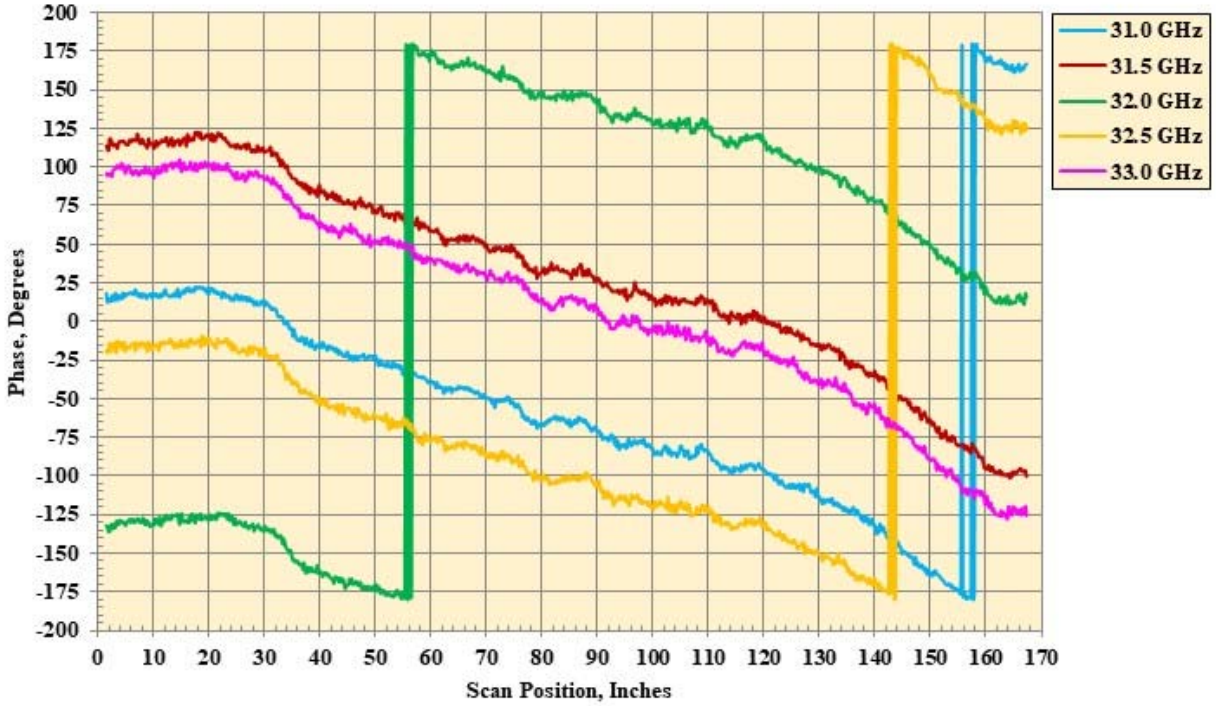

(rr) Phase probe data, Probe Angle = -60°, Pol = VV.
Figure 23. Continued.

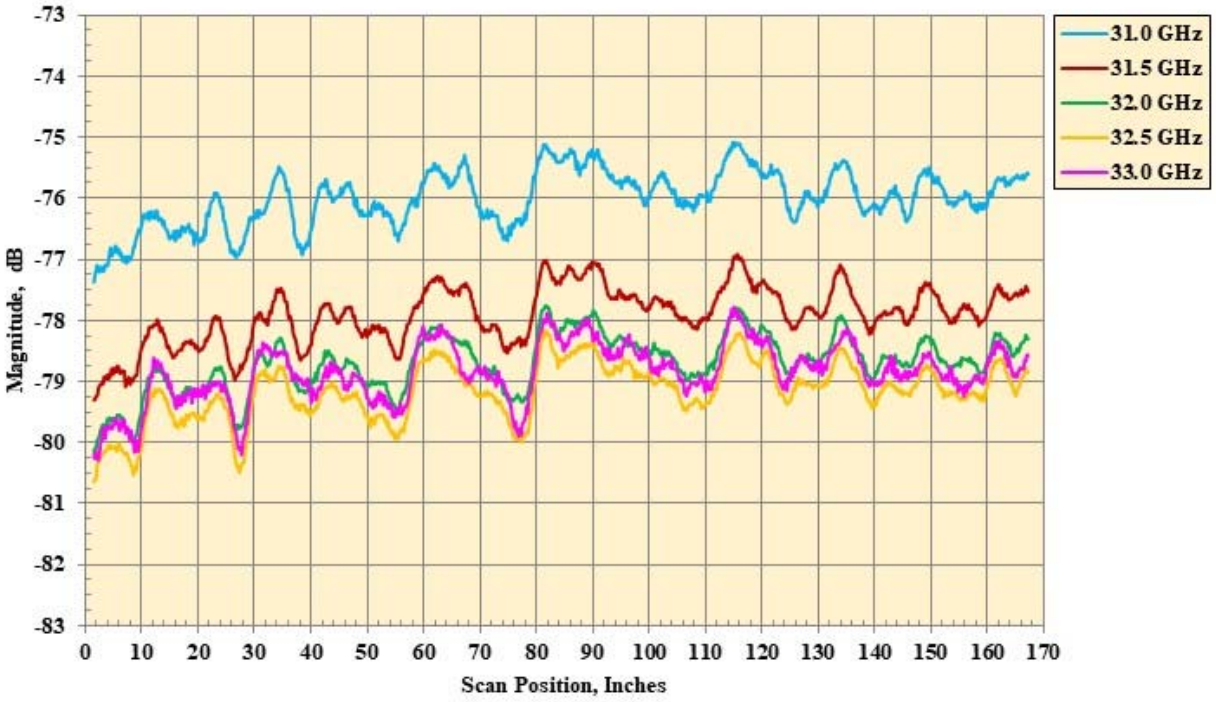

(ss) Magnitude probe data, Probe Angle = -75°, Pol = HH.
Figure 23. Continued.

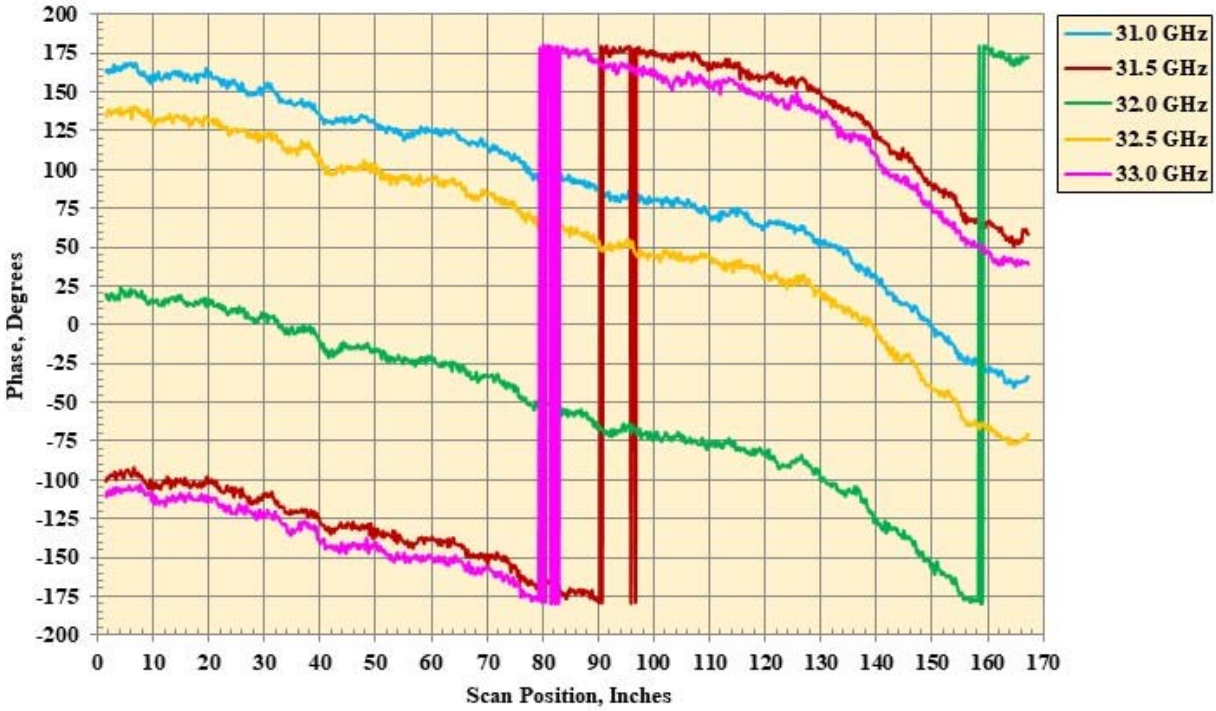

(tt) Phase probe data, Probe Angle = -75°, Pol = HH.
Figure 23. Continued.

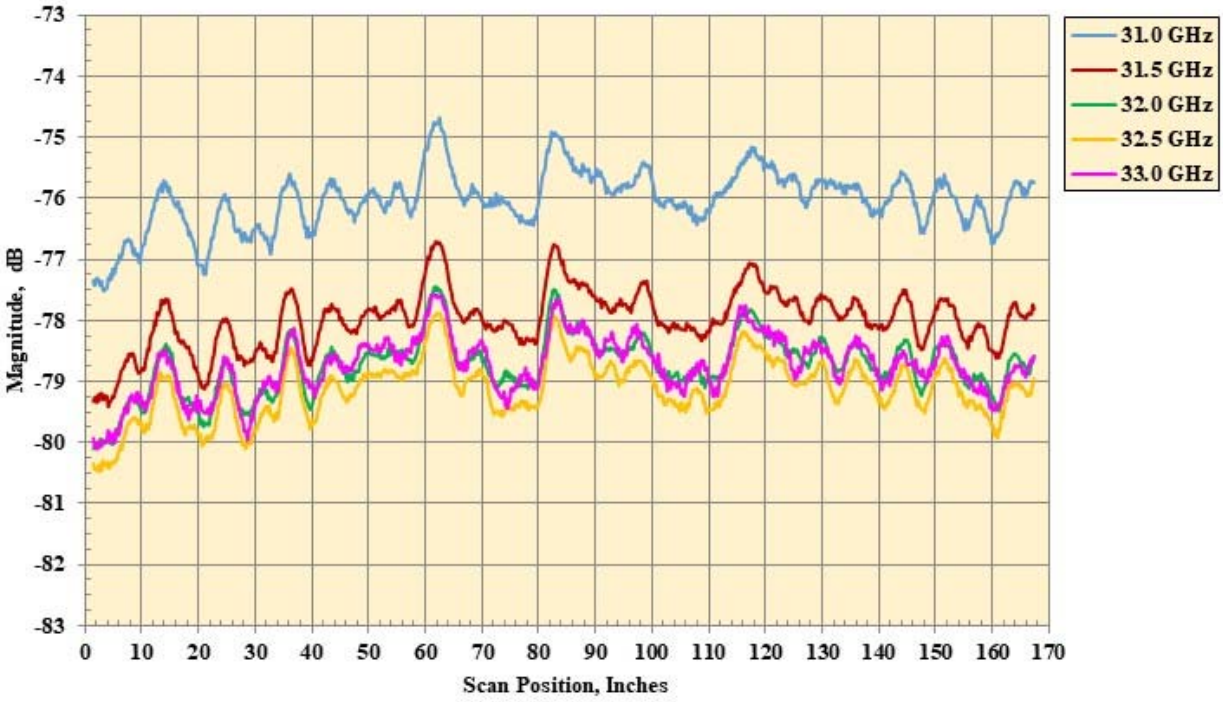

(uu) Magnitude probe data, Probe Angle = -75°, Pol = VV.
Figure 23. Continued.

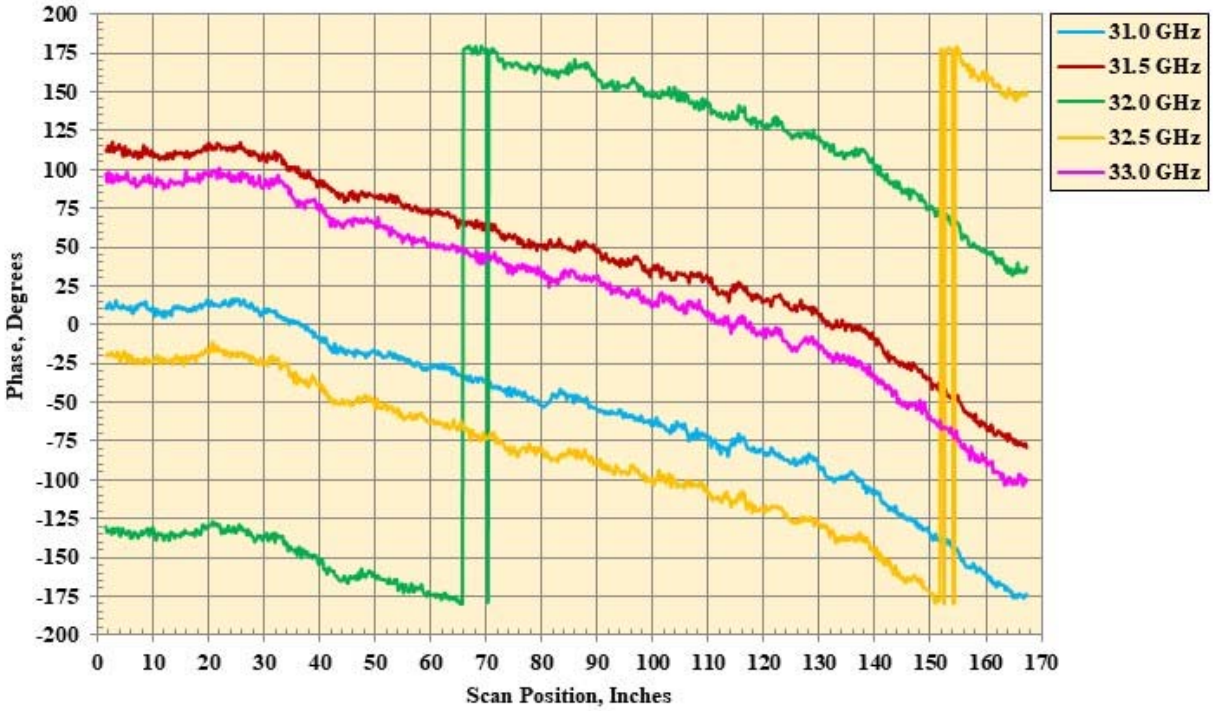

(vv) Phase probe data, Probe Angle = -75°, Pol = VV.
Figure 23. Continued.

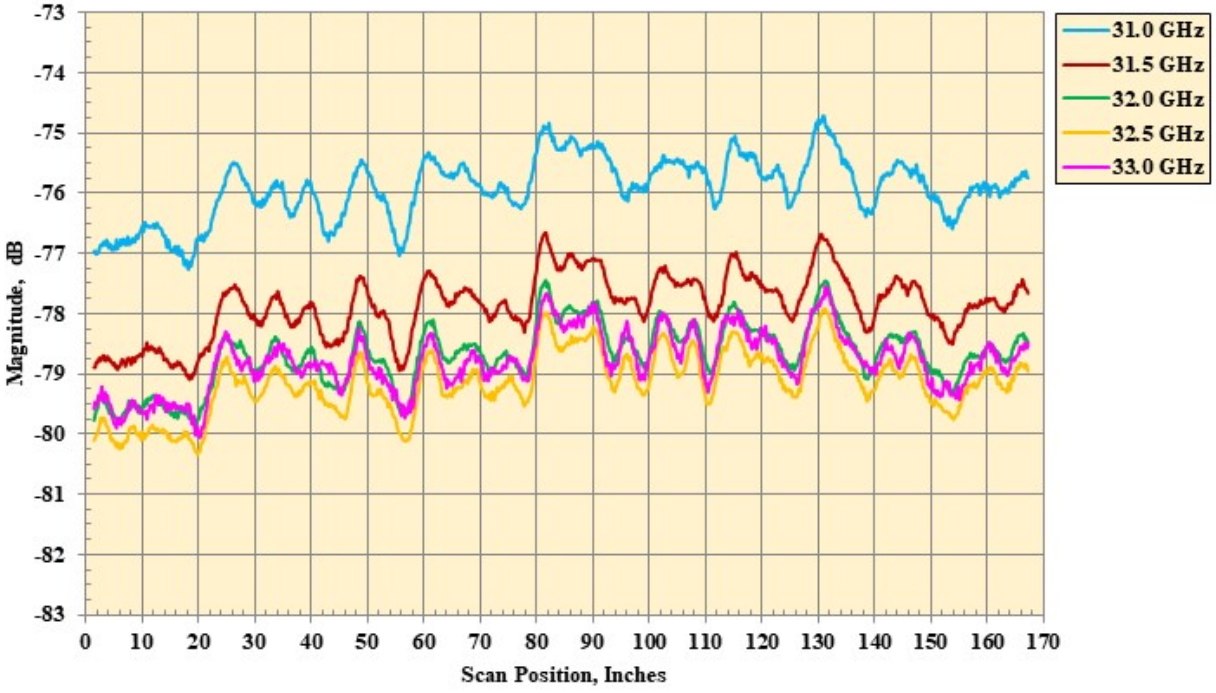

(ww) Magnitude probe data, Probe Angle = -90°, Pol = HH.
Figure 23. Continued.

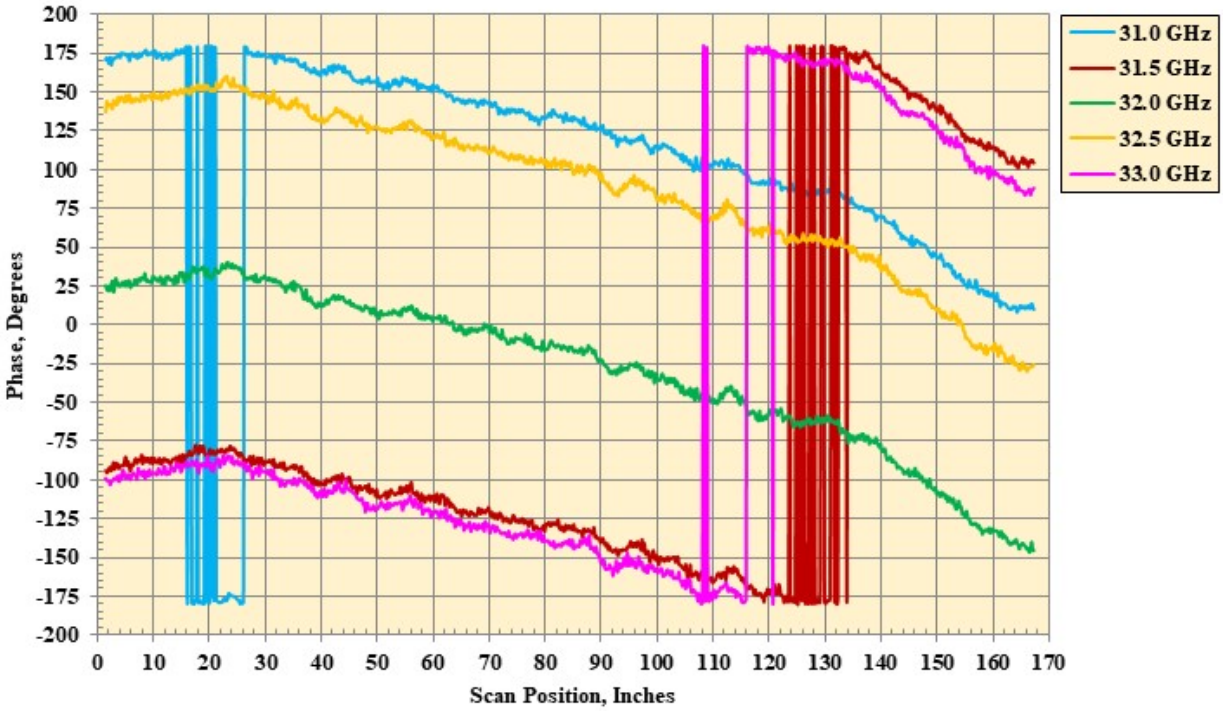

(xx) Phase probe data, Probe Angle = -90°, Pol = HH.
Figure 23. Continued.

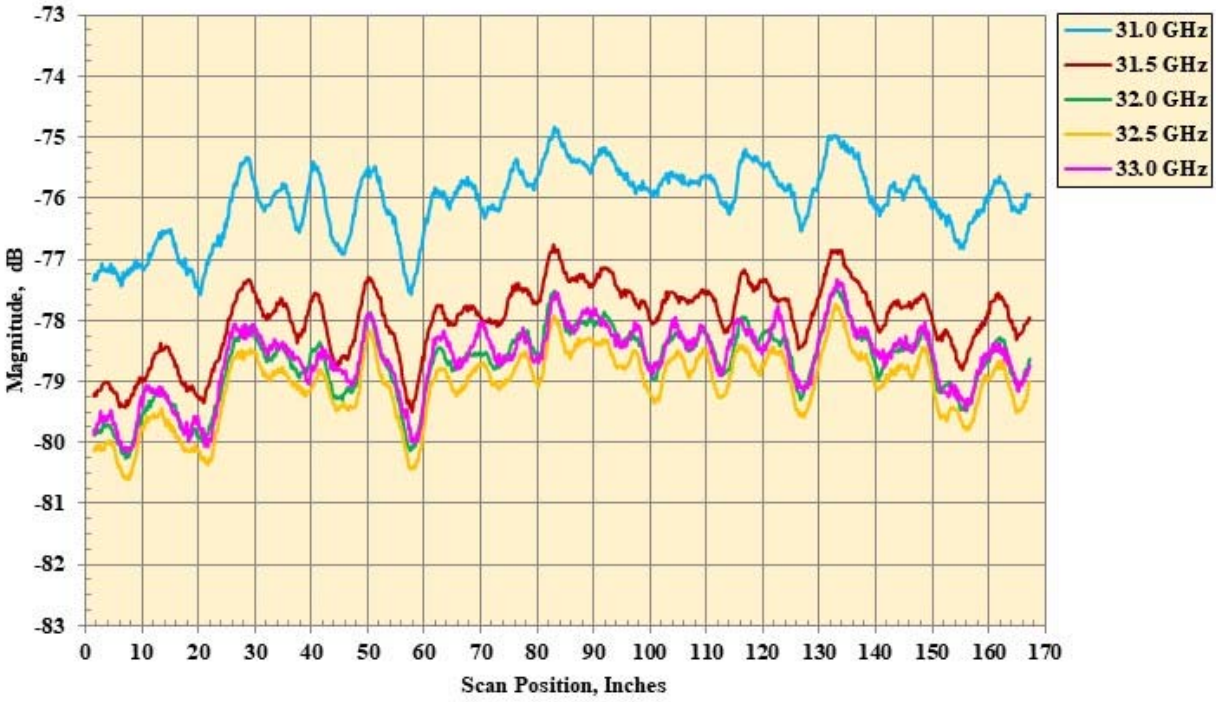

(yy) Magnitude probe data, Probe Angle = -90°, Pol = VV.
Figure 23. Continued.

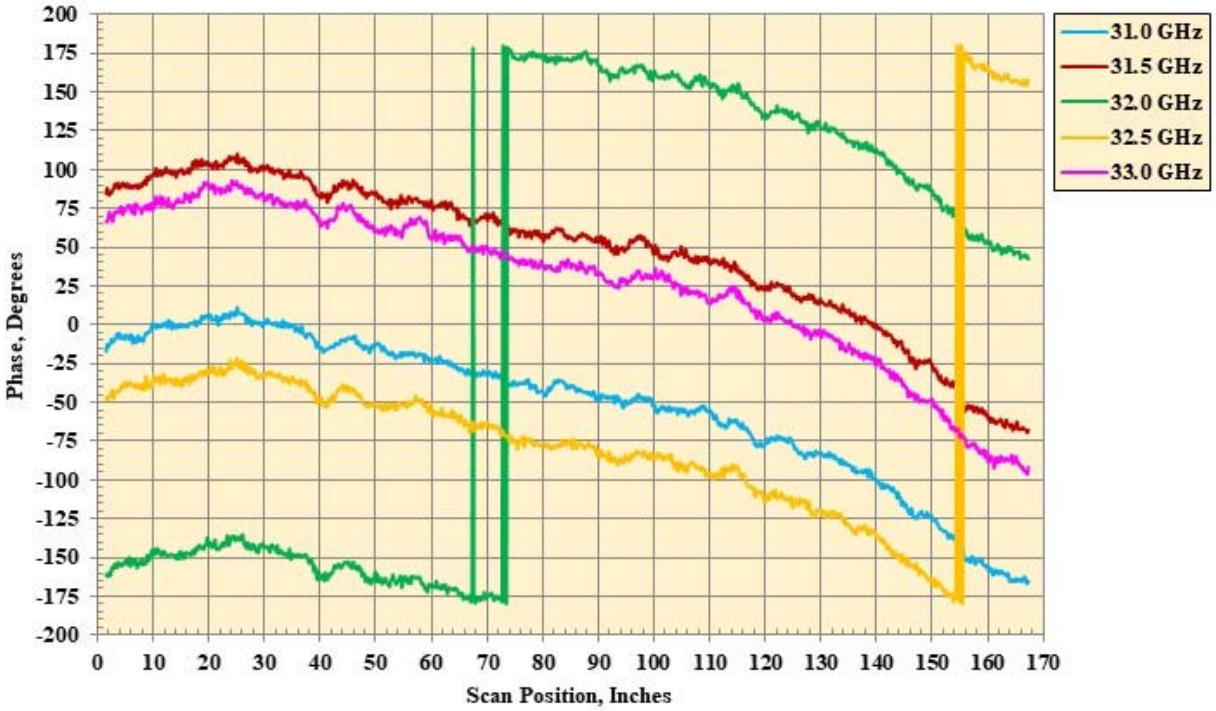

(zz) Phase probe data, Probe Angle = -90°, Pol = VV.
Figure 23. Concluded.

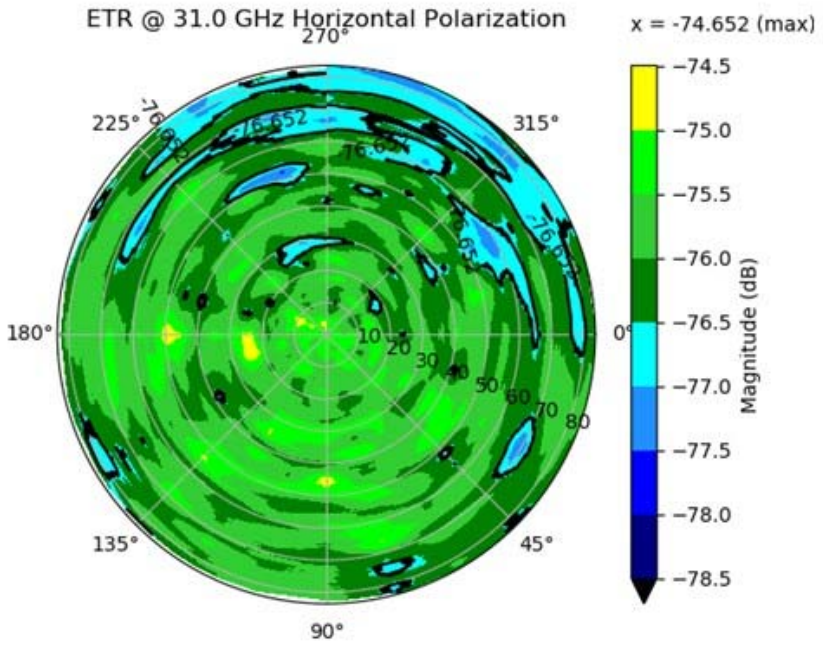

(a) Magnitude probe data, for all roll angles at 31.0 GHz, Pol HH.

Figure 24. Combined summary of all scan data at all roll angle for frequencies from 31 GHz to 33 GHz.

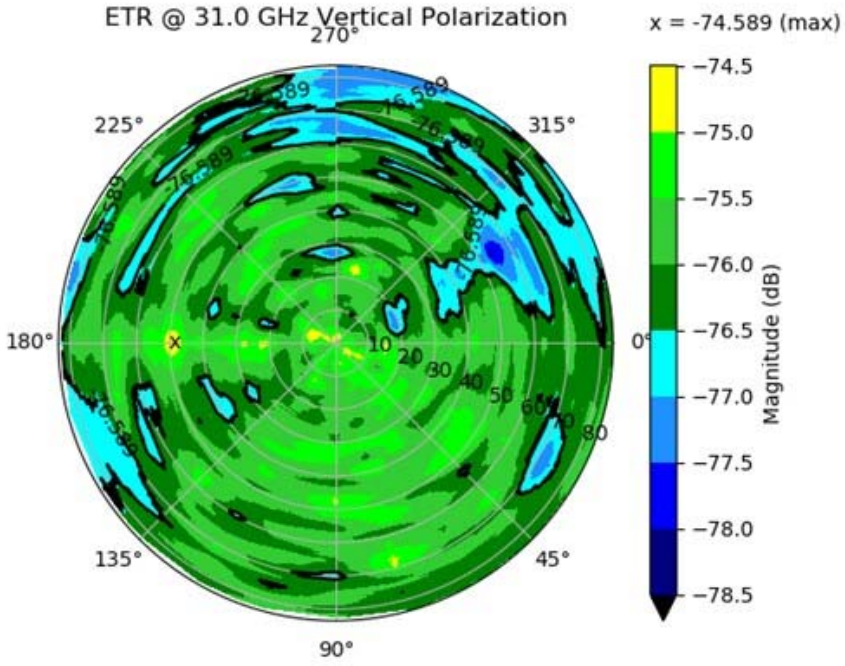

(b) Magnitude probe data, for all roll angles at 31.0 GHz, Pol VV.

Figure 24. Continued.

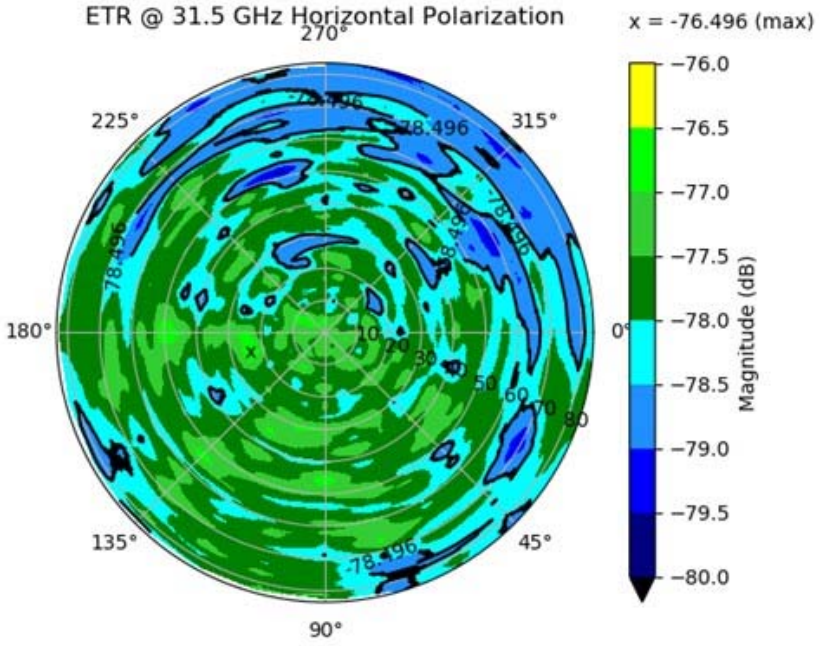

(c) Magnitude probe data, for all roll angles at 31.5 GHz, Pol HH.
Figure 24. Continued.

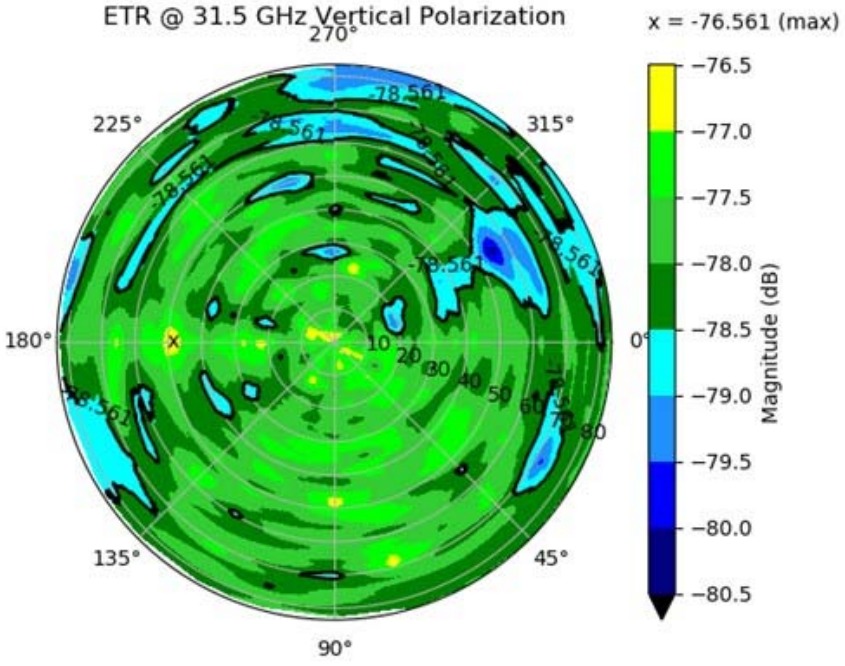

(d) Magnitude probe data, for all roll angles at 31.5 GHz, Pol VV.
Figure 24. Continued.

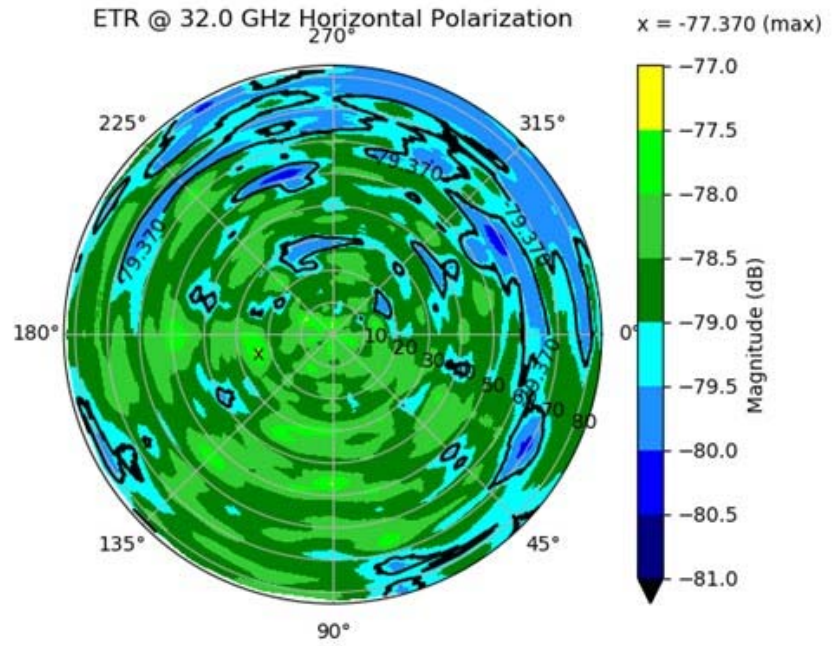

(e) Magnitude probe data, for all roll angles at 32.0 GHz, Pol HH.
Figure 24. Continued.

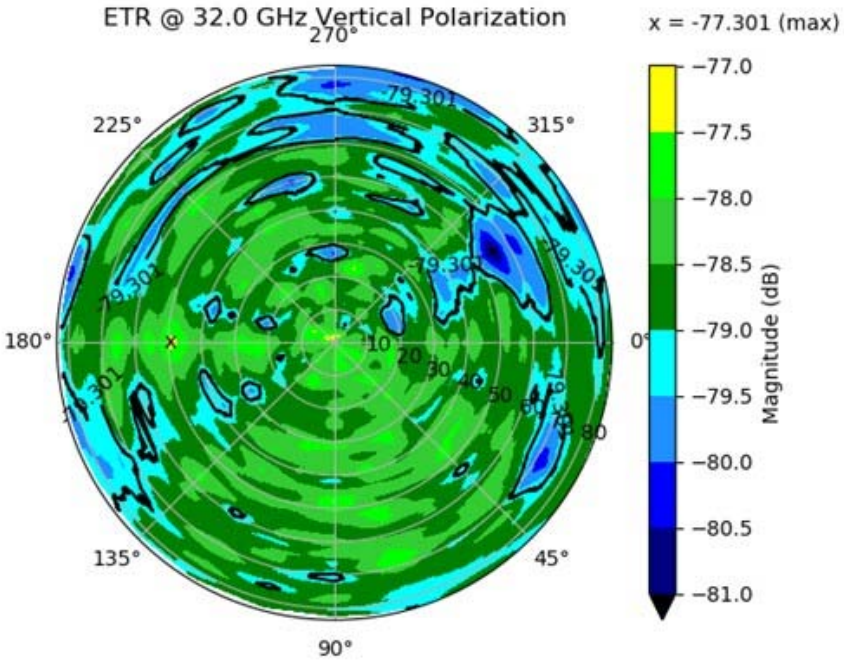

(f) Magnitude probe data, for all roll angles at 32.0 GHz, Pol VV.
Figure 24. Continued.

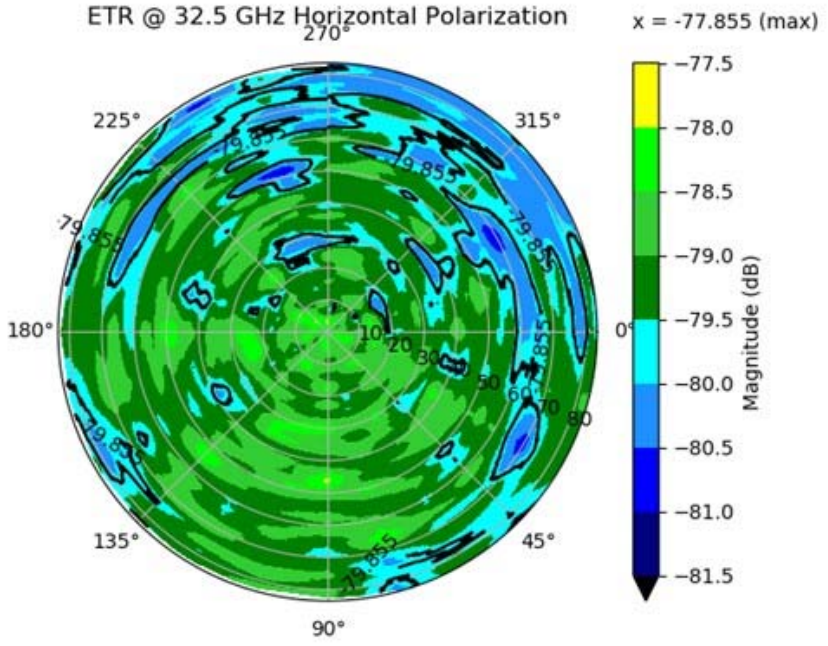

(g) Magnitude probe data, for all roll angles at 32.5 GHz, Pol HH.
Figure 24. Continued.

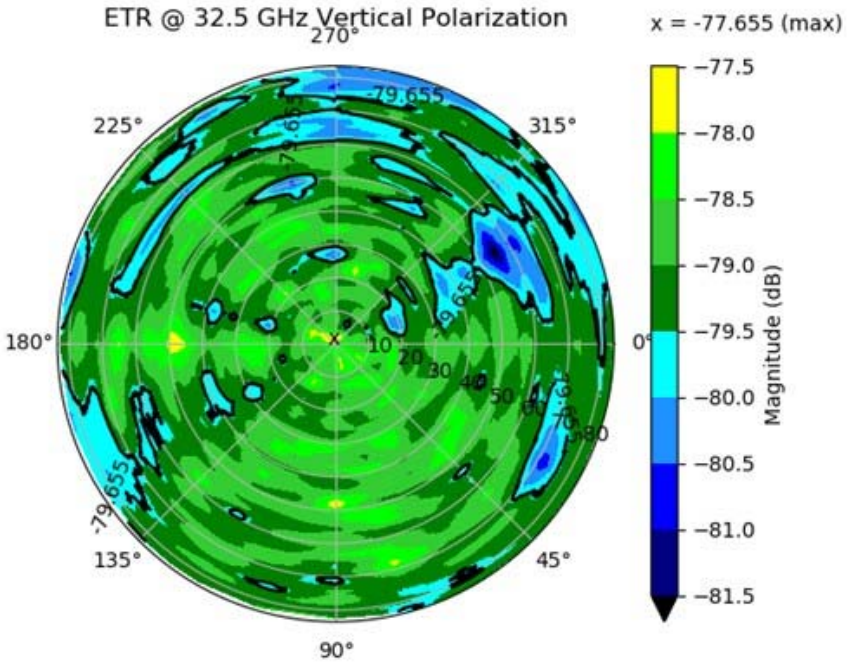

(h) Magnitude probe data, for all roll angles at 32.5 GHz, Pol VV.
Figure 24. Continued.

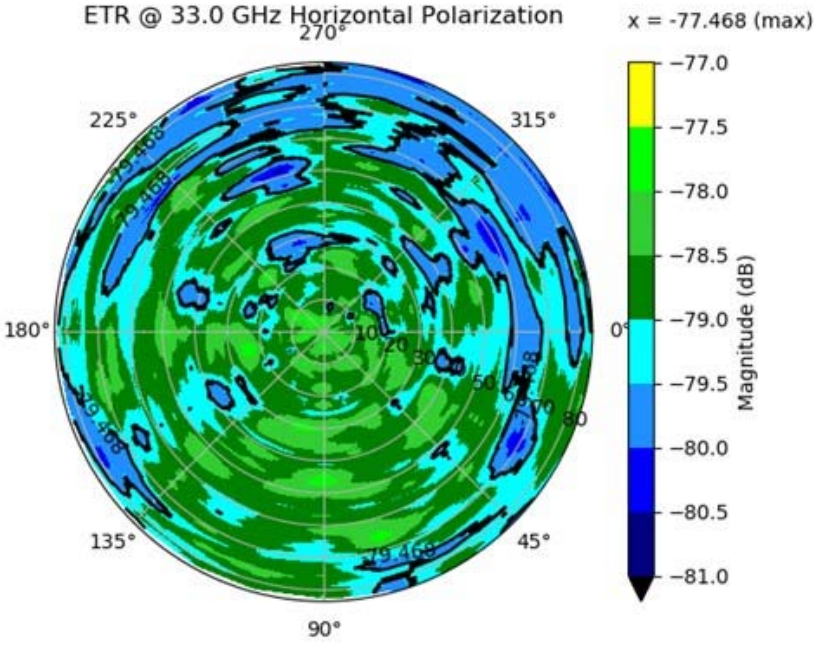

(i) Magnitude probe data, for all roll angles at 33.0 GHz, Pol HH.
Figure 24. Continued.

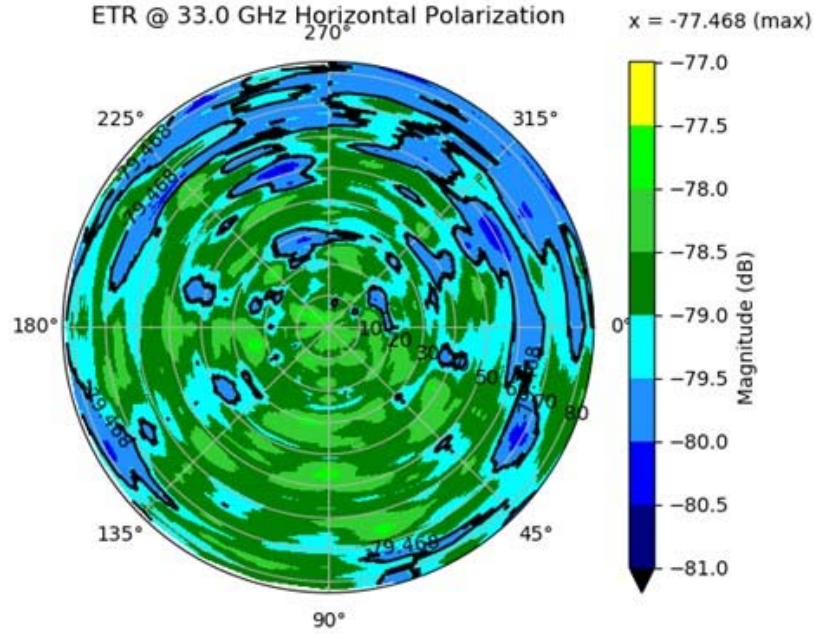

(j) Magnitude probe data, for all roll angles at 33.0 GHz, Pol VV.
Figure 24. Concluded

PNA	Frequency Band, GHz	22.0 to 34.0
	Number of data points inband	2001
	IF Bandwidth, Hz	700
	Average number of points	8
HH	Gate Center, ns	-66.8
HH	Gate Span, ns	1.325
VV	Gate Center, ns	-66.8
VV	Gate Span, ns	1.325
S1	Milltech SFH-28-R31560N A17503	
S2	DRG SAS-574	
S1	Amplifier RF-Lambda RLNA16G32G	Yes
S2	Amplifier	None
Prober	Step size, in.	0.5

Figure 25. Setup for the 22.0 to 34.0 GHz probe data acquisition.

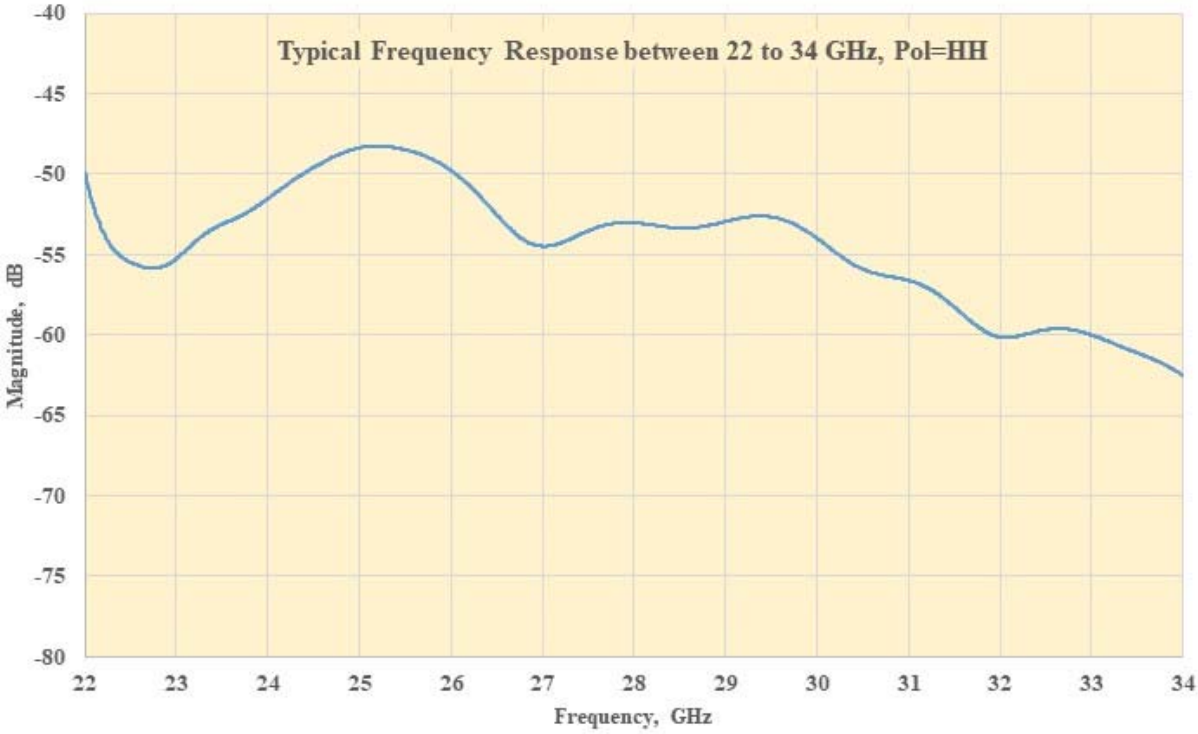

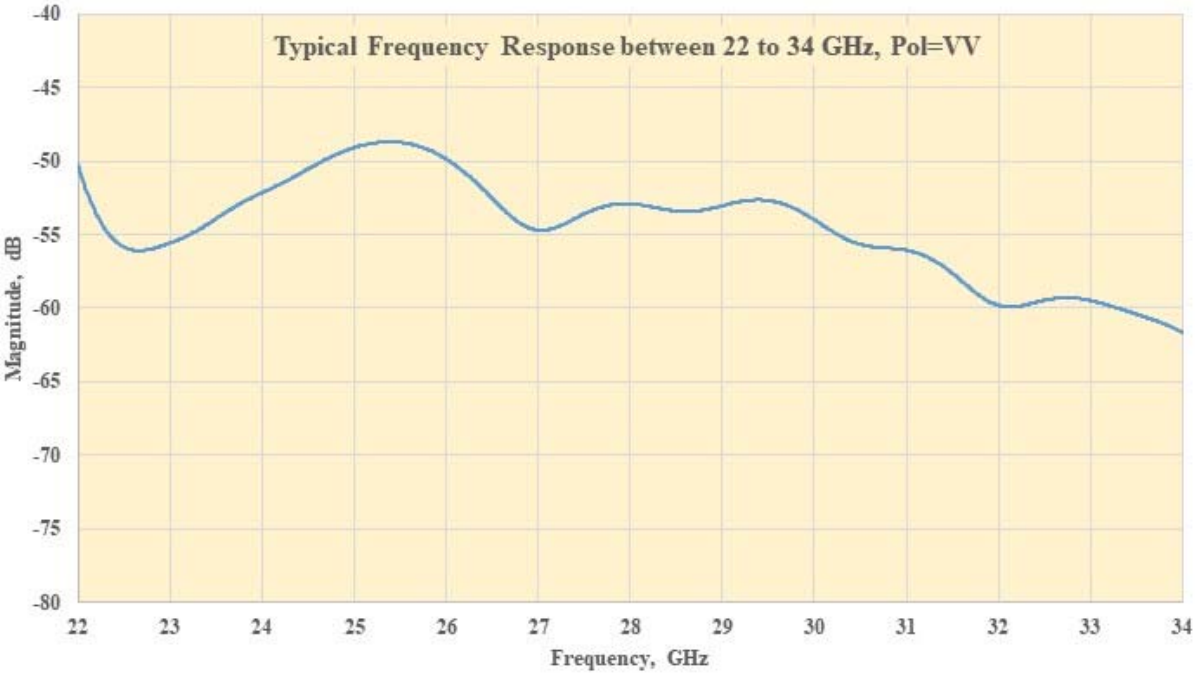

Figure 26. Typical frequency response data for HH and VV for 22.0 – 34.0 GHz probe data. Data acquired at probe arm center.

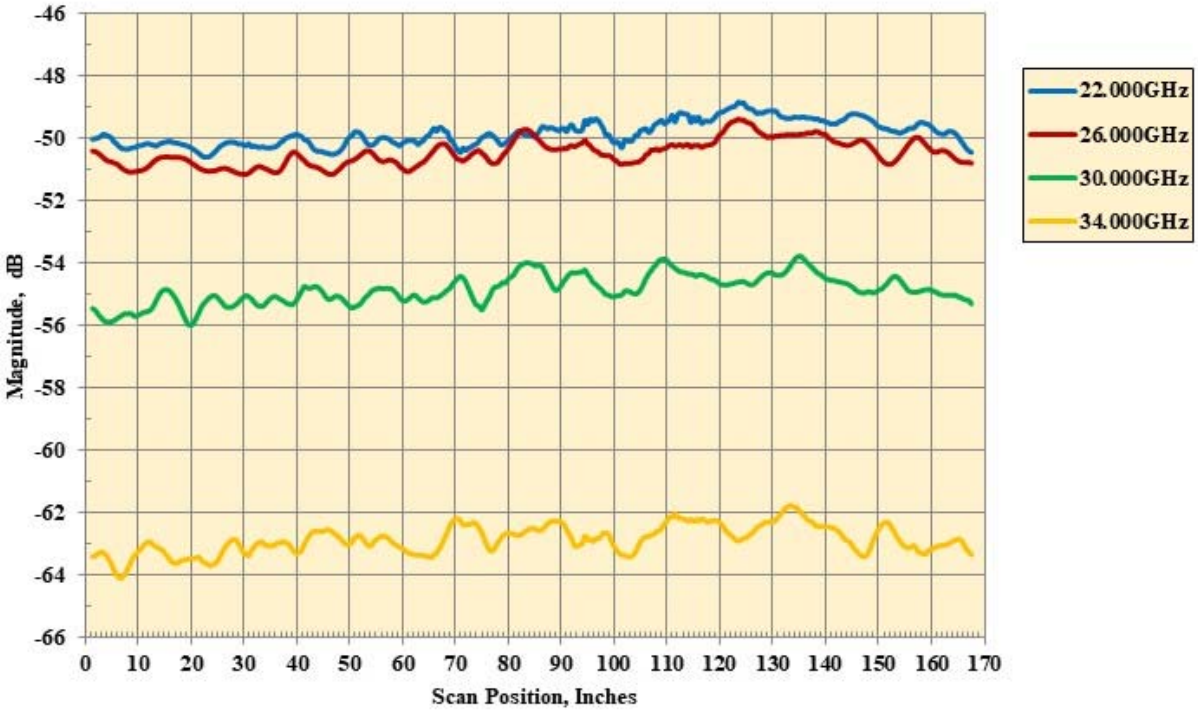

(a) Magnitude probe data, Probe Angle = 0°, Pol = HH.

Figure 27. Probe data at frequency = 22.0 GHz to 34.0 GHz using the S1 antenna = Milltech SFH-28-R31560N A17503 , S2 antenna = DRG SAS-574

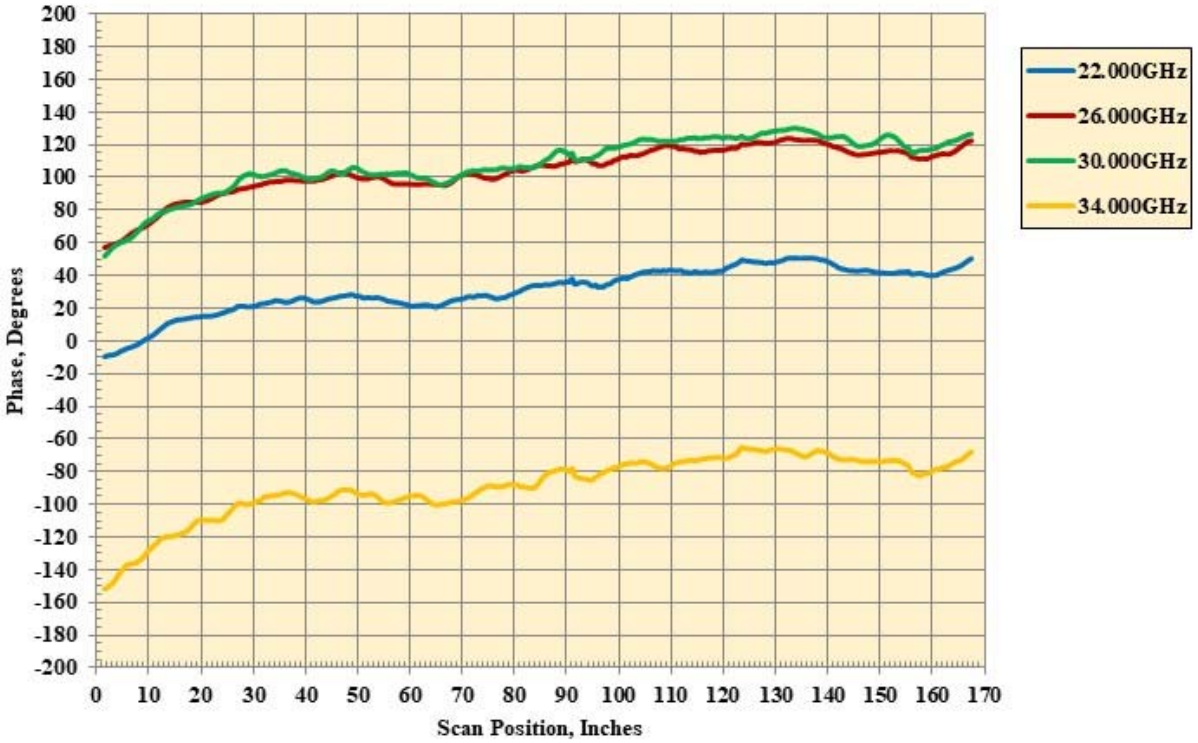

(b) Phase probe data, Probe Angle = 0°, Pol = HH.

Figure 27. Continued.

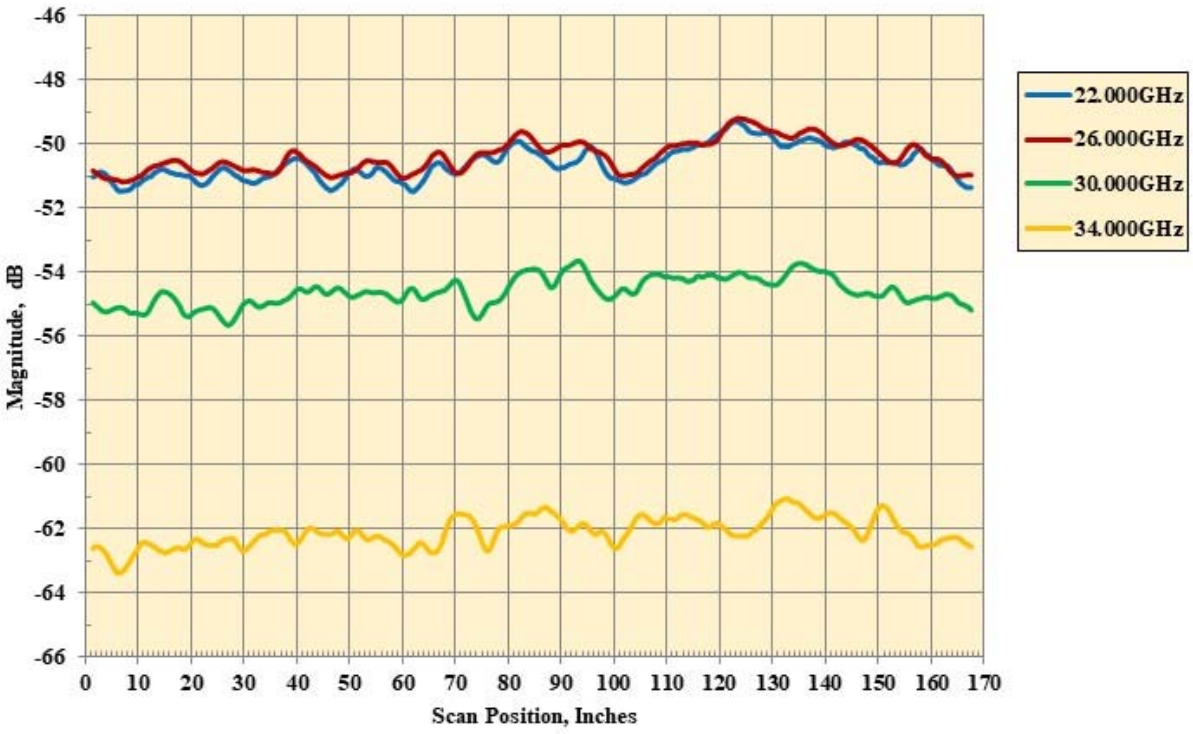

(c) Magnitude probe data, Probe Angle = 0°, Pol = VV.
Figure 27. Continued.

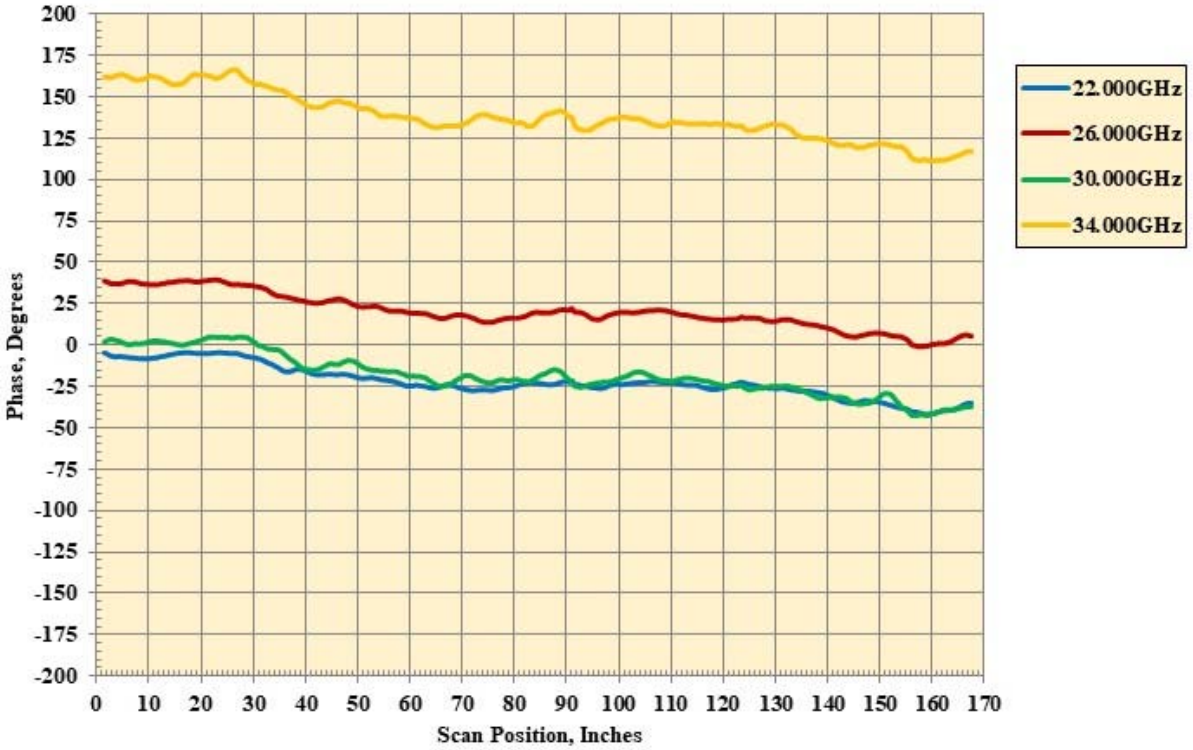

(d) Phase probe data, Probe Angle = 0°, Pol = VV.
Figure 27. Continued.

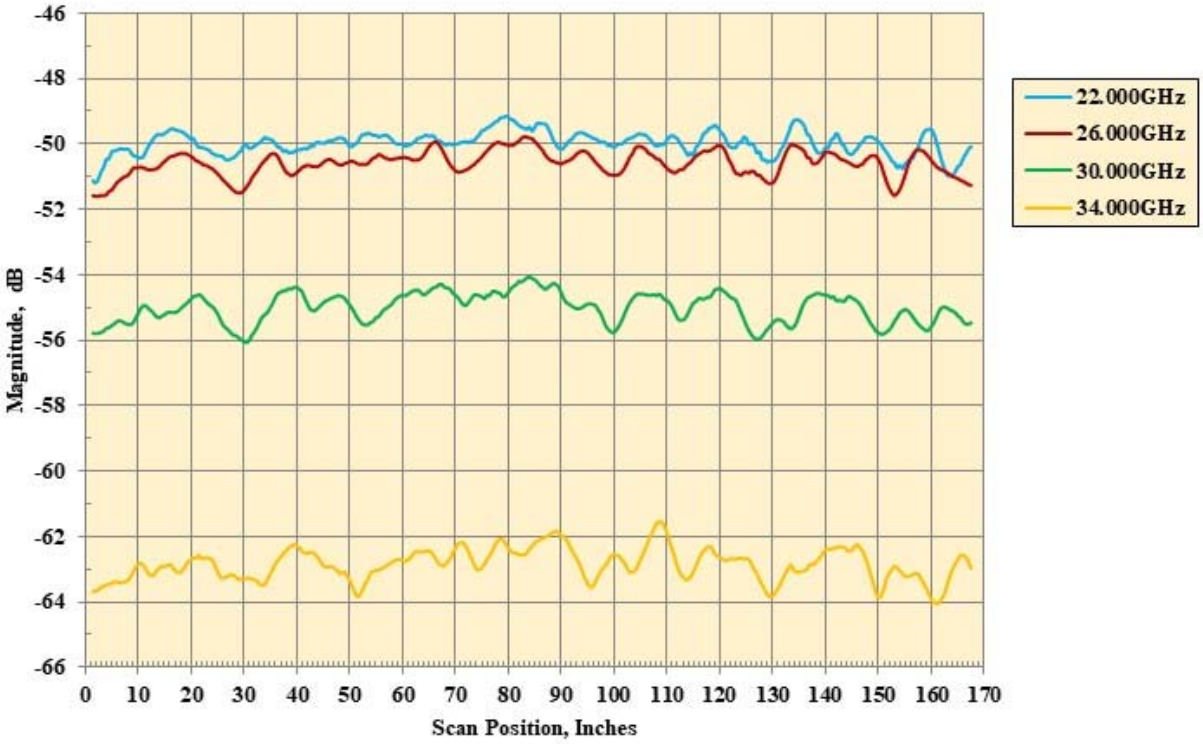

(e) Magnitude probe data, Probe Angle = 45°, Pol = HH.
Figure 27. Continued.

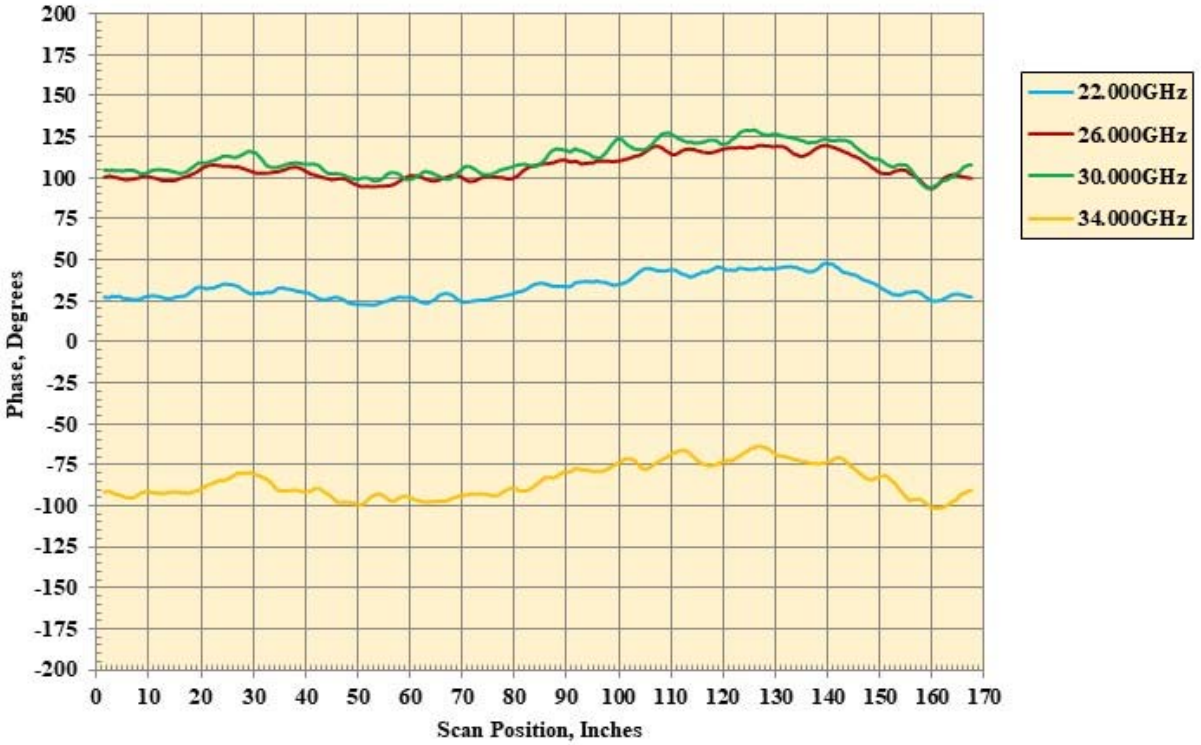

(f) Phase probe data, Probe Angle = 45°, Pol = HH.
Figure 27. Continued.

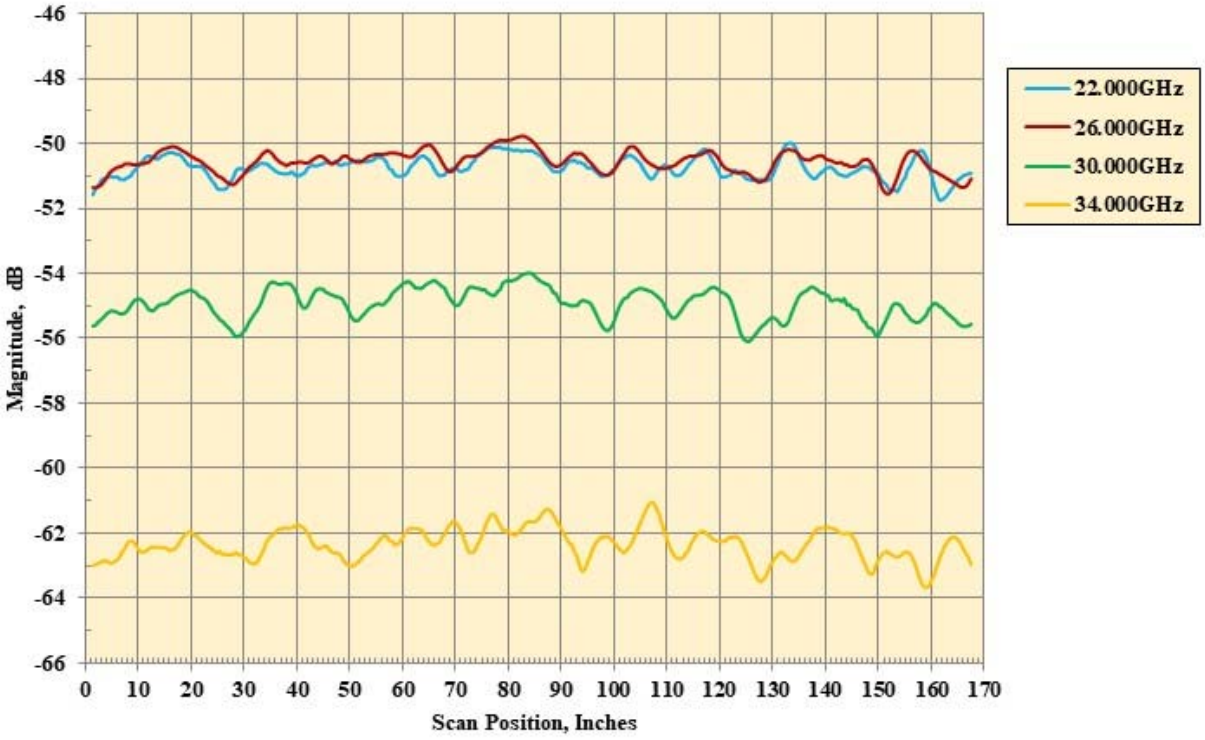

(g) Magnitude probe data, Probe Angle = 45°, Pol = VV.
Figure 27. Continued.

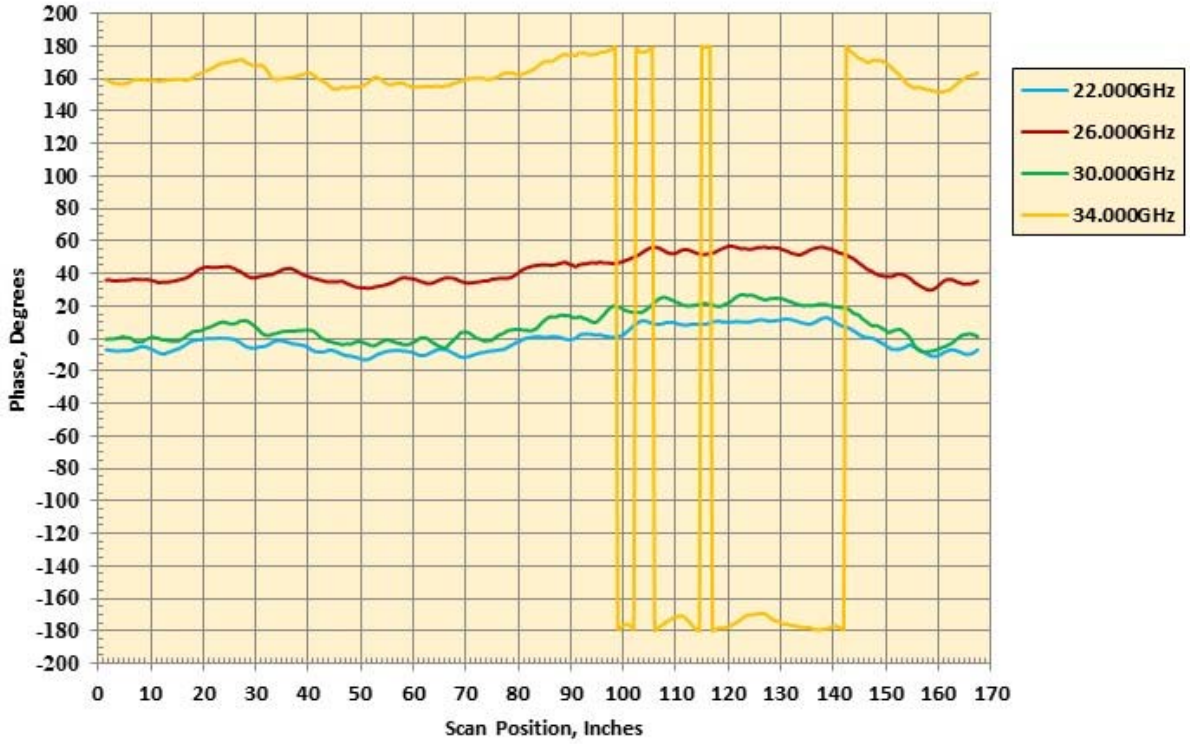

(h) Phase probe data, Probe Angle = 45°, Pol = VV.
Figure 27. Continued.

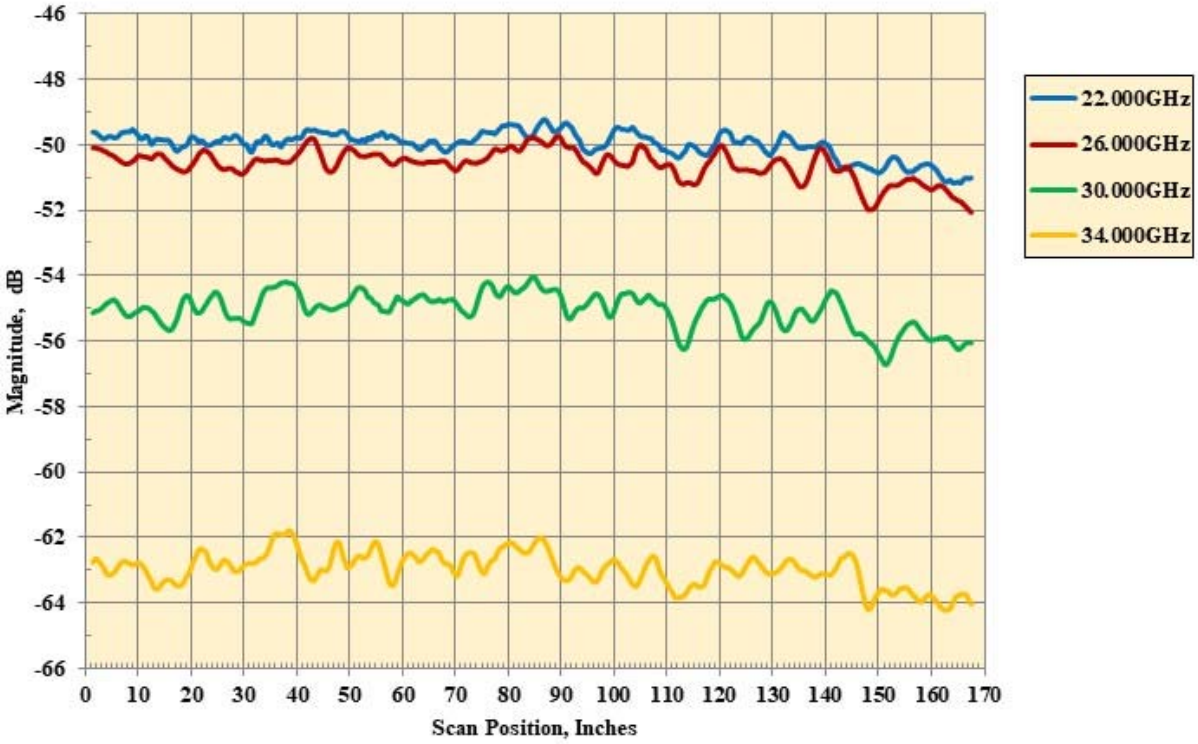

(i) Magnitude probe data, Probe Angle = 90°, Pol = HH.
Figure 27. Continued.

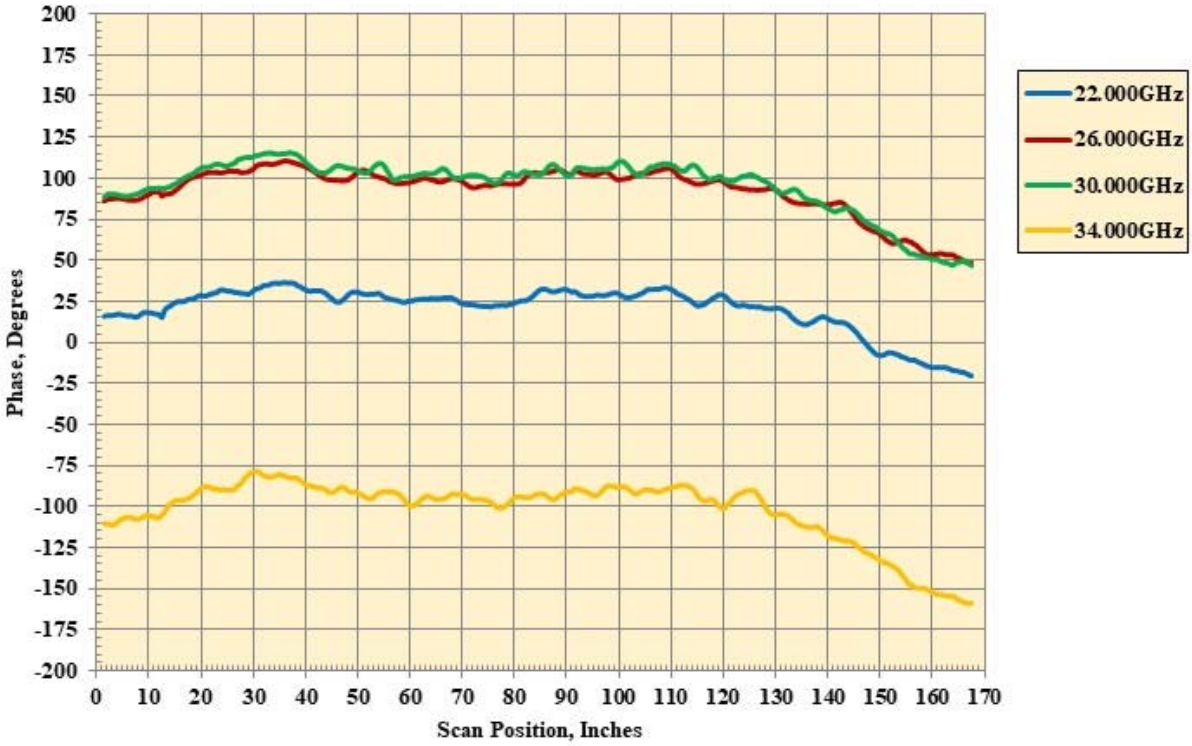

(j) Phase probe data, Probe Angle = 90°, Pol = HH.
Figure 27. Continued.

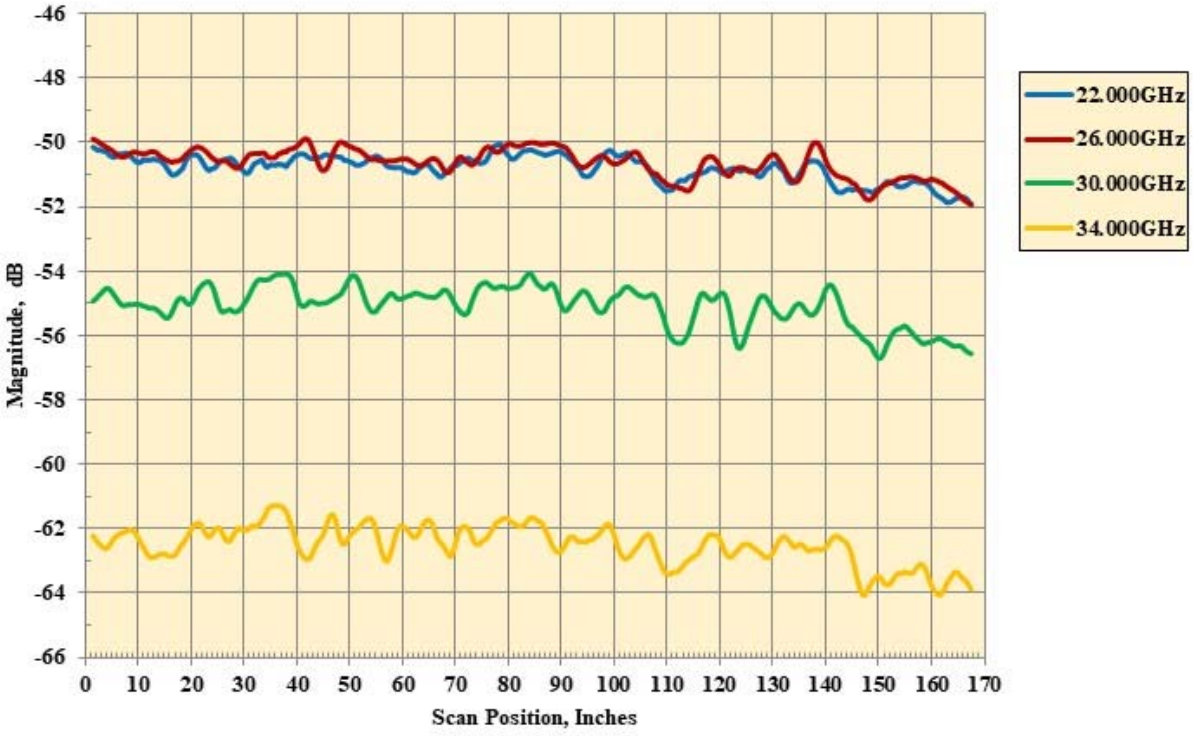

(k) Magnitude probe data, Probe Angle = 90°, Pol = VV.
Figure 27. Continued.

(l) Phase probe data, Probe Angle = 90°, Pol = VV.
Figure 27. Concluded.

REPORT DOCUMENTATION PAGE

Form Approved
OMB No. 0704-0188

The public reporting burden for this collection of information is estimated to average 1 hour per response, including the time for reviewing instructions, searching existing data sources, gathering and maintaining the data needed, and completing and reviewing the collection of information. Send comments regarding this burden estimate or any other aspect of this collection of information, including suggestions for reducing the burden, to Department of Defense, Washington Headquarters Services, Directorate for Information Operations and Reports (0704-0188), 1215 Jefferson Davis Highway, Suite 1204, Arlington, VA 22202-4302. Respondents should be aware that notwithstanding any other provision of law, no person shall be subject to any penalty for failing to comply with a collection of information if it does not display a currently valid OMB control number.
PLEASE DO NOT RETURN YOUR FORM TO THE ABOVE ADDRESS.

1. REPORT DATE *(DD-MM-YYYY)*
1-01-2020

2. REPORT TYPE
Technical Memorandum

3. DATES COVERED *(From - To)*

4. TITLE AND SUBTITLE
NASA ETR Quiet Zone Probe Study

5a. CONTRACT NUMBER

5b. GRANT NUMBER

5c. PROGRAM ELEMENT NUMBER

6. AUTHOR(S)
Ticatch, Larry A.; Szatkowski, George N.; Cavone, Angelo A.; Strickland, Justin K.

5d. PROJECT NUMBER

5e. TASK NUMBER

5f. WORK UNIT NUMBER
993975.04.02.04

7. PERFORMING ORGANIZATION NAME(S) AND ADDRESS(ES)
NASA Langley Research Center
Hampton, VA 23681-2199

8. PERFORMING ORGANIZATION REPORT NUMBER
L-21091

9. SPONSORING/MONITORING AGENCY NAME(S) AND ADDRESS(ES)
National Aeronautics and Space Administration
Washington, DC 20546-0001

10. SPONSOR/MONITOR'S ACRONYM(S)
NASA

11. SPONSOR/MONITOR'S REPORT NUMBER(S)
NASA-TM-2020-220434

12. DISTRIBUTION/AVAILABILITY STATEMENT
Unclassified-
Subject Category 09
Availability: NASA STI Program (757) 864-9658

13. SUPPLEMENTARY NOTES

14. ABSTRACT The NASA Langley Research Center's Experimental Test Range is an indoor anechoic compact range far field test facility used to conduct antenna and electromagnetic radiation measurements. The Experimental Test Range was designed to simulate far field illumination in the facility test volume over a broad band of frequencies by collimating the RF energy from the 26 ft by 26 ft parabolic reflector. The quality of the antenna and radiation measurements are dependent on the uniformity of the far field plane wave generated by the compact range reflector. While this facility is going through several upgrades, this report describes an assessment of the far field plane wave conducted after resurfacing the primary reflector to improve performance and extend the range of frequencies for which this facility can operate. This assessment addresses far field uniformity probe data measured in the test volume across the facility operational frequency bands.

15. SUBJECT TERMS
Antenna; Backscatter; Compact Range; Electromagnetics; Ground Test Facility

16. SECURITY CLASSIFICATION OF:			17. LIMITATION OF ABSTRACT	18. NUMBER OF PAGES	19a. NAME OF RESPONSIBLE PERSON
a. REPORT	b. ABSTRACT	c. THIS PAGE			STI Help Desk (email: help@sti.nasa.gov)
U	U	U	UU	123	19b. TELEPHONE NUMBER *(Include area code)* (757) 864-9658